Model Predictive and Nonlinear Control of Transport-Reaction Process Systems

by

Qingqing Xu

A thesis submitted in partial fulfillment of the requirements for the degree of

Doctor of Philosophy

in

Process Control

Department of Chemical and Material Engineering
University of Alberta

Abstract

Distributed parameter systems (DPS) are models of fundamental conservation laws in industrial processes, such as chemical, petroleum, metallurgical and solar thermal energy processes. The major drawback of DPS models is that they take form of partial differential equations (PDEs) containing higher order derivatives in space and time. The complexity of PDEs models lies in spatial approximation arriving to a finite dimensional model representation amenable for subsequent controller, observer and/or monitoring device design. This thesis provides foundation of systematic modelling framework for linear DPS which uses a finite and low dimensional setting for controller/observer/estimator design without application of any spatial approximation or order reduction. First, we develop a linear model predictive controller design for a class of linear DPS account for a constrained optimization based problem. The discrete model of a linear DPS is obtained by using energy preserving Cayley-Tustin transformation. We present our results applied to the DPS emerging from chemical transport-reaction processes and solar boreal thermal energy processes. Second, we address the servo controller design for a class of DPS described by coupled hyperbolic PDE and ODE. The simple and easily realizable servo control algorithm is applied to the solar thermal system with borehole seasonal storage in a real commercial com-

munity. Finally, we propose the nonlinear controller design for a class of distributed parameter system described by nonlinear hyperbolic PDEs. The nonlinear control methodology is an extension of single-step formulation of full state feedback control design which lies in the fact that both feedback control and stabilization design objectives given as target stable dynamics are accomplished in one step. The performance of controllers is assessed by numerical simulation with application on different distributed parameter systems.

Preface

Chapter 2 of this work has been published as Qingqing Xu, Stevan Dubljevic, "Linear Model Predictive Control for Transport-Reaction Processes", AIChE Journal (2016). I was responsible for the theory development, numerical simulation and analysis, as well as the manuscript composition. Stevan Dubljevic was the supervisory author and was involved with the guidance of concept formation and manuscript composition.

Chapter 3 of this work is published as Qingqing Xu, Stevan Dubljevic, "Modeling and Control of Solar Thermal System with Borehole Seasonal Storage", Renewable Energy 100 (2017) 114-128. I was responsible for the theory development, numerical simulation and analysis, as well as the manuscript composition. Stevan Dubljevic was the supervisory author and was involved with the guidance of concept formation and contributed to manuscript edits.

Chapter 4 of this work is submitted for publication as Qingqing Xu, Stevan Dubljevic, "Model Predictive Control of Solar Thermal System with Borehole Seasonal Storage", Computers & Chemical Engineering. I was responsible for the theory development, numerical simulation and analysis, as well as the manuscript composition. Stevan Dubljevic was the supervisory author and was involved with the guidance of

manuscript composition.

Chapter 5 of this work is submitted for publication as Qingqing Xu, Ilyasse Aksikas, Stevan Dubljevic, "Single-step Full State Feedback Control Design for Nonlinear Hyperbolic PDEs", European Journal of Control. I was responsible for the theory development, numerical simulation and analysis, as well as the manuscript composition. Ilyasse Aksikas assisted with the prove of theory development. Stevan Dubljevic was the supervisory author and was involved with the guidance of concept formation and manuscript composition.

Acknowledgements

First and foremost, I would like to express my deepest thanks to my supervisor Prof. Stevan Dubljevic. His patience, support, and immense knowledge were key motivations through my graduate studies. Without his assistance and dedicated involvement in every step throughout the process, this thesis would have never been accomplished.

At the beginning I know almost nothing about distributed parameter systems, it was Prof. Dubljevic who taught me step-by-step. I am truly thankful for his selfless help and dedication to both my personal and academic development. I cannot think of a better supervisor to have. I owe a great debt of gratitude to Prof. Dubljevic.

I would also like to express my deepest gratitude to my parents for supporting me spiritually throughout my life. Last but not the least, I am grateful to my fellow friends in distributed parameter systems group who supported me a lot: Liu Liu, Felicia Yapari, Azzam Hazim, Xiaodong Xu, Peyman Tajik and Navid Alavi Shoushtari.

Contents

List of Figures

List of Tables

Chapter 1

Introduction

1.1 Motivation

In a real world engineering control applications, the states, inputs and outputs of a mathematical model of a system depend on both temporal and spatial variables. These systems have parameters distributed in space and therefore they are named distributed parameter systems (DPS). On the contrary, systems which do not have distributed parameter nature are lumped parameter systems (LPS) and system variables do not depend on spatial parameters, see [1].

Many industrial processes, such as chemical, petroleum, metallurgical and solar thermal energy processes, belong to the class of DPS. In particular, an interesting subset of continuous DPS processes in chemical and solar thermal energy engineering is presented by the heat transport models. The above industrial processes are often described by a mathematical model, which consists of partial differential equations (PDEs), boundary conditions (BCs), as well as possible constraints on input, state and/or output.

In order to classify the above models, we look into the mathematical classifications of PDEs. Equations involving partial derivatives of a function of two or more independent variables are PDEs. The order of the highest derivative is the order of the equation. Because the properties of DPS depend strongly on the type of equations, the classification of linear, second-order PDE is by the equation of the following form:

$$\frac{\partial u}{\partial t} + \alpha(x,y)\frac{\partial^2 u}{\partial x^2} + \beta(x,y)\frac{\partial^2 u}{\partial x \partial y} + \gamma(x,y)\frac{\partial^2 u}{\partial y^2} = f(x,y,u,\frac{\partial u}{\partial x},\frac{\partial u}{\partial y}) \tag{1.1}$$

An equation of the above form is said to be: parabolic PDE, if $\beta^2 - 4\alpha\gamma = 0$; elliptic PDE, if $\beta^2 - 4\alpha\gamma < 0$; hyperbolic PDE, if $\beta^2 - 4\alpha\gamma > 0$.

In particular, the axial dispersion chemical reactor is described by parabolic PDE which is augmented with either Dirichlet or Neumann boundary conditions. Moreover, the plug flow reactor is modelled by hyperbolic PDEs. On the other hand, the solar thermal energy process contains coupled partial differential equations and ordinary differential equations (ODEs).

Advanced technology needs motivate control of physical and chemical DPS processes of fluid flows, temperature distribution and material structures. Advanced process control, monitoring and decision making in the context of DPS usually require information on all states variables. In particular, the advanced control realization is usually constrained by natural limits on the actuator power and/or the available position where actuation can take place (in domain or boundary of the system). Moreover, in the DPS setting, the knowledge of the system state variables is limited by the time delay in obtaining the measurements, the number of available sensors and the noise corrupting the data. This problem occurs in LPS, but is even more acute in DPS.

The objective of this thesis is to explore advanced controller design to improve the chemical transport-reaction and solar thermal energy processes operations. In

particular, the above PDEs models will be basis for the regulator (controller/observer) synthesis. One of regulator design methodologies to be explored in this thesis is model predictive control (MPC). MPC is an algorithm for optimal control synthesis in which the control action is obtained by solving a finite horizon open-loop optimal control problem at each sampling instant, see [2]. The optimization algorithm yields a sequence of optimal control moves and the fist move is applied to the process, see [3], [4]. The MPC in DPS setting has to account for distributed parameter nature for optimal process performance characteristics, for naturally present constraints and/or limitations on available measurements.

Another regulator design to be explored is the servo controller design for a class of DPS described by coupled hyperbolic PDE and ODE. Servo controller design is a well-know strategy that computes the required input which asymptotically attenuates error between the output and a reference trajectory or set point to zero.

Another interesting research direction is to explore nonlinear controller design for the DPS described by nonlinear PDEs. The nonlinear control methodology is an extension of single-step formulation of full state feedback control design. With a simultaneous implementation of a nonlinear coordinate transformation and a nonlinear state feedback law, both feedback control and stabilization design objectives given as target stable dynamics are accomplished in one step.

1.2 Literature Review

The controller design and state estimation of DPS are more complex than in the LPS. The presence of spatial variables imposes limitations to the controller design. For example, in some cases, boundary conditions are used as inputs and outputs. In

order to illustrate details, this section will review process models of DPS and advanced control methods of these processes. For controller design and state estimation of DPS, in general, there are two approaches taken, see [5], [6]:

(1) Early lumping: in which DPS is first discretized into an approximate LPS model consisting of a set of ODEs. Then, LPS control theory for controller design and state estimation is applied directly to DPS. However, one disadvantage of this approach is that conditions for controllability and stabilizability depend on the method of lumping and the location of discretization points.

(2) Late lumping: in which DPS control theory is applied first to DPS and approximation method is applied at the final stage. It takes full advantages of the available distributed parameter control theory and analyzes the full PDEs model for controllability and stabilizability. Once the design is accomplished, some type of finite dimensional approximation in the controller realization is performed.

The design procedure of early lumping and late lumping is shown in Fig.1.1.

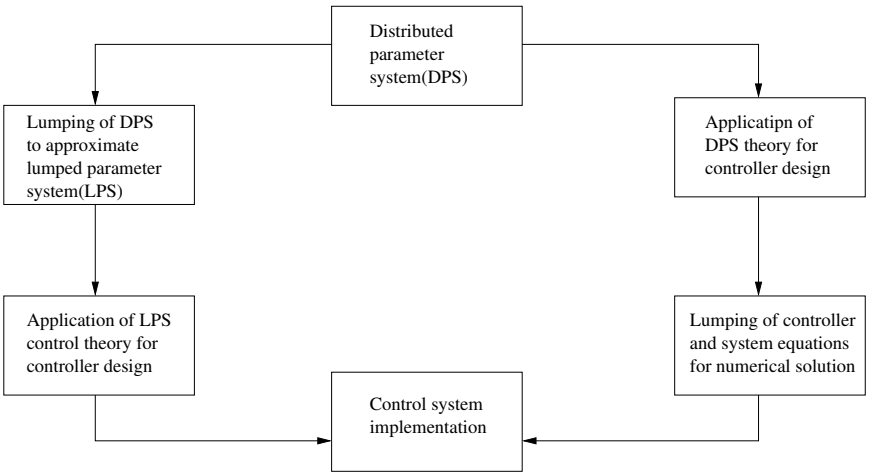

Fig. 1.1: Design procedure via early lumping and late lumping

Since distributed parameter systems are modelled by partial differential equations,

the evolution of states of a PDE is described in an infinite-dimensional space setting. A number of researchers have explored many problems related to control of a system described by PDE, such as dynamic optimization, output feedback controller design, nonlinear and robust control, see [7], [8].

The traditional approach for control of some PDE systems utilizes spatial discretization techniques to obtain systems of ODEs, which are subsequently utilized as the foundation of the finite-dimensional controllers design, see [9], [10]. This approach has a significant drawback since the number of states which must be preserved to obtain a system of ODEs, might be quite large, which leads to a high dimensional controller realization and complex controller design.

Optimal control is a problem of determining inputs to a dynamical system that optimize a specified performance while satisfying any constraints on the motion of the system. The theory of necessary conditions for optimal control problems is solution of multipoint boundary value problems, see [11], [12]. For such problems, shooting techniques have been established as efficient and reliable methods providing highly accurate solutions, see [13]. However, the shooting methods have a severe drawback: these methods need a rather precise initial guess of the optimal state, control and adjoint variables and require a detailed knowledge of the structure of the optimal solution.

Model predictive control refers to a class of control algorithms that compute an input profile by utilizing a linear process model to optimize an open loop quadratic objective function subject to constraints over a future time horizon, see [14]. In reality, actuators and sensors have their limits due to physical properties, or the system state is required not to be in excess of specified limit values. Motivated by this consideration, model predictive controller for distributed parameter system is developed.

Various development of MPC have been explored by Dubljevic, Christofides, Alonso and Armaou within the framework of distributed [15] and boundary applied actuation [16], and predictive output and full state feedback control [17].

In order to utilize model predictive control, the discrete version of the overall system is required. Traditional numerical time discretization approaches, such as Euler, Runge-Kutta, etc. have the disadvantage that the accuracy of the approximate discrete time system rapidly deteriorates as the sampling period increases [18]. The Cayley-Tustin time discretization methodology preserves the intrinsic energy and dynamical characteristics of distributed parameter systems [19, 20]. Along the line of Cayley-Tustin transformation, the PDEs system is kept without any type of spatial approximation and/or model reduction, see [21, 22, 23]. The issues arising from analytic transformation of continuous to discrete distributed parameter setting are addressed by providing guidance for appropriate choice of discretization parameters.

The discrete representation of distributed parameter systems obtained by the application of Cayley-Tustin transformation provides an insight into frequency analysis and controller design. The servo problem is a discrete controller which can be easily realized and implemented in practice. Servo controller design is a well-know strategy that computes the required input which asymptotically attenuates error between the output and a reference trajectory or set point to zero [24, 25]. One of the advantages of a servo controller is that it can account for disturbances which may affect the process.

The controller synthesis for nonlinear DPS which is given in an infinite dimensional setting is rather rare and difficult both in terms of design and/or implementation. Within the linear DPS, the extensions of state feedback regulation, optimal control, internal model control and backstepping are successfully realized [26, 27, 28, 29, 30,

31, 32, 33, 34]. However, only small number of nonlinear finite dimensional control design methodologies were extended to nonlinear DPS [35, 36, 37]. Motivated by Luenberger's early ideas on a single-step design approach for pole placement, the development of single-step controller design that achieves simultaneously the feedback linearization and desired pole placement is pursued for nonlinear DPS.

1.3 Semigroup Theory

The abstract formulation of linear infinite-dimensional system is described by the following state space system:

$$\dot{z}(\zeta, t) = Az(\zeta, t), \quad z(\zeta, 0) = z_0 \tag{1.2}$$

the state $z(\zeta, t) \in H$, where H is a real Hilbert space.

A C_0-semigroup is an operator-valued function $\mathcal{T}(t)$ from R^+ to (H) that satisfies the following properties [38]:

(1) $\mathcal{T}(t+\tau) = \mathcal{T}(t)\mathcal{T}(\tau)$ for $t, \tau \geq 0$;

(2) $\mathcal{T}(0) = I$;

(3) $||\mathcal{T}(t)z_0 - z_0|| \to 0$ as $t \to 0^+$ $\forall z_0 \in H$.

The operator $A : D(A) \subset H \to H$ is a generator of a C_0-semigroup on H and one can obtain:

$$z(\zeta, t) = \mathcal{T}(t)z_0 \tag{1.3}$$

Let us consider an example that a metal bar of length one is heated along its

length according to:

$$\frac{\partial z(\zeta,t)}{\partial t} = \frac{\partial^2 z(\zeta,t)}{\partial \zeta^2}, \quad z(\zeta,0) = z_0 \tag{1.4}$$
$$\frac{\partial z(0,t)}{\partial \zeta} = 0 = \frac{\partial z(1,t)}{\partial \zeta}$$

$z(\zeta,t)$ represents the temperature at position ζ at time$t$, z_0 the initial temperature profile. We define the operators A on H as:

$$Az = \frac{dz}{d\zeta^2} \tag{1.5}$$

with $D(A) = \{z \in L_2(0,1) |\ z, \frac{dz}{d\zeta}$ are absolutely continuous, $\frac{d^2z}{d\zeta^2} \in L_2(0,1)$ and $\frac{dz(0)}{d\zeta} = 0 = \frac{dz(1)}{d\zeta}\}$.

It is readily verified that A has the eigenvalues $\lambda_n = -n^2\pi^2, n \geq 0$, and that the corresponding eigenvectors $\phi_n(\zeta) = \sqrt{2}\cos(n\pi\zeta)$ for $n \geq 1$, $\phi_0 = 1$, form and orthonormal basis for $L_2(0,1)$. A is the Riesz-spectral operator given by

$$Az = \sum_{n=0}^{\infty} -n^2\pi^2 < z, \phi_n > \phi_n, \quad z \in D(A) \tag{1.6}$$

where $D(A) = \{z \in L_2(0,1) |\ \sum_{n=1}^{\infty} n^4\pi^4| < z, \phi_n > |^2 < \infty\}$.

A is the infinitesimal generator of the following C_0-semigroup:

$$\mathcal{T}(t)z_0 =< z_0, 1 > + \sum_{n=1}^{\infty} 2e^{-n^2\pi^2 t} < z_0, \cos(n\pi\zeta) > cos(n\pi\zeta) \tag{1.7}$$

Another example is the first-order hyperbolic PDE in the following form:

$$\frac{\partial z(\zeta,t)}{\partial t} = -\frac{\partial z(\zeta,t)}{\partial \zeta}, \quad z(\zeta,0) = z_0 \tag{1.8}$$

$$z(0,t) = 0$$

the following C_0-semigroup on $L_2(0,1)$ can be obtained:

$$\mathcal{T}(t)z_0 = \begin{cases} z_0(\zeta - t) & \zeta - t < 1 \\ 0 & \zeta - t > 1 \end{cases} \tag{1.9}$$

1.4 Thesis Outline and Contributions

This thesis is organized as follows:

In Chapter 2, a systematic linear model predictive control algorithm for linear distributed parameter systems emerging from chemical engineering industry is developed. We consider the systems varying from the convection dominated plug flow reactor models described by hyperbolic PDEs to the diffusion dominated axial dispersion reactor models described by parabolic PDEs. The discrete state space setting is developed by applying Cayley-Tustin time discretization without spatial discretization and model reduction. The issues of optimality and constrained stabilization are addressed within the controller design setting leading to the finite constrained quadratic regulator problem, which is easily realized and is no more computationally intensive than the existing algorithms.

In Chapter 3, the modelling of a complex solar boreal thermal storage system which is inspired by a real Drake Landing Solar Commercial Community is developed. The overall system is obtained from a coupled finite and infinite dimensional subsystems of solar power plant process, heat exchanger process, borehole energy storage process, hot tank process and district heating loop process. The discrete coupled PDEs and ODEs system is obtained by applying Cayley-Tustin time discretization

with the same sampling time. We address the problem of controlling a solar thermal storage system with the purpose of achieving a desired thermal comfort level and energy savings. As the energy output from the solar thermal plant with borehole seasonal storage varies, the control system maintains the thermal comfort by using a servo controller. A simple and easily realizable servo control algorithm is designed to regulate the system operating at desired thermal comfort level despite disturbances from the solar thermal plant system, the borehole geo-thermal energy storage system and/or the district heating loop system.

In Chapter 4, we consider the same discrete solar boreal thermal storage system developed in Chapter 3. The novel model predictive control addresses a house heat regulation by constrained optimization problem with the manipulation constraints, and accounts for possible unstable system dynamics and disturbances arising from solar and geothermal radiations. The realistic output regulation is considered by the inclusion of an observer which constructs finite and infinite dimensional states. The proposed model development and control regulation can successfully account for the long range variability in environmental and/or economic conditions associated with the overall operational costs of the large scale solar energy community.

In Chapter 5, the thesis proposes an extension of single-step formulation of full state feedback control design to the class of distributed parameter system described by nonlinear hyperbolic PDEs. We consider an exothermic plug-flow reactor system which is described by first-order hyperbolic PDE and a damped wave equation which takes the form of second-order hyperbolic PDE. The methodology lies in the fact that both feedback control and stabilization design objectives given as target stable dynamics are accomplished in one step under a simultaneous implementation of a nonlinear coordinate transformation and a nonlinear state feedback law. The mathe-

matical formulation of the problem is realized via a system of first-order quasi-linear singular PDEs. By using Lyapunov's auxiliary theorem for singular PDEs, the necessary and sufficient conditions for solvability are utilized. The solution to the singular PDEs is locally analytic, which enables development of a PDE series solution.

Chapter 6 summarizes the main results of this thesis and discusses future research directions.

Chapter 2

Linear Model Predictive Control for Transport-Reaction Processes

2.1 Introduction

Modelling of a transport process is the most important issue in the process analysis and control design of transport processes. It is currently addressed by phenomenological modelling arising from first-principles, experimental studies and/or with the help of the system identification theory. In many industries including chemical, petrochemical and pharmaceutical plants, model-based control has been very successful. In majority of them, the underlying plant model is low dimensional and linear. In general, mathematical models of many industrial relevant transport processes are obtained from conservation laws, such as mass, momentum and/or energy, and take forms represented by nonlinear partial differential equations (PDEs). The salient feature of these models is temporal and spatial dependence that captures the change in shape and material properties, and can be associated with well known physical

phenomena of the phase change, generation or/and consumption of chemical species by chemical reaction mechanisms, heat and mass transfer phenomena.

Chemical process control of lumped parameter systems is a well established and documented field of the process control. One of the most prominent achievements in the broad area of process control is development of model predictive control for lumped parameter systems [39, 40, 2, 41, 42, 43]. This refers to a class of control algorithms which compute a control variable by utilizing a plant process model to optimize a linear or quadratic open-loop performance objective subject to constraints over a future time horizon. The computed control variable profile over the horizon is utilized by applying only the first move and this process is repeated at each time interval in a repetitive manner. In the case of linear models [2], linear predictive control utilizes a linear state space or transfer function models obtained by the first principles, or obtained by the pulse and/or step response of the controlled plant. The great feature of linear model predictive control is that constrained and multivariable processes can be addressed with emphasis on a robust algorithm realization that can be implemented on-line.

Along the line of developed control areas, the control of linear distributed parameter systems is a mature control field [5, 44, 38, 45, 46]. The intrinsic feature of distributed parameter systems is that the models take the form in an infinite dimensional space setting which leads into infinite dimensional controller designs that are not implementable and realizable in practice. In other words, control designers are forced to apply some type of approximations in order to arrive at some finite dimensional model setting that can be consequently explored within a finite dimensional control design setting. Along this line of work, there are several contributions, for example, the seminal work of Harmon Ray [5] laid foundation for spectral treatment

for a class of distributed parameter systems, Ray and Seinfeld explored the design of nonlinear distributed state estimators using stochastic methods [47]. Other notable works addressed the issue of identification and multivarable predictive control applied to distributed parameter systems [48, 49]. More recently, Ng and Dubljevic considered the time-varying optimal control problem [50] and boundary control formulation [51] for the crystal growth model regulation with time-varying domain characteristic represented by the PDE as an abstract evolution equation on an infinite-dimensional function space with a non-autonomous parabolic operator which generates a two-parameter semigroup. Despite the aforementioned developments and a myriad of work on unconstrained stabilization, the issue of a low order constrained optimal/suboptimal controller design remained elusive.

In the last decade, there were several attempts to address control of distributed parameter systems within an input and/or state constrained optimal control setting. In the case of transport systems modelled by the first order hyperbolic systems, there were several works on dynamical analysis and control of hyperbolic PDEs systems, and in particular, the work of Aksikas *et. all.* on linear quadratic control application to a fixed-bed reactor [52] and optimal linear quadratic feedback controller design to hyperbolic distributed parameter systems [53]. Other contributions considered model predictive control applied to hyperbolic systems [54, 55]. In the same vein, the optimal and model predictive control realizations are extended to Riesz spectral systems (parabolic, and higher order dissipative PDEs) with a separable eigenspectrum of the underlying dissipative spectral operator with successful realization of algorithms that account for the input and PDE state constraints [56, 15, 57, 58, 59]. There are also other extensions in the area of nonlinear model predictive control [60] in which a combination of on-line model reduction and successive linearizations is applied. In

all aforementioned control design realizations, some type of appropriate approximation is applied to a continuous model to arrive to a discrete model, which is used for the controller design. It will be clear in subsequent sections, that one can treat the linear distributed parameter system intact and design a controller without any model approximation.

In this chapter, we provide development of an optimal constrained finite dimensional controller for linear transport-reaction systems with input and PDE state/output constraints which capture majority of linear transport-reaction chemical process systems of interest. The prominent feature of the proposed controller design is that no spatial discretization is required. The linear transport-reaction system is completely captured with the proposed transformations from a continuous to a discrete state space setting without consideration of spatial discretization and/or any other type of spatial approximation of the process model plant. The Cayley-Tustin time discretization transformation is applied to the parabolic PDE system and hyperbolic PDE system to preserve the infinite-dimensional nature of the distributed parameter system [19]. Along the line of Cayley-Tustin transformation, the time discretization lies in the fact that conservative characteristics of the system are preserved [20, 22, 23]. The issues arising from analytic transformation of continuous to discrete distributed parameter setting are addressed by providing guidance for appropriate choice of discretization parameters. An important resolvent operator for discretization realization of parabolic and hyperbolic PDE system is obtained. The underlying analytic form of a discrete model is utilized in the design of the model predictive controller which addresses the input and PDE state/output constraints satisfaction and stabilization by finite dimensional convex quadratic problem realization. The representative examples of the novel algorithm design applied to hyperbolic and parabolic transport-reaction

systems are discussed from the stability and optimality point of view.

This chapter is organized as follows. In Section 2.2, the Cayley-Tustin time discretization for distributed parameter systems is introduced. Further, the discrete-time model representations for the hyperbolic and parabolic PDE system are provided. In Section 2.3, the model predictive controller is designed and the issues related to stability, input and state constraints satisfaction are addressed. In Section 2.4, we demonstrate the features of the model predictive control algorithm built in the previous section through the simulation studies.

2.2 Time Discretization for Linear PDE

The linear infinite-dimensional system is described by the following state space system:

$$\begin{aligned} \dot{z}(\zeta,t) &= Az(\zeta,t) + Bu(t),\ z(\zeta,0) = z_0 \\ y(t) &= Cz(\zeta,t) + Du(t) \end{aligned} \tag{2.1}$$

where the following assumptions hold: the state $z(\zeta,t) \in H$, where H is a real Hilbert space endowed with the inner product $< \cdot\ ,\ \cdot >$; the input $u(t) \in U$ and the output $y(t) \in Y$, where U and Y are real Hilbert spaces; the operator $A : D(A) \subset H \to H$ is a generator of a C_0-semigroup on H and has a Yoshida extension operator A_{-1} (to accommodate for boundary or point actuation) [61]; B, C and D are linear operators associated with the actuation and output measurement or direct feed forward element, i.e., $B \in L(U,H)$, $C \in L(H,Y)$ and $D \in L(U,Y)$. In particular, the operator A is a linear spatial operator associated with the hyperbolic or parabolic transport reaction system.

Taking a type of Crank-Nicolson time discretization scheme and given a time discretization parameter $h > 0$, in the system engineering theory known as Tustin time discretization is given by [62]:

$$\begin{aligned} &\frac{z(jh) - z((j-1)h)}{h} \approx A\frac{z(jh) + z((j-1)h)}{2} + Bu(jh),\ z(0) = z_0 \\ &y(jh) \approx C\frac{z(jh) + z((j-1)h)}{2} + Du(jh) \end{aligned} \tag{2.2}$$

Let $u_j^h/\sqrt{h}$ be the approximation of $u(jh)$, the convergence of $y_j^h/\sqrt{h}$ to $y(jh)$ as $h \to 0$ under rather general assumptions, the above set of equations yields the discrete time dynamics:

$$\begin{aligned} &\frac{z_j^h - z_{j-1}^h}{h} = A\frac{z_j^h + z_{j-1}^h}{2} + B\frac{u_j^h}{\sqrt{h}},\ z_0^h = z_0 \\ &\frac{y_j^h}{\sqrt{h}} = C\frac{z_j^h + z_{j-1}^h}{2} + D\frac{u_j^h}{\sqrt{h}} \end{aligned} \tag{2.3}$$

After some basic manipulation, the discrete system takes the following form:

$$\begin{aligned} &z(\zeta, k) = A_d z(\zeta, k-1) + B_d u(k),\ z(\zeta, 0) = z_0 \\ &y(k) = C_d z(\zeta, k-1) + D_d u(k) \end{aligned} \tag{2.4}$$

where $\delta = 2/h$, A_d, B_d, C_d and D_d are discrete time linear system operators, given by

$$\mathcal{S} := \begin{bmatrix} A_d & B_d \\ C_d & D_d \end{bmatrix} = \begin{bmatrix} [\delta - A]^{-1}[\delta + A] & \sqrt{2\delta}[\delta - A_{-1}]^{-1}B \\ \sqrt{2\delta}C[\delta - A]^{-1} & G(\delta) \end{bmatrix} \tag{2.5}$$

where $G(\delta)$ denotes the transfer function of the system evaluated at δ and is defined as

$G(\delta) = C[\delta - A_{-1}]^{-1}B + D$. A continuous system with strictly proper transfer function has physical realization and does not have the feedthrough operator D (e.g. $D = 0$). However, the corresponding discrete representation for the linear transport reaction systems poses the feedthrough operator $D_d = G(\delta)$ [19]. This continuous and discrete infinite dimensional system representations discrepancy is nullified in the limit of $h \to 0$, which implies that discrete system given by Eq.2.4 becomes a continuous counterpart in the limit given by Eq.2.1. Moreover, it is important to notice that if the transfer function of the continuous system Eq.2.1 $G(\delta)$ is strictly proper, then the limit of $G(\delta)$ at infinity exists and is 0, [63] which ensures the well posedness of the system. An important notion is that all physically realizable dynamical systems usually do not contain feedthrough operator which represents instantaneous transfer of signal from the input to the output. The mapping between the continuous system (A, B, C, D) to $\mathcal{S}$ discrete infinite dimensional systems is referred as the Cayley-Tustin discretization method. Another important property of this discretization method is that the discretization does not change the nature of the transformed system. Namely, the classical application of the forward in time Euler discretization may potentially transform a stable continuous system into an unstable discrete system, while the backward in time Euler discretization may transform an unstable system into a discrete, stable one [64]. Finally, if the Cayley-Tustin discretization method is applied to a linear conservative continuous time system, then the resulting discrete system is conservative in the discrete time sense. This transformation preserves the energy equality among the continuous and the discrete model, in other words, it is simplectic or Hamiltonian preserving. The Cayley-Tustin discretization method applied is also a symmetric method, which means that the formula in Eq.2.2 is left unaltered after exchanging $z_j \leftrightarrow z_{j-1}$ and $h \leftrightarrow -h$ [65].

Remark 1: The Cayley-Tustin discretization method maps the generator A of the continuous time system to its *cogenerator* A_d of the corresponding discrete time system. The operator A_d can be also expressed as $A_d = [\delta - A]^{-1}[\delta + A] = -I + 2\delta[\delta - A]^{-1}$, with I being the identity operator.

Proof: One can easily show:

$$\begin{aligned} A_d(\cdot) &= [\delta - A]^{-1}[\delta + A](\cdot) \\ &= \frac{\delta + A}{\delta - A}(\cdot) \\ &= [-I + \frac{2\delta}{\delta - A}](\cdot) \\ &= [-I + 2\delta[\delta - A]^{-1}](\cdot) \end{aligned} \tag{2.6}$$

In addition to the transformation of a distributed parameter system from continuous to discrete representation, important technical difficulties associated with point and/or boundary actuation and observation in the continuous system representation are remediated with construction of bounded operators associated with (A_d, B_d, C_d, D_d). The Cayley-Tustin transform maps the unbounded operators A, B and C of the continuous time system into the bounded operators in the discrete-time counterpart, which brings technical advantages, since the generic properties, such as stability, controllability and observability are the same for both representations. In addition, one can extend the formalism of the above section to the analysis of parametric variations on the solution of Eq.2.1. This indeed goes well with the notions of dynamic simulators, so called "time-steppers" in [66, 67, 68] used to perform fixed-point and path following computations.

2.2.1 Linear Hyperbolic Scalar System

In this section, we are interested in the construction of a discrete model for the convection dominated system, such as the plug flow reactor model [5]. In general, one can apply a spatial discretization and/or use method of characteristic to obtain an approximate linear model suitable for the controller design. However, here we consider the Cayley-Tustin approach by applying a transformation which completely captures the nature of linear infinite-dimensional systems dynamics and translates a 1st order hyperbolic PDE from a continuous to a discrete state space setting.

Let us consider the model of transport-reaction system given by Eq.2.1, which is the linear infinite-dimensional system model on the Hilbert space $L_2(0,1)$, with the spatial linear operator $A = -v\frac{\partial}{\partial\zeta} + \psi(\zeta)$ defined on its domain $D(A) = \{z \in L_2(0,1) | z \textit{ is absolutely continuous } \frac{dz}{d\zeta} \in L_2(0,1), z(0) = 0\}$. The output is taken as the state at the exit of the reactor, that is at $\zeta = L$, and it is obtained by the operator $C(f(\zeta)) = \int_0^L f(\zeta)\delta(\zeta - L)d\zeta = f(L)$ and we assume that the continuous model does not contain a feedthrough term, that is $D = 0$. The discretized hyperbolic PDE system is obtained by the Cayley-Tustin transformation presented in the previous section by Eq.2.4 where the operators A_d, B_d, C_d and D_d are calculated by Eq.2.5. From Remark 1, one can notice that the realization of the operators in Eq.2.5 depends on the resolvent $R(\delta, A)$ of the operator A.

The resolvent operator for the scalar hyperbolic system can be obtained by utilizing the Laplace transform. Finding a Laplace transform is one of essential ingredients of obtaining the Cayley-Tustin transform. Under the zero-input condition, the following hyperbolic PDE system arising from Eq.2.1 is considered:

$$\dot{z}(\zeta, t) = A(\zeta)z(\zeta, t), \quad z(\zeta, 0) = z_0 \tag{2.7}$$

The operator A arises as a model of tubular reactors with a linearized spatial reaction term (that is $\psi(\zeta)$), which models a large number of convection dominated transport processes.

The resolvent operator $R(s,A) = [sI - A]^{-1}$ of the operator $A(\zeta)$ is obtained by applying the Laplace transform and expressed as follows:

$$\begin{aligned} R(s,A)z(\zeta,0) &= [sI-A]^{-1}(\cdot) \\ &= \Big[\int_0^{\zeta} \frac{1}{v}(\cdot)e^{-\frac{1}{v}\int_0^{\eta}(\psi(\phi)-sI)d\phi}d\eta\Big]e^{\frac{1}{v}\int_0^{\zeta}(\psi(\phi)-sI)d\phi} \end{aligned} \tag{2.8}$$

Proof: One can directly obtain the above expression by taking the Laplace transform of Eq.2.7, and integrating the expression in space, which is given as $z(\zeta,s) = [sI-A]^{-1}z(\zeta,0) = R(s,A)z(\zeta,0)$.

$$\frac{\partial z(\zeta,s)}{\partial \zeta} = \frac{1}{v}(\psi(\zeta) - sI)z(\zeta,s) + \frac{1}{v}z(\zeta,0) \tag{2.9}$$

By solving the above ODE, one obtains:

$$z(\zeta,s) = z(0,s)e^{\frac{1}{v}\int_0^{\zeta}(\psi-sI)d\phi} + \Big[\int_0^{\zeta}\frac{1}{v}z(\eta,0)e^{-\frac{1}{v}\int_0^{\eta}(\psi-sI)d\phi}d\eta\Big]e^{\frac{1}{v}\int_0^{\zeta}(\psi-sI)d\phi} \tag{2.10}$$

With the boundary condition $z(0,s) = 0$, the resolvent operator of the operator A applied on the state $z(\zeta,0)$ can be expressed as:

$$\begin{aligned} R(s,A)z(\zeta,0) &= [sI-A]^{-1}z(\zeta,0) \\ &= \Big[\int_0^{\zeta}\frac{1}{v}z(\eta,0)e^{-\frac{1}{v}\int_0^{\eta}(\psi-sI)d\phi}d\eta\Big]e^{\frac{1}{v}\int_0^{\zeta}(\psi-sI)d\phi} \end{aligned} \tag{2.11}$$

With the system resolvent operator described in the previous section, one can directly obtain the discrete time operators in Eq.2.4. The convenient form to express the operator A_d is in the following form:

$$\begin{aligned} A_d(\cdot) &= [\delta - A]^{-1}[\delta + A](\cdot) \\ &= -(\cdot) + 2\delta\big[\int_0^{\zeta} \frac{1}{v}(\cdot) e^{-\frac{1}{v}\int_0^{\eta}(\psi-\delta)d\phi} d\eta\big] e^{\frac{1}{v}\int_0^{\zeta}(\psi-\delta)d\phi} \end{aligned} \tag{2.12}$$

One can easily obtain the derivation of the A_d operator as below:

$$\begin{aligned} & A_d z(\zeta, k-1) = [\delta - A]^{-1}[\delta + A] z(\zeta, k-1) \\ & = [\delta - A]^{-1}[-v\frac{\partial z(\zeta, k-1)}{\partial \zeta} + (\psi + \delta) z(\zeta, k-1)] \\ & = \Big[\int_0^{\zeta} \frac{1}{v}[-v\frac{\partial z(\eta, k-1)}{\partial \eta} + (\psi + \delta) z(\eta, k-1)] e^{-\frac{1}{v}\int_0^{\eta}(\psi-\delta)d\phi} d\eta\Big] e^{\frac{1}{v}\int_0^{\zeta}(\psi-\delta)d\phi} \\ & = \Big[\int_0^{\zeta} \frac{1}{v}[-v\frac{\partial z(\eta, k-1)}{\partial \eta}] e^{-\frac{1}{v}\int_0^{\eta}(\psi-\delta)d\phi} d\eta\Big] e^{\frac{1}{v}\int_0^{\zeta}(\psi-\delta)d\phi} \\ & + \Big[\int_0^{\zeta} \frac{1}{v}[(\psi + \delta) z(\eta, k-1)] e^{-\frac{1}{v}\int_0^{\eta}(\psi-\delta)d\phi} d\eta\Big] e^{\frac{1}{v}\int_0^{\zeta}(\psi-\delta)d\phi} \\ & = \Big[\int_0^{\zeta} -e^{-\frac{1}{v}\int_0^{\eta}(\psi-\delta)d\phi} dz(\eta, k-1)\Big] e^{\frac{1}{v}\int_0^{\zeta}(\psi-\delta)d\phi} \\ & + \Big[\int_0^{\zeta} \frac{1}{v}[(\psi + \delta) z(\eta, k-1)] e^{-\frac{1}{v}\int_0^{\eta}(\psi-\delta)d\phi} d\eta\Big] e^{\frac{1}{v}\int_0^{\zeta}(\psi-\delta)d\phi} \\ & = \Big[-e^{-\frac{1}{v}\int_0^{\eta}(\psi-\delta)d\phi} z(\eta, k-1)\Big|_0^{\zeta} - \int_0^{\zeta} -z(\eta, k-1) d[e^{-\frac{1}{v}\int_0^{\eta}(\psi-\delta)d\phi}]\Big] e^{\frac{1}{v}\int_0^{\zeta}(\psi-\delta)d\phi} \\ & + \Big[\int_0^{\zeta} \frac{1}{v}[(\psi + \delta) z(\eta, k-1)] e^{-\frac{1}{v}\int_0^{\eta}(\psi-\delta)d\phi} d\eta\Big] e^{\frac{1}{v}\int_0^{\zeta}(\psi-\delta)d\phi} \\ & = \Big[-e^{-\frac{1}{v}\int_0^{\zeta}(\psi-\delta)d\phi} z(\zeta, k-1) + z(0) - \int_0^{\zeta} \frac{1}{v}[(\psi - \delta) z(\eta, k-1)] e^{-\frac{1}{v}\int_0^{\eta}(\psi-\delta)d\phi} d\eta\Big] e^{\frac{1}{v}\int_0^{\zeta}(\psi-\delta)d\phi} \\ & + \Big[\int_0^{\zeta} \frac{1}{v}[(\psi + \delta) z(\eta, k-1)] e^{-\frac{1}{v}\int_0^{\eta}(\psi-\delta)d\phi} d\eta\Big] e^{\frac{1}{v}\int_0^{\zeta}(\psi-\delta)d\phi} \end{aligned} \tag{2.13}$$

$$= -z(\zeta, k-1) + 2\delta\Big[\Big[\int_0^{\zeta} \frac{1}{v} z(\eta, k-1) e^{-\frac{1}{v}\int_0^{\eta}(\psi-\delta)d\phi} d\eta\Big] e^{\frac{1}{v}\int_0^{\zeta}(\psi-\delta)d\phi}\Big]$$
$$= [-I + 2\delta[\delta - A]^{-1}] z(\zeta, k-1)$$

In the above derivation, one can extend the class of systems considered with having velocity as spatial function $v(\zeta)$, and accordingly all above expressions can be easily rewritten to account for it.

Similarly, one can directly obtain the expression for the discrete operator B_d. The operator B in a continuous system can represent point or boundary actuation, or it can represent in-domain actuation. Hence, for $B(\zeta)$ describing an in-domain operator $B(\zeta)$, one can obtain the expression of B_d in the following form:

$$\begin{aligned} B_d \quad &= \sqrt{2\delta}[\delta - A]^{-1} B(\zeta) \\ &= \sqrt{2\delta}\Big[\int_0^{\zeta} \frac{1}{v} B(\eta) e^{-\frac{1}{v}\int_0^{\eta}(\psi-\delta)d\phi} d\eta\Big] e^{\frac{1}{v}\int_0^{\zeta}(\psi-\delta)d\phi} \end{aligned} \tag{2.14}$$

In the case of a point or boundary realized actuation, the input operator B is given as $B(\zeta) = \delta(\zeta - \zeta_0)$, with ζ_0 being a point position where the actuation is applied. Therefore, one obtains the expression of B_d in the following form:

$$B_d = \begin{cases} 0, & 0 \le \zeta < \zeta_0 \\ \frac{\sqrt{2\delta}}{v}, & \zeta_0 \le \zeta \le L \end{cases}$$

For example for boundary actuation at $\zeta_0 = 0$, one obtains $B_d = \frac{\sqrt{2\delta}}{v} e^{\frac{1}{v}\int_0^{\zeta}(\psi-\delta)d\phi}$. For boundary actuation at $\zeta_0 = L$, one obtains $B_d = \frac{\sqrt{2\delta}}{v}\delta(\zeta - L)$.

Similarly, one can directly obtain the expression of discrete operators C_d and D_d. In particular, C can be point and/or boundary observation, or the output can be

considered in some region. When C is a boundary operator at $\zeta = L$, the operator C_d is obtained as follows:

$$\begin{aligned} C_d(\cdot) &= \sqrt{2\delta} C[\delta - A]^{-1}(\cdot) \\ &= \sqrt{2\delta}\Big[\int_0^L \frac{1}{v}(\cdot) e^{-\frac{1}{v}\int_0^\eta (\psi-\delta)d\phi} d\eta\Big] e^{\frac{1}{v}\int_0^L (\psi-\delta)d\phi} \end{aligned} \tag{2.15}$$

The operator D_d is a straight forward representation of the transfer function of the system parameterized by the parameter δ.

$$\begin{aligned} D_d &= C[\delta - A_{-1}]^{-1} B + D \\ &= \Big[\int_0^L \frac{1}{v} B e^{-\frac{1}{v}\int_0^\eta (\psi-\delta)d\phi} d\eta\Big] e^{\frac{1}{v}\int_0^L (\psi-\delta)d\phi} \end{aligned} \tag{2.16}$$

One can notice that in the discrete state space representation, the operators (A_d, B_d, C_d, D_d) are parameterized by the term δ which contains the discretization time so that one can relate known spatial and temporal discretization numerical techniques and numerical outcomes associated with them with the Cayley-Tustin discrete state space realization. In particular, it is known that for the first order hyperbolic system, temporal and spatial discretization of the simple $\frac{\partial z}{\partial t} + c\frac{\partial z}{\partial \zeta} = 0$ transport problem leads to Courant-Friedrichs-Lewy stability conditions. Namely, for many explicit finite difference schemes for hyperbolic systems in one space dimension, the claim is that for numerical stability it is necessary that $|c\frac{h}{\triangle\zeta}| \leq 1$. In other words, this condition can be interpreted as $\frac{\triangle\zeta}{h} \geq |c|$ that the numerical speed of propagation must be greater than or equal to the speed of initial data propagation. Hence, if the numerical scheme cannot propagate the initial data at least as fast as the solution of the differential equation, then the solution of the scheme cannot converge to the solution of the partial differential equation. Since the numerical scheme given by Eqs.2.4-2.5 is

unconditionally stable, the numerical integration accuracy in Eqs.2.12-2.14-2.15-2.16 and the choice of δ needs to be selected adequately. In general, one must carefully choose a reasonable value of $\frac{h}{\triangle\zeta}$ in order to obtain an accurate enough solution, since the accuracy of the solution can be heavily impacted with arbitrary $\frac{h}{\triangle\zeta}$.

Remark 2: In the case of the application of spatial discretization methods and subsequent temporal discretization which is not a Cayley-Tustin, if there is no feed forward operator D, the discretized approximation system will generate realization $(\tilde{A}_d, \tilde{B}_d, \tilde{C}_d, 0)$, without a feedthrough term. Contrary to this case, the Cayley-Tustin discretization generates D_d term as a direct transfer function parameterized δ term.

Adjoint Operator

In the subsequent section, the construction of the model predictive controller requires finding adjoint operators of (A_d, B_d, C_d, D_d), that is $(A_d^*, B_d^*, C_d^*, D_d^*)$. Therefore, the adjoint operator A_d^* of the generator A_d is defined by the equation:

$$< \Phi, Ad^*\Psi^* >=< Ad\Phi, \Psi^* > \tag{2.17}$$

where Φ and Ψ^* are arbitrary spatial functions on the domain $L_2(0,1)$.

The expression of the adjoint operator A_d^* of the discrete operator A_d is given in the following form:

$$A_d^*(\cdot) = -(\cdot) + 2\delta\Big[\int_\zeta^L \frac{1}{v}(\cdot)e^{\frac{1}{v}\int_0^\eta(\psi-\delta)d\phi}d\eta\Big]e^{-\frac{1}{v}\int_0^\zeta(\psi-\delta)d\phi} \tag{2.18}$$

One can construct A_d^* of a hyperbolic PDE system as follows:

$$< A_d\Phi, \Psi^* >= \int_0^L \Big[-\Phi(\zeta) + 2\delta\Big[\int_0^\zeta \frac{1}{v}\Phi(\eta)e^{-\frac{1}{v}\int_0^\eta(\psi-\delta)d\phi}d\eta\Big]e^{\frac{1}{v}\int_0^\zeta(\psi-\delta)d\phi}\Big]\Psi^*(\zeta)d\zeta$$

$$
\begin{aligned}
&= \int_0^L -\Phi(\zeta)\Psi^*(\zeta)d\zeta + 2\delta \int_0^L \Big(\int_0^\zeta \frac{1}{v}\Phi(\eta)e^{-\frac{1}{v}\int_0^\eta(\psi-\delta)d\phi}d\eta\Big)\Psi^*(\zeta)e^{\frac{1}{v}\int_0^\zeta(\psi-\delta)d\phi}d\zeta \\
&= \int_0^L -\Phi(\zeta)\Psi^*(\zeta)d\zeta + 2\delta \int_0^L \int_0^\zeta \frac{1}{v}[\Phi(\eta)e^{-\frac{1}{v}\int_0^\eta(\psi-\delta)d\phi}][\Psi^*(\zeta)e^{\frac{1}{v}\int_0^\zeta(\psi-\delta)d\phi}]d\eta d\zeta \\
&= \int_0^L -\Phi(\zeta)\Psi^*(\zeta)d\zeta + 2\delta \int_0^L \int_\eta^L \frac{1}{v}[\Phi(\eta)e^{-\frac{1}{v}\int_0^\eta(\psi-\delta)d\phi}][\Psi^*(\zeta)e^{\frac{1}{v}\int_0^\zeta(\psi-\delta)d\phi}]d\zeta d\eta \\
&= \int_0^L -\Phi(\zeta)\Psi^*(\zeta)d\zeta + 2\delta \int_0^L \Big(\int_\eta^L \frac{1}{v}\Psi^*(\zeta)e^{\frac{1}{v}\int_0^\zeta(\psi-\delta)d\phi}d\zeta\Big)\Phi(\eta)e^{-\frac{1}{v}\int_0^\eta(\psi-\delta)d\phi}d\eta
\end{aligned}
$$

Interchanging the ζ and η, one obtains:

$$
\begin{aligned}
&< A_d\Phi, \Psi^* > \\
&= \int_0^L -\Phi(\zeta)\Psi^*(\zeta)d\zeta + 2\delta \int_0^L \Big(\int_\zeta^L \frac{1}{v}\Psi^*(\eta)e^{\frac{1}{v}\int_0^\eta(\psi-\delta)d\phi}d\eta\Big)\Phi(\zeta)e^{-\frac{1}{v}\int_0^\zeta(\psi-\delta)d\phi}d\zeta \\
&= \int_0^L \Big[-\Psi^*(\zeta) + 2\delta\big[\int_\zeta^L \frac{1}{v}\Psi^*(\eta)e^{\frac{1}{v}\int_0^\eta(\psi-\delta)d\phi}d\eta\big]e^{-\frac{1}{v}\int_0^\zeta(\psi-\delta)d\phi}\Big]\Phi(\zeta)d\zeta \\
&=< \Phi, A_d^*\Psi^* >
\end{aligned}
$$

Similarly, one can obtain the expression of the adjoint operator C_d^* of the discrete operator C_d as below:

$$
C_d^*(\cdot) = \sqrt{2\delta}\big[\int_0^L \frac{1}{v}(\cdot)d\eta\big]e^{-\frac{1}{v}\int_0^\zeta(\psi-\delta)d\phi}e^{\frac{1}{v}\int_0^L(\psi-\delta)d\phi} \tag{2.19}
$$

The construction of C_d^* for a hyperbolic PDE system is as follows:

$$
\begin{aligned}
&< C_d\Phi, \Psi^* >= \int_0^L \Big[\sqrt{2\delta}\big[\int_0^L \frac{1}{v}\Phi(\eta)e^{-\frac{1}{v}\int_0^\eta(\psi-\delta)d\phi}d\eta\big]e^{\frac{1}{v}\int_0^L(\psi-\delta)d\phi}\Big]\Psi^*(\zeta)d\zeta \\
&= \sqrt{2\delta}e^{\frac{1}{v}\int_0^L(\psi-\delta)d\phi}\int_0^L \int_0^L \frac{1}{v}\Phi(\eta)e^{-\frac{1}{v}\int_0^\eta(\psi-\delta)d\phi}\Psi^*(\zeta)d\eta d\zeta \\
&= \sqrt{2\delta}e^{\frac{1}{v}\int_0^L(\psi-\delta)d\phi}\int_0^L \int_0^L \frac{1}{v}\Phi(\eta)e^{-\frac{1}{v}\int_0^\eta(\psi-\delta)d\phi}\Psi^*(\zeta)d\zeta d\eta
\end{aligned}
$$

$$= \sqrt{2\delta} e^{\frac{1}{v}\int_0^L (\psi-\delta)d\phi} \int_0^L \big[\int_0^L \frac{1}{v}\Psi^*(\zeta)d\zeta \big] \Phi(\eta) e^{-\frac{1}{v}\int_0^\eta (\psi-\delta)d\phi} d\eta$$
$$= \sqrt{2\delta} e^{\frac{1}{v}\int_0^L (\psi-\delta)d\phi} \int_0^L \big[\int_0^L \frac{1}{v}\Psi^*(\eta)d\eta \big] \Phi(\zeta) e^{-\frac{1}{v}\int_0^\zeta (\psi-\delta)d\phi} d\zeta$$
$$= \int_0^L \Big[\sqrt{2\delta} \big[\int_0^L \frac{1}{v}\Psi^*(\eta)d\eta \big] e^{-\frac{1}{v}\int_0^\zeta (\psi-\delta)d\phi} e^{\frac{1}{v}\int_0^L (\psi-\delta)d\phi} \Big] \Phi(\zeta) d\zeta$$
$$=< \Phi, C_d^* \Psi^* >$$

The adjoint operators B_d^* and D_d^* are self-adjoint: $B_d^* = B_d$ and $D_d^* = D_d$.

2.2.2 Linear Parabolic System

In this section, we apply the Cayley-Tustin time discretization to the diffusion dominated model of an axial dispersion reactor described by the parabolic PDE with the Dirichlet, Neumann or Robin boundary condition [5].

Let us consider a diffusion dominated transport-reaction system which leads to the linear infinite-dimensional system model given by Eq.2.1 with the operator A defined on Hilbert space $H = L_2(0,1)$. In particular,

$$\begin{aligned} \dot{z}(\zeta,t) &= Az(\zeta,t) + Bu(t),\ z(\zeta,0) = z_0 \\ y(t) &= Cz(\zeta,t) + Du(t) \end{aligned} \tag{2.20}$$

$A(\zeta) = \frac{\partial^2}{\partial\zeta^2} + \psi I$ is the linear operator defined on its domain $D(A) = \{z \in L_2(0,1) |$ *z is absolutely continuous*, $\frac{dz}{d\zeta} \in L_2(0,1), \frac{d^2z}{d\zeta^2} \in L_2(0,1), \psi$ *is constant*, *Dirichlet boundary conditions* : $z(0) = 0 = z(1)$, *Neumann boundary conditions* : $\frac{dz(0)}{d\zeta} = 0 = \frac{dz(1)}{d\zeta}$, *Danckwerts boundary conditions* : $\frac{dz(0)}{d\zeta} = Pez(0), \frac{dz(1)}{d\zeta} = 0\}$. The output is the state of the PDE at a point within the domain, for example at $\zeta = \zeta_0$ and is obtained by the operator $C(f(\zeta)) = \int_0^L f(\zeta)\delta(\zeta - \zeta_0)d\zeta = f(\zeta_0)$ and $D = 0$.

The discretization of a parabolic PDE system described in Eq.2.4 is obtained by the Cayley-Tustin transformation presented in the previous section with the operators A_d, B_d, C_d and D_d calculated by Eq.2.5. In order to realize discrete system representation for parabolic PDE, let us consider the parabolic PDE system in the following form:

$$\dot{z}(\zeta, t) = A(\zeta) z(\zeta, t) \tag{2.21}$$

The realization of the discrete operator A_d is constructed by substitution of the s parameter with the δ in the resolvent operator in the expression for A_d in Eq.2.5. One needs to address if any constraints are arising as a result of freely choosing any discretization time $\delta = \frac{2}{h}$. In particular, only one constraint is that the discretization time does not coincide with the eigenvalues of the operator A, the $\delta \notin \sigma(A)$, where $\sigma(A)$ is the point spectrum of the spatial operator A.

Therefore, one may easily apply Laplace transform to the parabolic system described in Eq.2.21:

$$sz(\zeta, s) - z(\zeta, 0) = \frac{\partial^2 z(\zeta, s)}{\partial \zeta^2} + \psi z(\zeta, s) \tag{2.22}$$

which leads to:

$$\frac{\partial^2 z(\zeta, s)}{\partial \zeta^2} = (sI - \psi) z(\zeta, s) - z(\zeta, 0) \tag{2.23}$$

Further, one can obtain the following system:

$$\frac{\partial}{\partial\zeta}\begin{bmatrix} z(\zeta,s) \\ \frac{\partial z(\zeta,s)}{\partial\zeta} \end{bmatrix} = \begin{bmatrix} 0 & 1 \\ s-\psi & 0 \end{bmatrix}\begin{bmatrix} z(\zeta,s) \\ \frac{\partial z(\zeta,s)}{\partial\zeta} \end{bmatrix} + \begin{bmatrix} 0 \\ -z(\zeta,0) \end{bmatrix} \tag{2.24}$$

which leads to $\bar{Z}(\zeta,s) = \begin{bmatrix} z(\zeta,s) \\ \frac{\partial z(\zeta,s)}{\partial\zeta} \end{bmatrix}$, $\bar{A} = \begin{bmatrix} 0 & 1 \\ s-\psi & 0 \end{bmatrix}$ and $\bar{B} = \begin{bmatrix} 0 \\ -z(\zeta,0) \end{bmatrix}$:

$$\frac{\partial\bar{Z}(\zeta,s)}{\partial\zeta} = \bar{A}\bar{Z}(\zeta,s) + \bar{B} \tag{2.25}$$

We can obtain the solution of the above ODE:

$$\bar{Z}(\zeta,s) = e^{\bar{A}\zeta}\bar{Z}(0,s) + \int_0^\zeta e^{\bar{A}(\zeta-\eta)}\bar{B}d\eta \tag{2.26}$$

Since $\bar{A}$ is a constant matrix, one can calculate $e^{\bar{A}\bar{t}}$ with the Laplace inverse transform $e^{\bar{A}\bar{t}} = \mathcal{L}^{-1}\{[\bar{s}I - \bar{A}]^{-1}\}$:

$$e^{\bar{A}\bar{t}} = \begin{bmatrix} cosh(\sqrt{s-\psi}\bar{t}) & \frac{1}{\sqrt{s-\psi}}sinh(\sqrt{s-\psi}\bar{t}) \\ \sqrt{s-\psi}sinh(\sqrt{s-\psi}\bar{t}) & cosh(\sqrt{s-\psi}\bar{t}) \end{bmatrix} \tag{2.27}$$

which leads to the solution of Eq.2.26 as:

$$\begin{bmatrix} z(\zeta,s) \\ \frac{\partial z(\zeta,s)}{\partial\zeta} \end{bmatrix} = \begin{bmatrix} cosh(\sqrt{s-\psi}\zeta) & \frac{1}{\sqrt{s-\psi}}sinh(\sqrt{s-\psi}\zeta) \\ \sqrt{s-\psi}sinh(\sqrt{s-\psi}\zeta) & cosh(\sqrt{s-\psi}\zeta) \end{bmatrix}\begin{bmatrix} z(0,s) \\ \frac{\partial z(0,s)}{\partial\zeta} \end{bmatrix} + \int_0^\zeta \begin{bmatrix} -\frac{1}{\sqrt{s-\psi}}z(\eta,0)sinh[\sqrt{s-\psi}(\zeta-\eta)] \\ -z(\eta,0)cosh[\sqrt{s-\psi}(\zeta-\eta)] \end{bmatrix} d\eta \tag{2.28}$$

Finally, we obtains:

$$z(\zeta,s) = \quad cosh(\sqrt{s-\psi}\zeta)z(0,s) + \frac{1}{\sqrt{s-\psi}}sinh(\sqrt{s-\psi}\zeta)\frac{\partial z(0,s)}{\partial \zeta} \quad (2.29)$$
$$-\int_0^\zeta \frac{1}{\sqrt{s-\psi}}z(\eta,0)sinh[\sqrt{s-\psi}(\zeta-\eta)]d\eta$$

The above expression is obtained as a solution to $z(\zeta,s) = [sI-A]^{-1}z(\zeta,0)$, by the application of the Laplace transform to the parabolic system described in Eq.2.21 for the case when $s-\psi > 0$. However, it can be demonstrated that the similar and well posed expression will be obtained if $s-\psi < 0$. Assuming that, $s-\psi < 0$, one obtains $\sqrt{s-\psi} = i\sqrt{\psi-s}$, here $i^2 = -1$. We can obtain $sinh(\sqrt{s-\psi}\zeta) = sinh(i\sqrt{\psi-s}\zeta) = isin(\sqrt{\psi-s}\zeta)$ and $cosh(\sqrt{s-\psi}\zeta) = cosh(i\sqrt{\psi-s}\zeta) = cos(\sqrt{\psi-s}\zeta)$. Then, the state becomes:

$$z(\zeta,s) = \quad cos(\sqrt{\psi-s}\zeta)z(0,s) + \frac{1}{\sqrt{\psi-s}}sin(\sqrt{\psi-s}\zeta)\frac{\partial z(0,s)}{\partial \zeta} \quad (2.30)$$
$$-\int_0^\zeta \frac{1}{\sqrt{\psi-s}}z(\eta,0)sin[\sqrt{\psi-s}(\zeta-\eta)]d\eta$$

In the following section, without loss of generality we consider the case when the following $s-\psi > 0$ holds. As expected in the case of parabolic PDEs, different boundary conditions will lead to different expressions for the resolvent of operator A and associated cogenerator A_d.

Dirichlet Boundary Conditions

When Dirichlet boundary conditions are applied, $z(0,s) = 0 = z(1,s)$, one can utilize Eq.2.28 -2.29, and $\frac{\partial z(0,s)}{\partial \zeta} = \frac{1}{sinh(\sqrt{s-\psi})}\int_0^1 z(\eta,0)sinh[\sqrt{s-\psi}(1-\eta)]d\eta$. The resolvent

of the operator A is given as:

$$\begin{aligned} R(s,A)z(\zeta,0) = \quad & [sI-A]^{-1}z(\zeta,0) \\ = \quad & \frac{1}{\sqrt{s-\psi}}\frac{sinh(\sqrt{s-\psi}\zeta)}{sinh(\sqrt{s-\psi})}\int_0^1 z(\eta,0)sinh[\sqrt{s-\psi}(1-\eta)]d\eta \\ & -\int_0^\zeta \frac{1}{\sqrt{s-\psi}}z(\eta,0)sinh[\sqrt{s-\psi}(\zeta-\eta)]d\eta \end{aligned} \tag{2.31}$$

Neumann Boundary Conditions

When Neumann boundary conditions are applied, $\frac{dz(0,s)}{d\zeta} = 0 = \frac{dz(1,s)}{d\zeta}$ and from Eq.2.28 -2.29, one obtains $z(0,s) = \frac{1}{\sqrt{s-\psi}}\frac{1}{sinh(\sqrt{s-\psi})}\int_0^1 z(\eta,0)cosh[\sqrt{s-\psi}(1-\eta)]d\eta$. The resolvent of operator A is:

$$\begin{aligned} R(s,A)z(\zeta,0) = \quad & [sI-A]^{-1}z(\zeta,0) \\ = \quad & \frac{1}{\sqrt{s-\psi}}\frac{cosh(\sqrt{s-\psi}\zeta)}{sinh(\sqrt{s-\psi})}\int_0^1 z(\eta,0)cosh[\sqrt{s-\psi}(1-\eta)]d\eta \\ & -\int_0^\zeta \frac{1}{\sqrt{s-\psi}}z(\eta,0)sinh[\sqrt{s-\psi}(\zeta-\eta)]d\eta \end{aligned} \tag{2.32}$$

Danckwerts Boundary Conditions

Another important set of boundary conditions is arising from the description of an axial dispersion reactor [5]: $z'(0,t) = P_e z(0,t)$, $z'(1,t) = 0$, with P_e being a Peclet number. One obtains:

$$\begin{aligned} \frac{\partial z(1,s)}{\partial\zeta} \quad & = \sqrt{s-\psi}sinh(\sqrt{s-\psi})z(0,s) + cosh(\sqrt{s-\psi})\frac{\partial z(0,s)}{\partial\zeta} \\ & -\int_0^1 z(\eta,0)cosh[\sqrt{s-\psi}(1-\eta)]d\eta = 0 \end{aligned} \tag{2.33}$$

so that $z'(0,s) = P_e z(0,s)$, we obtain:

$$z(0,s) = \frac{\int_0^1 z(\eta,0)cosh[\sqrt{s-\psi}(1-\eta)]d\eta}{\sqrt{s-\psi}sinh(\sqrt{s-\psi}) + P_e cosh(\sqrt{s-\psi})} \tag{2.34}$$
$$z'(0,s) = \frac{p_e\int_0^1 z(\eta,0)cosh[\sqrt{s-\psi}(1-\eta)]d\eta}{\sqrt{s-\psi}sinh(\sqrt{s-\psi}) + P_e cosh(\sqrt{s-\psi})}$$

finally resolvent can be easily defined.

Discrete Time Operators and Its Adjoint Operators

Dirichlet Boundary Condition

With the system resolvent operator described in Eq.2.31, one can directly obtain the discrete time operators A_d, B_d, C_d and D_d of a parabolic system presented in Eq.2.5:

$$\begin{aligned} A_d(\cdot) = \quad & [-I + 2\delta[\delta - A]^{-1}](\cdot) \\ = \quad & -(\cdot) + 2\delta\Big[\frac{1}{\sqrt{\delta-\psi}}\frac{sinh(\sqrt{\delta-\psi}\zeta)}{sinh(\sqrt{\delta-\psi})}\int_0^1 (\cdot)sinh[\sqrt{\delta-\psi}(1-\eta)]d\eta \\ & -\int_0^\zeta \frac{1}{\sqrt{\delta-\psi}}(\cdot)sinh[\sqrt{\delta-\psi}(\zeta-\eta)]d\eta\Big] \end{aligned} \tag{2.35}$$

$$\begin{aligned} B_d = \quad & \sqrt{2\delta}[\delta - A_{-1}]^{-1}B \\ = \quad & \sqrt{2\delta}\Big[\frac{1}{\sqrt{\delta-\psi}}\frac{sinh(\sqrt{\delta-\psi}\zeta)}{sinh(\sqrt{\delta-\psi})}\int_0^1 Bsinh[\sqrt{\delta-\psi}(1-\eta)]d\eta \\ & -\int_0^\zeta \frac{1}{\sqrt{\delta-\psi}}Bsinh[\sqrt{\delta-\psi}(\zeta-\eta)]d\eta\Big] \end{aligned} \tag{2.36}$$

$$C_d(\cdot) = \quad \sqrt{2\delta}C[\delta - A]^{-1}(\cdot) \tag{2.37}$$

$$= \quad \sqrt{2\delta}\Big[\frac{1}{\sqrt{\delta-\psi}}\frac{sinh(\sqrt{\delta-\psi}\zeta_0)}{sinh(\sqrt{\delta-\psi})}\int_0^1(\cdot)sinh[\sqrt{\delta-\psi}(1-\eta)]d\eta$$
$$-\int_0^{\zeta_0}\frac{1}{\sqrt{\delta-\psi}}(\cdot)sinh[\sqrt{\delta-\psi}(\zeta_0-\eta)]d\eta\Big]$$

$$D_d = \quad C[\delta - A_{-1}]^{-1}B + D \tag{2.38}$$
$$= \quad \frac{1}{\sqrt{\delta-\psi}}\frac{sinh(\sqrt{\delta-\psi}\zeta_0)}{sinh(\sqrt{\delta-\psi})}\int_0^1 Bsinh[\sqrt{\delta-\psi}(1-\eta)]d\eta$$
$$-\int_0^{\zeta_0}\frac{1}{\sqrt{\delta-\psi}}Bsinh[\sqrt{\delta-\psi}(\zeta_0-\eta)]d\eta$$

The expression of an adjoint operator A_d^* of a discrete operator A_d is in the following form:

$$A_d^*(\cdot) = \quad -(\cdot) + 2\delta\Big[\frac{1}{\sqrt{\delta-\psi}}\frac{sinh[\sqrt{\delta-\psi}(L-\zeta)]}{sinh(\sqrt{\delta-\psi})}\int_0^1(\cdot)sinh(\sqrt{\delta-\psi}\eta)d\eta$$
$$-\int_\zeta^1\frac{1}{\sqrt{\delta-\psi}}(\cdot)sinh[\sqrt{\delta-\psi}(\eta-\zeta)]d\eta\Big] \tag{2.39}$$

One can obtain the construction of A_d^* for a parabolic PDE system with the Dirichlet boundary conditions as follows:

$$< A_d\Phi, \Psi^* >= \int_0^L\Big[-\Phi(\zeta) + 2\delta\Big(\frac{1}{\sqrt{\delta-\psi}}\frac{sinh(\sqrt{\delta-\psi}\zeta)}{sinh(\sqrt{\delta-\psi}L)}\int_0^L\Phi(\eta)sinh[\sqrt{\delta-\psi}(L-\eta)]d\eta$$
$$-\int_0^\zeta\frac{1}{\sqrt{\delta-\psi}}\Phi(\eta)sinh[\sqrt{\delta-\psi}(\zeta-\eta)]d\eta\Big)\Big]\Psi^*(\zeta)d\zeta$$
$$= \int_0^L -\Phi(\zeta)\Psi^*(\zeta)d\zeta + 2\delta\int_0^L\int_0^L\frac{1}{\sqrt{\delta-\psi}}\frac{sinh(\sqrt{\delta-\psi}\zeta)}{sinh(\sqrt{\delta-\psi}L)}\Phi(\eta)\Psi^*(\zeta)sinh[\sqrt{\delta-\psi}(L-\eta)]d\eta d\zeta$$
$$-2\delta\int_0^L\int_0^\zeta\frac{1}{\sqrt{\delta-\psi}}\Phi(\eta)\Psi^*(\zeta)sinh[\sqrt{\delta-\psi}(\zeta-\eta)]d\eta d\zeta$$
$$= \int_0^L -\Phi(\zeta)\Psi^*(\zeta)d\zeta + 2\delta\int_0^L\int_0^L\frac{1}{\sqrt{\delta-\psi}}\frac{sinh(\sqrt{\delta-\psi}\zeta)}{sinh(\sqrt{\delta-\psi}L)}\Phi(\eta)\Psi^*(\zeta)sinh[\sqrt{\delta-\psi}(L-\eta)]d\zeta d\eta$$

$$-2\delta \int_0^L \int_\eta^L \frac{1}{\sqrt{\delta-\psi}} \Phi(\eta)\Psi^*(\zeta) sinh[\sqrt{\delta-\psi}(\zeta-\eta)] d\zeta d\eta$$

Interchanging the ζ and η leads to:

$$\begin{aligned}
&< A_d\Phi, \Psi^* > \\
&= \int_0^L -\Phi(\zeta)\Psi^*(\zeta)d\zeta + 2\delta \int_0^L \int_0^L \frac{1}{\sqrt{\delta-\psi}} \frac{sinh(\sqrt{\delta-\psi}\eta)}{sinh(\sqrt{\delta-\psi}L)} \Phi(\zeta)\Psi^*(\eta) sinh[\sqrt{\delta-\psi}(L-\zeta)] d\eta d\zeta \\
&-2\delta \int_0^L \int_\zeta^L \frac{1}{\sqrt{\delta-\psi}} \Phi(\zeta)\Psi^*(\eta) sinh[\sqrt{\delta-\psi}(\eta-\zeta)] d\eta d\zeta \\
&= \int_0^L \Big[-\Psi^*(\zeta) + 2\delta \Big(\frac{1}{\sqrt{\delta-\psi}} \frac{sinh[\sqrt{\delta-\psi}(L-\zeta)]}{sinh(\sqrt{\delta-\psi}L)} \int_0^L \Psi^*(\eta) sinh(\sqrt{\delta-\psi}\eta) d\eta \\
&- \int_\zeta^L \frac{1}{\sqrt{\delta-\psi}} \Psi^*(\eta) sinh[\sqrt{\delta-\psi}(\eta-\zeta)] d\eta \Big) \Big] \Phi(\zeta) d\zeta \\
&=< \Phi, A_d^*\Psi^* >
\end{aligned}$$

The adjoint operator B_d^* is self-adjoint: $B_d^* = B_d$.

For other boundary conditions, one can easily find discrete operators and adjoint cogenerators which take the similar form as the one calculated in the case of Dirichlet boundary conditions. When the boundary condition is a Neumann Boundary Condition, with the system resolvent operator described in Eq.2.32, one can directly obtain the discrete time operators A_d, B_d, C_d and D_d of the parabolic system:

$$\begin{aligned}
A_d(\cdot) \quad &= [-I + 2\delta[\delta - A]^{-1}](\cdot) \qquad (2.40) \\
&= -(\cdot) + 2\delta \Big[\frac{1}{\sqrt{\delta-\psi}} \frac{cosh(\sqrt{\delta-\psi}\zeta)}{sinh(\sqrt{\delta-\psi})} \int_0^1 (\cdot) cosh[\sqrt{\delta-\psi}(1-\eta)] d\eta \\
&- \int_0^\zeta \frac{1}{\sqrt{\delta-\psi}} (\cdot) sinh[\sqrt{\delta-\psi}(\zeta-\eta)] d\eta \Big]
\end{aligned}$$

$$B_d \quad = \sqrt{2\delta}[\delta - A_{-1}]^{-1} B \qquad (2.41)$$

$$= \sqrt{2\delta}\Big[\frac{1}{\sqrt{\delta-\psi}}\frac{cosh(\sqrt{\delta-\psi}\zeta)}{sinh(\sqrt{\delta-\psi})}\int_0^1 Bcosh[\sqrt{\delta-\psi}(1-\eta)]d\eta$$
$$-\int_0^\zeta \frac{1}{\sqrt{\delta-\psi}}Bsinh[\sqrt{\delta-\psi}(\zeta-\eta)]d\eta\Big]$$

$$C_d(\cdot) = \sqrt{2\delta}C[\delta - A]^{-1}(\cdot) \tag{2.42}$$
$$= \sqrt{2\delta}\Big[\frac{1}{\sqrt{\delta-\psi}}\frac{cosh(\sqrt{\delta-\psi}\zeta_0)}{sinh(\sqrt{\delta-\psi})}\int_0^1 (\cdot)cosh[\sqrt{\delta-\psi}(1-\eta)]d\eta$$
$$-\int_0^{\zeta_0} \frac{1}{\sqrt{\delta-\psi}}(\cdot)sinh[\sqrt{\delta-\psi}(\zeta_0-\eta)]d\eta\Big]$$

$$D_d = C[\delta - A_{-1}]^{-1}B + D \tag{2.43}$$
$$= \frac{1}{\sqrt{\delta-\psi}}\frac{cosh(\sqrt{\delta-\psi}\zeta_0)}{sinh(\sqrt{\delta-\psi})}\int_0^1 Bcosh[\sqrt{\delta-\psi}(1-\eta)]d\eta$$
$$-\int_0^{\zeta_0} \frac{1}{\sqrt{\delta-\psi}}Bsinh[\sqrt{\delta-\psi}(\zeta_0-\eta)]d\eta$$

The expression of an adjoint operator A_d^* of a discrete operator A_d is in the following form:

$$A_d^*(\cdot) = -(\cdot) + 2\delta\Big[\frac{1}{\sqrt{\delta-\psi}}\frac{cosh[\sqrt{\delta-\psi}(L-\zeta)]}{sinh(\sqrt{\delta-\psi})}\int_0^1 (\cdot)cosh(\sqrt{\delta-\psi}\eta)d\eta$$
$$-\int_\zeta^1 \frac{1}{\sqrt{\delta-\psi}}(\cdot)sinh[\sqrt{\delta-\psi}(\eta-\zeta)]d\eta\Big] \tag{2.44}$$

The adjoint operator B_d^* is self-adjoint: $B_d^* = B_d$.

2.3 Model Predictive Control for Linear PDE

The linear discrete-time model dynamics developed in Eq.2.4 is utilized in the formulation of the model predictive control for linear transport-reaction systems. The regulator is based on the similar formulation emerging from the finite dimensional systems theory. In particular, there are similarities among constrained optimal controller design formulations for finite and infinite dimensional systems. The important differences in the controller synthesis are associated with the issue how the stable and unstable infinite dimensional systems are treated and this will be discussed in detail in the context of linear transport-reaction model equations. Along the line of similarities, the well known formulation of the quadratic form optimization functional on the infinite horizon is used for both infinite and finite dimensional systems. That is, minimization of the following open-loop objective functional is given in the form of inner products. Here, at a given sampling time k, the objective function with constraints is given as:

$$\min_{u^N} \sum_{j=0}^{\infty} < y(\zeta, k+j|k), Qy(\zeta, k+j|k) > + < u(k+j+1|k), Ru(k+j+1|k) > \tag{2.45}$$

$$\begin{aligned} s.t. \quad z(\zeta, k+j|k) &= A_d z(\zeta, k+j-1|k) + B_d u(k+j|k) \\ y(\zeta, k+j|k) &= C_d z(\zeta, k+j-1|k) + D_d u(k+j|k) \\ u^{min} &\leq u(k+j|k) \leq u^{max} \\ y^{min} &\leq y(\zeta, k+j|k) \leq y^{max} \end{aligned}$$

where Q is a positive semidefinite spatial operator associated with the output (state of PDE) and R is a positive definite spatial operator. The $y(k+j|k)$ and $u(k+j+1|k)$ represent the output and input variables at the future time $k+j$ given the current time k. The vectors Y and U are given as follows:

$$Y = \left[\begin{array}{ccccc} y(\zeta, k+1|k) & y(\zeta, k+2|k) & y(\zeta, k+3|k) & \cdots & y(\zeta, k+N-1|k) \end{array} \right]^T$$
$$U = \left[\begin{array}{ccccc} u(k+1|k) & u(k+2|k) & u(k+3|k) & \cdots & u(k+N-1|k) \end{array} \right]^T$$

The infinite horizon open-loop objective function in Eq.2.45 can be cast as the finite horizon open-loop objective function with an assumption that the input is zero beyond the control horizon, that is $u(k+N|k) = 0$, and with inclusion of the terminal penalty term:

$$\begin{aligned} \min_{u^N} \quad J = \quad & \sum_{j=0}^{N-1} < y(\zeta, k+j|k), Qy(\zeta, k+j|k) > + < u(k+j+1|k), Ru(k+j+1|k) > \\ & + < z(\zeta, k+N-1|k), \bar{Q}z(\zeta, k+N-1|k) > \end{aligned} \tag{2.46}$$

Without the loss of generality and with the assumption of observability, the output terminal penalty term is replaced with the corresponding state penalty operator term. The issue of how to determine the terminal state penalty term, the operator $\bar{Q}$, depends on the nature of the underlying transport-reaction linear model (that is a parabolic or a hyperbolic PDE system), and whether the system is a stable or unstable one. In general and in similar way as it is done for stable finite dimensional systems, the spatial operator $\bar{Q}$ for the stable PDE model is defined as the infinite sum $\bar{Q} = \sum_{i=0}^{\infty} A_d^{*i} C_d^* Q C_d A_d^i$. Therefore, the operator $\bar{Q}$ can be calculated from the

solution of the following operator discrete Lyapunov function:

$$A_d^* \bar{Q} A_d - \bar{Q} = -C_d^* Q C_d \tag{2.47}$$

The straightforward algebraic manipulation of the objective function presented in Eq.2.46 results in the following finite dimensional quadratic optimization problem:

$$\begin{aligned} \min_U \quad J = \quad & U^T < I, H > U + 2U^T < I, Pz(\zeta, k|k) > \\ & + < z(\zeta, k|k), \bar{Q} z(\zeta, k|k) > + < y(\zeta, k|k), Q y(\zeta, k|k) > \end{aligned} \tag{2.48}$$

where H and P are computed as below:

$$H = \begin{bmatrix} D_d^* Q D_d + B_d^* \bar{Q} B_d + R & B_d^* C_d^* Q D_d + B_d^* A_d^* \bar{Q} B_d & \cdots & B_d^* A_d^{*N-3} C_d^* Q D_d + B_d^* A_d^{*N-2} \bar{Q} B_d \\ D_d^* Q C_d B_d + B_d^* \bar{Q} A_d B_d & D_d^* Q D_d + B_d^* \bar{Q} B_d + R & \cdots & B_d^* A_d^{*N-4} C_d^* Q D_d + B_d^* A_d^{*N-3} \bar{Q} B_d \\ \vdots & \vdots & \ddots & \vdots \\ D_d^* Q C_d A_d^{N-3} B_d + B_d^* \bar{Q} A_d^{N-2} B_d & D_d^* Q C_d A_d^{N-4} B_d + B_d^* \bar{Q} A_d^{N-3} B_d & \cdots & D_d^* Q D_d + B_d^* \bar{Q} B_d + R \end{bmatrix}$$

$$P = \begin{bmatrix} D_d^* Q C_d + B_d^* \bar{Q} A_d \\ D_d^* Q C_d A_d + B_d^* \bar{Q} A_d^2 \\ \vdots \\ D_d^* Q C_d A_d^{N-2} + B_d^* \bar{Q} A_d^{N-1} \end{bmatrix}$$

The objective function given in Eq.2.48 is subjected to the following constraints:

$$\begin{aligned} & U^{min} \leq U \leq U^{max} \\ & Y^{min} \leq SU + Tz(\zeta, k|k) \leq Y^{max} \end{aligned} \tag{2.49}$$

One obtains:

$$\begin{bmatrix} I \\ -I \\ S \\ -S \end{bmatrix} U \leq \begin{bmatrix} U^{max} \\ -U^{min} \\ Y^{max} - Tz(\zeta, k|k) \\ -Y^{min} + Tz(\zeta, k|k) \end{bmatrix}$$

where

$$S = \begin{bmatrix} D_d & 0 & 0 & \cdots & 0 \\ C_d B_d & D_d & 0 & \cdots & 0 \\ C_d A_d B_d & C_d B_d & D_d & \cdots & 0 \\ \vdots & \vdots & \vdots & \ddots & \vdots \\ C_d A_d^{N-3} B_d & C_d A_d^{N-4} B_d & C_d A_d^{N-5} B_d & \cdots & D_d \end{bmatrix} \quad T = \begin{bmatrix} C_d \\ C_d A_d \\ C_d A_d^2 \\ \vdots \\ C_d A_d^{N-2} \end{bmatrix}$$

In the above case, the constraint is at the output which is taken as the state at $\zeta = L$. One can also have the constraint at any point within domain at $\zeta = \zeta_0$. As a result, the matrix S and T will change by using different discrete operators $\bar{C}_d$ and $\bar{D}_d$.

A standard formulation of the quadratic programming problem in Eq.2.48 with constraints leads to the finite dimensional quadratic programming problem with linear constraints that can be easily evaluated. This leads to the well known formulation of the model predictive controller design emerging from the finite dimensional theory, that if the system is optimizable then the system is stabilizable with satisfaction of input and state constraints, which is guaranteed under no disturbance conditions.

Remark 3: When the regulator is based on the state, the minimization of the

following open-loop objective function is considered:

$$\min_{u^N} \quad J = \sum_{j=0}^{N-1} < z(\zeta, k+j|k), Qz(\zeta, k+j|k) > + < u(k+j+1|k), Ru(k+j+1|k) > + < z(\zeta, k+N-1|k), \bar{Q}z(\zeta, k+N-1|k) > \tag{2.50}$$

the terminal state penalty operator becomes $\bar{Q} = \sum_{i=0}^{\infty} A_d^{*i} Q A_d^i$ and can be calculated from the solution of the following discrete Lyapunov function:

$$A_d^* \bar{Q} A_d - \bar{Q} = -Q \tag{2.51}$$

The operators H, P, S and T are given as follows:

$$H = \begin{bmatrix} B_d^*\bar{Q}B_d + R & B_d^*A_d^*\bar{Q}B_d & B_d^*A_d^{*2}\bar{Q}B_d & \cdots & B_d^*A_d^{*N-1}\bar{Q}B_d \\ B_d^*\bar{Q}A_dB_d & B_d^*\bar{Q}B_d + R & B_d^*A_d^*\bar{Q}B_d & \cdots & B_d^*A_d^{*N-2}\bar{Q}B_d \\ \vdots & \vdots & \vdots & \ddots & \vdots \\ B_d^*\bar{Q}A_d^{N-1}B_d & B_d^*\bar{Q}A_d^{N-2}B_d & B_d^*\bar{Q}A_d^{N-3}B_d & \cdots & B_d^*\bar{Q}B_d + R \end{bmatrix}$$

$$P = \begin{bmatrix} B_d^*\bar{Q}A_d \\ B_d^*\bar{Q}A_d^2 \\ \vdots \\ B_d^*\bar{Q}A_d^N \end{bmatrix}, \quad S = \begin{bmatrix} B_d & 0 & \cdots & 0 \\ A_dB_d & B_d & \cdots & 0 \\ \vdots & \vdots & \ddots & \vdots \\ A_d^{N-1}B_d & A_d^{N-2}B_d & \cdots & B_d \end{bmatrix}, \quad T = \begin{bmatrix} A_d \\ A_d^2 \\ \vdots \\ A_d^N \end{bmatrix}$$

2.3.1 Model predictive control for hyperbolic PDE

Discrete Lyapunov Function

The realization of the model predictive controller given in quadratic program Eq.2.48 contains the term $\bar{Q}$ which is obtained as solution of Eq.2.47 or Eq.2.51. The discrete

Lyapunov function $V(k)$ of the hyperbolic or parabolic PDE system is defined as below:

$$V(k) =< z(\zeta,k), \bar{Q}z(\zeta,k) >= \int_0^L z^T(\zeta,k)\bar{Q}z(\zeta,k)d\zeta \tag{2.52}$$

Straightforward algebraic manipulation of the above discrete Lyapunov function between instances $V(k)$ and $V(k+1)$ results in the following expression of a discrete Lyapunov equation:

$$< z(\zeta,k), [A_d^*\bar{Q}A_d - \bar{Q}]z(\zeta,k) >= - < z(\zeta,k), C_d^*QC_dz(\zeta,k) > \tag{2.53}$$

It is known that A_d is the infinitesimal cogenerator of the stable A operator that generates a stable C_0-semigroup $\mathcal{T}(t)$ on the Hilbert space H. Therefore, the corresponding power generator in a discrete setting T is power stable if and only if there exists a positive operator $\bar{Q} \in L_2(0,1)$ such that the expression in Eq.2.53 for Lyapunov function holds. In other words, the solution $\bar{Q}$ satisfies the following equation:

$$A_d^*\bar{Q}A_d - \bar{Q} = -C_d^*QC_d \tag{2.54}$$

However, one can notice that the operator $\bar{Q}$ needs to operate on some function which is also true for the operators A_d and C_d and a solution for $\bar{Q}$ in Eq.2.54 can not be directly determined by calculation. The way to calculate the operator $\bar{Q}$ is to link the solution of the discrete and continuous Lyapunov equation for the hyperbolic and parabolic linear transport-reaction PDEs. In particular, it can be demonstrated that the unique solution of the continuous Lyapunov equation is directly related to the

discrete one. One can find a unique solution $\bar{Q}$ of the continuous Lyapunov equation:

$$A^*\bar{Q} + \bar{Q}A = -C^*QC \tag{2.55}$$

and it can be shown that $\bar{Q}$ is also the solution to the discrete Lyapunov equation described in Eq.2.54.

One can demonstrate that if the continuous Lyapunov equation $A^*\bar{Q} + \bar{Q}A = -C^*QC$ holds, by simple algebraic manipulation one can obtain:

$$\begin{aligned} A_d^*\bar{Q}A_d - \bar{Q} &= \sqrt{2\delta}[\delta - A]^{-1*}[A^*\bar{Q} + \bar{Q}A]\sqrt{2\delta}[\delta - A]^{-1} \\ &= -\sqrt{2\delta}[\delta - A]^{-1*}[C^*QC]\sqrt{2\delta}[\delta - A]^{-1} \\ &= -[\sqrt{2\delta}C[\delta - A]^{-1}]^*Q[\sqrt{2\delta}C[\delta - A]^{-1}] \\ &= -C_d^*QC_d \end{aligned}$$

Therefore, by multiplying a spatial function $X(\zeta) \in L_2(0,1)$ on both sides of the continuous Lyapunov equation described in Eq.2.55 one obtains:

$$\begin{aligned} &A^*\bar{Q}X + \bar{Q}AX = -C^*QCX \\ &[v\frac{\partial \bar{Q}X}{\partial \zeta} + \psi\bar{Q}X] + \bar{Q}[-v\frac{\partial X}{\partial \zeta} + \psi X] = -C^*QCX \\ &v\bar{Q}\frac{\partial X}{\partial \zeta} + v\frac{\partial \bar{Q}}{\partial \zeta}X + \psi\bar{Q}X - v\bar{Q}\frac{\partial X}{\partial \zeta} + \psi\bar{Q}X = -C^*QCX \end{aligned}$$

Finally, one can obtain the solution of the continuous Lyapunov equation by obtaining the analytic solution for the operator $\bar{Q}$ in the case of a hyperbolic PDE in the

following equation:

$$v\frac{\partial \bar{Q}}{\partial \zeta}X + 2\psi\bar{Q}X = -C^*QCX \tag{2.56}$$
$$\bar{Q} \in \mathcal{D}(A^*)$$

In the case when the full state feedback is considered, which implies that the output operator C is a constant, for example $C = 1$, then $C^* = C$ which implies that one can remove the arbitrary test function $X(\zeta)$ on both sides in Eq.2.56. On the other hand, if C measurement is applied to boundary or point observation, for example at the exit of the reactor in the case of a hyperbolic PDE system, that is $C(f(\zeta)) = \int_0^L f(\zeta)\delta(\zeta - L)d\zeta = f(L)$, then C^* is a spatial operator $C^*(f(\zeta)) = \int_0^L f(\eta)d\eta\delta(\zeta - L)$, that operates on the arbitrary function $X(\zeta)$.

Remark 4: In the case of a scalar hyperbolic PDE, it can be shown that the form of a linear hyperbolic PDE given in this chapter is always stable one, and the issue of calculating the $\bar{Q}$ for an unstable PDE system can arise only in the case of a parabolic PDE.

Simulation Results of Model Predictive Controller design and application to scalar hyperbolic PDE

In simulation, we choose the output of the tubular reactor to represent the output operator, that is $C(f(\zeta)) = \int_0^L f(\zeta)\delta(\zeta - L)d\zeta = f(L)$, a uniform state weight function in the Lyapunov function is chosen as $Q(\zeta) = 5$, and the arbitrary function $X(\zeta) = 1$. By application of the following condition $\bar{Q} \in \mathcal{D}(A^*)$, the integration is obtained by integrating Eq.2.56 from $\bar{Q}(\zeta = L) = 0$ to $\zeta = 0$, see Fig.2.1. To demonstrate successful application of the model predictive controller, the discretization time $h =$

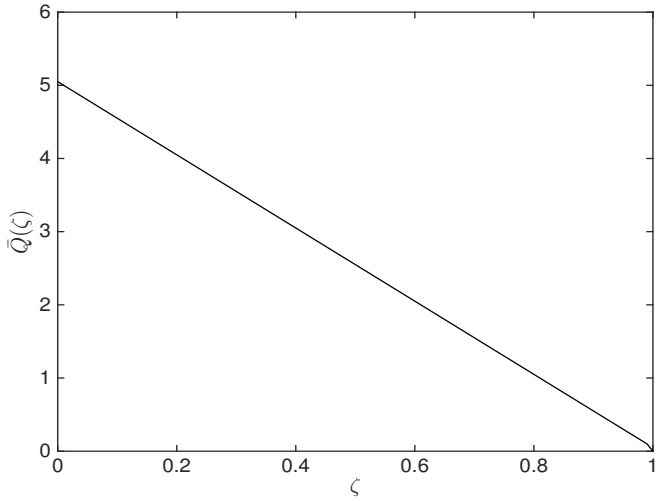

Fig. 2.1: Function $\bar{Q}(\zeta)$ obtained as solution of Eq.2.56.

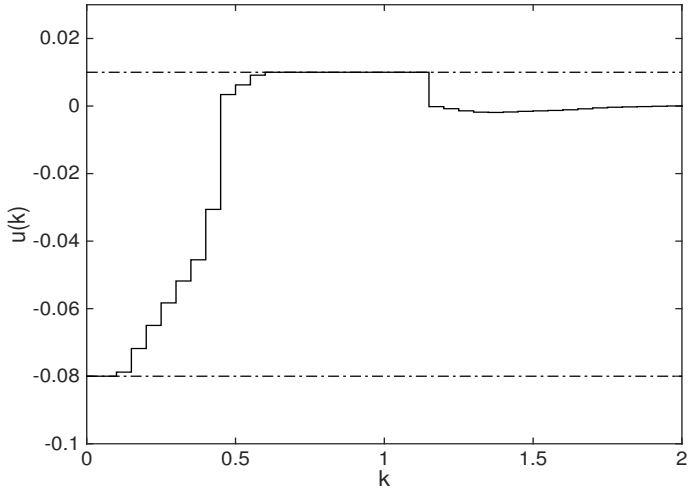

Fig. 2.2: Input profile model predictive control law Eq.2.46-Eq.2.49 constructed on the basis of a discrete time hyperbolic PDE system Eq.2.4 with input and output constraints (solid line); input constraints are given by (dash-dot line).

0.05 is chosen, which implies that the $\delta = 40$, and $d\zeta = 0.01$ is chosen for numerical integration. The model system parameters are chosen as $v = 1$, $\psi = 0.5$, with constant

spatial function $B = 2$, $Q = 5$ and $R = 10$. The initial condition is $z_0 = 1 - \cos(2\pi\zeta)$ and MPC horizon is 15. The constraints for the input and output/state are given as $-0.08 \leq u(k) \leq 0.01$ and $-0.1 \leq y(k) \leq 0.7$.

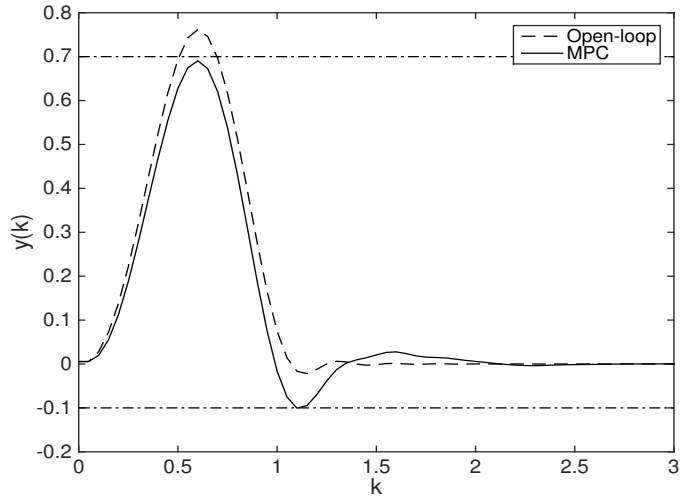

Fig. 2.3: Comparison between the profile of a closed-loop system under the implementation of the model predictive control law Eq.2.46-Eq.2.49 constructed on the discrete time hyperbolic PDE system Eq.2.4 with input and output constraints (solid line) and the profile of an open-loop system (dashed line); output constraints (dash-dot line).

The controller performance can be evaluated in Fig.2.3-2.4, and the corresponding control input is given in Fig.2.2. Fig.2.3 provides a comparison of outputs $y(k)$ evolution with and without MPC control applied. The state $z(\zeta, k)$ with MPC is shown in Fig.2.4.

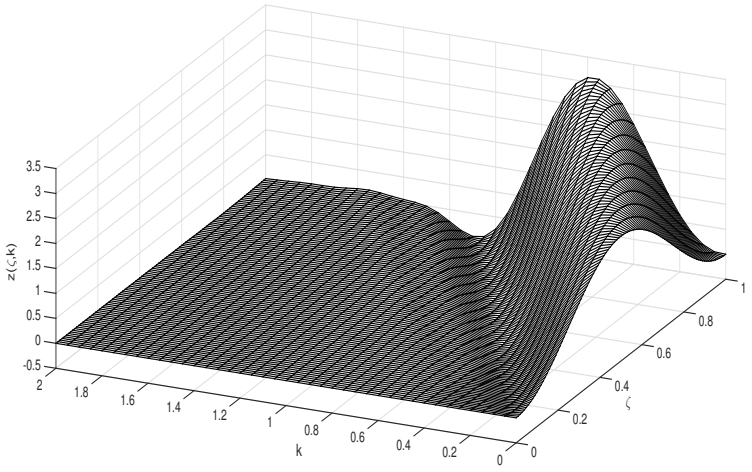

Fig. 2.4: State profile evolution under the applied model predictive control law Eq.2.46-Eq.2.49 constructed on the basis of the discrete time hyperbolic PDE system Eq.2.4 with input and output constraints.

2.3.2 Model predictive control for parabolic PDE

Discrete Lyapunov Function

In the previous section it has been demonstrated how one can calculate the terminal penalty operator $\bar{Q}$ in the case of a hyperbolic system. However, when it comes to parabolic systems the calculation of $\bar{Q}$ can not be completed in analytic sense. It can be shown that the solution of a discrete Lyapunov equation $A_d^* \bar{Q} A_d - \bar{Q} = -C_d^* Q C_d$ can be obtained by solving a continuous Lyapunov equation $A^* \bar{Q} + \bar{Q} A = -C^* Q C$. The continuous Lyapunov equation of parabolic PDE system is consider in the following inner product form [38]:

$$< Az_1, \bar{Q} z_2 > + < \bar{Q} z_1, Az_2 >= - < Cz_1, QCz_2 > \tag{2.57}$$

where $z_1,\ z_2 \in \mathcal{D}(A)$. Let us take $z_1 = \phi_n$ and $z_1 = \phi_m$, where ϕ_i represent normalized eigenfunctions of the parabolic linear operator A. Defining the operator $\bar{Q}_{nm} =< \phi_n, \bar{Q}\phi_m >$, one can obtain:

$$< A\phi_n, \bar{Q}\phi_m > + < \bar{Q}\phi_n, A\phi_m >= - < C\phi_n, QC\phi_m > \tag{2.58}$$

With $A\phi_n = \lambda_n\phi_n$, the above equation becomes:

$$\lambda_n\bar{Q}_{nm} + \lambda_m\bar{Q}_{nm} = - < C\phi_n, QC\phi_m > \tag{2.59}$$

then,

$$\bar{Q}_{nm} = -\frac{< C\phi_n, QC\phi_m >}{\lambda_n + \lambda_m} \tag{2.60}$$

Finally, one can obtain the operator $\bar{Q}$ as a solution of continuous Lyapunov equation by calculating the following equation:

$$\begin{aligned} \bar{Q}(\cdot) &= \sum_{n=0}^{\infty}\sum_{m=0}^{\infty} \bar{Q}_{nm} < \cdot, \phi_m > \phi_n \\ &= \sum_{n=0}^{\infty}\sum_{m=0}^{\infty} -\frac{< C\phi_n, QC\phi_m >}{\lambda_n + \lambda_m} < \cdot, \phi_m > \phi_n \end{aligned} \tag{2.61}$$

If the operator C is a constant spatial function, then $\bar{Q}_{nm} = -\frac{C^2 < \phi_n, Q\phi_m >}{\lambda_n + \lambda_m}$. Since $< \phi_n, Q\phi_m >= \delta_{nm}$, when $n \neq m$, $\bar{Q}_{nm} = 0$, thus, $\bar{Q}_{nn} = -\frac{C^2 < \phi_n, Q\phi_n >}{2\lambda_n}$, the expression for the operator $\bar{Q}$ simplifies to:

$$\bar{Q}(\cdot) = \sum_{n=0}^{\infty} -\frac{C^2 < \phi_n, Q\phi_n >}{2\lambda_n} < \cdot, \phi_n > \phi_n \tag{2.62}$$

Stability

The definition of a positive definite operator is that if the inner product $< \psi(\zeta), \bar{Q}\psi(\zeta) >$ is nonnegative, the operator $\bar{Q}$ is a positive definite operator. Here, it can be shown that the operator $\bar{Q}$ in Eq.2.62 is a positive definite operator. Let us consider:

$$
\begin{aligned}
&< \psi(\zeta), \bar{Q}\psi(\zeta) >= \int_0^1 \psi(\zeta)[\bar{Q}\psi(\zeta)]d\zeta \qquad (2.63)\\
&= \int_0^1 \psi(\zeta)[\sum_{n=0}^{\infty} -\frac{C^2 < \phi_n, Q\phi_n >}{2\lambda_n} < \psi(\eta), \phi_n(\eta) > \phi_n(\zeta)]d\zeta \\
&= \sum_{n=0}^{\infty} -\frac{C^2 < \phi_n, Q\phi_n >}{2\lambda_n} < \psi(\eta), \phi_n(\eta) > [\int_0^1 \psi(\zeta)\phi_n(\zeta)d\zeta] \\
&= \sum_{n=0}^{\infty} -\frac{C^2 < \phi_n, Q\phi_n >}{2\lambda_n} < \psi(\eta), \phi_n(\eta) >< \psi(\zeta), \phi_n(\zeta) > \\
&= \sum_{n=0}^{\infty} -\frac{C^2 < \phi_n, Q\phi_n >}{2\lambda_n} < \psi, \phi_n >^2
\end{aligned}
$$

Since $Q(\zeta)$ is a nonnegative spatial function, then $< \phi_n, Q\phi_n >= \int_0^1 Q(\zeta)\phi_n^2(\zeta)d\zeta$ is nonnegative. And the eigenvalues of the stable operator A are negative $\lambda_n < 0$, thus, the above inner product is nonnegative which implies that the operator $\bar{Q}$ is a positive operator.

If the system is unstable with nonnegative eigenvalues $\lambda_n \geq 0$, $\bar{Q}$ is not a positive definite operator. In order to address the unstable parabolic PDE, one needs to identify the unstable modes of the continuous linear PDE. The issue to address is that the unstable modes are associated with nonnegative eigenvalues λ_n. Therefore, in order to guarantee stabilization, one needs to employ the stability constraints in the optimization problem cast as equality constraints. Therefore, if optimization is feasible, the controller will achieve stabilization by cancelling the unstable modes.

The corresponding condition is given with the following inner product:

$$< z(\zeta, N), \phi_u >= 0 \tag{2.64}$$

where ϕ_u are the eigenfunctions associated with the nonnegative eigenvalues.

The above equation leads to the following equality constraint expressed as stabilization of unstable modes at the end of the horizon with the feasible input:

$$\begin{bmatrix} < A_d^{N-1} B_d, \phi_u > & < A_d^{N-2} B_d, \phi_u > & \cdots & < B_d \ , \phi_u > \end{bmatrix} \begin{bmatrix} u(1) \\ u(2) \\ \vdots \\ u(N) \end{bmatrix} \tag{2.65}$$
$$= - < A_d^N z(\zeta, 0), \phi_u >$$

Eq.2.65 needs to be integrated in the constrained convex optimization problem given by Eqs.2.50-2.51.

Simulation of model predictive controller design and application to scalar parabolic PDE

Dirichlet Boundary Condition

We consider the case of the Dirichlet boundary condition $z(0) = 0 = z(1)$, and linear operator $A = \frac{\partial^2}{\partial \zeta^2} + \psi$, with ψ being constant. The operator A has eigenvalues $\lambda_n = -n^2\pi^2 + \psi$ which determine stability of the system and associated eigenvectors $\phi_n(z) = \sqrt{2} sin(n\pi z)$, $n \geq 1$. In the case when $\psi < \pi^2$, which implies that the $\lambda < 0$, the parabolic system with the Dirichlet boundary condition is stable, see Fig.2.5. The application of the model predictive controller leads to the faster convergence to the

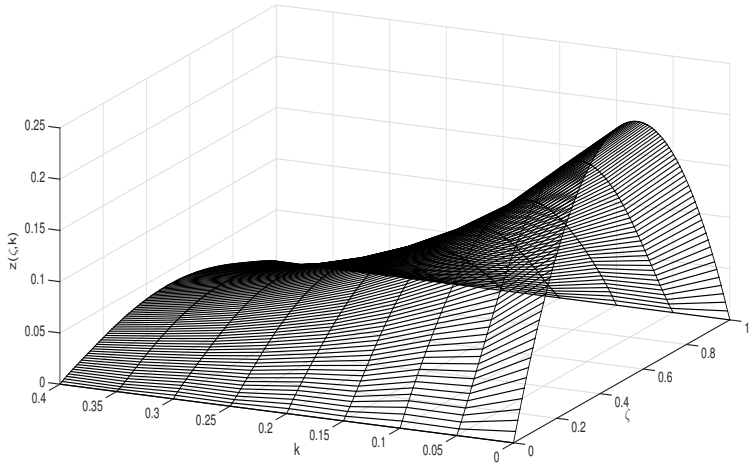

Fig. 2.5: Evolution of the state profile of an open-loop parabolic PDE system Eq.2.4 with Dirichlet boundary conditions.

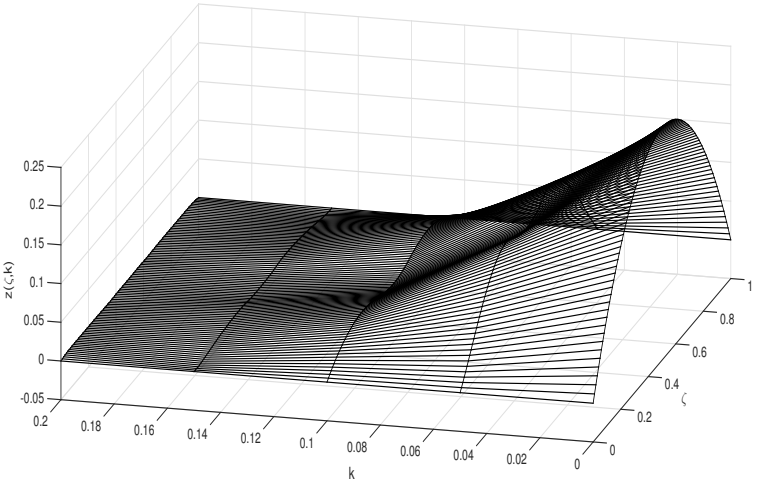

Fig. 2.6: Evolution of the state profile when the model predictive control law Eq.2.50 is applied with the Dirichlet boundary condition and input and state constraints.

stable steady state with satisfaction of the input and state constraints, see Fig.2.6-2.7-2.8. In simulation, the system parameters are $\psi = 5$, while the actuation distribution

function is given as $B = 0$ $(0 < \zeta < 0.4$ & $0.6 < \zeta < 1)$ and $B = 1$ $(0.4 < \zeta < 0.6)$, $Q = 5$ and $R = 0.01$. Initial condition is $z_0 = -(\zeta - 0.5)^2 + 0.5^2$, and $h = 0.05$, with MPC horizon 5. The value of the terminal penalty is calculated by accounting for 5 eigenmodes, that is $n = m = 5$. The constraints on the input and the state are given as $-0.16 \leq u(k) \leq 0$ and $0 \leq z(0.5, k) \leq 0.3$.

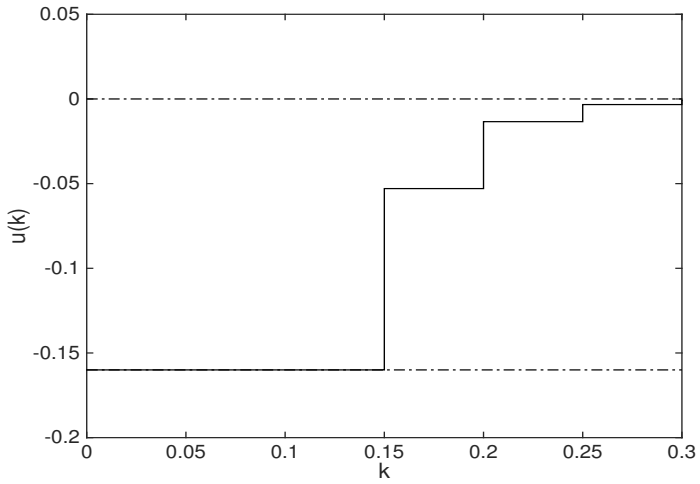

Fig. 2.7: Input profile evolution under the model predictive control law Eq.2.50 applied with the Dirichlet boundary condition, input and state constraints. (solid line); input constraints (dash-dot line).

Neumann Boundary Condition

The Neumann boundary condition $\frac{\partial z(0)}{\partial \zeta} = 0 = \frac{\partial z(1)}{\partial \zeta}$, with the linear operator $A = \frac{\partial^2}{\partial \zeta^2} + \psi$ is considered. The operator A has eigenvalues $\lambda_n = -n^2\pi^2 + \psi,\ n \geq 0$ and eigenvectors $\phi_n(z) = \sqrt{2}cos(n\pi z),\ n \geq 1,\ \phi_0(z) = 1$. When $\psi \geq 0,\ \lambda_0 \geq 0$, the parabolic system with Neumann Boundary Condition is unstable, see Fig.2.9. The application of MPC control law leads to simultaneous stabilization, input and stat/output constraints satisfaction providing that optimization is feasible, see 2.10-

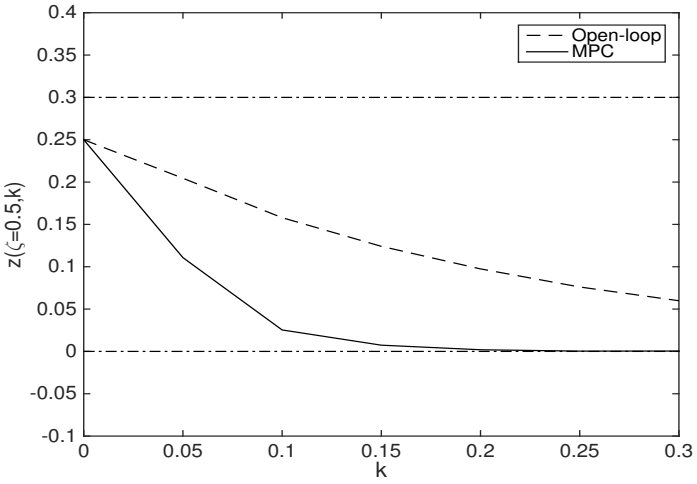

Fig. 2.8: Comparison among profiles of the closed-loop system under the implementation of the model predictive control law Eq.2.50 constructed as a discrete time parabolic PDE system in Eq.2.4 with the Dirichlet boundary condition and input and state constraints (solid line) and open-loop system profile (dashed line); state constraints (dash-dot line).

2.11-2.12. In simulation studies, the system parameters are $\psi = 2$, $B = 0$ ($0 < \zeta < 0.4$ & $0.6 < \zeta < 1$) and $B = 1$ ($0.4 < \zeta < 0.6$), $Q = 5$ and $R = 0.01$. The initial condition is $z_0 = -(\zeta - 0.5)^2 + 0.5^2$, $h = 0.01$ and the MPC horizon is 5. The value of the terminal penalty is calculated by accounting for 10 eigenmodes, that is $n = m = 10$. Since, the case of unstable PDE is considered, the first eigenmode is used in the stabilizing condition given by Eq.2.65. The constraints for the input and the state are $-3 \leq u(k) \leq 1$ and $-0.05 \leq z(0.5, k) \leq 0.3$.

It can be noticed that the model predictive control law for the infinite dimensional system achieves the input and state constraints satisfaction since the state evolution is exactly at the state constraint, see Fig.2.11. This confirms the previous findings in [56, 15] in which the model predictive control was realized on the basis of an approximate

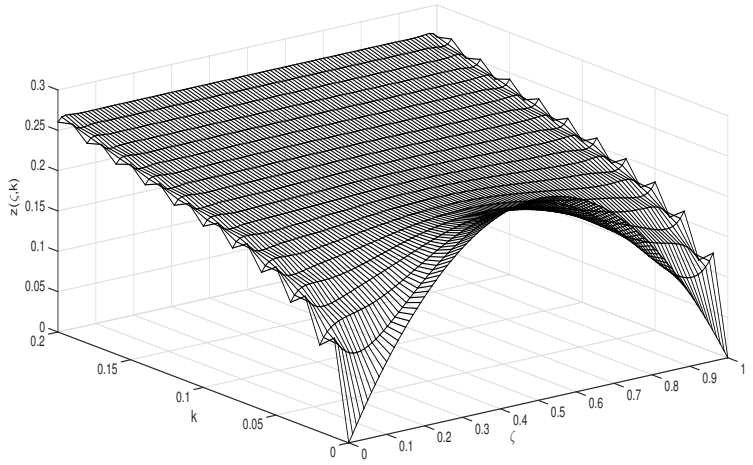

Fig. 2.9: The evolution of state profile of the open-loop parabolic PDE system Eq.2.4 with the Neumann boundary condition.

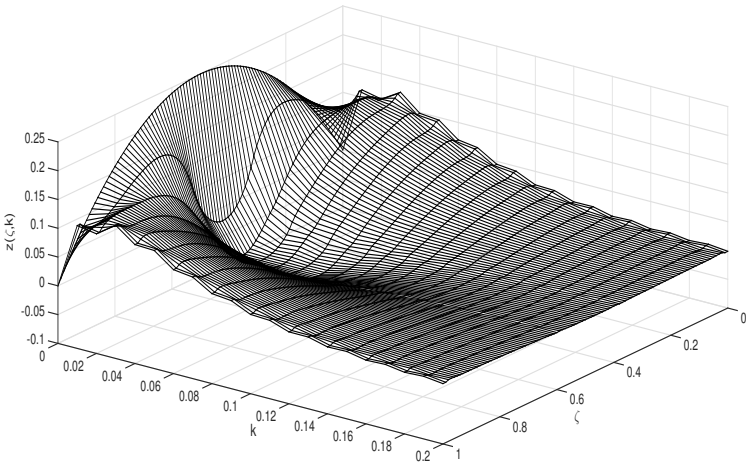

Fig. 2.10: The evolution of the state profile under the model predictive control law Eq.2.50 constructed using discrete time parabolic PDE system Eq.2.4 with the Neumann boundary condition and input and state constraints.

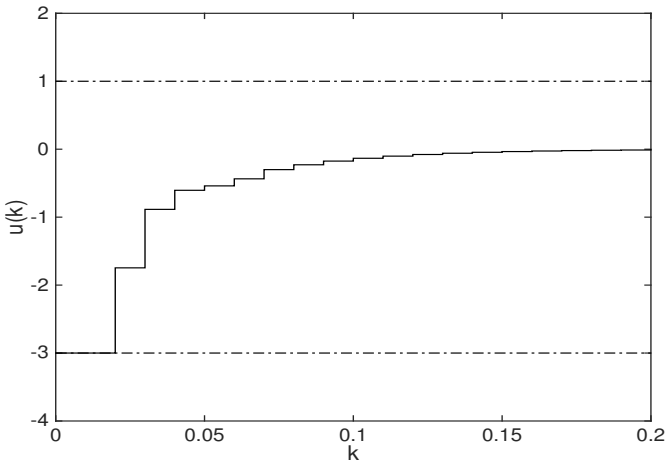

Fig. 2.11: Input evolution profile under the model predictive control law Eq.2.50 constructed using discrete time parabolic PDE system Eq.2.4 with the Neumann boundary condition and input and state constraints (solid line); input constraints (dash-dot line).

model obtained by the Galerkin method with the PDE state constraints considered and realized as slack variables in the model predictive control law. Contrary to any previous published case where a linear PDE model is approximated with some type of the spatial discretization, the proposed model predictive control law for single scalar transport equation leads to an easy realizable constrained control algorithm formulation which is not more complex than one when algorithms are dealing with the scalar finite dimensional models.

2.4 Summary

In summary, finite dimensional and computationally realizable model predictive control algorithms are developed in this chapter for a class of linear transport-reaction systems with consideration of input and state constraints arising in the context of a

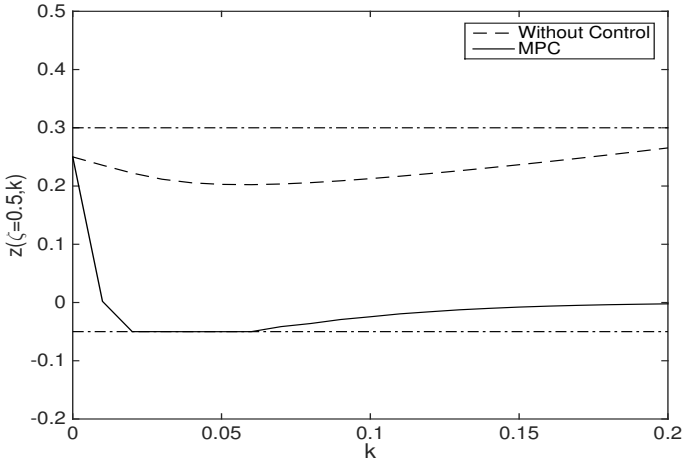

Fig. 2.12: The comparison between profiles of closed-loop system under the implementation of the model predictive control law Eq.2.50 constructed using discrete time parabolic PDE system Eq.2.4 with the Neumann boundary condition and input and state constraints (solid line) and profile of open-loop system (dashed line); state constraints (dash-dot line).

plug flow reactor and/or an axial dispersion reactor model. The dimensionless models described by hyperbolic PDE and/or parabolic PDE are explored and an exact time discretization algorithm is applied by introducing the Cayley-Tustin transform. The proposed discretization exactly maps from a continuous to a discrete infinite dimensional counterpart of the hyperbolic or parabolic PDE, and also preserves stability, controllability and observability properties of the system. The model predictive control formulation is developed in the inner product setting to account for the spatial nature of the problem, and various discrete models of hyperbolic PDE and/or parabolic PDE with different boundary conditions (Dirichlet, Neumann and Robin) are developed and used in the construction of the performance objective function, input and state constraints. Finally, the model predictive control laws are applied and if optimization is feasible, the controllers achieve the control objectives which are

demonstrated via simulation studies. An important issue of stabilization in the case of linear unstable systems is addressed by the application of the terminal penalty condition. The following framework can be easily extended to the systems of linear parabolic and/or hyperbolic problems, and to the class of second order hyperbolic systems that model wave propagation phenomena, or more complex models of Kuramoto-Sivashinsky, Ginzburg Landau equations with boundary or/and in domain actuation or observation.

Chapter 3

Modelling and Control of Solar Thermal System with Borehole Seasonal Storage

3.1 Introduction

The modelling and control of the solar thermal system with borehole seasonal storage is motivated by the need for accurate modelling and analysis of the state of the art community development of the Drake Landing Solar Community (DLSC) in Okotoks, Alberta, Canada [69]. The DLSC contains 52 energy-efficient houses with an innovative heating system which includes a solar thermal power plant, borehole thermal energy storage system (BTES), short term thermal storage system (STTS) and a district heating loop system. Solar thermal energy is collected through roof mounted plate collectors. A heat transfer fluid containing a high concentration of glycol is used to collect solar energy. The energy collected by the glycol loop is transferred to STTS

by a heat exchanger, see Fig.3.1. Depending on the season and energy requirements, the energy from the STTS can be distributed to the district heating loop or stored in the BTES. The BTES uses a grid of boreholes with single u-tube heat exchangers [70, 71]. Finally, the collected energy is sent to the district heating loop system to heat the energy efficient homes.

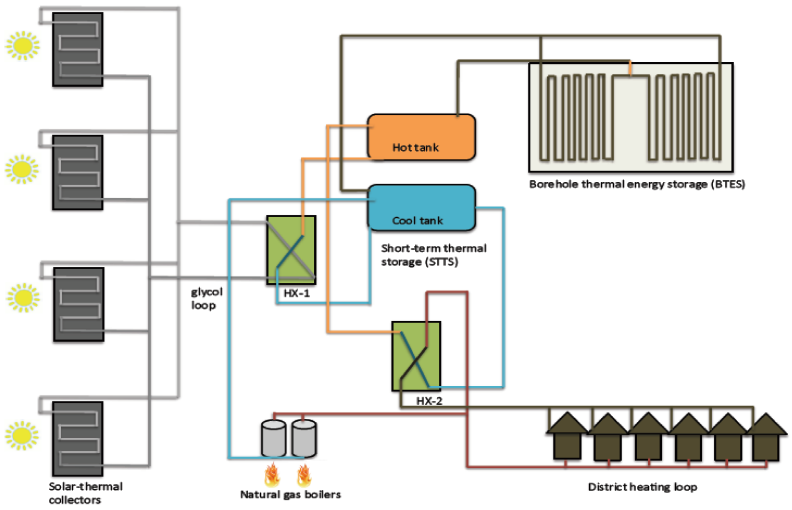

Fig. 3.1: Diagram of the solar thermal system with borehole seasonal storage.

A major step towards the completion of the control system is the development of a process model using detailed energy balances. The solar thermal plant system concentrates solar radiation using mirrors or lenses to heat a fluid [72]. The dynamic model of the solar thermal energy system is of distributed nature. However, the changes of solar radiation on warm sunny or cold cloudy days affect the dynamics of the solar thermal system. Due to this solar radiation variability, many advanced control techniques have been applied to the solar thermal energy system to account for possible problems caused by the solar radiation under variable solar energy supply

[73, 74, 75, 76].

The energy collected by a solar thermal plant system is sent to the STTS through heat exchanger. The dynamics of the heat exchanger system is distributed in nature and is modelled by the transport thermal distributed parameter system [77]. The energy from the solar thermal system is transferred to the heat exchanger system through the boundary and the counter-current flows exchange the energy, therefore, the boundary controlled system realization is considered in the modelling of the heat exchanger system.

The BTES uses a grid of boreholes with U-tube heat exchangers to preserve energy as a long-term storage device in the overall system. To fulfill energy requirements in different seasons, the BTES saves energy during the summer months by transferring available thermal energy to the ground and provides energy from the ground during the heating season. The energy balance and dynamics of the BTES is modelled as a transport thermal distributed parameter system [78, 79]. In particular, when it comes to the BTES, environmental temperature fluctuations make a possible sources of disturbances to the BTES system and may affect the time evolution of the model.

In the STTS, water-filled storage tanks act as a thermal buffer between the solar thermal plant system and the district heating loop system [70]. During the summer months, the hot tank utilizes thermal energy from the solar plant. When the temperature of the hot tank rises above the set-point, thermal energy from the hot tank is transferred to the BTES system. During the heating season, the hot tank charges thermal energy from both the solar plant and the BTES. Finally, the collected energy of the STTS is sent to a district heating loop system.

In order to heat the energy efficient homes in the district heating loop system, a backup gas boiler is provided to insure that heat is available to each and every

home at all times. One important performance specification is to heat homes to the prespecified temperature (which may fluctuate with seasonal changes in temperature), and therefore a controller for the natural gas boiler system is designed to track the desired temperature set-point. The temperature regulation of the solar thermal system with borehole seasonal storage is characterized by many uncertainties, such as environmental changes, occupancy status changes, and changes in the operating conditions of equipment in the building. Therefore, control systems play an important role in maintaining the performance of the systems in the presence of possible uncertainties and disturbances. The ultimate performance goal is that the proposed controller maintains the temperature at a desired set point and keeps the integrity of the energy demands in the district heating loop system.

Servo controller design is a well-know strategy that computes the required input which asymptotically attenuates error between the output and a reference trajectory or set point to zero [24, 25]. One of the advantages of a servo controller is that it can account for disturbances which may affect the process. We propose a servo control system design for the solar thermal system regulation with borehole seasonal storage, which takes into account measurable disturbances, such as changes in ambient temperature and disturbance predictions, such as weather forecast that may potentially assist in the prediction of the availability of the different energy sources.

From the literature review, most of the modelling of subsystems, such as solar thermal energy system [72], heat exchanger system [77], and BTES system [78, 79] are continuous and distributed in nature. In this chapter, in order to realize accurate modelling of the subsystems and to design a practical and usable controller, discrete models of the subsystems and a discrete controller design are developed. We utilize Cayley-Tustin time discretization which preserves the infinite-dimensional

nature of the distributed parameter system [19]. This transformation preserves the energy equality among the continuous and discrete model which provides a discrete model for controller design and frequency analysis. Other model reduction technique, such as explicit Euler discretization may potentially transfer the stable continuous system into unstable discrete system or require small time steps for approximation. This proposed discretization transforms the system from a continuous to a discrete state space setting without spatial discretization and/or any other type of spatial approximation of the distributed parameter system. In this chapter, according to the energy balance conservation laws, the processes in solar thermal system with borehole seasonal storage are modelled using ordinary differential equations (ODEs), hyperbolic partial differential equations (PDEs) or coupled PDEs-ODEs equations. In particular, by application of Cayley-Tustin time discretization we maintain the low dimensionality of the overall discrete model. The discrete representation of coupled partial and ordinary differential equations does not include any high order plant representation, which is contrary to the previous proposed methods [5]. In addition, a discrete infinite-dimensional representation of the system realized in this chapter provides an insight into frequency response of the subsystems and that of the overall plant. This is of importance, since all well known frequency analysis methods and controller synthesis can be easily applied, and one can obtain appropriate engineering insight into plant operation. Finally, the controller designed for the servo problem is a discrete controller which can be easily realized and implemented in practice.

The chapter is organized as follows: section 3.2 introduces the Cayley-Tustin time discretization. In section 3.3, we address the model of the solar thermal system with borehole seasonal storage and discretize the subsystems of the overall plant. Section 3.4 provides the servo controller design and the analysis of the system frequency

response. Finally, we demonstrate the performance of the servo control formulations built in previous section through simulation studies.

3.2 Time Discretization for Linear System

According to the energy balance, the processes in the solar thermal system with borehole seasonal storage can be modelled by ordinary differential equations (ODEs), hyperbolic partial differential equations (PDEs) and/or coupled PDEs-ODEs equations. In other words, the overall system contains internally coupled linear finite and infinite dimensional systems, see Fig.3.2. The Cayley-Tustin time discretization method is applied to obtain a discrete model version which provides an insight into the subsystem's performance and overall dynamical behaviour of the system.

3.2.1 Time Discretization for Linear Infinite-dimensional System

In this section, we introduce the time discretization called the Cayley-Tustin transformation of continuous time systems to discrete time systems [19]. The linear infinite-dimensional system is described by the following state space sy-stem:

$$\begin{aligned} \dot{x}(\zeta,t) &= Ax(\zeta,t) + Bu(t),\ x(\zeta,0) = x_0 \\ y(t) &= Cx(\zeta,t) + Du(t) \end{aligned} \tag{3.1}$$

where the following assumptions hold: the state $x(\zeta,t) \in H \oplus R^n$, H is a real Hilbert space with inner product $< \cdot\,,\, \cdot >$ and R^n is a real space, where n accounts for the states associated with the lumped parameter system. This state-space representation

accounts for coupled infinite and finite dimensional systems. The input $u(t) \in U$ and the output $y(t) \in Y$, where U and Y are real Hilbert spaces; operator $A : D(A) \subset H \to H$ is the generator of a C_0-semigroup on H and has a Yosida extension operator A_{-1}; B, C and D are linear operators associated with actuation and output measurement or a direct feed forward element, i.e., $B \in L(U, H)$, $C \in L(H, Y)$ and $D \in L(U, Y)$.

Given the time discretization parameter $h > 0$, the Tustin time discretization is given by [62]:

$$\begin{aligned} &\frac{x(jh) - x((j-1)h)}{h} \approx A\frac{x(jh) + x((j-1)h)}{2} + Bu(jh),\ x(0) = x_0 \\ &y(jh) \approx C\frac{x(jh) + x((j-1)h)}{2} + Du(jh) \end{aligned} \tag{3.2}$$

Let $u_j^h/\sqrt{h}$ be the approximation of $u(jh)$ and $y_j^h/\sqrt{h}$ be the approximation of $y(jh)$, the above set of equations yields the discrete time dynamics:

$$\begin{aligned} &\frac{x_j^h - x_{j-1}^h}{h} = A\frac{x_j^h + x_{j-1}^h}{2} + B\frac{u_j^h}{\sqrt{h}},\ x_0^{(h)} = x_0 \\ &\frac{y_j^h}{\sqrt{h}} = C\frac{x_j^h + x_{j-1}^h}{2} + D\frac{u_j^h}{\sqrt{h}} \end{aligned} \tag{3.3}$$

After some basic manipulation, the discrete system takes the following form:

$$\begin{aligned} &x(\zeta, k) = A_d x(\zeta, k-1) + B_d u(k),\ x(\zeta, 0) = x_0 \\ &y(k) = C_d x(\zeta, k-1) + D_d u(k) \end{aligned} \tag{3.4}$$

where $\delta = 2/h$, A_d, B_d, C_d and D_d are discrete time linear system operators, given

by:

$$\begin{bmatrix} A_d & B_d \\ C_d & D_d \end{bmatrix} = \begin{bmatrix} [\delta - A]^{-1}[\delta + A] & \sqrt{2\delta}[\delta - A_{-1}]^{-1}B \\ \sqrt{2\delta}C[\delta - A]^{-1} & G(\delta) \end{bmatrix} \tag{3.5}$$

where $G(\delta)$ denotes the transfer function of the system from input to the output and it is defined as $G(\delta) = C[\delta - A_{-1}]^{-1}B + D$.

In the most general case, Eq.3.1 can be extended by introducing the affine disturbance input, which leads to the following form:

$$\begin{aligned} \dot{x}(\zeta, t) &= Ax(\zeta, t) + Bu(t) + Ed(t),\ x(\zeta, 0) = x_0 \\ y(t) &= Cx(\zeta, t) + Du(t) + Fd(t) \end{aligned} \tag{3.6}$$

where $E \in L(R^n, H)$ and $F \in L(R^n, Y)$ are linear operators. The corresponding discrete operators are $E_d = \sqrt{2\delta}[\delta - A_{-1}]^{-1}E$ and $F_d = C[\delta - A_{-1}]^{-1}E + F$.

Remark 1: Discrete operator A_d can be expressed as $A_d = [\delta - A]^{-1}[\delta + A] = -I + 2\delta[\delta - A]^{-1}$, here I is the identity operator.

Proof: In order to demonstrate the results in Remark 1, one can show that:

$$\begin{aligned} A_d(\cdot) &= [\delta - A]^{-1}[\delta + A](\cdot) \\ &= \tfrac{\delta + A}{\delta - A}(\cdot) \\ &= [-I + \tfrac{2\delta}{\delta - A}](\cdot) \\ &= [-I + 2\delta[\delta - A]^{-1}](\cdot) \end{aligned}$$

Remark 2: The Cayley-Tustin transform maps infinite-dimensional system from continuous time to discrete time without spatial approximation. The novelty of using

Cayley-Tustin time discretization is that this implicit method can be applied freely with larger time steps for time integration compared to the explicit methods, such as explicit Euler and/or Runge-Kutta method.

In the next section, we apply the Cayley-Tustin discretization described above to the solar thermal system with borehole seasonal storage.

3.3 Model Formulation and Time Discretization

3.3.1 Overview of Solar Thermal System with Borehole Seasonal Storage

The solar thermal system with borehole seasonal storage modelled in this chapter uses the solar thermal system, heat exchanger, BTES system, STTS system, natural gas system and the district heating loop system, see Fig.3.2. The thermal energy transfers from the solar thermal system to the STTS system through a heat exchanger. The BTES system stores thermal energy to the STTS system directly. Then, the STTS system provides thermal energy to district the heating loop system. Finally, the inlet to the district heating loop system is maintained at a reference temperature through the control of the natural gas system.

In this chapter, the solar thermal system and the BTES system are described by coupled PDEs-ODEs equations. The contraflow heat exchanger is modelled by a series of first order hyperbolic PDES with consideration of boundary inputs. The STTS system and the natural gas system are represented by ODE equations. In this section, we introduce the modelling of these subsystems and discretize the subsystems with the Cayley-Tustin method described above.

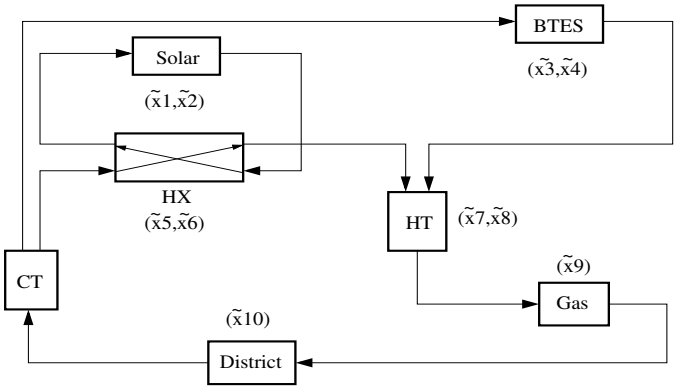

Fig. 3.2: Diagram of the solar thermal system with borehole seasonal storage: solar collector system (solar); borehole thermal energy storage system (BTES); heat exchanger system (HX); hot tank system (HT); cold tank system (CT); natural gas system (Gas); district heating loop system (District).

Remark 3: The system modelling in this chapter does not consider irreversible processes in thermal dynamic system representation. The time discretization of the closed-loop system has no modelling error associated with spatial domain discretization since Cayley-Tustin transformation preserves system energy.

3.3.2 Solar Thermal Energy System

The solar thermal energy system uses a plate collector to focus solar radiation onto the absorber pipe [72]. The energy balance of the flow in the solar collector is given as follows:

$$\rho_{gl} C_{pgl} s_{solar} \frac{\partial T_{solar}}{\partial t} = -C_{pgl} F_{solar} \frac{\partial T_{solar}}{\partial \zeta} + h_p p_A (T_A - T_{solar}) \tag{3.7}$$

and the energy balance of the absorber is:

$$\rho_A C_{pA} s_A \frac{dT_A}{dt} = h_p p_A (T_{solar-in} - T_A) + Q_{solar} w \tag{3.8}$$

The description of the system variables is shown in Table.3.1.

One can apply appropriate non-dimensional transformation of Eq.3.7-3.8, so that the following states $x_1 = \frac{T_{solar}-T_r}{T_r}$, $x_2 = \frac{T_A-T_r}{T_r}$, and input $u_1 = \frac{Q_{solar}}{Q_r}$ are obtained. Here T_r is the reference temperature and Q_r is the reference heat flux. The parameters of the system are $\alpha_1 = \frac{F_{solar}}{\rho_{gl}s_{solar}}$, $\beta_1 = \frac{h_p p_A}{\rho_{gl}C_{pgl}s_{solar}}$, $\beta_2 = \frac{h_p p_A}{\rho_A C_{pA} s_A}$ and $\gamma_1 = \frac{Q_r w}{\rho_A C_{pA} s_A T_r}$. Therefore, the solar collector system can be described by the following coupled PDE and ODE system:

$$\begin{aligned} \frac{\partial x_1}{\partial t} &= -\alpha_1 \frac{\partial x_1}{\partial \zeta} + \beta_1(x_2 - x_1) \\ \frac{dx_2}{dt} &= \beta_2(x_{1in} - x_2) + \gamma_1 u_1 \\ y_1(t) &= x_1(L,t) \end{aligned} \tag{3.9}$$

By considering steady state conditions, one can obtain the following linear system by applying $x_1(\zeta,t) = x_{1ss}(\zeta) + \tilde{x}_1(\zeta,t)$, $x_2(\zeta,t) = x_{2ss}(\zeta) + \tilde{x}_2(\zeta,t)$, and $u_1(t) = u_{1ss} + \tilde{u}_1(t)$:

$$\begin{aligned} \frac{\partial \tilde{x}_1}{\partial t} &= -\alpha_1 \frac{\partial \tilde{x}_1}{\partial \zeta} + \beta_1(\tilde{x}_2 - \tilde{x}_1),\ \tilde{x}_{1in} = \tilde{x}_1(0,t) \\ \frac{d\tilde{x}_2}{dt} &= \beta_2(\tilde{x}_{1in} - \tilde{x}_2) + \gamma_1 \tilde{u}_1 \\ \tilde{y}_1(t) &= \tilde{x}_1(L,t) \end{aligned} \tag{3.10}$$

and we assume $x_1(0,t)$ operates around steady state, thus $\tilde{x}_{1in} = \tilde{x}_1(0,t) = 0$.

The discrete system can be obtained by using the time discretization method described in Eq.3.4-3.5. According to Eq.3.4, the resolvent of the system is calculated by using Laplace transform and the following representation: $X_1(\zeta,t) = \begin{bmatrix} \tilde{x}_1(\zeta,t) \\ \tilde{x}_2(t) \end{bmatrix}$,

$U_1(t) = \tilde{u}_1(t)$, $A_1 = \begin{bmatrix} -\alpha_1 \frac{\partial}{\partial \zeta} - \beta_1 & \beta_1 \\ 0 & -\beta_2 \end{bmatrix}$, $B_1 = \begin{bmatrix} 0 \\ \gamma_1 \end{bmatrix}$ and $C_1 = \begin{bmatrix} C & 0 \end{bmatrix}$, here the operator $C[f(\zeta)] = \int_0^L f(\zeta)\delta(\zeta - L)d\zeta = f(L)$. Thus, the solar collector system can be expressed as:

$$\begin{aligned} \dot{X}_1(t) &= A_1 X_1(t) + B_1 U_1(t) \\ Y_1(t) &= C_1 X_1(t) \end{aligned} \tag{3.11}$$

From Eq.3.11, one can obtain the Laplace transformation with the mild assumption that $\alpha_1 = 1$ (in general even $\alpha_1(\zeta)$ can be considered):

$$\begin{aligned} s\tilde{x}_1(\zeta, s) - \tilde{x}_1(\zeta, 0) &= -\frac{\partial \tilde{x}_1(\zeta, s)}{\partial \zeta} + \beta_1[\tilde{x}_2(s) - \tilde{x}_1(\zeta, s)] \\ s\tilde{x}_2(s) - \tilde{x}_2(0) &= -\beta_2 \tilde{x}_2(s) \end{aligned} \tag{3.12}$$

Solving the above set of equations, the resolvent of the operator A_1 is expressed as:

$$R(s, A_1) = [sI - A_1]^{-1} X_1(\zeta, 0) = \begin{bmatrix} R_{11} & R_{12} \\ R_{21} & R_{22} \end{bmatrix} X_1(\zeta, 0) \tag{3.13}$$

where $R_{11} = \int_0^\zeta (\cdot) e^{\int_0^\eta (s+\beta_1)d\phi} d\eta e^{-\int_0^\zeta (s+\beta_1)d\phi}$,
$R_{12} = \frac{\beta_1}{s+\beta_2} \int_0^\zeta (\cdot) e^{\int_0^\eta (s+\beta_1)d\phi} d\eta e^{-\int_0^\zeta (s+\beta_1)d\phi}$, $R_{21} = 0$ and $R_{22} = \frac{1}{s+\beta_2}$.

Finally, the discrete system can be expressed as:

$$\begin{aligned} X_1(k) &= A_{d1} X_1(k-1) + B_{d1} U_1(k) \\ Y_1(k) &= C_{d1} X_1(k-1) + D_{d1} U_1(k) \end{aligned} \tag{3.14}$$

here, the discrete operators A_{d1}, B_{d1}, C_{d1} and D_{d1} are given directly as follows:

$$A_{d1}(\cdot) = [-I + 2\delta[\delta - A_1]^{-1}](\cdot) = \begin{bmatrix} A_{d1-11} & A_{d1-12} \\ A_{d1-21} & A_{d1-22} \end{bmatrix}(\cdot)$$

where $A_{d1-11} = -(\cdot) + 2\delta \int_0^{\zeta}(\cdot)e^{\int_0^{\eta}(\delta+\beta_1)d\phi}d\eta e^{-\int_0^{\zeta}(\delta+\beta_1)d\phi}$,
$A_{d1-12} = \frac{2\delta\beta_1}{\delta+\beta_2}\int_0^{\zeta}(\cdot)e^{\int_0^{\eta}(\delta+\beta_1)d\phi}d\eta e^{-\int_0^{\zeta}(\delta+\beta_1)d\phi}$, $A_{d1-21} = 0$, and $A_{d1-22} = -(\cdot) + \frac{2\delta}{\delta+\beta_2}(\cdot)$, while the discrete input operator is:

$$B_{d1} = \sqrt{2\delta}[\delta - A_1]^{-1}B_1 = \begin{bmatrix} B_{d1-1} \\ B_{d1-2} \end{bmatrix}$$

where $B_{d1-1} = \frac{\sqrt{2\delta}\beta_1}{\delta+\beta_2}\int_0^{\zeta}\gamma_1 e^{\int_0^{\eta}(\delta+\beta_1)d\phi}d\eta e^{-\int_0^{\zeta}(\delta+\beta_1)d\phi}$ and $B_{d1-2} = \frac{\sqrt{2\delta}}{\delta+\beta_2}\gamma_1$. The output operator,

$$C_{d1}(\cdot) = \sqrt{2\delta}C_1[\delta - A_1]^{-1}(\cdot) = \begin{bmatrix} C_{d1-1} & C_{d1-2} \end{bmatrix}(\cdot)$$

where $C_{d1-1} = \sqrt{2\delta}\int_0^{L}(\cdot)e^{\int_0^{\eta}(\delta+\beta_1)d\phi}d\eta e^{-\int_0^{L}(\delta+\beta_1)d\phi}$,
and $C_{d1-2} = \frac{\sqrt{2\delta}\beta_1}{\delta+\beta_2}\int_0^{L}(\cdot)e^{\int_0^{\eta}(\delta+\beta_1)d\phi}d\eta e^{-\int_0^{L}(\delta+\beta_1)d\phi}$, while the feedthrough operator is:

$$D_{d1} = C_1[\delta - A_1]^{-1}B_1 = \frac{\beta_1}{\delta+\beta_2}\int_0^{L}\gamma_1 e^{\int_0^{\eta}(\delta+\beta_1)d\phi}d\eta e^{-\int_0^{L}(\delta+\beta_1)d\phi}$$

3.3.3 Borehole Thermal Energy Storage System

The borehole thermal energy storage system uses a grid of boreholes with U-tube heat exchangers [79]. The energy balance of the flow in the U-tube heat exchanger is

Table 3.1: Parameters of the solar system used to model Eq.3.7-3.8.

Variable	Unit	Description
T_{solar}	K	Flow temperature out of solar system
T_A	K	Temperature of the absorber
F_{solar}	kg/s	Flow rate of the solar system
C_{pgl}	J/kgK	Heat capacity of glycol in the solar system
C_{pA}	J/kgK	Pipe heat capacity
Q_{solar}	W/m^2	Solar system heat flux
w	m	Solar collector width
ρ_{gl}	kg/m^3	Density of hot glycol flow
ρ_A	kg/m^3	Density of pipe
s_{solar}	m^2	Area of glycol flow
h_p	W/m^2K	Convective heat transfer coefficient for the pipe
p_A	m	Absorber pipe perimeter

given as:

$$\rho_{H_2O} C_{pH_2O} s_{borehole} \frac{\partial T_{borehole}}{\partial t} = -C_{pH_2O} F_{borehole} \frac{\partial T_{borehole}}{\partial \zeta} + h_w p_W (T_W - T_{borehole}) \tag{3.15}$$

The energy balance of the pipe wall is:

$$\rho_W C_{pW} s_W \frac{dT_W}{dt} = h_w p_W (T_{borehole-in} - T_W) + Q_{borehole} w \tag{3.16}$$

the description of the system variables is shown in Table.3.2.

We consider the following change of variables with states $x_3 = \frac{T_{borehole} - T_r}{T_r}$, $x_4 = \frac{T_W - T_r}{T_r}$, and input $u_2 = \frac{Q_{borehole}}{Q_r}$. The system parameters are $\alpha_3 = \frac{F_{borehole}}{\rho_{H_2O} s_{borehole}}$, $\beta_3 = \frac{h_w p_W}{\rho_{H_2O} C_{pH_2O} s_{borehole}}$, $\beta_4 = \frac{h_w p_W}{\rho_W C_{pW} s_W}$ and $\gamma_2 = \frac{Q_r w}{\rho_W C_{pW} s_W T_r}$. By applying linearization around the steady state of interest, the BTES system is described by the following

Table 3.2: Parameters of the borehole thermal energy storage system used to model Eq.3.15-3.16

Variable	Unit	Description
$T_{borehole}$	K	Flow temperature out of borehole system
T_W	K	Temperature of the pipe wall
$F_{borehole}$	kg/s	Flow rate of the borehole system
C_{pH_2O}	J/kgK	Heat capacity of water in the borehole system
C_{pW}	J/kgK	Heat capacity of the pipe wall
$Q_{borehole}$	W/m^2	Collected Energy of the borehole system
w	m	Width of the borehole system
ρ_{H_2O}	kg/m^3	Density of hot water flow
ρ_W	kg/m^3	Density of pipe wall
$s_{borehole}$	m^2	Area of water flow
h_w	W/m^2K	Convective heat transfer coefficient for the pipe wall
p_W	m	Pipe wall perimeter

coupled PDE and ODE:

$$\begin{aligned} \frac{\partial \tilde{x}_3}{\partial t} &= -\alpha_3 \frac{\partial \tilde{x}_3}{\partial \zeta} + \beta_3(\tilde{x}_4 - \tilde{x}_3),\ \tilde{x}_{3in} = \tilde{x}_3(0,t) \\ \frac{d\tilde{x}_4}{dt} &= \beta_4(\tilde{x}_{3in} - \tilde{x}_4) + \gamma_2 \tilde{u}_2 \\ \tilde{y}_2(t) &= \tilde{x}_3(L,t) \end{aligned} \tag{3.17}$$

and we assume that $x_3(0,t)$ operates around the steady state of interest, thus $\tilde{x}_{3in} = \tilde{x}_3(0,t) = 0$. By considering $X_2(\zeta,t) = \begin{bmatrix} \tilde{x}_3(\zeta,t) \\ \tilde{x}_4(t) \end{bmatrix}$, $U_2(t) = \tilde{u}_2(t)$,

$A_2 = \begin{bmatrix} -\alpha_3 \frac{\partial}{\partial \zeta} - \beta_3 & \beta_3 \\ 0 & -\beta_4 \end{bmatrix}$, $B_2 = \begin{bmatrix} 0 \\ \gamma_2 \end{bmatrix}$ and $C_2 = \begin{bmatrix} C & 0 \end{bmatrix}$, here operator

$C[f(\zeta)] = \int_0^L f(\zeta)\delta(\zeta - L)d\zeta = f(L)$. Finally, the BTES system can be expressed as:

$$\begin{aligned} \dot{X}_2(t) &= A_2 X_2(t) + B_2 U_2(t) \\ Y_2(t) &= C_2 X_2(t) \end{aligned} \tag{3.18}$$

and discrete system can be expressed as:

$$\begin{aligned} X_2(k) &= A_{d2} X_2(k-1) + B_{d2} U_2(k) \\ Y_2(k) &= C_{d2} X_2(k-1) + D_{d2} U_2(k) \end{aligned} \tag{3.19}$$

The model of BTES system is similar to the model of the solar collector system, thus, the expression of a discrete BTES system is similar to the solar thermal energy system with different parameters.

3.3.4 System of Heat Exchanger

The heat exchanger in the solar thermal system is a counter-current heat exchanger which is modelled by a set of coupled first-order hyperbolic partial differential equations [77]. Despite the non-linearity of the controlled system, an explicit characterization of the equilibrium profiles can be given. As a consequence, the linearized system around an equilibrium profile is obtained as a linear infinite dimensional time-invariant system.

According to the heat exchange balance, we obtain the following differential equations for the heat exchanger HX-1:

$$\frac{\partial T_{HX-11}(\zeta,t)}{\partial t} = \frac{F_{HX-11}}{\rho_{gl} s_1} \frac{\partial T_{HX-11}(\zeta,t)}{\partial \zeta} - \frac{kl}{C_{pgl}\rho_{gl} s_1}[T_{HX-11}(\zeta,t) - T_{HX-12}(\zeta,t)] \tag{3.20}$$

$$\frac{\partial T_{HX-12}(\zeta,t)}{\partial t} = -\frac{F_{HX-12}}{\rho_{H_2O}s_2}\frac{\partial T_{HX-12}(\zeta,t)}{\partial \zeta} + \frac{kl}{C_{pH_2O}\rho_{H_2O}s_2}[T_{HX-11}(\zeta,t) - T_{HX-12}(\zeta,t)]$$

the description of the system variables is shown in Table.3.3.

Table 3.3: Parameters of heat exchanger HX-1 used to model Eq.3.20

Variable	Unit	Description
$T_{HX-11}(\zeta,t)$	K	Temperature of hot flow in the HX-1 system
$T_{HX-12}(\zeta,t)$	K	Temperature of cold flow in the HX-1 system
$T_{HX-11}(L,t) = T_{solarin}$	K	Temperature of hot flow into the HX-1 system
$T_{HX-11}(0,t) = T_{solar}$	K	Temperature of hot flow out of the HX-1 system
$T_{HX-12}(L,t) = T_{HT-1}$	K	Temperature of cold flow out of the HX-1 system
$T_{HX-12}(0,t) = T_{CT-1}$	K	Temperature of cold flow into the HX-1 system
$F_{HX-11} = F_{solar}$	kg/s	Flow rate of hot flow into the HX-1 system
$F_{HX-12} = F_{HX-1}$	kg/s	Flow rate of cold flow into the HX-1 system
k	W/m^2K	Exchange coefficient
$l = 2\pi r_2$	m	Contact circumference of the exchanger
$s_1 = \pi(r_1^2 - r_2^2)$,$r_1 > r_2$	m^2	Area of hot flow
$s_2 = \pi r_2^2$	m^2	Area of cold flow

The change of variables leads to the states given as $x_5 = \frac{T_{HX-11}-T_r}{T_r}$ and $x_6 = \frac{T_{HX-12}-T_r}{T_r}$, input $u_3 = \frac{F_{HX-12}}{F_r}$, and parameters $F_1 = \frac{F_{HX-11}}{F_r}$, $\alpha_5 = \frac{F_r}{\rho_{gl}s_1}$, $\beta_5 = \frac{kl}{C_{pgl}\rho_{gl}s_1}$, $\alpha_6 = \frac{F_r}{\rho_{H_2O}s_2}$ and $\beta_6 = \frac{kl}{C_{pH_2O}\rho_{H_2O}s_2}$. The linearized heat exchanger system is described

by the following hyperbolic PDEs:

$$\begin{aligned}
&\frac{\partial \tilde{x}_5(\zeta,t)}{\partial t} = \alpha_5 F_1 \frac{\partial \tilde{x}_5(\zeta,t)}{\partial \zeta} - \beta_5[\tilde{x}_5(\zeta,t) - \tilde{x}_6(\zeta,t)] \\
&\frac{\partial \tilde{x}_6(\zeta,t)}{\partial t} = -\alpha_6 u_3(t) \frac{\partial \tilde{x}_6(\zeta,t)}{\partial \zeta} + \beta_6[\tilde{x}_5(\zeta,t) - \tilde{x}_6(\zeta,t)] - \alpha_6 \tilde{u}_3(t) \frac{dx_{6ss}(\zeta)}{d\zeta} \\
&\tilde{y}_6(t) = z_6(L,t) + B_6(L)\tilde{x}_6(0,t)
\end{aligned} \tag{3.21}$$

It is important to note that the linearized system around an equilibrium point is governed by the above equations with $u_3(t)$ replaced by u_{3ss}.

The heat exchanger transfers the energy from the solar system to the hot tank system, the flow into the state x_5 is the flow out of the solar system which enters the heat exchanger at $\zeta = L$, thus, $\tilde{x}_5(L,t) = \tilde{x}_1(L,t)$, see Fig.3.2. The flow into the heat exchanger state x_6 at $\zeta = 0$ is the flow out of the cold tank system. Since the cold tank is at the reference temperature, one can obtain $\tilde{x}_6(0,t) = 0$.

Since the heat exchanger system is potentially exposed to boundary disturbances, the boundary conditions need to be adequately considered in this coupled hyperbolic PDEs system. In the ensuing section, we accurately account for boundary influence and transfer the boundary applied disturbance to the in-domain disturbance.

The standard methodology to accurately account for transfer of boundary actuation to in-domain is to apply state transformation. Let $\tilde{x}_5(\zeta,t) = z_5(\zeta,t) + B_5(\zeta)\tilde{x}_5(L,t)$, then $z_5(L,t) = 0$, $B_5(L) = 1$, $\tilde{x}_6(\zeta,t) = z_6(\zeta,t) + B_6(\zeta)\tilde{x}_6(0,t)$, then $z_6(0,t) = 0$, $B_6(0) = 1$. With the assumptions $\alpha_5 F_1 = 1$, $\alpha_6 u_{3ss} = 1$, $\gamma_3 = \alpha_6 \frac{dx_{6ss}(\zeta)}{d\zeta}$, the above system becomes:

$$\frac{\partial z_5(\zeta,t)}{\partial t} = \frac{\partial z_5(\zeta,t)}{\partial \zeta} - \beta_5[z_5(\zeta,t) - z_6(\zeta,t)] - B_5(\zeta)\frac{\partial \tilde{x}_5(L,t)}{\partial t} \tag{3.22}$$

$$
\begin{aligned}
&+[\frac{\partial B_5(\zeta)}{\partial \zeta} - \beta_5 B_5(\zeta)]\tilde{x}_5(L,t) + \beta_5 B_6(\zeta)\tilde{x}_6(0,t) \\
&\frac{\partial z_6(\zeta,t)}{\partial t} = -\frac{\partial z_6(\zeta,t)}{\partial \zeta} + \beta_6[z_5(\zeta,t) - z_6(\zeta,t)] - B_6(\zeta)\frac{\partial \tilde{x}_6(0,t)}{\partial t} \\
&-[\frac{\partial B_6(\zeta)}{\partial \zeta} + \beta_6 B_6(\zeta)]\tilde{x}_6(0,t) + \beta_6 B_5(\zeta)\tilde{x}_5(L,t) - \gamma_3 \tilde{u}_3(t)
\end{aligned}
$$

With the assumption $\frac{\partial B_5(\zeta)}{\partial \zeta} - \beta_5 B_5(\zeta) = 0$ and $\frac{\partial B_6(\zeta)}{\partial \zeta} + \beta_6 B_6(\zeta) = 0$, one can obtain the analytic expressions of $B_5(\zeta)$ and $B_6(\zeta)$. Finally, the extended system can be expressed as follows:

$$
\begin{aligned}
\frac{\partial}{\partial t}\begin{bmatrix} z_5(\zeta,t) \\ z_6(\zeta,t) \\ \tilde{x}_5(L,t) \\ \tilde{x}_6(0,t) \end{bmatrix} &= \begin{bmatrix} \frac{\partial}{\partial \zeta} - \beta_5 & \beta_5 & 0 & \beta_5 B_6(\zeta) \\ \beta_6 & -\frac{\partial}{\partial \zeta} - \beta_6 & \beta_6 B_5(\zeta) & 0 \\ 0 & 0 & 0 & 0 \\ 0 & 0 & 0 & 0 \end{bmatrix}\begin{bmatrix} z_5(\zeta,t) \\ z_6(\zeta,t) \\ \tilde{x}_5(L,t) \\ \tilde{x}_6(0,t) \end{bmatrix} \\
&+ \begin{bmatrix} -B_5(\zeta) & 0 \\ 0 & -B_6(\zeta) \\ 1 & 0 \\ 0 & 1 \end{bmatrix}\begin{bmatrix} \bar{x}_5(L,t) \\ \bar{x}_6(0,t) \end{bmatrix} + \begin{bmatrix} 0 \\ -\gamma_3 \\ 0 \\ 0 \end{bmatrix}\tilde{u}_3(t) \qquad (3.23) \\
\tilde{y}_6(t) &= \begin{bmatrix} 0 & C & 0 & B_6(L) \end{bmatrix}\begin{bmatrix} z_5(\zeta,t) \\ z_6(\zeta,t) \\ \tilde{x}_5(L,t) \\ \tilde{x}_6(0,t) \end{bmatrix}
\end{aligned}
$$

where $\bar{x}_5(L,t) = \frac{\partial \tilde{x}_5(L,t)}{\partial t}$, $\bar{x}_6(0,t) = \frac{\partial \tilde{x}_6(0,t)}{\partial t}$ and the operator $C[f(\zeta)] = \int_0^L f(\zeta)\delta(\zeta - L)d\zeta = f(L)$.

We define extended state to be $Z_3 = \begin{bmatrix} z_5(\zeta,t) & z_6(\zeta,t) & \tilde{x}_5(L,t) & \tilde{x}_6(0,t) \end{bmatrix}^T$,

then, the above system can be expressed as:

$$\dot{Z}_3(t) = A_{z3}Z_3(t) + B_{z3}U_3(t) + E_{z3}G_3(t) \tag{3.24}$$
$$Y_3(t) = C_{z3}Z_3(t)$$

By applying Laplace transform with the boundary conditions $z_5(1,s) = 0$ and $z_6(0,s) = 0$, the resolvent of the operator A_{z3} can be expressed as follows:

$$R(s, A_{z3}) = [sI - A_{z3}]^{-1}Z_3(\zeta, 0) = \begin{bmatrix} R_{11} & R_{12} & R_{13} & R_{14} \\ R_{21} & R_{22} & R_{23} & R_{24} \\ 0 & 0 & R_{33} & 0 \\ 0 & 0 & 0 & R_{44} \end{bmatrix} Z_3(\zeta, 0) \tag{3.25}$$

where

$$R_{11} = \frac{e^{a\zeta}cosh(b\zeta) + ce^{a\zeta}sinh(b\zeta)}{e^a cosh(b) + ce^a sinh(b)} \int_0^1 [e^{a(1-\eta)}cosh(b(1-\eta)) + ce^{a(1-\eta)}sinh(b(1-\eta))](\cdot)d\eta$$
$$- \int_0^\zeta [e^{a(\zeta-\eta)}cosh(b(\zeta-\eta)) + ce^{a(\zeta-\eta)}sinh(b(\zeta-\eta))](\cdot)d\eta$$
$$R_{12} = \frac{e^{a\zeta}cosh(b\zeta) + ce^{a\zeta}sinh(b\zeta)}{e^a cosh(b) + ce^a sinh(b)} \int_0^1 \frac{\beta_5}{b} e^{a(1-\eta)}sinh(b(1-\eta))(\cdot)d\eta$$
$$- \int_0^\zeta \frac{\beta_5}{b} e^{a(\zeta-\eta)}sinh(b(\zeta-\eta))(\cdot)d\eta$$
$$R_{21} = \frac{\frac{\beta_6}{b}e^{a\zeta}sinh(b\zeta)}{e^a cosh(b) + ce^a sinh(b)} \int_0^1 [e^{a(1-\eta)}cosh(b(1-\eta)) + ce^{a(1-\eta)}sinh(b(1-\eta))](\cdot)d\eta$$
$$- \int_0^\zeta \frac{\beta_6}{b} e^{a(\zeta-\eta)}sinh(b(\zeta-\eta))(\cdot)d\eta$$
$$R_{22} = \frac{\frac{\beta_6}{b}e^{a\zeta}sinh(b\zeta)}{e^a cosh(b) + ce^a sinh(b)} \int_0^1 \frac{\beta_5}{b} e^{a(1-\eta)}sinh(b(1-\eta))(\cdot)d\eta$$
$$+ \int_0^\zeta [e^{a(\zeta-\eta)}cosh(b(\zeta-\eta)) - ce^{a(\zeta-\eta)}sinh(b(\zeta-\eta))](\cdot)d\eta$$

$$R_{13} = \frac{e^{a\zeta}cosh(b\zeta) + ce^{a\zeta}sinh(b\zeta)}{e^{a}cosh(b) + ce^{a}sinh(b)} \int_0^1 \frac{\beta_5}{b} e^{a(1-\eta)}sinh(b(1-\eta))\beta_6 B_5(\eta)\frac{1}{s}(\cdot)d\eta$$
$$- \int_0^\zeta \frac{\beta_5}{b} e^{a(\zeta-\eta)}sinh(b(\zeta-\eta))\beta_6 B_5(\eta)\frac{1}{s}(\cdot)d\eta$$
$$R_{14} = \frac{e^{a\zeta}cosh(b\zeta) + ce^{a\zeta}sinh(b\zeta)}{e^{a}cosh(b) + ce^{a}sinh(b)} \int_0^1 [e^{a(1-\eta)}cosh(b(1-\eta)) + ce^{a(1-\eta)}sinh(b(1-\eta))]\beta_5 B_6(\eta)\frac{1}{s}(\cdot)d\eta$$
$$- \int_0^\zeta [e^{a(\zeta-\eta)}cosh(b(\zeta-\eta)) + ce^{a(\zeta-\eta)}sinh(b(\zeta-\eta))]\beta_5 B_6(\eta)\frac{1}{s}(\cdot)d\eta$$
$$R_{23} = \frac{\frac{\beta_6}{b}e^{a\zeta}sinh(b\zeta)}{e^{a}cosh(b) + ce^{a}sinh(b)} \int_0^1 \frac{\beta_5}{b} e^{a(1-\eta)}sinh(b(1-\eta))\beta_6 B_5(\eta)\frac{1}{s}(\cdot)d\eta$$
$$+ \int_0^\zeta [e^{a(\zeta-\eta)}cosh(b(\zeta-\eta)) - ce^{a(\zeta-\eta)}sinh(b(\zeta-\eta))]\beta_6 B_5(\eta)\frac{1}{s}(\cdot)d\eta$$
$$R_{24} = \frac{\frac{\beta_6}{b}e^{a\zeta}sinh(b\zeta)}{e^{a}cosh(b) + ce^{a}sinh(b)} \int_0^1 [e^{a(1-\eta)}cosh(b(1-\eta)) + ce^{a(1-\eta)}sinh(b(1-\eta))]\beta_5 B_6(\eta)\frac{1}{s}(\cdot)d\eta$$
$$- \int_0^\zeta \frac{\beta_6}{b} e^{a(\zeta-\eta)}sinh(b(\zeta-\eta))\beta_5 B_6(\eta)\frac{1}{s}(\cdot)d\eta$$
$$R_{33} = \frac{1}{s}(\cdot)$$
$$R_{44} = \frac{1}{s}(\cdot)$$

with $a = \frac{\beta_5-\beta_6}{2}$, $b = \sqrt{\frac{(\beta_5-\beta_6)^2}{4} + s^2 + (\beta_5+\beta_6)s}$ and $c = \frac{2s+\beta_5+\beta_6}{2b}$.

The discrete system is expressed as:

$$Z_3(k) = A_{dz3}Z_3(k-1) + B_{dz3}U_3(k) + E_{dz3}G_3(k) \tag{3.26}$$
$$Y_3(k) = C_{dz3}Z_3(k-1) + D_{dz3}U_3(k) + F_{dz3}G_3(k)$$

The discrete operators in the above equation are $A_{dz3}(\cdot) = [-I + 2\delta[\delta - A_{z3}]^{-1}](\cdot)$, $B_{dz3} = \sqrt{2\delta}[\delta - A_{z3}]^{-1}B_{z3}$, $C_{dz3}(\cdot) = \sqrt{2\delta}C_{z3}[\delta - A_{z3}]^{-1}(\cdot)$, $D_{dz3} = C_{z3}[\delta - A_{z3}]^{-1}B_{z3}$, $E_{dz3} = \sqrt{2\delta}[\delta - A_{z3}]^{-1}E_{z3}$ and $F_{dz3} = C_{z3}[\delta - A_{z3}]^{-1}E_{z3}$.

The original states are obtained by the following transform:

$$\begin{bmatrix} \tilde{x}_5(\zeta,k) \\ \tilde{x}_6(\zeta,k) \end{bmatrix} = \begin{bmatrix} z_5(\zeta,k) \\ z_6(\zeta,k) \end{bmatrix} + \begin{bmatrix} B_5(\zeta)\tilde{x}_5(L,k) \\ B_6(\zeta)\tilde{x}_6(0,k) \end{bmatrix}.$$

3.3.5 Short Term Thermal Storage System

Hot Tank System

The mass balance and energy balance of the hot tank system is modelled by the following equations [5]:

$$\begin{aligned} A_{HT}\frac{dh_{HT}}{dt} &= F_{HT-1} + F_{HT-2} - F_{HT-3} \\ \rho_{H_2O}C_{pH_2O}A_{HT}\frac{dh_{HT}T_{HT}}{dt} &= \rho_{H_2O}C_{pH_2O}[F_{HX-1}T_{HT-1} + F_{HT-2}T_{HT-2} - F_{HT-3}T_{HT}] \end{aligned} \tag{3.27}$$

where F_{HT-1} and F_{HT-2} are flow rates from the heat exchanger system and the BTES system. F_{HT-3} is flow rate out of the hot tank and $F_{HT-3} = \frac{1}{K_1}h_{HT}$. The description of the system variables is shown in Table.3.4.

The following change of variables is considered, states $x_7 = \frac{h_{HT}}{h_r}$ and $x_8 = \frac{T_{HT}-T_r}{T_r}$, and inputs $u_4 = \frac{F_{HT-1}}{F_r}$, $u_5 = \frac{F_{HT-2}}{F_r}$ and $u_6 = \frac{F_{HT-3}}{F_r}$. Disturbances $x_{8in1} = \frac{T_{HT-1}-T_r}{T_r}$ and $x_{8in2} = \frac{T_{HT-2}-T_r}{T_r}$, and parameter $\beta_7 = \frac{F_r}{h_r A_{HT}}$, the hot tank system is described by the following ODEs:

$$\begin{aligned} \frac{dx_7}{dt} &= \beta_7(u_4 + u_5 - u_6) \\ \frac{d[x_7(x_8+1)]}{dt} &= \beta_7(u_4(x_{8in1}+1) + u_5(x_{8in2}+1) - u_6(x_8+1)) \\ y_8(t) &= x_8(t) \end{aligned} \tag{3.28}$$

One can obtain the linearized system, $x_7(t) = x_{7ss} + \tilde{x}_7(t)$, $x_8(t) = x_{8ss} + \tilde{x}_8(t)$, $u_4(t) = u_{4ss} + \tilde{u}_4(t)$, $u_5(t) = u_{5ss} + \tilde{u}_5(t)$ and $u_6(t) = \frac{1}{K_1}x_7(t) = \frac{1}{K_1}(x_{7ss} + \tilde{x}_7(t))$. The Taylor

expansion around steady state yields $x_7(x_8+1) \simeq x_{7ss}(x_{8ss}+1)+x_{7ss}\tilde{x}_8+(x_{8ss}+1)\tilde{x}_7$ and $u_6(x_8+1)=\frac{1}{K_1}x_7(x_8+1)$, so the system becomes:

$$\begin{aligned}
&\frac{d\tilde{x}_7(t)}{dt} = \beta_7[\tilde{u}_4(t)+\tilde{u}_7(t)-\frac{1}{K_1}\tilde{x}_7(t)] \\
&\frac{d\tilde{x}_8(t)}{dt} = \frac{\beta_7}{x_{7ss}}[(x_{8in1ss}-x_{8ss})\tilde{u}_4(t)+(x_{8in2ss}-x_{8ss})\tilde{u}_5(t) \\
&+u_{4ss}\tilde{x}_{8in1}+u_{5ss}\tilde{x}_{8in2}-\frac{1}{K_1}x_{7ss}\tilde{x}_8(t)] \\
&\tilde{y}_8(t) = \tilde{x}_8(t)
\end{aligned} \tag{3.29}$$

The flows which come into the hot tank are from the heat exchanger system and the borehole thermal energy storage system, see Fig.3.2, thus, we have the conditions: $\tilde{x}_{8in1} = \tilde{x}_6(L,t)$ and $\tilde{x}_{8in2} = \tilde{x}_3(L,t)$. With the representations of $X_4(\zeta,t)=\begin{bmatrix}\tilde{x}_7(t)\\ \tilde{x}_8(t)\end{bmatrix}$, $U_4(t)=\begin{bmatrix}\tilde{u}_4(t)\\ \tilde{u}_5(t)\end{bmatrix}$, $G_4=\begin{bmatrix}\tilde{x}_{8in1}(t)\\ \tilde{x}_{8in2}(t)\end{bmatrix}$, $A_4=\begin{bmatrix}-\frac{\beta_7}{K_1} & 0\\ 0 & -\frac{\beta_7}{K_1}\end{bmatrix}$, $B_4=\begin{bmatrix}\beta_7 & \beta_7\\ \frac{\beta_7(x_{8in1ss}-x_{8ss})}{x_{7ss}} & \frac{\beta_7(x_{8in2ss}-x_{8ss})}{x_{7ss}}\end{bmatrix}$, $E_4=\begin{bmatrix}0 & 0\\ u_{4ss} & u_{5ss}\end{bmatrix}$ and $C_4=\begin{bmatrix}0 & 1\end{bmatrix}$, the hot tank system is expressed as:

$$\begin{aligned}
&\dot{X}_4(t) = A_4X_4(t)+B_4U_4(t)+E_4G_4(t) \\
&Y_4(t) = C_4X_4(t)
\end{aligned} \tag{3.30}$$

and the discrete system can be expressed as:

$$\begin{aligned}
&X_4(k) = A_{d4}X_4(k-1)+B_{d4}U_4(k)+E_{d4}G_4(k) \\
&Y_4(k) = C_{d4}X_4(k-1)+D_{d4}U_4(k)+F_{d4}G_4(k)
\end{aligned} \tag{3.31}$$

here $A_{d4} = \begin{bmatrix} \frac{2\delta}{\delta+\frac{\beta_7}{K_1}} - 1 & 0 \\ 0 & \frac{2\delta}{\delta+\frac{\beta_7}{K_1}} - 1 \end{bmatrix}$, $B_{d4} = \sqrt{2\delta} \begin{bmatrix} \frac{\frac{\beta_7}{\delta+\frac{\beta_7}{K_1}}}{\frac{\beta_7}{x_{7ss}}(x_{8in1}-x_{8ss})} & \frac{\frac{\beta_7}{\delta+\frac{\beta_7}{K_1}}}{\frac{\beta_7}{x_{7ss}}(x_{8in2}-x_{8ss})} \\ \delta+\frac{\beta_7}{K_1} & \delta+\frac{\beta_7}{K_1} \end{bmatrix}$,

$C_{d4} = \sqrt{2\delta} \begin{bmatrix} 0 & \frac{1}{\delta+\frac{\beta_7}{K_1}} \end{bmatrix}$, $D_{d4} = \begin{bmatrix} \frac{\frac{\beta_7}{x_{7ss}}(x_{8in1}-x_{8ss})}{\delta+\frac{\beta_7}{K_1}} & \frac{\frac{\beta_7}{x_{7ss}}(x_{8in2}-x_{8ss})}{\delta+\frac{\beta_7}{K_1}} \end{bmatrix}$,

$E_{d4} = \sqrt{2\delta} \begin{bmatrix} 0 & 0 \\ \frac{\beta_7 u_{4ss}}{x_{7ss}(\delta+\frac{\beta_7}{K_1})} & \frac{\beta_7 u_{7ss}}{x_{7ss}(\delta+\frac{\beta_7}{K_1})} \end{bmatrix}$, and $F_{d4} = \begin{bmatrix} \frac{\beta_7 u_{4ss}}{x_{7ss}(\delta+\frac{\beta_7}{K_1})} & \frac{\beta_7 u_{7ss}}{x_{7ss}(\delta+\frac{\beta_7}{K_1})} \end{bmatrix}$.

Table 3.4: Parameters of hot tank system used to model Eq.3.27.

Variable		Unit	Description
h_{HT}		m	Height of flow in the hot tank
T_{HT-1}	=	K	Temperature of hot flow from the HX-1 system
$T_{HX-12}(L,t)$			
$T_{HT-2} = T_{borehole}$		K	Temperature of hot flow from the borehole system
$T_{HT} = T_{boilerin}$		K	Temperature of hot flow to the natural gas boiler system
$F_{HT-1} = F_{HX-1}$		kg/s	Flow rate of hot flow from the HX-1 system
$F_{HT-2} = F_{borehole}$		kg/s	Flow rate of hot flow from the borehole system
$F_{HT-3} = F_{boiler}$		kg/s	Flow rate of hot flow to the natural gas boiler system
A_{HT}		m^2	Hot tank area

Cold Tank System

In Fig.3.2, the flow coming into the cold tank F_{CT-1} is from the district heating loop system. The flows out of the cold tank are linked to the solar thermal system and the BTES system, which are F_{CT-2} and F_{CT-3}. Here, we assume that the flow temperature out of the cold tank is at reference environment temperature, which is

$T_{CT-2} = T_{CT-3} = T_{CT} = T_r$. Thus, the disturbances to the solar thermal system and the BTES system are considered as zero. In simulations studies, we do not model the cold tank system.

3.3.6 Natural Gas Boiler System

The energy balance of the flow in the natural gas boiler system is given as follows:

$$\rho_{H_2O} C_{pH_2O} V_{boiler} \frac{dT_{boiler}}{dt} = C_{pH_2O} F_{boiler} (T_{boilerin} - T_{boiler}) + Q_{boiler} s_{boiler} \tag{3.32}$$

The description of the system variables is shown in Table.3.5.

Table 3.5: Parameters of the natural gas boiler system used to model Eq.3.32.

Variable	Unit	Description
T_{boiler}	K	Temperature of flow out of the boiler system
F_{boiler}	kg/s	Boiler system flow rate
V_{boiler}	m^3	Boiler system flow volum
Q_{boiler}	W/m^2	Boiler system collected energy
s_{boiler}	m^2	Boiler system area

Let us consider the following change of variables: state $x_9(t) = \frac{x_9(t) - T_r}{T_r}$, input $u_6(t) = \frac{Q_{boiler}}{Q_r}$ and parameters $\beta_9 = \frac{F_{boiler}}{\rho_{H_2O} V_{boiler}}$ and $\gamma_6 = \frac{Q_{boiler} s_{boiler} Q_r}{\rho_{H_2O} C_{pH_2O} V_{boiler} T_r}$. The linearized natural gas system is described by the following ODE:

$$\begin{aligned} \frac{d\tilde{x}_9(t)}{dt} &= \beta_9(\tilde{x}_{9in} - \tilde{x}_9(t)) + \gamma_6 \tilde{u}_6(t) \\ \tilde{y}_9(t) &= \tilde{x}_9(t) \end{aligned} \tag{3.33}$$

here, the flow into the natural gas boiler system is the flow out of the hot tank system,

thus $\tilde{x}_{9in} = \tilde{x}_8$.

The discrete gas boiler system can be expressed as:

$$\begin{aligned} \tilde{x}_9(k) &= A_{d5}\tilde{x}_9(k-1) + B_{d5}\tilde{u}_6(k) + E_{d5}\tilde{x}_{9in}(k) \\ \tilde{y}_9(k) &= C_{d5}\tilde{x}_9(k-1) + D_{d5}\tilde{u}_6(k) + F_{d5}\tilde{x}_{9in}(k) \end{aligned} \tag{3.34}$$

here $A_{d5} = \frac{2\delta}{\delta+\beta_9} - 1$, $B_{d5} = \frac{\sqrt{2\delta}\gamma_6}{\delta+\beta_9}$, $C_{d5} = \frac{\sqrt{2\delta}}{\delta+\beta_9}$, $D_{d5} = \frac{\gamma_6}{\delta+\beta_9}$, $E_{d5} = \frac{\sqrt{2\delta}\beta_9}{\delta+\beta_9}$ and $F_{d5} = \frac{\beta_9}{\delta+\beta_9}$.

3.3.7 District Heating Loop System

The district heating loop system is modelled as a hyperbolic PDE system with the heat sink $Q_{district}$:

$$\rho_{H_2O}C_{pH_2O}s_{district}\frac{\partial T_{district}}{\partial t} = -C_{pH_2O}F_{district}\frac{\partial T_{district}}{\partial \zeta} - Q_{district}w \tag{3.35}$$

The description of the system variables is shown in Table.3.6.

Table 3.6: Parameters of district heating loop system used to model Eq.3.35.

Variable	Unit	Description
$T_{district}$	K	Temperature of flow out of the district system
$F_{district}$	kg/s	Flow rate of the district system
$Q_{district}$	W/m^2	Heat flux of the district system
$s_{district}$	m^2	Area of water flow
w	m	District system width

The dimensionless system is obtained by considering the following change of variables: state $x_{10} = \frac{T_{district}-T_r}{T_r}$, input $u_7 = \frac{Q_{district}}{Q_r}$, and parameters $\alpha_{10} = \frac{F_{district}}{\rho_{H_2O}s_{district}}$

and $\gamma_7 = \frac{wQ_r}{\rho_{H_2O} C_{pH_2O} s_{district} T_r}$. By applying linearization, the district heating loop system becomes:

$$\begin{aligned} \frac{\partial \tilde{x}_{10}}{\partial t} &= -\alpha_{10} \frac{\partial \tilde{x}_{10}}{\partial \zeta} - \gamma_7 \tilde{u}_7 \\ \tilde{y}_{10}(t) &= \tilde{x}_{10}(L,t) \end{aligned} \tag{3.36}$$

The flow into the district heating loop system is the flow out of the natural gas boiler system, thus, $\tilde{x}_{10}(0,t) = \tilde{x}_9(t)$. With the consideration of boundary disturbance, let $\tilde{x}_{10}(\zeta,t) = z_{10}(\zeta,t) + B_{10}(\zeta)\tilde{x}_{10}(0,t)$, then $z_{10}(0,t) = 0$, $B_{10}(0) = 1$. With the assumption $\alpha_{10} = 1$, the above system becomes:

$$\begin{aligned} \frac{\partial z_{10}(\zeta,t)}{\partial t} &= -\frac{\partial z_{10}(\zeta,t)}{\partial \zeta} - B_{10}(\zeta)\frac{\partial \tilde{x}_{10}(0,t)}{\partial t} - \frac{\partial B_{10}(\zeta)}{\partial \zeta}\tilde{x}_{10}(0,t) - \gamma_7 \tilde{u}_7 \\ \tilde{y}_{10}(t) &= z_{10}(L,t) + B_{10}(L)\tilde{x}_{10}(0,t) \end{aligned} \tag{3.37}$$

With the assumption $\frac{\partial B_{10}(\zeta)}{\partial \zeta} = 0$, one can obtain the constant function $B_{10}(\zeta) = 1$. The extension of the system can be expressed as follows:

$$\begin{aligned} \frac{\partial}{\partial t}\begin{bmatrix} z_{10}(\zeta,t) \\ \tilde{x}_{10}(0,t) \end{bmatrix} &= \begin{bmatrix} -\frac{\partial}{\partial \zeta} & 0 \\ 0 & 0 \end{bmatrix}\begin{bmatrix} z_{10}(\zeta,t) \\ \tilde{x}_{10}(0,t) \end{bmatrix} + \begin{bmatrix} -1 \\ 1 \end{bmatrix}\bar{x}_{10}(0,t) + \begin{bmatrix} -\gamma_7 \\ 0 \end{bmatrix}\tilde{u}_7(t) \\ \tilde{y}_{10}(t) &= \begin{bmatrix} C & B_{10}(L) \end{bmatrix}\begin{bmatrix} z_{10}(\zeta,t) \\ \tilde{x}_{10}(0,t) \end{bmatrix} \end{aligned} \tag{3.38}$$

where $\bar{x}_{10}(0,t) = \frac{\partial \tilde{x}_{10}(0,t)}{\partial t}$ and the operator $C[f(\zeta)] = \int_0^L f(\zeta)\delta(\zeta - L)d\zeta = f(L)$.

Applying the Laplace transform to the above system, one obtains:

$$\begin{bmatrix} z_{10}(\zeta, s) \\ \tilde{x}_{10}(0, s) \end{bmatrix} = \begin{bmatrix} R_{11} & 0 \\ 0 & R_{22} \end{bmatrix} \begin{bmatrix} z_{10}(\zeta, 0) \\ \tilde{x}_{10}(0, 0) \end{bmatrix} \tag{3.39}$$

where $R_{11} = \int_0^{\zeta}(\cdot)e^{\int_0^{\eta} sd\phi}d\eta e^{-\int_0^{\zeta} sd\phi}$ and $R_{22} = \frac{1}{s}(\cdot)$.

The discrete system can be expressed as:

$$\begin{aligned} Z_6(k) &= A_{dz6}Z_6(k-1) + B_{dz6}U_6(k) + E_{dz6}G_6(k) \\ Y_6(k) &= C_{dz6}Z_6(k-1) + D_{dz6}U_6(k) + F_{dz6}G_6(k) \end{aligned} \tag{3.40}$$

The discrete operators A_{dz6}, B_{dz6}, C_{dz6}, D_{dz6}, E_{dz6} and F_{dz6} can be directly obtained. The original state can be obtained by the transform: $\tilde{x}_{10}(\zeta, k) = z_{10}(\zeta, k) + B_{10}(\zeta)\tilde{x}_{10}(0, k)$.

In this section, the discrete state space settings of the solar thermal system, BTES system, heat exchanger system, STTS system, natural gas boiler system and the district heating loop system are obtained. In the next section, we design a controller which maintains the temperature at desired set point, while still fulfilling the energy demands of the district heating loop.

3.4 Controller Design and System Analysis

Since large disturbances from the solar thermal plant system, borehole thermal energy storage system or the district heating loop system greatly impact system operation, the control system plays an important role in maintaining the system's performance. In this section, we propose a servo controller design which successfully rejects unde-

sired disturbances and tracks a reference trajectory or a set point.

One of the important analysis tools of the controlled system performance is given by the frequency analysis. The core of the frequency analysis is the frequency response of the system. In particular, we obtain frequency responses of the subsystems described in the previous section. The frequency response of the subsystems and units provides an insight into operational and performance capabilities, and also provides information on disturbance influence on the overall system's performance.

3.4.1 Servo Control for Linear Discrete System

The performance of the servo controller design requirement is to maintain desired temperature of the flow supplied to the district heating loop system and reject disturbances simultaneously. In this chapter, we consider that the system operates during the heating season. If the solar thermal system and the BTES can not provide enough thermal energy, a backup natural gas boiler system is provided to ensure the necessary supply of thermal energy. Therefore, the control strategy of the solar thermal system with borehole seasonal storage is realized by the servo controller design for the natural gas system, see Fig.3.3.

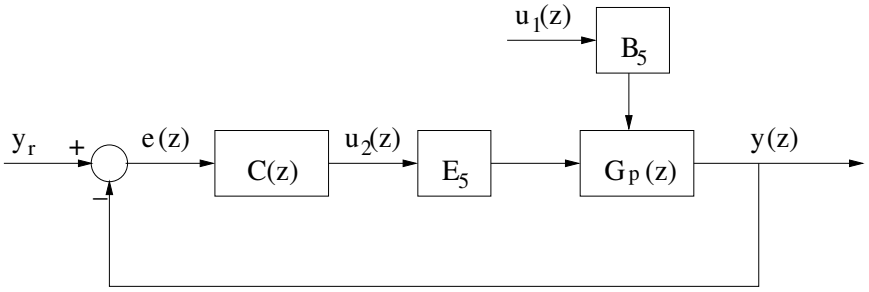

Fig. 3.3: Block diagram of the closed-loop system for the controller design of the natural gas system.

In this section, we design a servo controller for the discrete natural gas system. According to Eq.3.34, the transfer function of the discrete system can be expressed as follows:

$$G_p(z) = \frac{z+1}{(z+\beta_9)z - (z-\beta_9)} \tag{3.41}$$

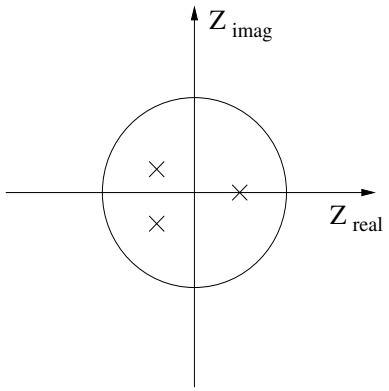

Fig. 3.4: Diagram of the pole placement of the controller design

Here, we assume that disturbances from different systems (solar thermal system, heat exchanger system, BTES and hot tank system) are harmonic function which model various sources with different frequencies. The servo control problem design is to track step reference trajectory and reject harmonic disturbances with the frequencies ω_1 and ω_2. Therefore, the transfer function of the controller contains the family of poles of functions chosen to be tracked and rejected as disturbance signals, such that:

$$C(z) = \frac{\alpha_0 + \alpha_1 z + \alpha_2 z^2 + \alpha_3 z^3 + \alpha_4 z^4 + \alpha_5 z^5}{(z-1)(z^2 - 2\cos(\omega_1 h)z + 1)(z^2 - 2\cos(\omega_2 h)z + 1)} \tag{3.42}$$

here the parameters α_0, α_1, α_2, α_3, α_4 and α_5 are determined to stabilize the following

characteristic equation:

$$\begin{aligned}\pi(z) = \quad & (z-1)(z^2 - 2\cos(\omega_1 h)z + 1)(z^2 - 2\cos(\omega_2 h)z + 1)((z+\beta_9)z - (z-\beta_9)) \\ & +(\alpha_0 + \alpha_1 z + \alpha_2 z^2 + \alpha_3 z^3 + \alpha_4 z^4 + \alpha_5 z^5)(\gamma_6(z+1)) \end{aligned} \tag{3.43}$$

In the ensuing section, we apply a pole placement regulator design for the closed-loop system. The basic idea of the pole placement regulation is that the controller design is realized such that all poles of the closed-loop system are placed at prescribed desired values. Eq.3.43 provides enough design freedom to achieve a pole placement regulation as desired. In particular, for a discrete system, the poles are assigned within the unit circle to guarantee the closed-loop system's stability, see Fig.3.4.

Remark 4: When it comes to the realization of a discrete controller, one needs to be careful in designing digital discrete state space realization of elements formulated in the Cayley-Tustin discretization framework. In particular, the appropriate care is required for application of the algorithm to the nominal discrete plant in the real time control setting.

3.4.2 System Analysis based on Frequency Response

The frequency response is based on the fact that a linear system can be completely characterized by its steady-state response to harmonic signals [80, 81]. Therefore, we can extend these results to discrete infinite and coupled infinite and finite dimensional systems. Based on frequency response, performance requirements can be expressed and in addition the evaluation of the effects of noise in the system can be achieved. In this section, we will explore frequency responses of the discrete subsystems described above.

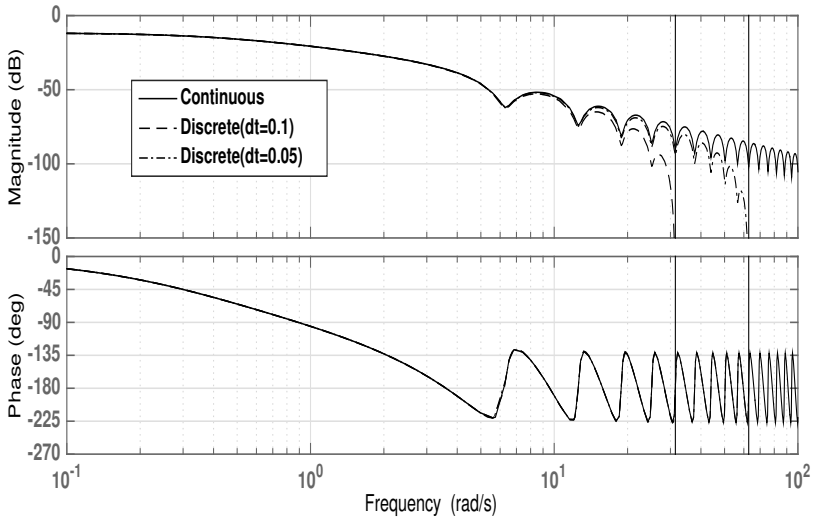

Fig. 3.5: Bode plot for the continuous solar thermal system (solid line), discrete solar thermal system by Cayley-Tustin discretization with $dt = 0.1$ (dash line) and discrete solar thermal system by Cayley-Tustin discretization with $dt = 0.05$ (dash-dot line). Vertical solid lines indicate the Nyquist frequencies.

First, let us consider the frequency response of the solar thermal energy system. The continuous transfer function of the solar thermal energy system is obtained from Laplace transform as follows:

$$G_1(s) = \frac{Y_1(s)}{U_1(s)} = \frac{\beta_1\gamma_1}{(s+\beta_1)(s+\beta_2)}[1 - e^{(s+\beta_1)}] \tag{3.44}$$

The variables z and s are related as $z = e^{s\Delta t}$ when the system is mapped from continuous time domain to discrete time domain. Using Cayley-Tustin time discretization, the difference approximation corresponds to the series expansion of

$z = e^{s\Delta t} \approx \frac{1+s\frac{\Delta t}{2}}{1-s\frac{\Delta t}{2}}$, which yields the following expression:

$$s = \frac{2}{\Delta t}\frac{z-1}{z+1} \tag{3.45}$$

here Δt is the sampling period. The discrete transfer function is obtained by replacing s in $G_1(s)$ by the above equation.

The frequency response of the above solar thermal system is plotted in Bode diagram, see Fig.3.5. In this Bode diagram, a comparison between continuous (solid line) and discrete frequency responses (dash line or dash-dot line) with different sampling times is given. The Nyquist frequency for two different discretization sampling times are given as $\omega_{N1} = 34.14 rad/s(\Delta t = 0.1)$ and $\omega_{N2} = 62.83 rad/s(\Delta t = 0.05)$. From the figures, it can be seen that the magnitude curves are very close for frequencies that are much smaller than the Nyquist frequency and the phase curves coincide. This is in agreement with physical plant features that high frequency signals will be attenuated in the solar thermal plant system. It is obvious that as the sampling time decreases, the magnitude curve is closer to the magnitude curve of the continuous system. In addition, if one would consider to apply an output feedback control realization by placing a local gain based controller, the gain margin of the solar thermal system is $35dB$.

The frequency response of the BTES system is similar in nature to the frequency response of the solar thermal system with different parameters. The continuous transfer function of the BTES is given as follows:

$$G_2(s) = \frac{Y_2(s)}{U_2(s)} = \frac{\beta_3\gamma_2}{(s+\beta_3)(s+\beta_4)}[1 - e^{(s+\beta_3)}] \tag{3.46}$$

The Bode plot of BTES system is given in Fig.3.6-3.7.

For the heat exchanger system, the continuous transfer function relates output $\tilde{x}_6(L,t)$ to the input $\tilde{x}_5(L,t)$, and is given as follows:

$$G_3(s) = \frac{\tilde{x}_6(L,s)}{\tilde{x}_5(L,s)} = \frac{2\beta_6 \sinh(b)}{2b\cosh(b) + (2s + \beta_5 + \beta_6)\sinh(b)} \tag{3.47}$$

where $b = \sqrt{\frac{(\beta_5-\beta_6)^2}{4} + s^2 + (\beta_5 + \beta_6)s}$. One can directly obtain the discrete transfer function and frequency response based on the above continuous transfer function of the system. The Bode plot is also given in Fig.3.6-3.7.

The inlet flows into the hot tank are from the heat exchanger system and the BTES system. The continuous transfer function from the heat exchanger system $\tilde{x}_{8in1}(t)$ to $\tilde{y}_4(t)$ is obtained as follows:

$$G_{41}(s) = \frac{\tilde{y}_4(s)}{\tilde{x}_{8in1}(s)} = \frac{\beta_7 u_{4ss}}{x_{7ss}(s + \frac{\beta_7}{K_1})} \tag{3.48}$$

Similarly, the continuous transfer function from $\tilde{x}_{8in2}(t)$ in the BTES system to $\tilde{y}_4(t)$ is obtained as follows:

$$G_{42}(s) = \frac{\tilde{y}_4(s)}{\tilde{x}_{8in2}(s)} = \frac{\beta_7 u_{5ss}}{x_{7ss}(s + \frac{\beta_7}{K_1})} \tag{3.49}$$

The discrete transfer functions and frequency responses are directly obtained based on the above continuous transfer functions of the system. The Bode plots of G_{41} and G_{42} are given in Fig.3.6-3.7.

For the natural gas system, the open loop system discrete transfer function is described in Eq.3.41 and the discrete transfer function of the controller is described in Eq.3.42. Thus, the discrete transfer function of the close loop system from $\tilde{x}_{9in}(k)$

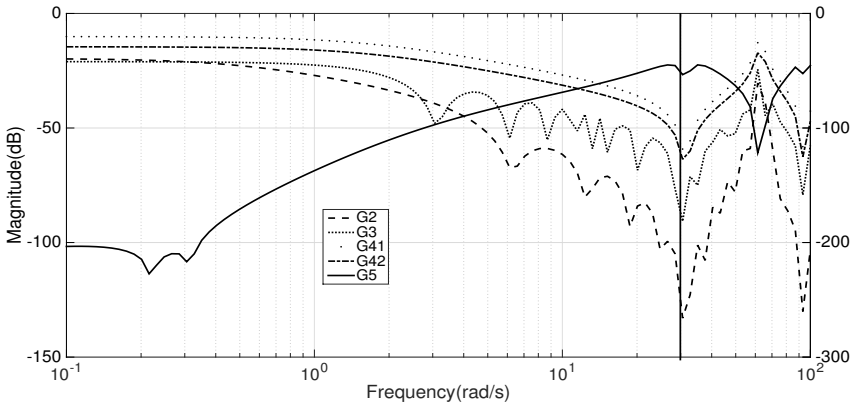

Fig. 3.6: Magnitudes of Bode diagrams for the discrete BTES system in Eq.3.46 ($G2$), heat exchanger system in Eq.3.47 ($G3$), hot tank system in Eq.3.48-3.49 ($G41$ and $G42$) and natural gas system in Eq.3.50 ($G5$). The y-axis on the left hand side is for $G2$, $G3$, $G41$ and $G42$ and the y-axis on the right hand side is for $G5$. The sampling period is $\Delta t = 0.1$.

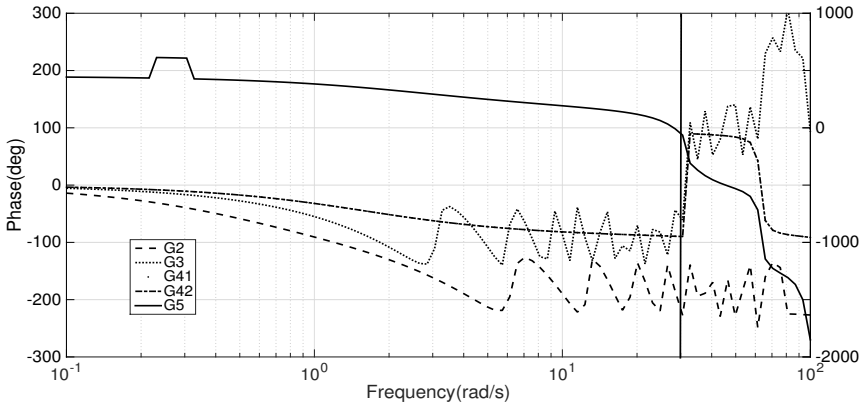

Fig. 3.7: Phases of Bode diagrams for the discrete BTES system in Eq.3.46 ($G2$), heat exchanger system in Eq.3.47 ($G3$), hot tank system in Eq.3.48-3.49 ($G41$ and $G42$) and natural gas system in Eq.3.50 ($G5$). The y-axis on the left hand side is for $G2$, $G3$, $G41$ and $G42$ and the y-axis on the right hand side is for $G5$. The sampling period is $\Delta t = 0.1$.

to $\tilde{y}_5(k)$ is expressed as follows:

$$G_5(z) = \frac{\tilde{y}_5(z)}{\tilde{x}_{9in}(z)} = \frac{\beta_9 G_p(z)}{1 + \gamma_6 G_p(z) C(z)} \tag{3.50}$$

The discrete frequency response is obtained from the above discrete close-loop system. The Bode plot is given in Fig.3.6-3.7.

Finally, the transfer function of the district heating loop system from $\tilde{x}_{10}(0,t)$ to $\tilde{y}_6(t)$ is obtained as follows:

$$G_6(s) = \frac{\tilde{y}_6(s)}{\tilde{x}_{10}(0,s)} = e^{-s} \tag{3.51}$$

This district heating loop system is a pure time delay system. The magnitude of the system is 0 and the phase of the system is $-\pi$.

The frequency response of the above subsystems are plotted in Bode diagram, see Fig.3.6 and Fig.3.7. The sampling period is $\Delta t = 0.1$. In the natural gas system, we assume the disturbances are with frequencies of $\omega_1 = 0.3142$ and $\omega_2 = 0.2199$. These frequencies can be reflected in the Bode diagram of the transfer function G_5.

3.5 Simulation Results

In this section, we demonstrate the implementation of the servo control system to improve the overall efficiency of the system. The dynamic model of the collection-storage-district heating loop system is simulated according to the energy balance models developed in the previous section. With plant model available, a servo problem is set up to compute the control input that maintains the energy demand constant and rejects disturbances, with guaranteed asymptotic stabilization despite uncertainties present within the system.

In the next, we introduce two simulation scenarios. First, the servo control problem rejects disturbances arising in the solar thermal system. In the second scenario, the disturbances are arising from operating conditions of the district heating loop

system and the BTES system.

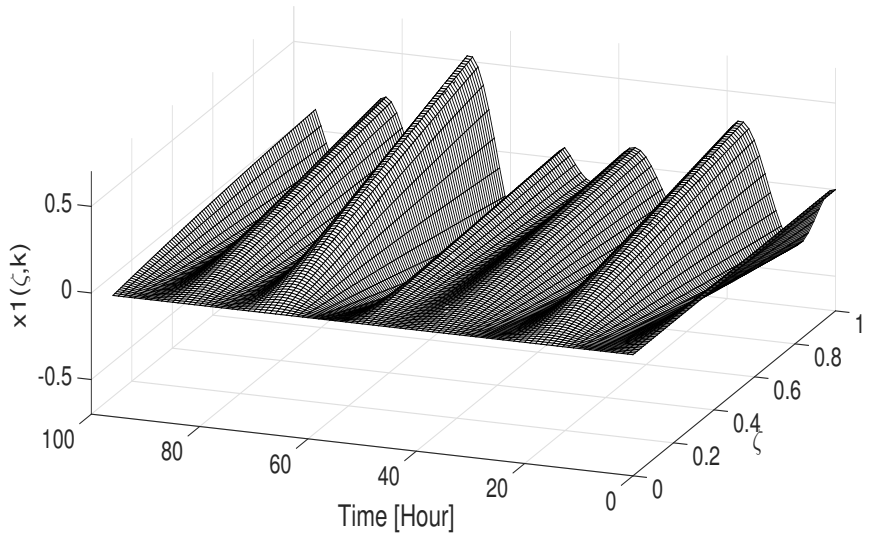

Fig. 3.8: Simulation of the solar thermal system profile given by the implementation of the discrete system in Eq.3.14. The parameters of the system are $\alpha_1 = 1$, $\beta_1 = 0.3$, $\beta_2 = 0.4$ and $\gamma_1 = 0.4$. The input $\tilde{u}_1(t)$ is the periodic harmonic function containing two frequencies $\omega_1 = 0.3142$ and $\omega_2 = 0.4084$.

3.5.1 Cloudy Day: Disturbances from the Solar Thermal System

We consider a scenario when a cloudy day with larger variations of available solar energy, the solar thermal system undergoes disturbance in the power output. Due to the weather changes and according to the weather forecast, the possible disturbances to the solar thermal system with the borehole seasonal storage can be considered as periodic harmonic disturbances with different frequencies. The control goal is to maintain the temperature of hot flow to the district heating loop system at desired set point and to reject two disturbances described above. The simulation results show

4 days (96 hours) operation of the solar thermal system with $d\zeta = 0.01$ and $dt = 0.1$, see Fig.3.8-3.12. The initial conditions of all states are zeros.

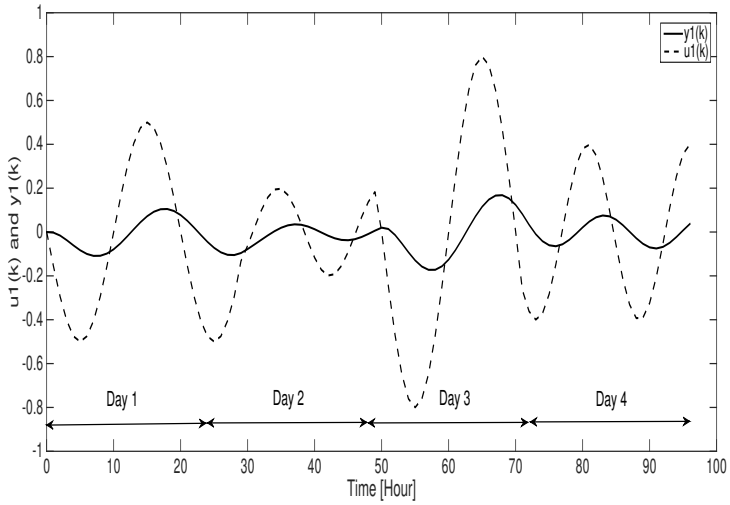

Fig. 3.9: Output profile of simulation of the solar thermal system given by the implementation of discrete system in Eq.3.14.

The solar thermal system is simulated as exposed to periodic harmonic disturbances given by two frequencies $\omega_1 = 0.3142$ and $\omega_2 = 0.4084$, see Fig.3.8 and Fig.3.9, where the input and output of the solar thermal system are given. Fig.3.11 shows the simulation result of the heat exchanger's two states. The natural gas system with servo control is given in Fig.3.10. The desired poles of the designed controller are $\sigma(A_{CL}) = \{0.65, 0.65, -0.75, -0.75, -0.55, 0.85\}$. It can be seen that the system can track the step reference $y_r = 1$ and reject periodic harmonic disturbances with different frequencies. The designed controller has good performance since it can achieve tracking the step reference in less than 5 hours. However, one can easily reconfigure the controller and have faster tracking by placing $\sigma(A_{CL})$ closer to the center within the unit circle. Finally, Fig.3.12 shows the simulation result of the district heating

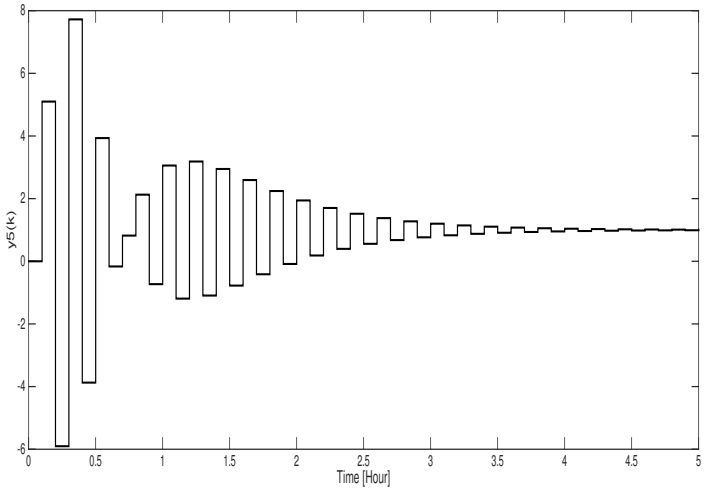

Fig. 3.10: Simulation of the natural gas system profile given by the implementation of the discrete system in Eq.3.34. The parameters of the system are $\beta_9 = 1$ and $\gamma_6 = 1.5$. The input $\tilde{u}_6(t)$ is obtained by the servo controller in Eq.3.42.

loop system. From the simulation result, it is obvious that the district heating loop system is driven by the input from the natural gas system.

3.5.2 Disturbances from Operating Conditions of the District Heating Loop System

When the operating conditions of the district heating loop system are affected by the environment changes, the heating loop system undergoes disturbance in power output. When the BTES system undergoes disturbance from the perturbations of the environmental temperature, these two disturbances will influence the solar thermal system with borehole seasonal storage. In this scenario, the control goal of the controller design is similar as the previous scenario. Therefore, the controller rejects disturbances in the district heating loop system and the BTES system and maintains

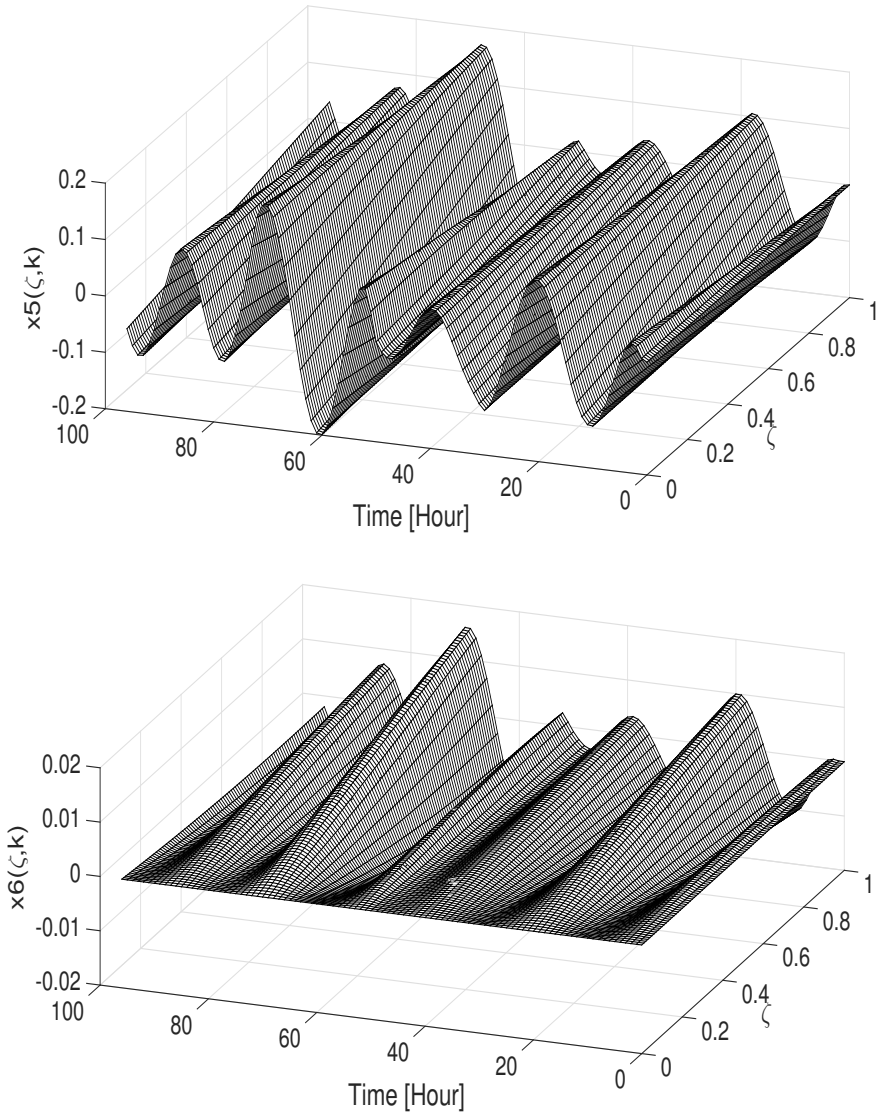

Fig. 3.11: Simulation of the evolution of the heat exchanger system profile given by the implementation of the discrete system in Eq.3.26. The parameters of the system are $\alpha_5 F_1 = 1$, $\alpha_6 u_{3ss} = 1$, $\beta_5 = 0.15$, $\beta_6 = 0.1$. The input is a constant function $\tilde{u}_3(t) = 0$.

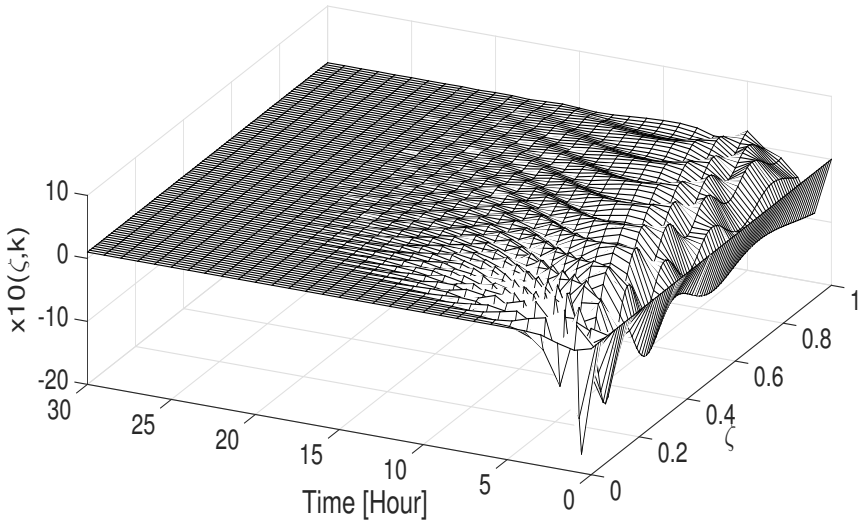

Fig. 3.12: Simulation of the district heating loop system profile given by the implementation of the discrete system in Eq.3.40. The parameters of the system are $\alpha_{10} = 1$ and $\gamma_7 = 1$. The input is a constant function $\tilde{u}_7(t) = 0$.

the required flow temperature into the homes in the district heating loop system. The simulation results are shown in Fig.3.13-3.17. The initial conditions of all states are zeros.

The BTES system is simulated with harmonic disturbance in the frequency of $\omega_1 = 0.2199$, see Fig.3.13. Fig.3.14 gives the input and output of the BTES system. Here, the harmonic disturbance with the frequency of $\omega_2 = 0.3142$ is also considered as in-domain input to the heating loop system, see Fig.3.16. The natural gas system with servo control is shown in Fig.3.15. The desired poles of the designed controller are $\sigma(A_{CL}) = \{0.5, 0.5, -0.8, -0.8, -0.7, 0.6\}$. As it can be seen from the simulation result, the designed controller has good tracking and rejecting performance. Finally, Fig.3.17 shows the simulation result of the district heating loop system. This second scenario study shows that the designed controller has the ability to reject any linear

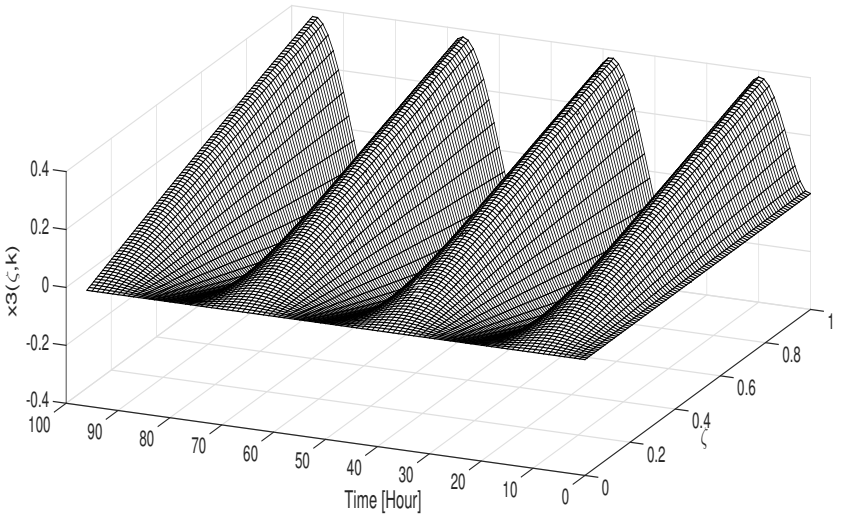

Fig. 3.13: Simulation of the BTES system profile given by the implementation of the discrete system in Eq.3.19. The parameters of the system are $\alpha_3 = 1$, $\beta_3 = 0.3$, $\beta_4 = 0.5$ and $\gamma_2 = 0.2$. The input $\tilde{u}_2(t)$ is the periodic harmonic function with frequency $\omega_1 = 0.2199$.

combination of signals with known frequencies. In addition, the designed controller is easily realized in practice to address a wide range of disturbances.

3.6 Conclusion

In this chapter, we provided a model of the state-of-the-art in the solar thermal system with borehole seasonal storage mathematically modelled by ordinary differential equations (ODEs), hyperbolic partial differential equation (PDEs) and coupled PDEs-ODEs according to the energy balance. Then, the discrete systems of these integrated systems are obtained by the application of the Cayley-Tustin time discretization method. We developed a simple servo controller design for the solar ther-

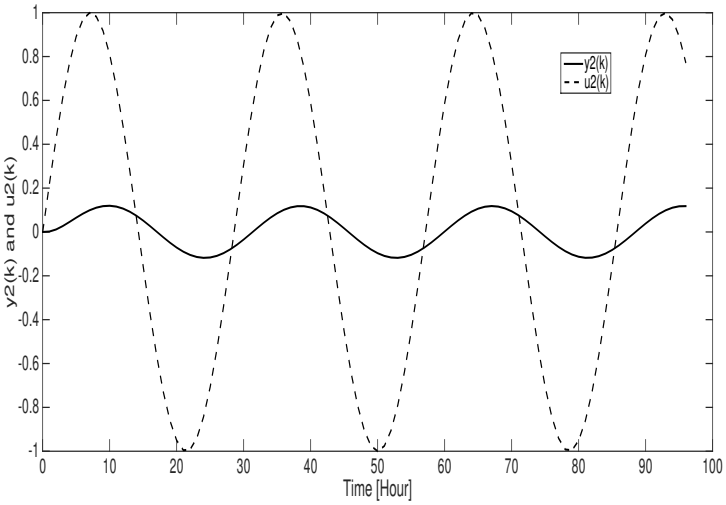

Fig. 3.14: Output profile of simulation of the BTES system given by the implementation of the discrete system in Eq.3.19.

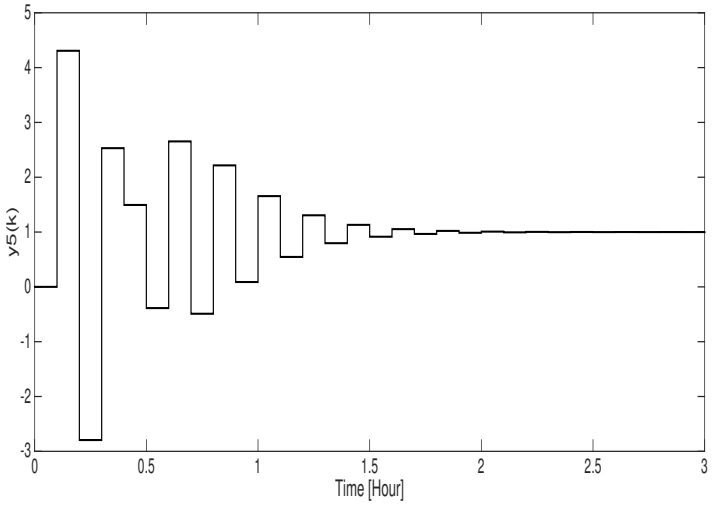

Fig. 3.15: Simulation of the natural gas system profile given by the implementation of the discrete system in Eq.3.34. The parameters of the system are $\beta_9 = 1$ and $\gamma_6 = 1.5$. The input $\tilde{u}_6(t)$ is obtained by the servo controller in Eq.3.42.

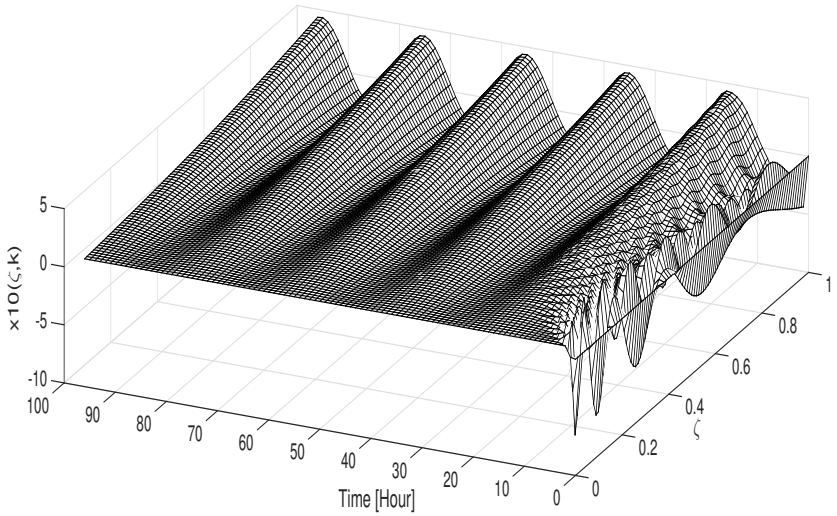

Fig. 3.16: Simulation of the district heating loop system profile given by the implementation of the discrete system in Eq.3.40. The parameters of the system are $\alpha_{10} = 1$ and $\gamma_7 = 1$. The input $\tilde{u}_7(t)$ is the periodic harmonic function with frequency $\omega_2 = 0.3142$, which is $\tilde{u}_7(t) = 0.6e^{\zeta}\sin(\omega_2 t)$.

mal system which takes into account measurements of the disturbances. The control system manipulates the natural gas energy into the system in order to track a step reference for fulfilling the demands of space heating in the district heating loop system. The simulation results of different scenarios show that, the discrete servo controller tracks step reference and rejects harmonic disturbances with different frequencies. More advanced control and optimization schemes can be pursued in order to leverage the thermal energy storage. It is recommended that optimal control schemes are developed to help the solar thermal system with borehole seasonal storage to operate more efficiently.

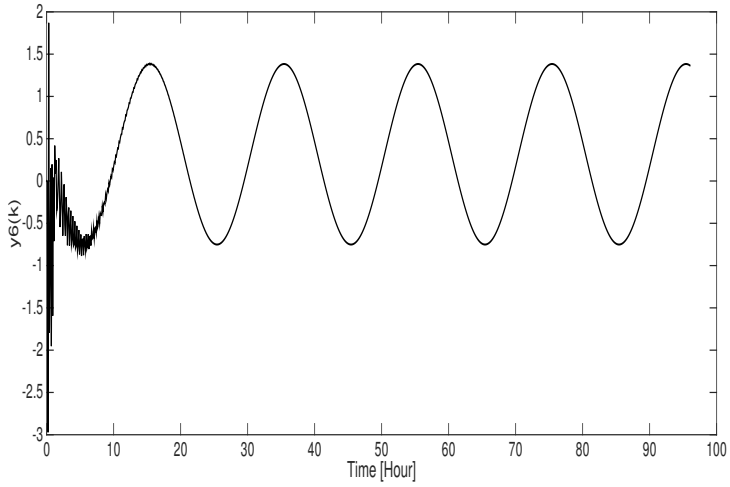

Fig. 3.17: Output profile of simulation of the district heating loop system given by the implementation of the discrete system in Eq.3.40.

Chapter 4

Model Predictive Control of Solar Thermal System with Borehole Seasonal Storage

4.1 Introduction

The development and utilization of the solar thermal system with borehole seasonal storage for a commercial community is one of the most promising topics in the renewable energy field. A typical commercial community is the Drake Landing Solar Community (DLSC) in Okotoks, Alberta, Canada which has successfully integrated the solar thermal system with borehole seasonal storage and supplied efficient renewable energy to its district heating system [69]. The energy efficiency of existing houses in a commercial community can be improved through temperature operation control of the complex solar boreal thermal storage system.

The temperature regulation of the solar thermal system with borehole seasonal

storage is characterized by many uncertainties, such as environmental changes, occupancy status changes, and changes in the operating conditions of equipment in the houses. The ultimate performance goal is that the proposed controller stabilizes the temperature around steady state and keeps the integrity of economic demands in the district heating loop system. Conventional solar thermal system control with borehole seasonal storage uses control action to maintain temperature around steady state [76, 73, 74]. However, this control strategy does not always result in optimal performance. In literature, different optimization-based control strategies have been used to improve the energy efficiency of a solar thermal system. Some examples include the hierarchical control strategy presented in [82], the supervisory optimal control strategy described in [75], and the model predictive control (MPC) strategy presented in [83].

Model predictive control is a strategy that explicitly uses a model of the process to compute the required manipulation that will minimize the energy cost [2]. One of the advantages of model predictive control is that input/state/output constraints can be taken explicitly in the computation of control law. We propose a model predictive control design for the solar thermal system with borehole seasonal storage, which will take into account measurements of the input disturbances, such as changes in ambient temperature, and disturbances predictions, such as weather forecasts, which can assist in the prediction of the availability of different energy sources. The Luenberger output observer is considered to observe a real complex spatial solar boreal thermal system. In addition, constraints can be enforced as limits on the actuators, manipulated and controlled variables (e.g. upper and lower limits of the temperature, supply flow rate limits, and energy sources limits).

The overall system includes a solar thermal energy system, borehole thermal en-

ergy storage system (BTES), short term thermal storage system (STTS) and a district heating loop system, see Fig.4.1. The solar thermal energy system collects solar thermal energy through plate collectors mounted on the roof of the houses and transfers the energy to the STTS by a heat exchanger [72, 77]. Then, the collected energy is sent from the STTS to the district heating loop system to heat the 52 energy-efficient houses. During the summer months, the borehole thermal storage system stores the energy from the STTS to heat the ground and cool the storage tanks. During the heating season, the BTES collects geothermal energy to send to the STTS by a grid of boreholes with single U-tube heat exchangers [70]. If the stored water temperature is insufficient to meet the current heating load, the natural gas boiler in the district heating loop system is provided as a backup to ensure heating of each houses. The system operation which fulfills the heat energy requirement of each house leads the turn on and/or turn off operating modes of the natural gas boiler. The heat fluctuations due to on and off operation is caused by the burning of natural gas, making the natural gas boiler system operation possibly as unstable fluctuations and chattering around desired temperature requirement. Therefore, the model predictive controller for the district heating loop system is designed to ensure the system optimal and stable working performance at desired steady state with the consideration of constraints.

According to the energy balance conservation laws, the solar thermal system with borehole seasonal storage is modelled using a combination of ordinary differential equations (ODEs), hyperbolic partial differential equations (PDEs) and/or coupled PDEs-ODEs. Initially, the thermal energy is transferred from the solar thermal system to the STTS system through a heat exchanger. The solar thermal system is described by coupled PDE-ODE and the counterflow heat exchanger is modelled by a

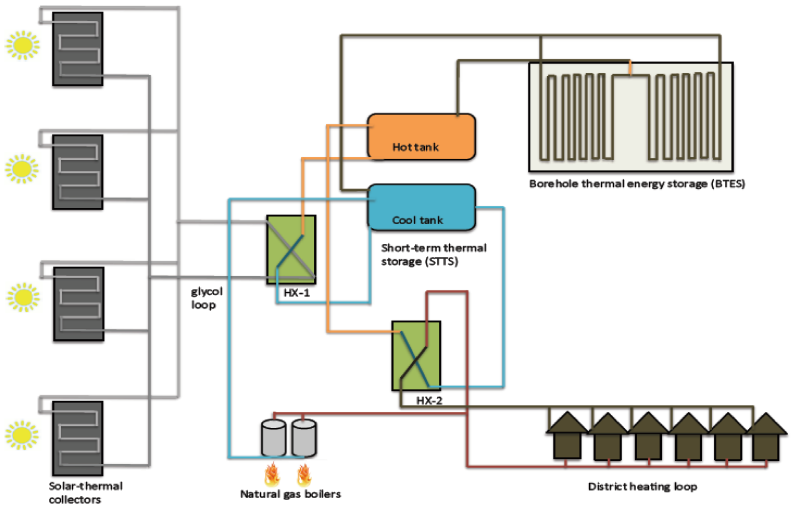

Fig. 4.1: Diagram of the solar thermal system with borehole seasonal storage.

series of first order hyperbolic PDEs. The energy from the solar thermal power plant is transferred to the heat exchanger through the boundary, therefore, the boundary controlled system realization is considered in the modelling of the heat exchanger system. The BTES system is described by a coupled PDE-ODE and stores thermal energy to the STTS system directly. Then, the STTS system, which is represented by ODEs, provides thermal energy to the district heating loop system, which is represented by coupled a PDE-ODE.

In this chapter, in order to utilize model predictive control, the discrete version of the overall system is required. Traditional numerical time discretization approaches, such as Euler, Runge-Kutta, etc. have the disadvantage that the accuracy of the approximate discrete time system rapidly deteriorates as the sampling period increases [18]. This chapter explores an adequate discretization method in order to preserve the intrinsic energy and dynamical characteristics of the coupled PDEs-ODEs system,

which is realized by the Cayley-Tustin time discretization transformation [19]. The novelty of the Cayley-Tustin time discretization transformation provides that both PDEs and/or ODEs systems are discretized with the same sampling time, in addition, the PDEs system is kept without any type of model reduction, see [21].

The novel model predictive controller developed in this chapter is designed by construction of a finite dimensional constrained optimization problem accounting for input disturbance rejection. In addition, a realistic discrete output observer which constructs finite and infinite states is considered without spatial discretization and state reduction. The solution to this discrete output observer is realized by solving discrete Lyapunov equation which is related to the corresponding continuous Lyapunov equation.

The chapter is organized as follows: section 4.2 addresses the model of the solar thermal system with borehole seasonal storage. In section 4.3, the discrete version of the overall system is obtained by using Cayley-Tustin time discretization. Section 4.4 introduces model predictive controller design for a coupled PDEs-ODEs system with the consideration of an output observer. Finally, we demonstrate the performance of the model predictive control built in previous sections through simulation studies in section 4.5.

4.2 Model Formulation of Solar Thermal System with Borehole Seasonal Storage

The overall solar thermal system with borehole seasonal storage contains solar thermal system, BTES system, STTS system and district heating loop system, see Fig.4.2. The first principle modelling of the overall system is in more details addressed in [84].

Hence, we consider only important subsections of the overall model in this section.

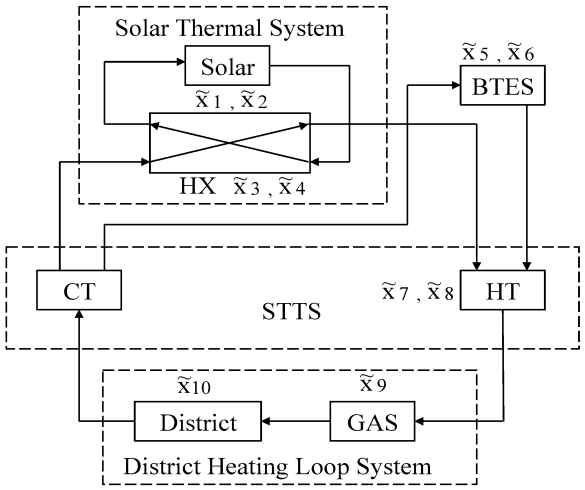

Fig. 4.2: Diagram of the solar thermal system with borehole seasonal storage: solar thermal system (Solar); borehole thermal energy storage system (BTES); heat exchanger system (HX); hot tank system (HT); cold tank system (CT); natural gas system (GAS); district heating loop system (District).

4.2.1 Model of Solar Thermal System

Solar energy is collected during the year by solar collectors which use mirrors or lenses to heat a fluid. The energy balance of the flow and the absorber in the solar power plant which uses a plate collector to focus solar radiation onto the absorber pipe is given as follows [72, 77]:

$$\rho_{gl} C_{pgl} s_{solar} \frac{\partial T_{solar}}{\partial t} = -C_{pgl} F_{solar} \frac{\partial T_{solar}}{\partial \zeta} + h_p p_A (T_A - T_{solar}) \tag{4.1}$$

$$\rho_A C_{pA} s_A \frac{dT_A}{dt} = h_p p_A (T_{solar-in} - T_A) + Q_{solar} w_{solar}$$

where $T_{solar-in} = T_{solar}(\zeta = 0)$. The variables of solar power plant system are shown in Table.4.1. One can apply appropriate non-dimensional transformation on Eq.4.1 with the following definition of states $x_1(\zeta, t) = \frac{T_{solar} - T_r}{T_r}$ and $x_2(t) = \frac{T_A - T_r}{T_r}$, and input $u_1(t) = \frac{Q_{solar}}{Q_r}$. Here, T_r and Q_r are the reference temperature and the reference heat flux. The parameters of the system are $\alpha_1 = \frac{F_{solar}}{\rho_{gl} s_{solar}}$, $\beta_1 = \frac{h_p p_A}{\rho_{gl} C_{pgl} s_{solar}}$, $\beta_2 = \frac{h_p p_A}{\rho_A C_{pA} s_A}$ and $\gamma_1 = \frac{Q_r w_{solar}}{\rho_A C_{pA} s_A T_r}$. Therefore, the solar power plant system can be described by the following coupled PDE-ODE:

$$\begin{aligned} \frac{\partial x_1(\zeta, t)}{\partial t} &= -\alpha_1 \frac{\partial x_1(\zeta, t)}{\partial \zeta} + \beta_1 [x_2(t) - x_1(\zeta, t)] \\ \frac{dx_2(t)}{dt} &= \beta_2 [x_{1in}(t) - x_2(t)] + \gamma_1 u_1(t) \end{aligned} \tag{4.2}$$

Table 4.1: Parameters of the solar system used to model Eq.4.1.

Variable	Unit	Description
T_{solar}	K	Temperature of glycol flow
T_A	K	Temperature of absorber
Q_{solar}	W/m^2	Heat flux in solar system
F_{solar}	kg/s	Flow rate of glycol flow
C_{pgl}	J/kgK	Heat capacity of glycol flow
C_{pA}	J/kgK	Heat capacity of absorber
h_p	W/m^2K	Convective heat transfer coefficient of absorber
ρ_{gl}	kg/m^3	Density of glycol flow
ρ_A	kg/m^3	Density of absorber
s_{solar}	m^2	Area of glycol flow
s_A	m^2	Area of absorber
w_{solar}	m	Solar collector width
p_A	m	Absorber pipe perimeter

With the consideration of steady state conditions $x_1(\zeta, t) = x_{1ss}(\zeta) + \tilde{x}_1(\zeta, t)$,

$x_2(t) = x_{2ss} + \tilde{x}_2(t)$, and $u_1(t) = u_{1ss} + \tilde{u}_1(t)$, the coupled PDE-ODE in Eq.4.2 becomes:

$$\begin{aligned} \frac{\partial \tilde{x}_1(\zeta,t)}{\partial t} &= -\alpha_1 \frac{\partial \tilde{x}_1(\zeta,t)}{\partial \zeta} + \beta_1[\tilde{x}_2(t) - \tilde{x}_1(\zeta,t)] \\ \frac{d\tilde{x}_2(t)}{dt} &= \beta_2[\tilde{x}_{1in}(t) - \tilde{x}_2(t)] + \gamma_1 \tilde{u}_1(t) \end{aligned} \tag{4.3}$$

with $\tilde{x}_{1in}(t) = \tilde{x}_1(0,t) = 0$ and $\tilde{x}_1(\zeta,0) = \varphi_1(\zeta)$, where the variables $\zeta \in [0,l]$ and $t \geq 0$ denote the space and time domains.

4.2.2 Model of Heat Exchanger System

The heat exchanger HX-1 in the solar thermal system is a counter-current heat exchanger which is modelled by a set of coupled first-order hyperbolic PDEs [77]. Despite the non-linearity of the controlled system, an explicit characterization of the equilibrium profiles can be given. As a consequence, the linearized system around an equilibrium profile is obtained as a linear infinite dimensional time-invariant system given as below:

$$\begin{aligned} \frac{\partial T_{HX-11}}{\partial t} &= \frac{F_{HX-11}}{\rho_{gl} s_1} \frac{\partial T_{HX-11}}{\partial \zeta} - \frac{kl}{C_{pgl}\rho_{gl} s_1}[T_{HX-11} - T_{HX-12}] \\ \frac{\partial T_{HX-12}}{\partial t} &= -\frac{F_{HX-12}}{\rho_{H_2O} s_2} \frac{\partial T_{HX-12}}{\partial \zeta} + \frac{kl}{C_{pH_2O}\rho_{H_2O} s_2}[T_{HX-11} - T_{HX-12}] \end{aligned} \tag{4.4}$$

where $T_{HX-11}(l,t) = T_{solar}(l,t)$ and $T_{HX-12}(0,t) = T_{CT}$.

The description of the variables in heat exchanger system is shown in Table.4.2. The change of variables leads to the states given as $x_3(\zeta,t) = \frac{T_{HX-11}-T_r}{T_r}$ and $x_4(\zeta,t) = \frac{T_{HX-12}-T_r}{T_r}$, input $u_2(t) = \frac{F_{HX-12}}{F_r}$, and parameters $F_1 = \frac{F_{HX-11}}{F_r}$, $\alpha_3 = \frac{F_r}{\rho_{gl} s_1}$, $\beta_3 = \frac{kl}{C_{pgl}\rho_{gl} s_1}$, $\alpha_4 = \frac{F_r}{\rho_{H_2O} s_2}$ and $\beta_4 = \frac{kl}{C_{pH_2O}\rho_{H_2O} s_2}$. The linearized heat exchanger system

Table 4.2: Parameters of the heat exchanger HX-1 used to model Eq.4.4.

Variable	Unit	Description
$T_{HX-11}(\zeta,t)$	K	Temperature of hot flow
$T_{HX-12}(\zeta,t)$	K	Temperature of cold flow
$F_{HX-11}=F_{solar}$	kg/s	Flow rate of hot flow
$F_{HX-12}=F_{HX-1}$	kg/s	Flow rate of cold flow
C_{pH_2O}	J/kgK	Heat capacity of water flow
ρ_{H_2O}	kg/m^3	Density of water flow
k	W/m^2K	Heat exchange coefficient
$l=2\pi r_2$	m	Contact circumference of heat exchanger
$s_1=\pi(r_1^2-r_2^2)$,$r_1>r_2$	m^2	Area of hot flow
$s_2=\pi r_2^2$	m^2	Area of cold flow

with the steady state conditions $x_3(\zeta,t) = x_{3ss}(\zeta) + \tilde{x}_3(\zeta,t)$, $x_4(\zeta,t) = x_{4ss}(\zeta) + \tilde{x}_4(\zeta,t)$, and $u_2(t) = u_{2ss} + \tilde{u}_2(t)$ is described by the following hyperbolic PDEs:

$$\begin{aligned}\frac{\partial\tilde{x}_3(\zeta,t)}{\partial t} &= \alpha_3 F_1\frac{\partial\tilde{x}_3(\zeta,t)}{\partial\zeta} - \beta_3[\tilde{x}_3(\zeta,t)-\tilde{x}_4(\zeta,t)] \\ \frac{\partial\tilde{x}_4(\zeta,t)}{\partial t} &= -\alpha_4 u_2(t)\frac{\partial\tilde{x}_4(\zeta,t)}{\partial\zeta} + \beta_4[\tilde{x}_3(\zeta,t)-\tilde{x}_4(\zeta,t)] - \alpha_4\tilde{u}_2(t)\frac{dx_{4ss}(\zeta)}{d\zeta}\end{aligned} \tag{4.5}$$

It is important to note that the linearized system around an equilibrium point is governed by the above equations with $u_2(t)$ replaced by u_{2ss}.

The heat exchanger system is potentially exposed to boundary disturbances, and therefore boundary conditions need to be adequately considered in this coupled hyperbolic PDEs system. The flow which enters the heat exchanger is the flow out of the solar power plant at $\zeta = l$ of the state $x_3(\zeta,t)$, thus, $\tilde{x}_3(l,t) = \tilde{x}_1(l,t)$, see Fig.4.2. The flow into the heat exchanger state $x_4(\zeta,t)$ at $\zeta = 0$ is the flow out of the cold tank system, which is at the reference temperature, then, $\tilde{x}_4(0,t) = 0$.

The standard methodology to accurately account for transfer of boundary actuation to in-domain is to apply state transformation [85]. Let $\tilde{x}_3(\zeta,t) = z_3(\zeta,t) + B_{b3}(\zeta)\tilde{x}_3(l,t)$, then $z_3(l,t) = 0$, $B_{b3}(l) = 1$, and $\tilde{x}_4(\zeta,t) = z_4(\zeta,t) + B_{b4}(\zeta)\tilde{x}_4(0,t)$, then $z_4(0,t) = 0,\ B_{b4}(0) = 1$. With the assumptions $\alpha_3 F_1 = 1$, $\alpha_4 u_{2ss} = 1$, $\gamma_2 = \alpha_4 \frac{dx_{4ss}(\zeta)}{d\zeta}$, the above PDEs system in Eq.4.5 becomes:

$$\begin{aligned}
&\frac{\partial z_3(\zeta,t)}{\partial t} = \frac{\partial z_3(\zeta,t)}{\partial \zeta} - \beta_3[z_3(\zeta,t) - z_4(\zeta,t)] - B_{b3}(\zeta)\frac{\partial \tilde{x}_3(l,t)}{\partial t} \qquad (4.6)\\
&+[\frac{\partial B_{b3}(\zeta)}{\partial \zeta} - \beta_3 B_{b3}(\zeta)]\tilde{x}_3(l,t) + \beta_3 B_{b4}(\zeta)\tilde{x}_4(0,t)\\
&\frac{\partial z_4(\zeta,t)}{\partial t} = -\frac{\partial z_4(\zeta,t)}{\partial \zeta} + \beta_4[z_3(\zeta,t) - z_4(\zeta,t)] - B_{b4}(\zeta)\frac{\partial \tilde{x}_4(0,t)}{\partial t}\\
&-[\frac{\partial B_{b4}(\zeta)}{\partial \zeta} + \beta_4 B_{b4}(\zeta)]\tilde{x}_4(0,t) + \beta_4 B_{b3}(\zeta)\tilde{x}_3(l,t) - \gamma_2 \tilde{u}_2(t)
\end{aligned}$$

The functions $B_{b3}(\zeta)$ and $B_{b4}(\zeta)$ can be calculated by taking that $\frac{\partial B_{b3}(\zeta)}{\partial \zeta} - \beta_3 B_{b3}(\zeta) = 0$ and $\frac{\partial B_{b4}(\zeta)}{\partial \zeta} + \beta_4 B_{b4}(\zeta) = 0$, which simplifies the system of Eq.4.6.

4.2.3 Model of Borehole Energy Storage System

The borehole thermal energy storage system uses a grid of boreholes with U-tube heat exchangers [78, 79]. The energy balance of the flow in the U-tube heat exchanger and the energy balance of the pipe wall are given as:

$$\begin{aligned}
&\rho_{H_2O} C_{pH_2O} s_{bore} \frac{\partial T_{bore}}{\partial t} = -C_{pH_2O} F_{bore} \frac{\partial T_{bore}}{\partial \zeta} + h_w p_W (T_W - T_{bore}) \qquad (4.7)\\
&\rho_W C_{pW} s_W \frac{dT_W}{dt} = h_w p_W (T_{bore-in} - T_W) + Q_{bore} w
\end{aligned}$$

where $T_{bore-in} = T_{bore}(\zeta = 0)$.

Table.4.3 gives the description of the variables in BTES system. We consider

Table 4.3: Parameters of the borehole thermal energy storage system used to model Eq.4.7.

Variable	Unit	Description
T_{bore}	K	Temperature of water flow
T_W	K	Temperature of pipe wall
Q_{bore}	W/m^2	Collected Energy in borehole system
F_{bore}	kg/s	Flow rate of water flow
C_{pW}	J/kgK	Heat capacity of pipe wall
h_w	W/m^2K	Convective heat transfer coefficient of pipe wall
ρ_W	kg/m^3	Density of pipe wall
s_{bore}	m^2	Area of water flow
w	m	Borehole system width
p_W	m	Pipe wall perimeter

the following change of variables with states $x_5(\zeta,t) = \frac{T_{bore}-T_r}{T_r}$, $x_6(t) = \frac{T_W-T_r}{T_r}$, and input $u_3(t) = \frac{Q_{bore}}{Q_r}$. The system parameters are $\alpha_5 = \frac{F_{bore}}{\rho_{H_2O} s_{bore}}$, $\beta_5 = \frac{h_w p_W}{\rho_{H_2O} C_{pH_2O} s_{bore}}$, $\beta_6 = \frac{h_w p_W}{\rho_W C_{pW} s_W}$ and $\gamma_3 = \frac{Q_r w_{bore}}{\rho_W C_{pW} s_W T_r}$. By applying linearization around the steady state of interest with the assumptions $x_5(\zeta,t) = x_{5ss}(\zeta) + \tilde{x}_5(\zeta,t)$, $x_6(t) = x_{6ss} + \tilde{x}_6(t)$, and $u_3(t) = u_{3ss} + \tilde{u}_3(t)$, the BTES system is described by the following coupled PDE-ODE:

$$\begin{aligned} \frac{\partial \tilde{x}_5(\zeta,t)}{\partial t} &= -\alpha_5 \frac{\partial \tilde{x}_5(\zeta,t)}{\partial \zeta} + \beta_5(\tilde{x}_6(t) - \tilde{x}_5(\zeta,t)) \\ \frac{d\tilde{x}_6(t)}{dt} &= \beta_6(\tilde{x}_{5in}(t) - \tilde{x}_6(t)) + \gamma_3 \tilde{u}_3(t) \end{aligned} \tag{4.8}$$

Similar to the solar power plant system, we assume that that $x_5(0,t)$ operates around the steady state of interest, thus $\tilde{x}_{5in}(t) = \tilde{x}_5(0,t) = 0$.

4.2.4 Model of Short Term Thermal Storage System

The short term thermal storage system utilizes the hot tank and cold tank to transfer the thermal energy obtained from the solar thermal system and the borehole energy storage system to the district heating subsystem, see Fig.4.2.

The mass balance and energy balance of the hot tank system is modelled by the following ODEs [5]:

$$A_{HT}\frac{dh_{HT}}{dt} = F_{HT1} + F_{HT2} - F_{HT} \tag{4.9}$$
$$\rho_{H_2O}C_{pH_2O}A_{HT}\frac{dh_{HT}T_{HT}}{dt} = \rho_{H_2O}C_{pH_2O}[F_{HX1}T_{HT1} + F_{HT2}T_{HT2} - F_{HT}T_{HT}]$$

where F_{HT1} and F_{HT2} are flow rates from the heat exchanger system and the BTES system. F_{HT} is flow rate out of the hot tank and $F_{HT} = \frac{1}{K_1}h_{HT}$. The variable description of the hot tank system is shown in Table.4.4.

Table 4.4: Parameters of the hot tank system used to model Eq.4.9.

Variable	Unit	Description
h_{HT}	m	Flow height in hot tank
T_{HT}	K	Temperature of flow out of hot tank
F_{HT}	kg/s	Flow rate out of hot tank
A_{HT}	m^2	Hot tank area
T_{HT1}	K	Temperature of flow into hot tank
T_{HT2}	K	Temperature of flow into hot tank
F_{HT1}	kg/s	Flow rate into hot tank
F_{HT2}	kg/s	Flow rate into hot tank

The following change of variables are considered in hot tank system: states $x_7(t) = \frac{h_{HT}}{h_r}$ and $x_8(t) = \frac{T_{HT}-T_r}{T_r}$; inputs $u_4(t) = \frac{F_{HT1}}{F_r}$, $u_5(t) = \frac{F_{HT2}}{F_r}$ and $u_6(t) = \frac{F_{HT}}{F_r}$; disturbances $x_{8in1}(t) = \frac{T_{HT1}-T_r}{T_r}$ and $x_{8in2}(t) = \frac{T_{HT2}-T_r}{T_r}$; parameter $\beta_7 = \frac{F_r}{h_r A_{HT}}$. One

obtains the model of hot tank system as below:

$$\begin{aligned}
&\frac{dx_7(t)}{dt} = \beta_7(u_4(t) + u_5(t) - u_6(t)) \\
&\frac{d[x_7(t)(x_8(t)+1)]}{dt} = \beta_7[u_4(t)(x_{8in1}(t)+1) + u_5(t)(x_{8in2}(t)+1) \\
&-u_6(t)(x_8(t)+1)]
\end{aligned} \tag{4.10}$$

With the Taylor expansion around steady state in the following expressions $x_7(t) = x_{7ss} + \tilde{x}_7(t)$, $x_8(t) = x_{8ss} + \tilde{x}_8(t)$, $u_4(t) = u_{4ss} + \tilde{u}_4(t)$, $u_5(t) = u_{5ss} + \tilde{u}_5(t)$, $u_6(t) = \frac{1}{K_1}x_7(t) = \frac{1}{K_1}(x_{7ss} + \tilde{x}_7(t))$, $x_7(x_8+1) \simeq x_{7ss}(x_{8ss}+1) + x_{7ss}\tilde{x}_8 + (x_{8ss}+1)\tilde{x}_7$ and $u_6(x_8+1) = \frac{1}{K_1}x_7(x_8+1)$, the linearized model of hot tank system is given as below:

$$\begin{aligned}
&\frac{d\tilde{x}_7(t)}{dt} = \beta_7[\tilde{u}_4(t) + \tilde{u}_5(t) - \frac{1}{K_1}\tilde{x}_7(t)] \\
&\frac{d\tilde{x}_8(t)}{dt} = \frac{\beta_7}{x_{7ss}}[(x_{8in1ss} - x_{8ss})\tilde{u}_4(t) + (x_{8in2ss} - x_{8ss})\tilde{u}_5(t) \\
&+u_{4ss}\tilde{x}_{8in1} + u_{5ss}\tilde{x}_{8in2} - \frac{1}{K_1}x_{7ss}\tilde{x}_8(t)]
\end{aligned} \tag{4.11}$$

The flows which come into the hot tank are from the heat exchanger system and the BTES system, see Fig.4.2. Therefore, we have the conditions for Eq.4.6 as $\tilde{x}_{8in1}(t) = \tilde{x}_4(l,t)$ and $\tilde{x}_{8in2}(t) = \tilde{x}_5(l,t)$.

The cold tank system plays an important role in the solar boreal thermal storage system due to the fact that the cold tank flow temperature is assumed to be at reference environment temperature. In Fig.4.2, the flow coming into the cold tank F_{CT} is from the district heating loop system. The flows out of the cold tank are linked to the solar thermal system and the BTES system at reference environment temperature, which are $F_{CT1} = T_r$ and $F_{CT2} = T_r$. Therefore, the disturbances to

the solar thermal system and the BTES system are considered as zero.

4.2.5 Model of District Heating Loop System

The district heating loop system is consist of coupled natural gas boiler model and district heating model. The energy balance of the flow in the natural gas boiler model is given as follows:

$$\rho_{H_2O} C_{pH_2O} V_{boiler} \frac{dT_{boiler}}{dt} = C_{pH_2O} F_{boiler} (T_{boiler-in} - T_{boiler}) + Q_{boiler} s_{boiler} \quad (4.12)$$

The district heating model is a hyperbolic PDE system with the heat sink $Q_{district}$ as below:

$$\rho_{H_2O} C_{pH_2O} s_{district} \frac{\partial T_{district}}{\partial t} = -C_{pH_2O} F_{district} \frac{\partial T_{district}}{\partial \zeta} - Q_{district} w_{district} \quad (4.13)$$

The variable description of the district heating model is shown in Table.4.5. The district heating loop system described in Eq.4.12-4.13 has coupled hyperbolic PDE and ODE connected through the boundary of hyperbolic PDE, which is $T_{district}(0,t) = T_{boiler}(t)$.

The dimensionless system is obtained by considering the following change of variables: states $x_9(t) = \frac{T_{boiler}-T_r}{T_r}$ and $x_{10}(\zeta,t) = \frac{T_{district}-T_r}{T_r}$; inputs $u_7(t) = \frac{Q_{boiler}}{Q_r}$ and $u_8(t) = \frac{Q_{district}}{Q_r}$; disturbance $x_{9in}(t) = \frac{T_{boiler-in}-T_r}{T_r}$; parameters $\beta_9 = \frac{F_{boiler}}{\rho_{H_2O} V_{boiler}}$, $\gamma_7 = \frac{Q_{boiler} s_{boiler} Q_r}{\rho_{H_2O} C_{pH_2O} V_{boiler} T_r}$, $\alpha_{10} = \frac{F_{district}}{\rho_{H_2O} s_{district}}$ and $\gamma_8 = \frac{Q_r w_{district}}{\rho_{H_2O} C_{pH_2O} s_{district} T_r}$. By applying system linearization with the conditions $x_9(t) = x_{9ss} + \tilde{x}_9(t)$, $x_{10}(\zeta,t) = x_{10ss}(\zeta) + \tilde{x}_{10}(\zeta,t)$, $u_7(t) = u_{7ss} + \tilde{u}_7(t)$, $u_8(t) = u_{8ss} + \tilde{u}_8(t)$ and $x_{9in}(t) = x_{9inss} + \tilde{x}_{9in}(t)$, the district

Table 4.5: Parameters of the district heating loop model used to model Eq.4.12 and Eq.4.13.

Variable	Unit	Description
T_{boiler}	K	Temperature of flow in boiler
$T_{boiler-in}$	K	Temperature of flow into boiler
Q_{boiler}	W/m^2	Energy collected by boiler
F_{boiler}	kg/s	Flow rate of water flow in boiler
V_{boiler}	m^3	Flow volume in boiler
s_{boiler}	m^2	Boiler area
$T_{district}$	K	Temperature of flow in district system
$Q_{district}$	W/m^2	Heat flux of district system
$F_{district}$	kg/s	Flow rate of water flow in district system
$s_{district}$	m^2	District system area
$w_{district}$	m	District system width

heating loop system is described by the following coupled PDE-ODE:

$$\begin{aligned} \frac{d\tilde{x}_9(t)}{dt} &= \beta_9(\tilde{x}_{9in}(t) - \tilde{x}_9(t)) + \gamma_7\tilde{u}_7(t) \\ \frac{\partial\tilde{x}_{10}(\zeta,t)}{\partial t} &= -\alpha_{10}\frac{\partial\tilde{x}_{10}(\zeta,t)}{\partial\zeta} - \gamma_8\tilde{u}_8(t) \\ \tilde{y}_5(t) &= \tilde{x}_{10}(l,t) \end{aligned} \tag{4.14}$$

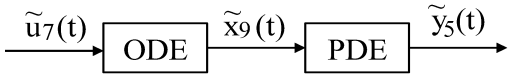

Fig. 4.3: Scheme of coupled ODE and hyperbolic PDE system connected through boundary.

The the flow into the natural gas boiler model equals the flow out of the hot tank system, such that $\tilde{x}_{9in}(t) = \tilde{x}_8(t)$. The natural gas boiler model and the district heat-

ing model is connected by the boundary condition $\tilde{x}_{10}(0,t) = \tilde{x}_9(t)$, see Fig.4.3. With the consideration of boundary disturbance, let $\tilde{x}_{10}(\zeta,t) = z_{10}(\zeta,t) + B_{b10}(\zeta)\tilde{x}_{10}(0,t)$, then $z_{10}(0,t) = 0,\ B_{b10}(0) = 1$. We assume $\alpha_{10} = 1$, and the above district heating loop system in Eq.4.14 becomes:

$$\begin{aligned}
&\frac{d\tilde{x}_9(t)}{dt} = \beta_9(\tilde{x}_{9in}(t) - \tilde{x}_9(t)) + \gamma_7\tilde{u}_7(t) \\
&\frac{\partial z_{10}(\zeta,t)}{\partial t} = -\frac{\partial z_{10}(\zeta,t)}{\partial \zeta} - B_{b10}(\zeta)[\beta_9\tilde{x}_{9in}(t) + \gamma_7\tilde{u}_7(t)] \\
&-[\frac{\partial B_{b10}(\zeta)}{\partial \zeta} - B_{b10}(\zeta)\beta_9]\tilde{x}_9(t) - \gamma_8\tilde{u}_8(t) \\
&\tilde{y}_5(t) = z_{10}(l,t) + B_{b10}(l)\tilde{x}_9(t)
\end{aligned} \tag{4.15}$$

The function $B_{b10}(\zeta)$ can be calculated from the assumption $\frac{\partial B_{b10}(\zeta)}{\partial \zeta} - B_{b10}(\zeta)\beta_9 = 0$. The coupled PDE-ODE system in Eq.4.15 is decoupled by this assumption.

4.3 Discrete Model of Solar Boreal Thermal System

According to the energy balance, the modelling of the solar thermal system with borehole seasonal storage contains internally coupled PDEs-ODEs, see Fig.4.2. The Cayley-Tustin time discretization method is applied to obtain a discrete model version which provides an insight into the subsystem's performance and overall dynamical behaviour of the system [19].

4.3.1 Infinite Dimensional System Representation

The linear first-order hyperbolic PDE system is described by the following state space system:

$$\begin{aligned} \dot{x}(\zeta,t) &= Ax(\zeta,t) + Bu(t), \quad x(\zeta,0) = x_0 \\ y(t) &= Cx(\zeta,t) \end{aligned} \tag{4.16}$$

where the variables $\zeta \in [0,1]$ and $t \geq 0$ denote the space and time domains; the state $x(\zeta,t) \in X$ and X is a Hilbert space $L_2[0,1]$; the input $u(t) \in U$ and the output $y(t) \in Y$, where U and Y are Hilbert spaces; the operator A is linear operator defined in the domain: $D(A) = \{x \in X : x(\zeta)\ is\ a.c.\ \frac{dx}{d\zeta} \in X\ and\ x(0) = 0\}$; the input operator $B = b(\zeta) \cdot I$, where I is identity operator; the output operator is given by $Cx(\zeta,t) = x(l,t)$, where $l = 1$ is the boundary point of the state $x(\zeta,t)$, see [85].

The output in infinite dimensional system is a point observation or point measurement, so let us induce the space X_1. The operator A generates an exponentially stable strongly continuous semigroup T_A on the space X [52]. The space X_1 is in the domain $D(A)$ with the norm $||x||_1 = ||(\lambda I - A)x||$, where $\lambda \in \rho(A)$ and $\rho(A)$ is the resolvent set [86]. Since this norm is equivalent to the graph norm of A, the restriction of T_A on X_1 is a semigroup on X_1, which is isomorphic to the original one. Then, we denote the restriction of T_A on X_1 by the same symbol T_A, which is the restriction of A to X. Denoting this restriction also by A, we have $A \in \mathcal{L}(X_1, X)$. This technical extension allows us to treat boundary and/or point actuation or/and point measurements.

The input operator B is bounded $B \in \mathcal{L}(U,X)$ and the output operator $C \in \mathcal{L}(X_1,Y)$ is an admissible observation operator for the semigroup T_A [87, 88]. Then,

the system in Eq.4.16 is regular and can be defined as follows:

$$\begin{aligned} \dot{x}(\zeta,t) &= Ax(\zeta,t) + Bu(t), \quad x(\zeta,0) = x_0 \\ y(t) &= C_\Lambda x(\zeta,t) \end{aligned} \tag{4.17}$$

where $C_\Lambda \in \mathcal{L}(X,Y)$ is Λ-extension of the operator C defined by:

$$C_\Lambda x = \lim_{\lambda \to +\infty} C\lambda(\lambda I - A)^{-1}x, \quad x \in X \tag{4.18}$$

where $\lambda \in \rho(A)$ and $\rho(A)$ is the resolvent set.

Now, we can see that the system in Eq.4.17 has well defined the state space X, the input space U and the output space Y. For any initial state $x_0 \in X$ and for any $u(t) \in L_2([0,\infty),U)$, Eq.4.17 has unique solutions $x(\zeta,t)$ and $y(t)$ such that $x(\zeta,t)$ is continuous on X and $y(t) \in L_2([0,\infty),Y)$.

4.3.2 Model Formulation of the System

With the physical models of solar thermal system, BTES system, STTS system and district heating loop system described in the previous section, the model formulation of the overall system is presented in this section.

The following representations are defined according to the solar power plant model described in Eq.4.3: $X_1(\zeta,t) = \begin{bmatrix} \tilde{x}_1(\zeta,t) & \tilde{x}_2(t) \end{bmatrix}^T$, $U_1(t) = \tilde{u}_1(t)$, $G_1(t) = \tilde{x}_{1in}(t)$, $A_1 = \begin{bmatrix} -\alpha_1 \frac{\partial}{\partial \zeta} - \beta_1 & \beta_1 \\ 0 & -\beta_2 \end{bmatrix}$, $B_1 = \begin{bmatrix} 0 \\ \gamma_1 \end{bmatrix}$ and $E_1 = \begin{bmatrix} 0 \\ \beta_2 \end{bmatrix}$.

Similarly, for the heat exchanger model in Eq.4.6, we have the following expressions: $X_2(\zeta,t) = \begin{bmatrix} z_3(\zeta,t) & z_4(\zeta,t) & \tilde{x}_3(l,t) & \tilde{x}_4(0,t) \end{bmatrix}^T$, $U_2(t) = \tilde{u}_2(t)$, $G_2(t) =$

$\begin{bmatrix} \frac{\partial \tilde{x}_3(l,t)}{\partial t} & \frac{\partial \tilde{x}_4(0,t)}{\partial t} \end{bmatrix}$, $A_2 = \begin{bmatrix} \frac{\partial}{\partial \zeta} - \beta_3 & \beta_3 & 0 & \beta_3 B_{b4}(\zeta) \\ \beta_4 & -\frac{\partial}{\partial \zeta} - \beta_4 & \beta_4 B_{b3}(\zeta) & 0 \\ 0 & 0 & 0 & 0 \\ 0 & 0 & 0 & 0 \end{bmatrix}$, $B_2 = \begin{bmatrix} 0 \\ -\gamma_2 \\ 0 \\ 0 \end{bmatrix}$ and $E_2 = \begin{bmatrix} -B_{b3}(\zeta) & 0 \\ 0 & -B_{b4}(\zeta) \\ 1 & 0 \\ 0 & 1 \end{bmatrix}$.

Let us define the following expressions from BTES system in Eq.4.8 as $X_3(\zeta,t) = \begin{bmatrix} \tilde{x}_5(\zeta,t) & \tilde{x}_6(t) \end{bmatrix}^T$, $U_3(t) = \tilde{u}_3(t)$, $G_3(t) = \tilde{x}_{5in}(t)$, $A_3 = \begin{bmatrix} -\alpha_5 \frac{\partial}{\partial \zeta} - \beta_5 & \beta_5 \\ 0 & -\beta_6 \end{bmatrix}$, $B_3 = \begin{bmatrix} 0 \\ \gamma_3 \end{bmatrix}$ and $E_3 = \begin{bmatrix} 0 \\ \beta_6 \end{bmatrix}$.

For the hot tank system described by Eq.4.11, we have the representations of states and inputs as $X_4(t) = \begin{bmatrix} \tilde{x}_7(t) & \tilde{x}_8(t) \end{bmatrix}^T$, $U_4(t) = \begin{bmatrix} \tilde{u}_4(t) & \tilde{u}_5(t) \end{bmatrix}^T$, $G_4(t) = \begin{bmatrix} \tilde{x}_{8in1}(t) & \tilde{x}_{8in2}(t) \end{bmatrix}^T$, $A_4 = \begin{bmatrix} -\frac{\beta_7}{K_1} & 0 \\ 0 & -\frac{\beta_7}{K_1} \end{bmatrix}$, $B_4 = \begin{bmatrix} \beta_7 & \beta_7 \\ \frac{\beta_7(x_{8in1ss} - x_{8ss})}{x_{7ss}} & \frac{\beta_7(x_{8in2ss} - x_{8ss})}{x_{7ss}} \end{bmatrix}$ and $E_4 = \begin{bmatrix} 0 & 0 \\ u_{4ss} & u_{5ss} \end{bmatrix}$.

The representations in district heating loop system in Eq.4.15 are defined as $X_5(\zeta,t) = \begin{bmatrix} \tilde{x}_9(t) & z_{10}(\zeta,t) \end{bmatrix}^T$, $U_5(t) = \begin{bmatrix} \tilde{u}_7(t) & \tilde{u}_8(t) \end{bmatrix}^T$, $G_5(t) = \tilde{x}_{9in}(t)$, $Y_5(t) = \tilde{y}_5(t)$, $A_5 = \begin{bmatrix} -\beta_9 & 0 \\ 0 & -\frac{\partial}{\partial \zeta} \end{bmatrix}$, $B_5 = \begin{bmatrix} \gamma_7 & 0 \\ -B_{b10}\gamma_7 & -\gamma_8 \end{bmatrix}$, $E_5 = \begin{bmatrix} \beta_9 \\ -B_{b10}\beta_9 \end{bmatrix}$ and $C_5 = \begin{bmatrix} B_{b10}(l) & C_\Lambda \end{bmatrix}$.

The model of overall solar boreal thermal energy system is given with the state

$x(\zeta,t) = \begin{bmatrix} X_1(\zeta,t) & X_2(\zeta,t) & X_3(\zeta,t) & X_4(t) & X_5(\zeta,t) \end{bmatrix}^T$, the input
$u(t) = \begin{bmatrix} U_1(t) & U_2(t) & U_3(t) & U_4(t) & U_5(t) \end{bmatrix}^T$, the disturbance
$g(t) = \begin{bmatrix} G_1(t) & G_2(t) & G_3(t) & G_4(t) & G_5(t) \end{bmatrix}^T$ and the output $y(t) = Y_5(t)$ in the following form:

$$\begin{aligned} \dot{x}(\zeta,t) &= Ax(\zeta,t) + Bu(t) + Eg(t), \quad x(\zeta,0) = x_0 \\ y(t) &= Cx(\zeta,t) \end{aligned} \tag{4.19}$$

where $A = \begin{bmatrix} A_1 & 0 & 0 & 0 & 0 \\ 0 & A_2 & 0 & 0 & 0 \\ 0 & 0 & A_3 & 0 & 0 \\ 0 & 0 & 0 & A_4 & 0 \\ 0 & 0 & 0 & 0 & A_5 \end{bmatrix}$, $B = \begin{bmatrix} B_1 & 0 & 0 & 0 & 0 \\ 0 & B_2 & 0 & 0 & 0 \\ 0 & 0 & B_3 & 0 & 0 \\ 0 & 0 & 0 & B_4 & 0 \\ 0 & 0 & 0 & 0 & B_5 \end{bmatrix}$,

$E = \begin{bmatrix} E_1 & 0 & 0 & 0 & 0 \\ 0 & E_2 & 0 & 0 & 0 \\ 0 & 0 & E_3 & 0 & 0 \\ 0 & 0 & 0 & E_4 & 0 \\ 0 & 0 & 0 & 0 & E_5 \end{bmatrix}$ and $C = \begin{bmatrix} 0 & 0 & 0 & 0 & C_5 \end{bmatrix}$.

This state-space representation accounts for coupled infinite and finite dimensional systems. The state $x(\zeta,t) \in X \oplus R^n$, X is a real Hilbert space and R^n is a real space, where n accounts for the states associated with the lumped parameter system. The input $u(t) \in U$, the disturbance $g(t) \in G$ and the output $y(t) \in Y$, where U, G and Y are real Hilbert spaces. The operator $A \in \mathcal{L}(X_1, X)$ generates semigroup T_A on X; $B \in \mathcal{L}(U, X)$ and $E \in \mathcal{L}(G, X)$ are operators associated with actuation and disturbance; $C \in \mathcal{L}(X, Y)$ is linear output measurement operator.

4.3.3 System Time Discretization

In the next subsection, we apply the Cayley-Tustin transformation on the above coupled PDEs-ODEs system, which maps the system from a continuous time to a discrete time space setting and preserves all energy properties of the system without spatial model reduction. With the sampling time Δt, the discrete time version of the system in Eq.4.19 takes the following form:

$$\begin{aligned} x(\zeta,k) &= A_d x(\zeta,k-1) + B_d u(k) + E_d g(k), \quad x(\zeta,0) = x_0 \\ y(k) &= C_d x(\zeta,k-1) + D_d u(k) + F_d g(k) \end{aligned} \tag{4.20}$$

where A_d, B_d, C_d, D_d, E_d and F_d are discrete time operators, given by $A_d = [\delta + A][\delta - A]^{-1} = -I + 2\delta[\delta - A]^{-1}$, $B_d = \sqrt{2\delta}[\delta - A]^{-1}B$, $C_d = \sqrt{2\delta}C[\delta - A]^{-1}$, $D_d = C[\delta - A]^{-1}B + D$, $E_d = \sqrt{2\delta}[\delta - A]^{-1}E$ and $F_d = C[\delta - A]^{-1}E + F$. The parameter is $\delta = 2/\Delta t$.

Remark 1: It is known that for many explicit finite difference schemes for hyperbolic PDEs in one space dimension, temporal and spatial discretization of the system leads to the Courant-Friedrichs-Lewy stability condition, which is $\frac{\Delta\zeta}{\Delta t} \geq |v|$. The advantage of the implicit scheme of the Cayley-Tustin transformation given by Eq.4.20 is that the transformation is unconditionally stable. In addition, the implicit scheme preserves the distributed nature of the hyperbolic PDEs system without spatial approximation. Therefore, the Cayley-Tustin discretization needs the choice of δ to be selected adequately for both PDEs and ODEs in the solar boreal thermal system described in Eq.4.19.

The discrete operators in Eq.4.20 can be obtained with the consideration of resolvent operator by replacing s with δ. The resolvent of the linear operator A of the

overall solar boreal thermal system in Eq.4.19 is defined as below:

$$R(s, A) = [sI - A]^{-1} \tag{4.21}$$

and it can be obtained from Laplace transform applied on the continuous system described in Eq.4.19. Since the subsystems in the overall solar boreal thermal system in Eq.4.19 are decoupled and connected through boundaries, the resolvent of the operator A in Eq.4.19 is expressed as below by applying Laplace transform:

$$R(s, A) = [sI - A]^{-1} = \begin{bmatrix} R_1 & 0 & 0 & 0 & 0 \\ 0 & R_2 & 0 & 0 & 0 \\ 0 & 0 & R_3 & 0 & 0 \\ 0 & 0 & 0 & R_4 & 0 \\ 0 & 0 & 0 & 0 & R_5 \end{bmatrix} \tag{4.22}$$

where the resolvent operators R_1, R_2, R_3, R_4 and R_5 are related to operators A_1, A_2, A_3, A_4 and A_5.

The resolvent of the operator A_1 in can be expressed as follows:

$$R_1(s, A_1)(\cdot) = [sI - A_1]^{-1}(\cdot) = \begin{bmatrix} R_{11} & R_{12} \\ R_{21} & R_{22} \end{bmatrix} (\cdot) \tag{4.23}$$

where

$$\begin{aligned} R_{11} &= \int_0^{\zeta} (\cdot) e^{\int_0^{\eta} (s+\beta_1) d\phi} d\eta e^{-\int_0^{\zeta} (s+\beta_1) d\phi} \\ R_{12} &= \frac{\beta_1}{s+\beta_2} \int_0^{\zeta} (\cdot) e^{\int_0^{\eta} (s+\beta_1) d\phi} d\eta e^{-\int_0^{\zeta} (s+\beta_1) d\phi} \\ R_{21} &= 0 \end{aligned}$$

$$R_{22} = \frac{1}{s+\beta_2}$$

The resolvent of the operator A_2 can be expressed as follows:

$$R_2(s, A_2)(\cdot) = [sI - A_2]^{-1}(\cdot) = \begin{bmatrix} R_{11} & R_{12} & R_{13} & R_{14} \\ R_{21} & R_{22} & R_{23} & R_{24} \\ R_{31} & R_{32} & R_{33} & R_{34} \\ R_{41} & R_{42} & R_{43} & R_{44} \end{bmatrix} (\cdot) \tag{4.24}$$

where

$$R_{11} = \frac{e^{a\zeta}cosh(b\zeta) + ce^{a\zeta}sinh(b\zeta)}{e^a cosh(b) + ce^a sinh(b)} \int_0^1 [e^{a(1-\eta)}cosh(b(1-\eta)) + ce^{a(1-\eta)}sinh(b(1-\eta))](\cdot)d\eta$$
$$- \int_0^\zeta [e^{a(\zeta-\eta)}cosh(b(\zeta-\eta)) + ce^{a(\zeta-\eta)}sinh(b(\zeta-\eta))](\cdot)d\eta$$
$$R_{12} = \frac{e^{a\zeta}cosh(b\zeta) + ce^{a\zeta}sinh(b\zeta)}{e^a cosh(b) + ce^a sinh(b)} \int_0^1 \frac{\beta_3}{b} e^{a(1-\eta)}sinh(b(1-\eta))(\cdot)d\eta$$
$$- \int_0^\zeta \frac{\beta_3}{b} e^{a(\zeta-\eta)}sinh(b(\zeta-\eta))(\cdot)d\eta$$
$$R_{21} = \frac{\frac{\beta_4}{b}e^{a\zeta}sinh(b\zeta)}{e^a cosh(b) + ce^a sinh(b)} \int_0^1 [e^{a(1-\eta)}cosh(b(1-\eta)) + ce^{a(1-\eta)}sinh(b(1-\eta))](\cdot)d\eta$$
$$- \int_0^\zeta \frac{\beta_4}{b} e^{a(\zeta-\eta)}sinh(b(\zeta-\eta))(\cdot)d\eta$$
$$R_{22} = \frac{\frac{\beta_4}{b}e^{a\zeta}sinh(b\zeta)}{e^a cosh(b) + ce^a sinh(b)} \int_0^1 \frac{\beta_3}{b} e^{a(1-\eta)}sinh(b(1-\eta))(\cdot)d\eta$$
$$+ \int_0^\zeta [e^{a(\zeta-\eta)}cosh(b(\zeta-\eta)) - ce^{a(\zeta-\eta)}sinh(b(\zeta-\eta))](\cdot)d\eta$$
$$R_{13} = \frac{e^{a\zeta}cosh(b\zeta) + ce^{a\zeta}sinh(b\zeta)}{e^a cosh(b) + ce^a sinh(b)} \int_0^1 \frac{\beta_3}{b} e^{a(1-\eta)}sinh(b(1-\eta))\beta_4 B_{b3}(\eta)\frac{1}{s}(\cdot)d\eta$$
$$- \int_0^\zeta \frac{\beta_3}{b} e^{a(\zeta-\eta)}sinh(b(\zeta-\eta))\beta_4 B_{b3}(\eta)\frac{1}{s}(\cdot)d\eta$$
$$R_{14} = \frac{e^{a\zeta}cosh(b\zeta) + ce^{a\zeta}sinh(b\zeta)}{e^a cosh(b) + ce^a sinh(b)} \int_0^1 [e^{a(1-\eta)}cosh(b(1-\eta)) + ce^{a(1-\eta)}sinh(b(1-\eta))]\beta_3 B_{b4}(\eta)\frac{(\cdot)}{s}d\eta$$

$$-\int_0^{\zeta}[e^{a(\zeta-\eta)}cosh(b(\zeta-\eta))+ce^{a(\zeta-\eta)}sinh(b(\zeta-\eta))]\beta_3 B_{b4}(\eta)\frac{1}{s}(\cdot)d\eta$$

$$R_{23}=\frac{\frac{\beta_4}{b}e^{a\zeta}sinh(b\zeta)}{e^a cosh(b)+ce^a sinh(b)}\int_0^1\frac{\beta_3}{b}e^{a(1-\eta)}sinh(b(1-\eta))\beta_4 B_{b3}(\eta)\frac{1}{s}(\cdot)d\eta$$

$$+\int_0^{\zeta}[e^{a(\zeta-\eta)}cosh(b(\zeta-\eta))-ce^{a(\zeta-\eta)}sinh(b(\zeta-\eta))]\beta_4 B_{b3}(\eta)\frac{1}{s}(\cdot)d\eta$$

$$R_{24}=\frac{\frac{\beta_4}{b}e^{a\zeta}sinh(b\zeta)}{e^a cosh(b)+ce^a sinh(b)}\int_0^1[e^{a(1-\eta)}cosh(b(1-\eta))+ce^{a(1-\eta)}sinh(b(1-\eta))]\beta_3 B_{b4}(\eta)\frac{1}{s}(\cdot)d\eta$$

$$-\int_0^{\zeta}\frac{\beta_4}{b}e^{a(\zeta-\eta)}sinh(b(\zeta-\eta))\beta_3 B_{b4}(\eta)\frac{1}{s}(\cdot)d\eta$$

$$R_{33}=\frac{1}{s}(\cdot)$$

$$R_{44}=\frac{1}{s}(\cdot)$$

with $a=\frac{\beta_3-\beta_4}{2}$, $b=\sqrt{\frac{(\beta_3-\beta_4)^2}{4}+s^2+(\beta_3+\beta_4)s}$ and $c=\frac{2s+\beta_3+\beta_4}{2b}$.

The resolvent of the operator A_3 in can be expressed as follows:

$$R_3(s,A_3)(\cdot)=[sI-A_3]^{-1}(\cdot)=\begin{bmatrix}R_{11} & R_{12}\\ R_{21} & R_{22}\end{bmatrix}(\cdot) \tag{4.25}$$

where

$$R_{11}=\int_0^{\zeta}(\cdot)e^{\int_0^{\eta}(s+\beta_5)d\phi}d\eta e^{-\int_0^{\zeta}(s+\beta_5)d\phi}$$

$$R_{12}=\frac{\beta_5}{s+\beta_6}\int_0^{\zeta}(\cdot)e^{\int_0^{\eta}(s+\beta_5)d\phi}d\eta e^{-\int_0^{\zeta}(s+\beta_5)d\phi}$$

$$R_{21}=0$$

$$R_{22}=\frac{1}{s+\beta_6}$$

The resolvent of the operator A_4 in can be expressed as follows:

$$R_4(s, A_4)(\cdot) = [sI - A_4]^{-1}(\cdot) = \begin{bmatrix} R_{11} & 0 \\ 0 & R_{22} \end{bmatrix}(\cdot) \tag{4.26}$$

where

$$R_{11} = R_{22} = \frac{1}{s + \frac{\beta_7}{K_1}}$$

The resolvent of the operator A_5 in can be expressed as follows:

$$R_5(s, A_5)(\cdot) = [sI - A_5]^{-1}(\cdot) = \begin{bmatrix} R_{11} & 0 \\ 0 & R_{22} \end{bmatrix}(\cdot) \tag{4.27}$$

where

$$R_{11} = \frac{1}{s + \beta_9}$$
$$R_{22} = \int_0^{\zeta} (\cdot) e^{s\eta} d\eta e^{-s\zeta}$$

4.4 Model Predictive Control for Linear System

The formulation of the model predictive control is developed for the unstable discrete coupled PDE-ODE inspired by district heating loop system accounting for input disturbance rejection and constraints. The constrained optimal controller design for coupled finite-dimensional and infinite-dimensional system is based on the similar formulation emerging from the finite-dimensional system theory. In addition, since the MPC is using the system state $x(\zeta, t)$, one needs to design observer in order to

reconstruct the state. Therefore, the Luenberger boundary applied output observer is considered in this section to reconstruct the state of plant system.

4.4.1 Input Disturbance Rejection

The continuous district heating loop system described in Eq.4.15 is a coupled hyperbolic PDE-ODE system. Let us rewrite Eq.4.15 as below:

$$\begin{aligned}
&\frac{d\tilde{x}_9(t)}{dt} = -\beta_9\tilde{x}_9(t) + \gamma_7[\tilde{u}_7(t) + \frac{\beta_9}{\gamma_7}\tilde{x}_{9in}(t)] \\
&\frac{\partial z_{10}(\zeta,t)}{\partial t} = -\frac{\partial z_{10}(\zeta,t)}{\partial \zeta} - B_{b10}(\zeta)\gamma_7[\tilde{u}_7(t) + \frac{\beta_9}{\gamma_7}\tilde{x}_{9in}(t)] - \gamma_8\tilde{u}_8(t) \\
&\tilde{y}_5(t) = z_{10}(l,t) + B_{b10}(l)\tilde{x}_9(t)
\end{aligned} \tag{4.28}$$

The input $\tilde{u}_8(t)$ in district system is thermal energy disturbance from houses and we consider it as $\tilde{u}_8(t) = 0$ in this work.

The variables in the district heating loop system become $X_5(\zeta,t) = \begin{bmatrix} \tilde{x}_9(t) & z_{10}(\zeta,t) \end{bmatrix}^T$, $U_5(t) = \tilde{u}_7(t)$, $G_5(t) = \tilde{x}_{9in}(t)$, $Y_5(t) = \tilde{y}_5(t)$, $A_5 = \begin{bmatrix} -\beta_9 & 0 \\ 0 & -\frac{\partial}{\partial\zeta} \end{bmatrix}$, $B_5 = \begin{bmatrix} \gamma_7 \\ -B_{b10}\gamma_7 \end{bmatrix}$ and $C_5 = \begin{bmatrix} B_{b10}(l) & C_\Lambda \end{bmatrix}$. By defining the parameter $\beta_u = \frac{\beta_9}{\gamma_7}$ and the input with disturbance $\bar{U}_5(t) = U_5(t) + \beta_u G_5(t)$, the representation of the district heating loop system is in the following form:

$$\begin{aligned}
&\dot{X}_5(\zeta,t) = A_5X_5(\zeta,t) + B_5\bar{U}_5(t) \\
&Y_5(t) = C_5X_5(\zeta,t)
\end{aligned} \tag{4.29}$$

The discrete version of the above coupled hyperbolic PDE-ODE system is obtained

by applying Cayley-Tustin discretization as follows:

$$
\begin{aligned}
X_5(\zeta,k) &= A_{d5}X_5(\zeta,k-1) + B_{d5}\bar{U}_5(k) \\
Y_5(k) &= C_{d5}X_5(\zeta,k-1) + D_{d5}\bar{U}_5(k)
\end{aligned}
\tag{4.30}
$$

The model predictive controller design in the following section will be applied on the above discrete coupled hyperbolic PDE-ODE system with the consideration of input disturbance rejection.

4.4.2 Model Predictive Control for Unstable Coupled PDE-ODE System

For model predictive control, the regulator is based on the minimization of the following open-loop objective function at sampling time k [2]:

$$
\begin{aligned}
\min_{u^N} \quad & \sum_{j=0}^{\infty} \left[< x(\zeta,k+j|k), Qx(\zeta,k+j|k) > + < \bar{u}(k+j+1|k), R\bar{u}(k+j+1|k) > \right] \\
s.t. \quad & x(\zeta,k+j|k) = A_d x(\zeta,k+j-1|k) + B_d\bar{u}(k+j|k) \\
& \bar{u}^{min} \leq \bar{u}(k+j|k) \leq \bar{u}^{max} \\
& x^{min} \leq x(\zeta,k+j|k) \leq x^{max}
\end{aligned}
\tag{4.31}
$$

where Q is positive semidefinite penalty spatial operator and R is positive definite penalty spatial operator, $x(k+j|k)$ and $\bar{u}(k+j+1|k)$ represent the state variable and input variable with disturbance at future time $k+j$ predicted at current time k.

The infinite horizon open-loop objective function in Eq.4.31 can be expressed as the finite horizon open-loop objective function with $\bar{u}(k+N+1|k) = 0$ in the following

form:

$$\begin{aligned}
\min_{\bar{u}^N} \quad & J = \sum_{j=0}^{N-1} \big[< x(\zeta, k+j|k), Qx(\zeta, k+j|k) > + < \bar{u}(k+j+1|k), R\bar{u}(k+j+1|k) > \big] \\
& + < x(\zeta, k+N|k), \bar{Q}x(\zeta, k+N|k) > \qquad (4.32) \\
s.t. \quad & x(\zeta, k+j|k) = A_d x(\zeta, k+j-1|k) + B_d \bar{u}(k+j|k) \\
& \bar{u}^{min} \leq \bar{u}(k+j|k) \leq \bar{u}^{max} \\
& x^{min} \leq x(\zeta, k+j|k) \leq x^{max}
\end{aligned}$$

where the state penalty term $\bar{Q}$ is defined as the infinite sum $\bar{Q} = \sum_{i=0}^{\infty} A_d^{*i} Q A_d^i$. The calculation of terminal state penalty term $\bar{Q}$ for unstable system is presented in [2].

Since the input variable contains disturbance term $g(k)$ in the form of $\bar{u}(k) = u(k) + \beta_u g(k)$, the finite horizon open-loop objective function in Eq.4.32 can be rewritten as follows:

$$\begin{aligned}
\min_{u^N} \quad & J = \sum_{j=0}^{N-1} \big[< x(\zeta, k+j|k), Qx(\zeta, k+j|k) > \qquad (4.33) \\
& + < [u(k+j+1|k) + \beta_u g(k+j+1|k)], R[u(k+j+1|k) + \beta_u g(k+j+1|k)] > \big] \\
& + < x(\zeta, k+N|k), \bar{Q}x(\zeta, k+N|k) > \\
s.t. \quad & x(\zeta, k+j|k) = A_d x(\zeta, k+j-1|k) + B_d [u(k+j|k) + \beta_u g(k+j|k)] \\
& \bar{u}^{min} - \beta_u g(k+j|k) \leq u(k+j|k) \leq \bar{u}^{max} - \beta_u g(k+j|k) \\
& x^{min} \leq x(\zeta, k+j|k) \leq x^{max}
\end{aligned}$$

Since the hyperbolic PDE system is stable, if the ODE system is stable, the coupled PDE-ODE system is a stable one. Otherwise, the unstable ODE system leads the coupled PDE-ODE system to be an unstable one. To deal with this instability of

coupled PDE-ODE system, the finite horizon open-loop objective function described in Eq.4.33 is subject to the following equality constraint on the unstable state $x^u(k)$ at time $k+N$:

$$A_d^u \; x^u(k+N|k) = 0 \tag{4.34}$$

where A_d^u denotes the discrete unstable operator associated with unstable subspace.

By denoting the vectors of state X, input U and disturbance G as follows:

$$\begin{aligned} X &= \left[\begin{array}{cccc} x(\zeta,k+1|k) & x(\zeta,k+2|k) & \cdots & x(\zeta,k+N|k) \end{array} \right]^T \\ U &= \left[\begin{array}{cccc} u(k+1|k) & u(k+2|k) & \cdots & u(k+N|k) \end{array} \right]^T \\ G &= \left[\begin{array}{cccc} g(k+1|k) & g(k+2|k) & \cdots & g(k+N|k) \end{array} \right]^T \end{aligned}$$

the objective function presented in Eq.4.33 results in the following program by straightforward algebraic manipulation:

$$\begin{aligned} \min_{U} \quad & J = U^T < I, H > U + 2U^T \big[< I, Px(\zeta,k|k) > + < I, R\beta_u G > \big] \\ & + < x(\zeta,k|k), \bar{Q}x(\zeta,k|k) > + < \beta_u G, R\beta_u G > \\ s.t. \quad & \left[\begin{array}{c} I \\ -I \\ S \\ -S \\ \bar{S} \end{array} \right] U \leq \left[\begin{array}{c} \bar{U}^{max} - \beta_u G \\ -\bar{U}^{min} + \beta_u G \\ X^{max} - Tx(\zeta,k|k) - S\beta_u G \\ -X^{min} + Tx(\zeta,k|k) + S\beta_u G \\ -\bar{T}x^u(k|k) - \bar{S}\beta_u G \end{array} \right] \end{aligned} \tag{4.35}$$

where

$$H = \begin{bmatrix} B_d^*\bar{Q}B_d + R & B_d^*A_d^*\bar{Q}B_d & \cdots & B_d^*A_d^{*N-1}\bar{Q}B_d \\ B_d^*\bar{Q}A_dB_d & B_d^*\bar{Q}B_d + R & \cdots & B_d^*A_d^{*N-2}\bar{Q}B_d \\ \vdots & \vdots & \ddots & \vdots \\ B_d^*\bar{Q}A_d^{N-1}B_d & B_d^*\bar{Q}A_d^{N-2}B_d & \cdots & B_d^*\bar{Q}B_d + R \end{bmatrix},$$

$$P = \begin{bmatrix} B_d^*\bar{Q}A_d \\ B_d^*\bar{Q}A_d^2 \\ \vdots \\ B_d^*\bar{Q}A_d^N \end{bmatrix}, \quad S = \begin{bmatrix} B_d & 0 & \cdots & 0 \\ A_dB_d & B_d & \cdots & 0 \\ \vdots & \vdots & \ddots & \vdots \\ A_d^{N-1}B_d & A_d^{N-2}B_d & \cdots & B_d \end{bmatrix}, \quad T = \begin{bmatrix} A_d \\ A_d^2 \\ \vdots \\ A_d^N \end{bmatrix},$$

$$\bar{S} = \begin{bmatrix} A_d^{uN-1}B_d^u & A_d^{uN-2}B_d^u & \cdots & B_d^u \end{bmatrix}, \quad \bar{T} = \begin{bmatrix} A_d^{uN} \end{bmatrix}.$$

The inner products $< I, H >$, $< I, Px(\zeta, k|k) >$ and $< I, R\beta_u G >$ in Eq.4.35 are real numbers, thus the optimization problem described in Eq.4.35 is a standard finite dimensional quadratic optimization problem. If feasible, then system stabilization is guaranteed and constraints and optimality are satisfied.

4.4.3 Luenberger Observer Design

In order to reconstruct the state and utilize in MPC controller design, we consider observer design. In particular, the coupled hyperbolic PDE-ODE system described in the following form is considered:

$$\begin{aligned} &\dot{x}(\zeta, t) = Ax(\zeta, t) + B\bar{u}(t), \quad x(\zeta, 0) = x_0 \\ &y(t) = Cx(\zeta, t) \end{aligned} \tag{4.36}$$

where the operators $A = \begin{bmatrix} A_o & 0 \\ 0 & A_p \end{bmatrix}$ and $C = \begin{bmatrix} C_o & C_p \end{bmatrix}$ with $C_p = C_\Lambda$. The input variable contains disturbance term, $\bar{u}(k) = u(k) + \beta_u g(k)$.

The Luenberger state observer is presented by the following equations:

$$\begin{aligned} \dot{\hat{x}}(\zeta, t) &= A\hat{x}(\zeta, t) + B\bar{u}(t) + L_o[y(t) - \hat{y}(t)], \quad \hat{x}(\zeta, 0) = \hat{x}_0 \\ \hat{y}(t) &= C\hat{x}(\zeta, t) \end{aligned} \tag{4.37}$$

where the gain $L_o = \begin{bmatrix} L_{o1} \\ L_{o2} \end{bmatrix}$. The state estimation error $\epsilon(\zeta, t) = x(\zeta, t) - \hat{x}(\zeta, t)$ satisfies the following equation:

$$\dot{\epsilon}(\zeta, t) = [A - L_o C]\epsilon(\zeta, t) \tag{4.38}$$

The design problem of the above state observer is to compute the observer gain L_o such that the state estimation error system described in Eq.4.38 is a stable one. The solution of the observer gain L_o in Eq.4.37 can be obtained by solving the following Lyapunov equation:

$$< \tilde{A}x, Q_o x > + < x, Q_o \tilde{A}x > = - < \tilde{C}x, N_o \tilde{C}x > \quad x \in D(\tilde{A}^*) \tag{4.39}$$

where $\tilde{A} = A - L_o C$, $\tilde{C} = 1$, Q_o is nonnegative self-adjoint operator and N_o is positive definite operator. The following theorem describes a general approach finding the observer gain L_o in Eq.4.37 [89].

Theorem 1: Under the assumption that the pair $\left(\begin{bmatrix} A_o & 0 \\ 0 & A_p \end{bmatrix}, \begin{bmatrix} C_o & C_p \end{bmatrix} \right)$ is exponentially detectable. If there exist the nonnegative self-adjoint operators Q_1 and

Q_2 that solve the following constrained operator Riccati equations:

$$\begin{aligned} A_o Q_1 + Q_1 A_o^* - 2Q_1 C_o^* C_o Q_1 + N_{11} = 0 \\ A_p Q_2 + Q_2 A_p^* - 2Q_2 C_p^* C_p Q_2 + N_{22} = 0 \\ -2Q_1 C_o^* C_p Q_2 + N_{12} = 0 \end{aligned} \tag{4.40}$$

where N_{11} is positive matrix and N_{22} is positive definite operator, and N_{12} satisfies $N_{12} = 2Q_1 C_o^* C_p Q_2$ such that $N_o = \begin{bmatrix} N_{11} & N_{12} \\ N_{12}^* & N_{22} \end{bmatrix}$ is positive definite. Then, $L_o = \begin{bmatrix} L_{o1} \\ L_{o2} \end{bmatrix} = \begin{bmatrix} Q_1 C_o^* \\ Q_2 C_p^* \end{bmatrix}$ is the observer gain.

Remark 2: The Luenberger observer gain designed for continuous coupled PDE-ODE system is related to the corresponding discrete system, see [21]. The unique solution Q_o to the continuous Lyapunov equation in Eq.4.39 is also the solution to the discrete Lyapunov equation in the following form:

$$< x, [\tilde{A}_d^* Q_o \tilde{A}_d - Q_o] x >= - < x, [\tilde{C}_d^* N_o \tilde{C}_d] x > \quad x \in D(\tilde{A}_d^*) \tag{4.41}$$

where $\tilde{A}_d = A_d - L_d C_d$ and $\tilde{C}_d = \sqrt{2\delta}\tilde{C}[\delta - \tilde{A}_d]^{-1}$.

4.5 Simulation Results

In this section, we demonstrate the implementation of the model predictive control to stabilize the subsystem at steady state and reject input disturbance, see Fig.4.4. The optimal controller is designed to satisfy input constraint and achieve the requirement of minimizing energy cost to improve the efficiency of the system. The output observer

is considered in the controller design to observer the real physical plant system.

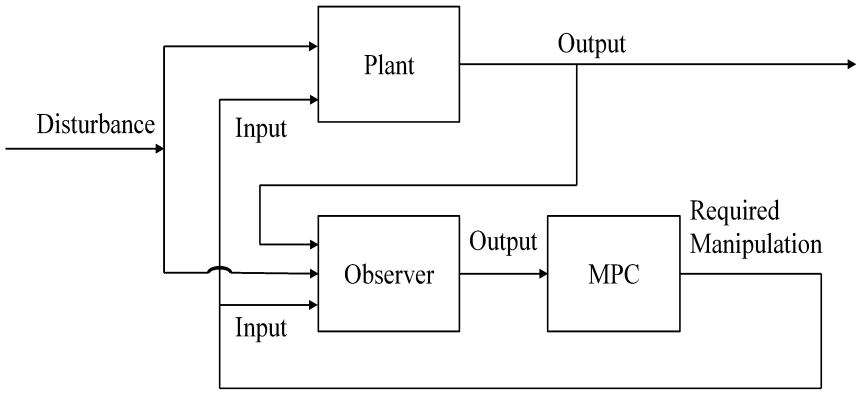

Fig. 4.4: Scheme of model predictive control for solar thermal system with borehole seasonal storage.

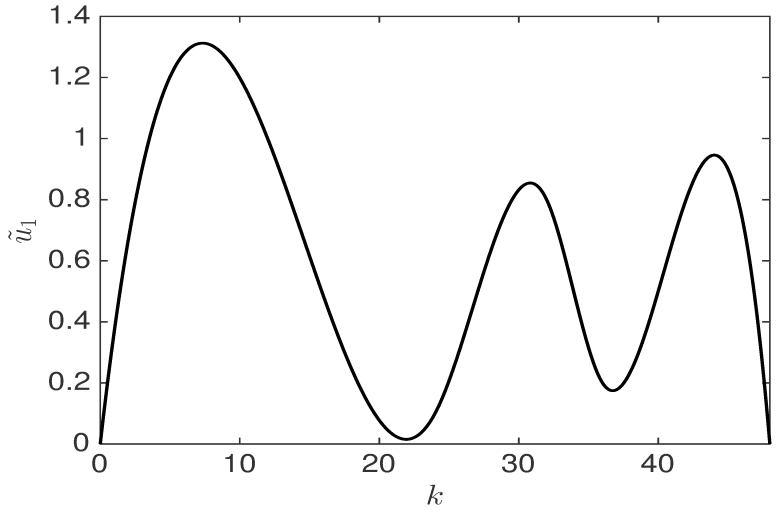

Fig. 4.5: Simulation of the solar radiation $\tilde{u}_1(t)$ in 48 hours.

We consider a scenario when the system is operating during the heating season, such that both solar power plant and geothermal system provide thermal energy to the district heating loop system. However, the solar power plant undergoes distur-

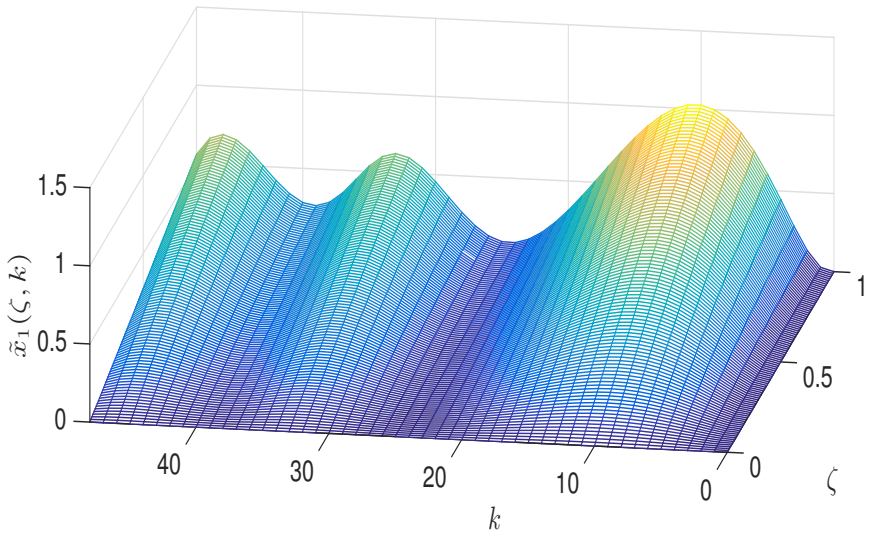

Fig. 4.6: Simulation of the solar thermal system profile given by the discrete system in Eq.4.3. The parameters of the system are $\alpha_1 = 1$, $\beta_1 = 0.3$, $\beta_2 = 0.4$ and $\gamma_1 = 0.4$. The input $\tilde{u}_1(t)$ is the periodic harmonic function.

bance due to larger variations of the weather. According to the weather forecast, the possible disturbance to the solar thermal system can be considered as periodic harmonic disturbance, see Fig.4.5. In simulation of 2 days solar radiation, we consider day 1 as a sunny day and day 2 as a cloudy day. Similarly, we consider the disturbance from borehole thermal system as uniform disturbance with reasonable assumption. These fluctuations cause a large burden on the rest of the energy system, therefore, the control goal is to maintain the temperature of hot flow to the district heating loop system at steady state and to reject two input disturbances described above.

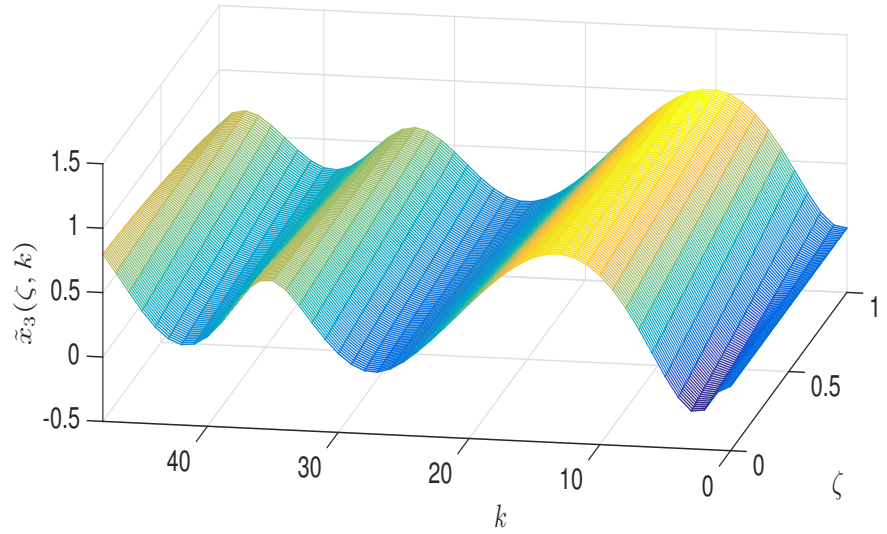

(a) State $\tilde{x}_3(\zeta, k)$

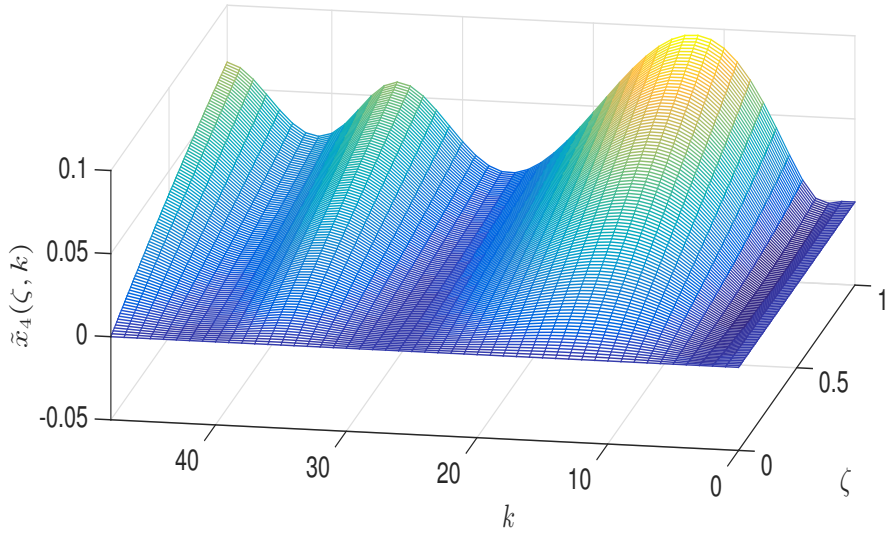

(b) State $\tilde{x}_4(\zeta, k)$

Fig. 4.7: Simulation of the heat exchanger system given by the discrete system in Eq.4.4.6. The parameters of the system are $\alpha_3 F_1 = 1$, $\alpha_4 u_{2ss} = 1$, $\beta_3 = 0.15$, $\beta_4 = 0.1$. The input $\tilde{u}_2(t) = 0$.

In the overall system, the inputs $U_1(t)$ and $U_3(t)$ are the solar and geothermal radiations, which are transferred to district heating loop system as input disturbances. We consider the flow rate in heat exchanger system and hot tank system operate at steady state, which implies that the inputs $U_2(t)$ and $U_4(t)$ are zero in this modelling. For the control of district heating loop system, the input $\tilde{u}_7(t)$ in $U_5(t)$ is the manipulation obtained from the application of model predictive control and the input $\tilde{u}_8(t)$ in $U_5(t)$ is the district radiation which is considered as zero here.

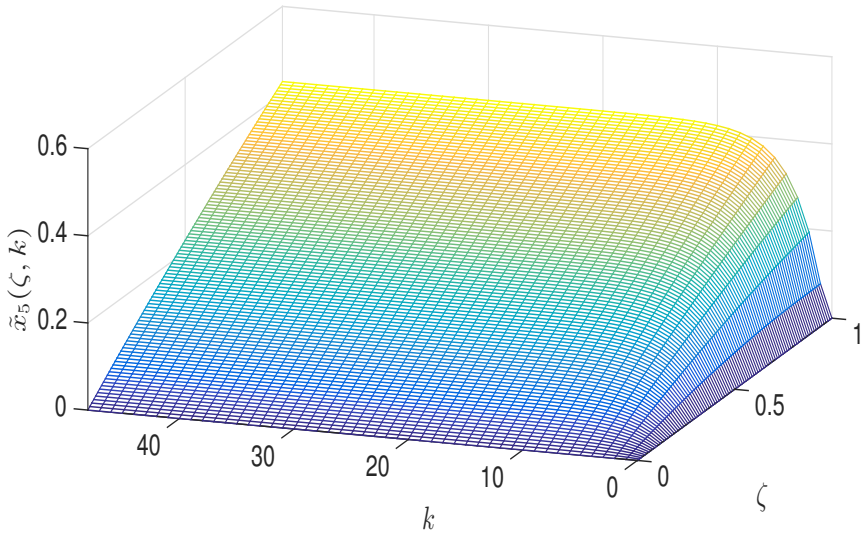

Fig. 4.8: Simulation of the BTES system given by the discrete system in Eq.4.8. The parameters of the system are $\alpha_5 = 1$, $\beta_5 = 0.3$, $\beta_6 = 0.5$ and $\gamma_3 = 0.2$. The input is a constant function $\tilde{u}_3(t) = 1$.

The disturbances in the solar thermal system $G_1(t)$ and the BTES system $G_3(t)$ are from the cold tank system and they are assumed as zero in this chapter. The disturbances $G_2(t)$ in the heat exchanger system, $G_4(t)$ in the hot tank system, and $G_5(t)$ in the district heating loop system are transferred from the solar thermal system and the BTES system due to solar and geothermal radiations. Therefore, the model

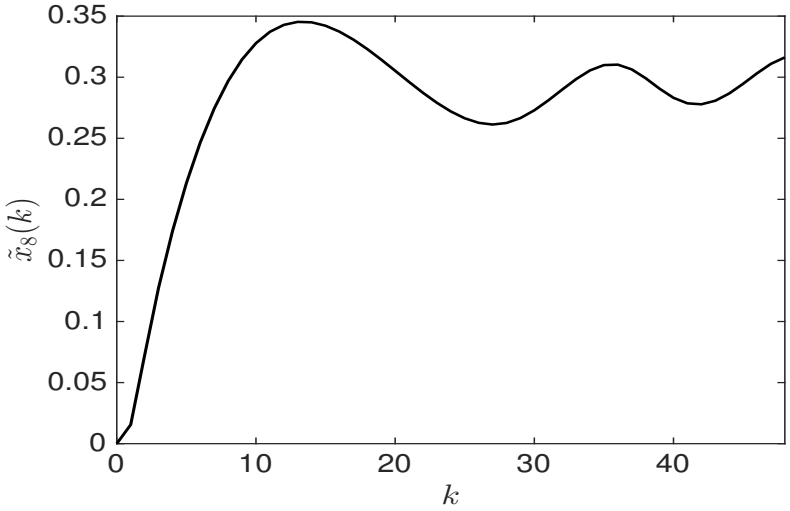

Fig. 4.9: Simulation of the hot tank system given by the discrete system in Eq.4.11. The parameters of the system are $\beta_7 = 0.8$ and $K_1 = 0.5$. The inputs $\tilde{u}_4(t) = \tilde{u}_5(t) = 0$.

predictive controller for the district heating loop system is designed to reject input disturbance $G_5(t)$ caused by solar and geothermal radiations.

The changes of solar radiation on warm sunny or cold cloudy days affect the dynamics of the solar thermal system, see Fig.4.6. The energy can be quickly and effectively retrieved from the heat exchanger and supplied to the houses without losing too much energy to the environment, see Fig.4.7. When space heating is required, energy from the STTS heats the district heating loop system. If there is insufficient energy in the STTS to meet the anticipated heating requirement, heat is transferred from the BTES into the STTS to meet the requirement. Fig.4.8 and Fig.4.9 show simulation results of the BTES system and the hot tank system, separately. If the stored water temperature is insufficient to meet the current heating load, natural gas boilers raise the temperature of the district loop as required. Fig.4.10-Fig.4.12

give the simulation of the model predictive control proposed in Eq.4.35 applied on the district heating loop system described in Eq.4.15. In simulation, the initial conditions of all states are zeros and $d\zeta = 0.01$ and $dt = 0.1$.

The manipulation of natural gas fired boilers in the turn on and off modes leads to the possibly instability of district heating looping system. From the simulation result given in Fig.4.10, it can be seen that the model predictive control stabilizes the unstable coupled PDE-ODE system presented in Eq.4.15. Solar and geothermal radiations are transferred to the district heating loop system as input disturbance through the hot tank system, see Fig.4.9. The model predictive controller proposed in this chapter rejects this input disturbance with good performance.

Fig.4.11 shows the input manipulation obtained from MPC, which is the solution to the constrained optimization problem with the parameters $Q = \begin{bmatrix} 1 & 0 \\ 0 & 1 \end{bmatrix}$, $R = 0.001$, and horizon $N = 3$. From Fig.4.11a, it can be seen that the input satisfies the input constraints, which are upper and lower limitations of realistic manipulations in the natural gas fired boilers system. In other words, this controller prevents the excessiveness of inputs which may cause damage to equipment or shutdown of system. Fig.4.11b gives the simulation result of input with disturbance and it shows that the range of input constraints changes respect to the time.

Fig.4.12 gives simulate output of the solar boreal thermal system in 3 case studies. In case study 1, Fig.4.12a shows the output of the district heating loop system without the consideration of observer. The output profile indicates that the controller works well to keep the district heating loop system operate at desired steady state.

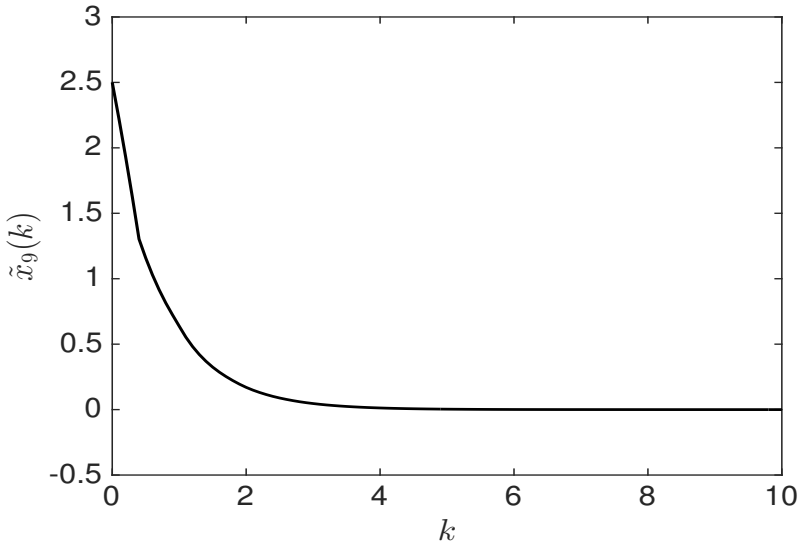

(a) State $\tilde{x}_9(k)$

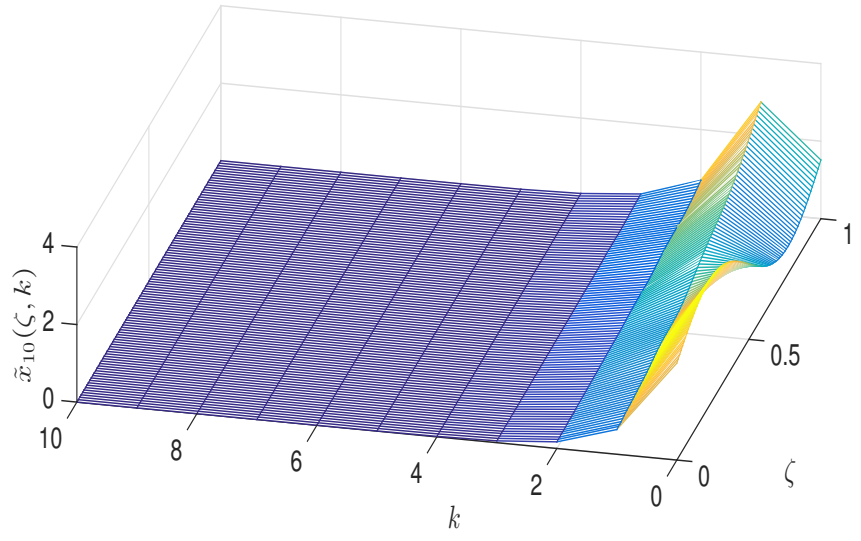

(b) State $\tilde{x}_{10}(\zeta, k)$

Fig. 4.10: Simulation of the district heating loop system given by the discrete system in Eq.4.15 under the implementation of model predictive control described in Eq.4.35. The parameters of the system are $\beta_9 = -0.5$, $\gamma_7 = 2.5$ and $\alpha_{10} = 1$. The input $\tilde{u}_8(t) = 0$ and the input $\tilde{u}_7(t)$ is calculated from the model predictive controller design.

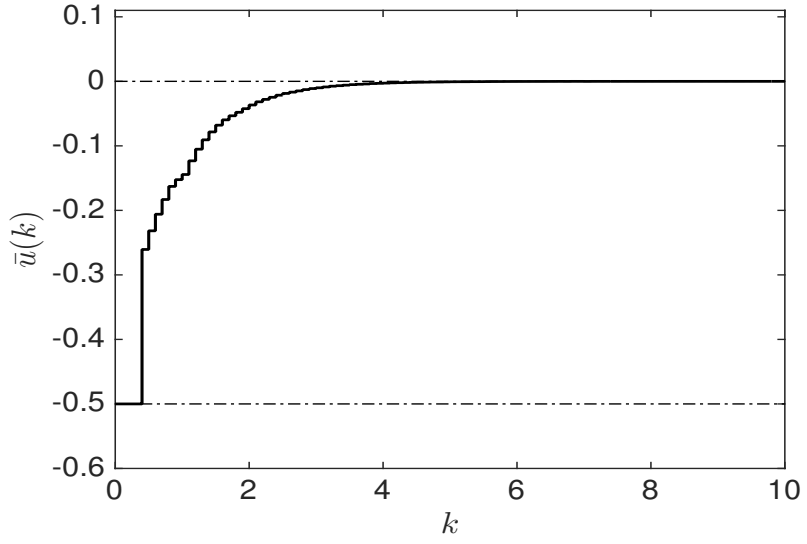

(a) Input with disturbance $\bar{u}(k)$

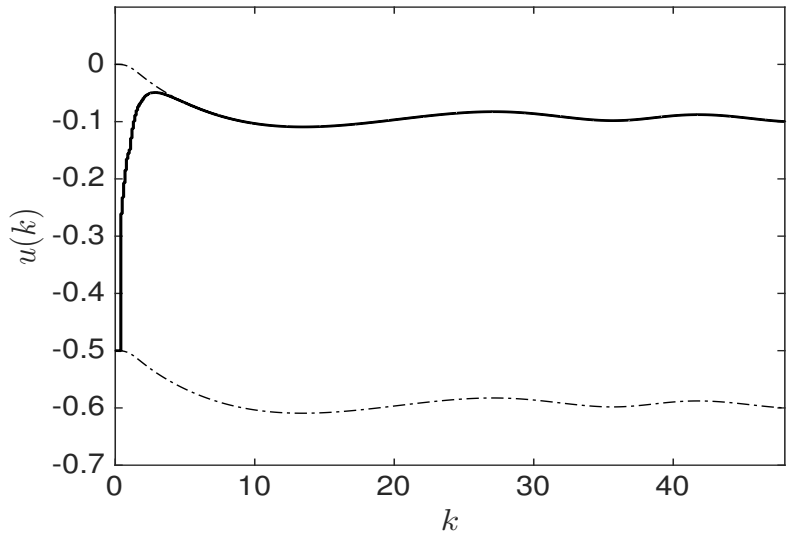

(b) Input $u(k)$

Fig. 4.11: Simulation of the input profile with disturbance $\bar{u}(k)$ and the input profile $u(k)$ in the district heating loop system given by the discrete system in Eq.4.15 under the implementation of model predictive control described in Eq.4.35.

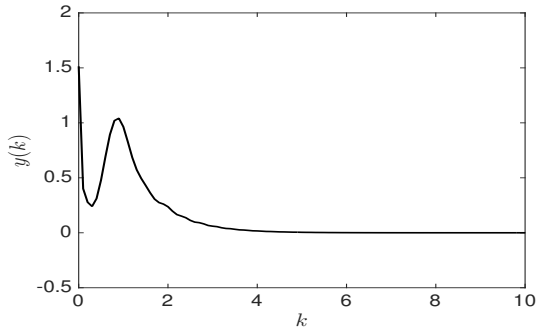

(a) System output $y(k)$

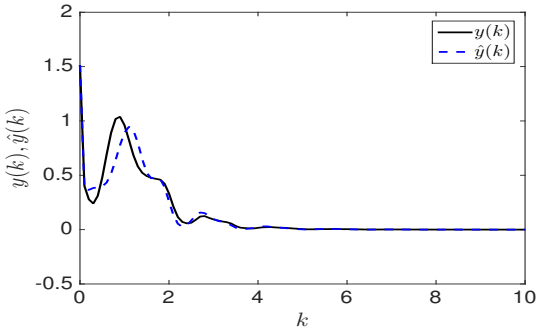

(b) System output $y(k)$ and observer output $\hat{y}(k)$

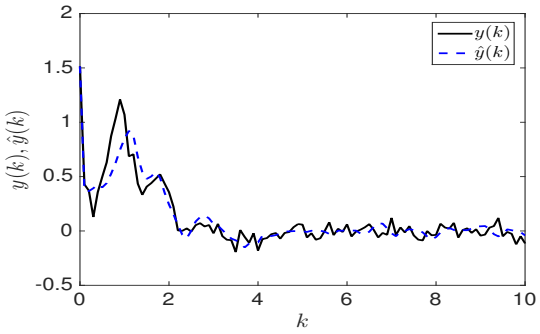

(c) System output $y(k)$ with noise and observer output $\hat{y}(k)$

Fig. 4.12: Comparison of the system output profile $y(k)$ (solid line) and the observer output profile $\hat{y}(k)$ (dashed line) in the district heating loop system given by the discrete system in Eq.4.15 under the implementation of model predictive control described in Eq.4.35 with the consideration of Luenberger observer in Eq.4.37.

However, case study 1 suits the case that the states of the district heating loop system are measurable. Due to the limitation of measurement in realistic system, the output observer is designed to reconstruct the states of the district heating loop system as case study 2, see Fig.4.4. Fig.4.12b gives the comparison of the system output $y(k)$ (solid line) and the observer output $\hat{y}(k)$ (dashed line). In simulation, we assume $N_{11} = N_{22} = 1$, by solving Riccati equation in Eq.4.40, we obtain $Q_1 = 2.0328$ and $Q_2(\zeta)$ as a spatial function. $N_{12} = 0.4926$ satisfies the condition that $N_o = \begin{bmatrix} N_{11} & N_{12} \\ N_{12}^* & N_{22} \end{bmatrix}$ is positive definite. According to Theorem 1, we have observer gain $L_{o1} = Q_1 C_o^* = 1.2314$ and $L_{o2} = Q_2 C_p^* = 0.2000$. The profiles indicate that the output observer has good performance, such that the model predictive controller designed in this case study can be applied in realistic system with the output measurement.

In the realistic district heating loop system, the noise from the operation environment can also affect the control manipulation. Therefore, we give the simulation of case study 3, such that a measurement noise is considered for the system output. In Fig.4.12c, the output $y(k)$ is simulated with measurement noise which is modelled as white noise with zero mean and standard variance as $\sigma = 0.05$, and it can be seen that the model predictive controller has good control performance to let the district heating loop system operate at desired steady state.

From the above 3 case studies, it indicates that the implementation of the model predictive control on the solar boreal thermal system can stabilize the district heating loop system at steady state and reject input disturbance from solar and/or geothermal system. The optimal controller is designed to satisfy the input constraints, which prevents damage to equipment or shutdown of system. In addition, the output boundary observer has good performance to reconstruct the states of the district heating loop system such that MPC is applicable in real physical plant system. The constrained

optimal controller developed in this section minimizes the energy cost to improve the efficiency of the system.

4.6 Conclusion

In this chapter, we provide a mathematical model of the solar thermal system with borehole seasonal storage which is a coupled finite and infinite dimensional space setting. The discrete system is obtained by applying the Cayley-Tustin time discretization on coupled a PDEs-ODEs system modelled according to the energy balance. We develop a model predictive controller design for the solar boreal thermal system which takes into account the measurements of the input disturbances and the consideration of the output observer. The control system regulates the natural gas energy into the system in order to fulfil the demands of space heating in the district heating loop system. The simulation results show that, the model predictive controller with an output observer has good performance to stabilize the unstable coupled PDE-ODE system and rejects input disturbances. This optimal control scheme with the consideration of input constraints is developed to help the solar thermal system with borehole seasonal storage to operate more efficiently.

Chapter 5

Single-step Full State Feedback Control Design for Nonlinear Hyperbolic PDEs

5.1 Introduction

The most desirable feedback control design for finite dimensional nonlinear system is based on the system's feedback linearization and subsequent pole placement application by the full state feedback control structure [90, 91, 92]. This exact feedback linearization with pole placement is realized by the two-step procedure. The first step, the implementation of nonlinear coordinate transformation to transform the original nonlinear system to a linear and controllable one, and subsequent second step, the employment of pole placement techniques with desired "target" closed-loop eigenvalues for the transformed linear system.

Although intuitive and straightforward, the two-step approach has drawbacks that

the nonlinear coordinate transformation, which is based on very restrictive conditions, is hardly met by any relevant physical system of higher order [90, 91]. Motivated by Luenberger's early ideas on a single-step design approach for pole placement, the development of single-step controller design that achieves simultaneously the feedback linearization and desired pole placement has been accomplished by Kazantzis and Kravaris [93, 94]. In particular, the design method successfully solves the system of singular first-order quasi-linear partial differential equations (PDEs) by applying Lyapunov's auxiliary theorem, and yields the nonlinear locally invertible coordinate transformation that accompanies pole placement design.

Contrary to the abundance of results considering controller design methods for nonlinear finite dimensional system, the controller synthesis for nonlinear distributed parameter system (DPS) which is given in an infinite dimensional setting is rather rare and difficult both in terms of design and/or implementation. Within the linear infinite dimensional setting, the extensions of full state feedback, output feedback regulation, optimal control, internal model control, and backstepping are successfully realized [26, 27, 28, 29, 30, 31, 32, 33, 34]. However, only small number of nonlinear finite dimensional control design methodologies were extended to nonlinear infinite dimensional systems [35], and only some results of associated Lyapunov based methods have been explored in the infinite dimensional setting [36, 37]. Consequently, an extension of finite dimensional design methods to DPS in infinite dimensional setting is pursued as possible extension of finite dimensional controller design by intuitive single-step method which achieves simultaneously state coordinate transformation and pole placement.

In this chapter, we seek a novel extension of a single-step design method that achieves simultaneous coordinate transformation and closed-loop desired target dy-

namics assignment for the broad class of first-order nonlinear hyperbolic PDEs systems and second-order hyperbolic PDEs systems. Firstly, a scalar hyperbolic PDE system which describes the dynamics of a tubular reactor is explored to develop a solution of the associated system of first-order quasi-linear PDE. Specifically, we consider the class of transport-reaction systems described by the first-order hyperbolic PDEs, which are physical relevant models of industrial exothermic plug-flow reactors. In practice, reactor design and operation often involve a trade-off between conflicting costs and in particular conversion and energy costs. For industrially important exothermic plug-flow reactors, the aim is to maximize reactant conversion, while minimizing side products and compression power. In contrast to optimizing a finite number of parameters, the optimal solution for conflicting conversion and energy costs is derived from optimal heat exchanger temperature, which has been accomplished by Smets, Dochain and Van Impe [95, 96]. The optimal solution with respect to a defined cost function is the steady state of the temperature and reactant concentration in an exothermic plug-flow reactor. However, the optimal temperature and reactant concentration profiles of interest are unstable steady-states. Therefore, we utilize the single-step full state feedback control design with a nonlinear coordinate transformation that achieves desired stabilization of the closed-loop system dynamics.

In addition to the physically interesting and appealing exothermic plug-flow reactors, we also consider the second example of the single-step full state feedback control design realization in the case of second-order hyperbolic PDE system which describes damped wave equation. The second-order hyperbolic PDE can be reduced to the first-order hyperbolic PDEs by state transformation. Similarly, linear and quadratic full state feedback control laws are proposed and utilized by single-step linearization and simultaneous coordinate transformation to the target system. The appealing

of single-step coordinate transformation is that all eigenvalues of the damped wave equation are shifted from unstable complex plain to the stable one. In some sense, this transformation mimics the "backstepping" approach which assigns target PDE behaviour through the transformation.

The chapter is organized as follows. In section 5.2, the extension of single-step design for the class of first-order nonlinear hyperbolic PDEs system is introduced. In section 5.3, we explore the solution of the associated system of first-order quasi-linear PDE by using scalar hyperbolic PDE system. In section 5.4, we explore the single-step full state feedback control by applying the design methodology to two systems and we demonstrate the method through simulation studies.

5.2 Preliminaries

We extend the single-step controller design of feedback linearization with desired stable target system assignment applied to a certain class of distributed parameter systems. In particular, we are interested in the class of the transport-reaction system described by the first-order nonlinear hyperbolic PDEs. We consider the general system representation which is described by the following form:

$$\begin{aligned} &\frac{\partial x}{\partial t}(\zeta,t) = -v\frac{\partial x}{\partial \zeta}(\zeta,t) + f[x(\zeta,t)] + g[x(\zeta,t)]u(t) \\ &x(0,t) = x_0, \quad x(\zeta,0) = \bar{x}_0 \end{aligned} \tag{5.1}$$

where the state $x(\zeta,t) \in H^n$, H is a real Hilbert space, $\zeta \in [0,L]$ and $t \in [0,\infty]$ denote the spatial and time coordinates; the input $u(t) \in U$; $f[x(\zeta,t)]$, $g[x(\zeta,t)]$ are nonlinear spatial vector fields on R^n; v is diagonal matrix. We assume that there is a well defined spatial equilibrium state $[x_{ss}(\zeta), u_{ss}]$ such that $-v\frac{\partial x_{ss}}{\partial \zeta}(\zeta) + f[x_{ss}(\zeta)] + g[x_{ss}(\zeta)]u_{ss} = 0$

holds, which can be obtained as spatially uniform steady state x_{ss} in the case of the scalar conservative law or as a set of spatially nonuniform steady state profiles for the system of first-order hyperbolic PDEs.

To apply the extension of the full state feedback linearization design from the finite dimensional state space geometric control theory to the hyperbolic PDE class of distributed parameter setting, we seek a nonlinear coordinate transformation $z(\zeta,t) = w[x(\zeta,t)]$ defined in the neighborhood of the steady state x_{ss} and application of static state feedback control law $u(t) = -Kz(\zeta,t)$, with $Kw[x(\zeta,t)]$ being defined on input space U. By applying the nonlinear coordinate transformation through the static full state feedback control law, the closed-loop system admits the behaviour of "target" stable distributed parameter system, so that Eq.5.1 is transformed to the following form:

$$\frac{\partial z}{\partial t}(\zeta,t) = \mathcal{A}z(\zeta,t) = -\bar{v}\frac{\partial z}{\partial \zeta}(\zeta,t) + \sigma z(\zeta,t), \quad z(\zeta,0) = w^{-1}\bar{x}_0 \tag{5.2}$$

where $\mathcal{A}$ is a stable linear operator which contains features of the spatial operator identical to the one given by Eq.5.1.

The extension of Luenberger's single-step design is a combination of a simultaneous locally invertible nonlinear coordinate transformation $z(\zeta,t) = w[x(\zeta,t)]$ by means of a linear static state feedback $u(t) = -Kz(\zeta,t)$ induces desired "target" closed-loop dynamics. In other words,

$$\begin{aligned} &\frac{\partial x}{\partial t}(\zeta,t) = -v\frac{\partial x}{\partial \zeta}(\zeta,t) + f[x(\zeta,t)] + g[x(\zeta,t)]u(t) \\ &\underset{z(\zeta,t)=w[x(\zeta,t)]}{\overset{u(t)=-Kz(\zeta,t)}{\Longrightarrow}} \frac{\partial z}{\partial t}(\zeta,t) = -\bar{v}\frac{\partial z}{\partial \zeta}(\zeta,t) + \sigma(\zeta)z(\zeta,t) \end{aligned} \tag{5.3}$$

in the core of the design procedure is to identify locally invertible nonlinear transformation which achieves target behaviour of desired closed-loop system through the application of Lyapunov Auxiliary theory.

5.3 Scalar Hyperbolic PDE System

A typical conservative system found in the process control is governed by the following scalar hyperbolic equation:

$$\frac{\partial x}{\partial t} + v\frac{\partial x}{\partial \zeta} = \alpha e^{x} - \beta(x-u), \quad x(0,t) = 0 \tag{5.4}$$

which represents common tubular reactor realization with simplified chemical kinetics. The above expression confirms the existence of spatially uniform nontrivial steady-state. The form e^x is for the temperature dependence result when the usual Arrhenuius form $k_0 e^{-E/T}$ is approximated by $k_0 e^{-E/T_0} e^{E(T-T_0)/T_0^2}$ through a Taylor series expansion of E/T about a reference temperature T_0 [97], and the scaling leads the state to be bounded as $||x(\zeta,t)|| \leq 1$.

The design method implies to propose a nonlinear transformation $z(w_1, w_2, \cdots, x) = \sum_{i=1}^{\infty} w_i(\zeta)x^i(\zeta,t) = WX$ (matrices $W = [w_1 \quad w_2 \quad \cdots]$ and $X = [x \quad x^2 \quad \cdots]^T$), such that the transformed target system admits stable desired dynamics given by the following form:

$$\frac{\partial z(w_i,x)}{\partial t} = -\bar{v}\frac{\partial z(w_i,x)}{\partial \zeta} \tag{5.5}$$

where $i = 1, 2, \cdots$. Then, one can obtain an associated system of first-order quasi-

linear PDE with full state feedback $u = -Kz(w_i, x)$ given as below:

$$\frac{\partial z(w_i,x)}{\partial x}[-v\frac{\partial x}{\partial \zeta} + \alpha e^x - \beta x - \beta K z(w_i,x)] = -\bar{v}\frac{\partial z(w_i,x)}{\partial \zeta} \tag{5.6}$$

Remark 1: Under the reasonable assumption that the control input does not change the velocity term associated with the spatial derivative, we have $\bar{v} = v$ in the scalar case. Although, the velocity term v can be a spatial function $v(\zeta)$, in this analysis, we consider that velocity term v is a constant.

We now present the so-called Lyapunov's Auxiliary Theorem that can be employed to guarantee the existence and uniqueness of solution to the first-order quasi-linear PDE in Eq.5.6.

5.3.1 Lyapunov's Auxiliary Theorem for Scalar System

Consider the following system of first-order quasi-linear partial differential equation, see [98]:

$$\begin{gathered} \tfrac{\partial w(x)}{\partial x}\phi(x,w) = \psi(x,w) \\ w(0) = 0 \end{gathered} \tag{5.7}$$

with

$$\begin{gathered} \phi(0,0) = 0 \\ \psi(0,0) = 0 \\ \tfrac{\partial \psi(0,0)}{\partial x} = 0 \end{gathered}$$

where $w \in R$ is the unknown solution of Eq.5.7 and $\phi(x,w) : R \times R \to R$, $\psi(x,w) : R \times R \to R$ are analytic functions. The above system of first-order quasi-linear PDE admits a unique analytic solution $w(x)$ in a neighborhood of $x^0 = 0$ with $\frac{\partial w(0)}{\partial x} = 0$.

Theorem 1: The system of first-order quasi-linear singular PDE of the form in Eq.5.6 with initial condition $z(x=0) = 0$ admits a unique locally invertible analytic solution $z = S(x)$ in a neighborhood of the equilibrium point $x^0 = 0$.

Proof: With the assumptions that $\alpha e^x - \beta x = f(x) = \frac{1}{1!}\frac{\partial f(x)}{\partial x}x + \frac{1}{2!}\frac{\partial^2 f(x)}{\partial x^2}x^2 + \cdots + \frac{1}{N!}\frac{\partial^N f(x)}{\partial x^N}x^N + \cdots = Fx + \bar{f}(x)$ and $z(w_i, x) = w_1 x + \bar{z} = w_1 x + \bar{W}\bar{X}$, here, we denote matrices $\bar{W} = [w_2 \quad w_3 \quad \cdots]$ and $\bar{X} = [x^2 \quad x^3 \quad \cdots]^T$, so the first-order quasi-linear PDE in Eq.5.6 becomes:

$$\begin{aligned} &[w_1 + \frac{\partial[\bar{W}\bar{X}]}{\partial x}][-v\frac{\partial x}{\partial \zeta} + Fx + \bar{f}(x) - \beta K(w_1 x + \bar{W}\bar{X})] \\ &= -vw_1\frac{\partial x}{\partial \zeta} - v\frac{\partial w_1(\zeta)}{\partial \zeta}x - v\frac{\partial[\bar{W}\bar{X}]}{\partial x}\frac{\partial x}{\partial \zeta} - v < \frac{\partial[\bar{W}\bar{X}]}{\partial \bar{W}}, \frac{\partial \bar{W}}{\partial \zeta} > \end{aligned} \tag{5.8}$$

From the Eq.5.8, $w_1(\zeta)$ has to satisfy the following equation:

$$w_1 F - w_1 \beta K w_1 = -v\frac{\partial w_1(\zeta)}{\partial \zeta} \tag{5.9}$$

and the unknown function $\bar{z} = \bar{W}\bar{X}$ in the following first-order system of quasi-linear PDE:

$$\begin{aligned} \frac{\partial \bar{z}}{\partial x}\phi(x,\bar{z}) &= \psi(x,\bar{z}) \\ \bar{z}(x=0) &= 0 \end{aligned} \tag{5.10}$$

where

$$\phi(x,\bar{z}) = (F - \beta KW)x + \bar{f}(x) - \beta K\bar{z}$$
$$\psi(x,\bar{z}) = -v < \frac{\partial[\bar{W}\bar{X}]}{\partial \bar{W}}, \frac{\partial \bar{W}}{\partial \zeta} > -W\bar{f}(x) + W\beta K\bar{z}$$

Note that:

$$\phi(0,0) = 0$$
$$\psi(0,0) = 0$$
$$\frac{\partial \psi(0,0)}{\partial x} = 0$$

Theorem 1 guarantees the existence and uniqueness of an analytic solution $\bar{z}$ of the system with $\frac{\partial \bar{z}(0)}{\partial x} = 0$. Given an initial condition $w_1(\zeta = 0) \neq 0$, the ordinary differential equation Eq.5.9 has a unique solution [98]. We may conclude that the associated first-order system of quasi-linear PDE in Eq.5.6 admits a unique analytic solution in a neighborhood $x^0 = 0$.

5.3.2 Analytical Solution of Quasi-linear PDE

The proof of existence and uniqueness of solution to the first-order quasi-linear PDE can also be obtained by finding analytical solution of Eq.5.6, and is demonstrated below.

Let us rewrite Eq.5.6 in the following form:

$$\frac{\partial[WX]}{\partial x}[-v\frac{\partial x}{\partial \zeta} + JX - \beta KWX] = -\bar{v}\frac{\partial[WX]}{\partial \zeta} \tag{5.11}$$

here, $J = [\frac{1}{1!}\frac{\partial f(x)}{\partial x} \quad \frac{1}{2!}\frac{\partial f^2(x)}{\partial x^2} \quad \cdots]$. By straightforward algebraic manipulation, one can obtain:

$$-v\frac{\partial[WX]}{\partial x}\frac{\partial x}{\partial \zeta} + \frac{\partial[WX]}{\partial x}[JX - \beta KWX] = -v\frac{\partial[WX]}{\partial x}\frac{\partial x}{\partial \zeta} - v < \frac{\partial[WX]}{\partial W}, \frac{\partial W}{\partial \zeta} > \tag{5.12}$$

After cancelling the term $-v\frac{\partial[WX]}{\partial x}\frac{\partial x}{\partial \zeta}$ on both hand sides, we have:

$$< W, \tilde{X} > [JX - \beta KWX] = -v < \frac{\partial[WX]}{\partial W}, \frac{\partial W}{\partial \zeta} > \tag{5.13}$$

here, $\tilde{X} = [1 \quad 2x \quad 3x^2 \quad \cdots \quad Nx^{N-1} \quad \cdots]^T$.

The solution of Eq.5.12 becomes a set of equations in the following summation form:

$$\begin{aligned} v\frac{\partial w_1}{\partial \zeta} &= \beta K w_1^2 - \frac{\partial f(x)}{\partial x} w_1 \\ v\frac{\partial w_2}{\partial \zeta} &= [3\beta K w_1 - 2\frac{\partial f(x)}{\partial x}]w_2 - \frac{1}{2}\frac{\partial^2 f(x)}{\partial x^2} w_1 \\ &\vdots \\ v\frac{\partial w_N}{\partial \zeta} &= \beta K \sum_{i=1}^{N} i w_i w_{N+1-i} - \sum_{i=1}^{N} i w_i \frac{1}{(N+1-i)!}\frac{\partial^{N+1-i} f(x)}{\partial x^{N+1-i}} \\ &\vdots \end{aligned} \tag{5.14}$$

The ordinary differential equation of $w_1(\zeta)$ yields the following Bernoulli equation:

$$\frac{dw_1}{d\zeta} = p(\zeta)w_1 + q(\zeta)w_1^2 \tag{5.15}$$

here $p(\zeta) = -\frac{1}{v}\frac{\partial f(x)}{\partial x}$ and $q(\zeta) = \frac{1}{v}\beta K$. The function $w_1(\zeta)$ is a solution of the Bernoulli equation in Eq.5.15 if the function $y(\zeta) = \frac{1}{w_1(\zeta)}$ is solution of the linear

differential equation as below:

$$\frac{dy}{d\zeta} = -p(\zeta)y - q(\zeta) \tag{5.16}$$

Given the constants $\zeta_0 \in [0,1]$ and $y_0 \in R$, the above linear differential equation is the initial value problem with $y(\zeta_0) = y_0$ and has the unique solution $y(\zeta)$ on the domain $[0,1]$.

The ordinary differential equations of $w_2(\zeta), w_3(\zeta), \cdots, w_N(\zeta), \cdots$ yield the well-posed initial value problem. Let us take $w_2(\zeta)$ as an example which yields the following equation:

$$\frac{dw_2}{d\zeta} = a(\zeta)w_2 + b(\zeta) \tag{5.17}$$

here $a(\zeta) = \frac{1}{v}[3\beta K w_1 - 2\frac{\partial f(x)}{\partial x}]$ and $b(\zeta) = -\frac{1}{v}\frac{\partial^2 f(x)}{\partial x^2}w_1$. $w_1(\zeta)$ is the known function obtained from Eq.5.15. Given the continuous functions $a(\zeta)$ and $b(\zeta)$, and constants $\zeta_0 \in [0,1]$ and $y_0 \in R$, the initial value problem yielded as below:

$$\frac{dy}{d\zeta} = a(\zeta)y + b(\zeta), \quad y(\zeta_0) = y_0 \tag{5.18}$$

has the unique solution $y(\zeta)$ on the domain $[0,1]$, given by the following expression:

$$y(\zeta) = e^{A(\zeta)}[y_0 + \int_{\zeta_0}^{\zeta} e^{-A(s)}b(s)ds] \tag{5.19}$$

where the function $A(\zeta) = \int_{\zeta_0}^{\zeta} a(s)ds$ is a particular primitive of function $a(\zeta)$.

Since $w_2(\zeta)$ in Eq.5.17 has unique solution, the subsequent
$w_3(\zeta), w_4(\zeta), \cdots, w_N(\zeta), \cdots$ are recursive functions and also have unique solutions.

Next, we show that the sum $\sum_{i=1}^{\infty} w_i(\zeta)x^i(\zeta,t)$ converges to an analytic function.

Theorem 2: The solution of initial value problem obtained in Eq.5.18 is bounded.

Proof: $||A(\zeta)|| = ||\int_{\zeta_0}^{\zeta} a(s)ds|| \leq \int_{\zeta_0}^{\zeta} ||a(s)||ds \leq A_m T$ for all $\zeta \in [0,1]$, where $A_m = max||A(\zeta)||$ for all $\zeta \in [0,1]$ and $T = 1 - 0 = 1$. One can obtain $e^{A(\zeta)} \leq e^{||A(\zeta)||} \leq e^{A_m}$ for all $\zeta \in [0,1]$. Then, $||\int_{\zeta_0}^{\zeta} e^{-A(s)}b(s)ds|| \leq \int_{\zeta_0}^{\zeta} ||e^{-A(s)}||||b(s)||ds \leq e^{A_m}B_m$ for all $\zeta \in [0,1]$, where $B_m = max||b(\zeta)||$. Finally, $||y(\zeta)|| = ||e^{A(\zeta)}[y_0 + \int_{\zeta_0}^{\zeta} e^{-A(s)}b(s)ds]|| \leq ||e^{A(\zeta)}||||y_0 + \int_{\zeta_0}^{\zeta} e^{-A(s)}b(s)ds|| \leq e^{A_m}(y_0 + e^{A_m}B_m)$ for all $\zeta \in [0,1]$.

Theorem 2 guarantees that $w_1(\zeta), w_2(\zeta), \cdots, w_N(\zeta), \cdots$ are bounded solutions. We assume that in domain $\zeta \in [0,1]$, $w_M = max||w_i(\zeta)||$ for $i = 1, 2, \cdots$. Then, one can obtain $||\sum_{i=1}^{\infty} w_i(\zeta)x^i(\zeta,t)|| \leq w_M||\sum_{i=1}^{\infty} x^i(\zeta,t)||$ for all $\zeta \in [0,1]$. Since $||x(\zeta,t)|| \leq 1$, the sum $\sum_{i=1}^{\infty} w_i(\zeta)x^i(\zeta,t)$ converges to an analytic function.

In the next design realization, we consider the stable target system given in Eq.5.5 with a design parameter σ in the following form:

$$\frac{\partial z(w_i,x)}{\partial t} = -\bar{v}\frac{\partial z(w_i,x)}{\partial \zeta} + \sigma z(w_i,x) \tag{5.20}$$

The analytical solution of $w_1(\zeta)$ in Eq.5.15 is expressed as below with design parameter σ:

$$w_1(\zeta) = \frac{e^{\frac{1}{v}[\sigma - \frac{\partial f(x)}{\partial x}](\zeta-1)}}{[\frac{\beta K}{\sigma - \frac{\partial f(x)}{\partial x}}e^{\frac{1}{v}[\sigma - \frac{\partial f(x)}{\partial x}](\zeta-1)} + \frac{1}{w_1(1)}]} \tag{5.21}$$

The simulation of $w_1(\zeta)$ obtained above is given in Fig.5.1. Fig.5.1 also shows the simulation of analytical solutions of $w_2(\zeta)$, $w_3(\zeta)$ and $w_4(\zeta)$ with design parameter σ.

We also consider the case when $\sigma = \frac{\partial f(x)}{\partial x}$, and the analytical solution of $w_1(\zeta)$ in

Eq.5.15 is expressed as below:

$$w_1(\zeta) = \frac{1}{\frac{1}{w_1(1)} - \frac{\beta k}{v}(\zeta - 1)} \tag{5.22}$$

Similarly, the numerical simulation of analytical solutions of $w_1(\zeta)$, $w_2(\zeta)$, $w_3(\zeta)$ and $w_4(\zeta)$ are given in Fig.5.2.

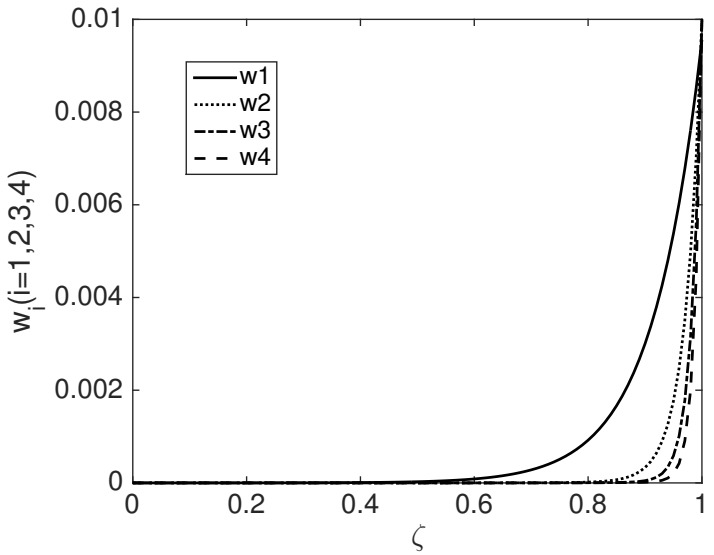

Fig. 5.1: Transform operator w_i in Eq.5.14 with $\sigma = -1$, for $i = 1, 2, 3, 4$.

5.4 Problem Formulation for the Class of Distributed Parameter Systems

Motivated by the design procedure described above, we extend the single-step coordinate transformation and stabilization of scalar hyperbolic PDE to the class of system of hyperbolic PDEs, see Eq.5.1. For the class of system of hyperbolic PDEs, we apply

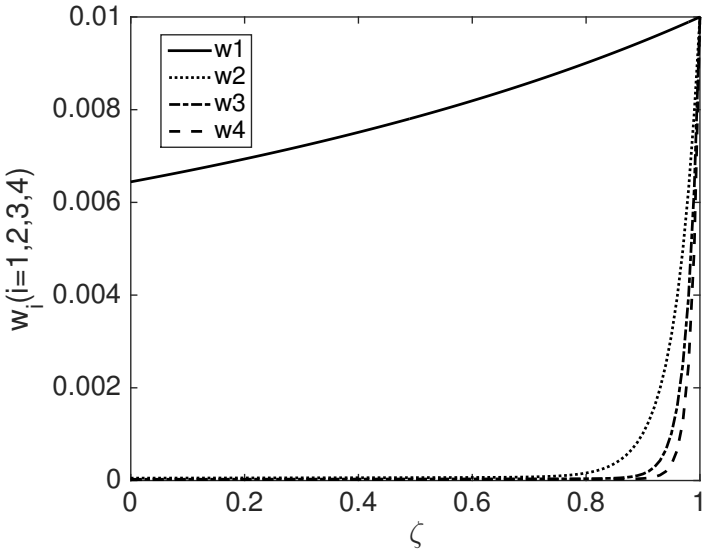

Fig. 5.2: Transform operator w_i in Eq.5.14 with $\sigma = \frac{\partial f(x)}{\partial x}$, for $i = 1, 2, 3, 4$.

the single-step state feedback control design procedure described in the above section. In particular, one may seek for the simplest spatial linear coordinate transformation given by:

$$z[x(\zeta, t)] = W(\zeta)x(\zeta, t) \tag{5.23}$$

where $W(\zeta)$ is a spatial matrix. Eq.5.1 becomes the following expression with coordinate transformation:

$$\begin{aligned} &\frac{\partial}{\partial x}\left[W(\zeta)x\right]\left[-v\frac{\partial x}{\partial \zeta} + \sigma(\zeta)x + \bar{f}(x) + b(\zeta)(-KW(\zeta)x)\right] \\ &= -\bar{v}\frac{\partial}{\partial \zeta}\left[W(\zeta)x\right] + \sigma(\zeta)\left[W(\zeta)x\right] \end{aligned} \tag{5.24}$$

which yields linear term in $x(\zeta, t)$. So that the following equation is obtained:

$$(-Wv + \bar{v}W)\frac{\partial x}{\partial \zeta} + \bar{v}\frac{\partial W}{\partial \zeta}x + W\sigma x - \sigma W x - Wb(\zeta)KWx = 0 \tag{5.25}$$

Remark 2: The velocity term in the target system yields $\bar{v} = WvW^{-1}$ under the reasonable assumption that the control input does not change the velocity term associated with the spatial derivative.

The above equation becomes the equation in $W(\zeta)$. The solution to the following equation provides the spatial transformation function $W(\zeta)$:

$$\bar{v}\frac{\partial W}{\partial \zeta} + W\sigma(\zeta) - \sigma(\zeta)W - Wb(\zeta)KW = 0, \;\; W(0) \neq 0 \tag{5.26}$$

For higher order approximation of the nonlinear coordinate transformation:

$$z(x(\zeta, t)) = W(\zeta)x(\zeta, t) + P(\zeta)x^2(\zeta, t) \tag{5.27}$$

we account for the approximation of the nonlinear vector field given by the term $\bar{f}(x) = \frac{\partial f(x)}{\partial x}|_{x_{ss}} x^2$. In other words, the expansion of higher order terms of the nonlinear transformation is required to be done to enlarge the region of stabilizing nonlinear coordinate transformation and control law.

5.4.1 First-Order Hyperbolic PDEs

Let us consider the case of nonlinear exothermic plug-flow reactor which takes the following hyperbolic PDEs form [99]:

$$\frac{\partial T}{\partial t} = -v\frac{\partial T}{\partial \zeta} - \frac{\Delta H}{\rho C_p}k_0 C e^{-\frac{E}{RT}} - \frac{4h}{\rho C_p d}(T - T_w) \tag{5.28}$$

$$\frac{\partial C}{\partial t} = -v\frac{\partial C}{\partial \zeta} - k_0 C e^{-\frac{E}{RT}}$$

with initial conditions and boundary conditions:

$$t = 0, \quad T(\zeta, 0) = T_{in}, \quad C(\zeta, 0) = C_{in}$$
$$\zeta = 0, \quad T(0, t) = T_0, \quad C(0, t) = C_0$$

where $\zeta \in [0, L]$ and $t \in [0, \infty]$, the temperature in the reactor $T(\zeta, t)$ and the reactant concentration $C(\zeta, t)$ are state variables, and the heat exchanger temperature $T_w(\zeta, t)$ is input variable.

After some basic manipulation and transformation of the system, the above set of equations is transformed to dimensionless form by defining state and input variables as $x_1 = \frac{T - T_{in}}{T_{in}}$, $x_2 = \frac{C_{in} - C}{C_{in}}$ and $u = \frac{T_w - T_{in}}{T_{in}}$ and process parameters as $\alpha = k_0 e^{-E/RT_{in}}$, $\beta = \frac{4h}{\rho C_p d}$, $\delta = -\frac{\Delta H}{\rho C_p}\frac{C_{in}}{T_{in}}$ and $\gamma = \frac{E}{RT_{in}}$. We assume initial conditions and boundary conditions as $T_{in} = 340(K)$, $C_{in} = 0.02(mol \cdot L^{-1})$, $T_0 = 340(K)$ and $C_0 = 0.02(mol \cdot L^{-1})$, so that the system becomes:

$$\frac{\partial x_1}{\partial t} = -v\frac{\partial x_1}{\partial \zeta} + \alpha\delta(1 - x_2)e^{\gamma x_1/1+x_1} - \beta x_1 + \beta u \tag{5.29}$$
$$\frac{\partial x_2}{\partial t} = -v\frac{\partial x_2}{\partial \zeta} + \alpha(1 - x_2)e^{\gamma x_1/1+x_1}$$

with initial conditions and boundary conditions:

$$x_1(\zeta, 0) = 0, \quad x_2(\zeta, 0) = 0$$
$$x_1(0, t) = 0, \quad x_2(0, t) = 0$$

where process parameters are $v = 0.1(m \cdot s^{-1})$, $\alpha = 0.0581$, $\beta = 0.2$, $\delta = 0.25$, $\gamma = 16.6607$.

In steady state, the above partial deferential equations of the system reduce to ordinary differential equations:

$$\begin{aligned} v\frac{dx_{1ss}}{d\zeta} &= \alpha\delta(1 - x_{2ss})e^{\gamma x_{1ss}/1+x_{1ss}} - \beta x_{1ss} + \beta u_{ss}, \quad x_{1ss}(0) = 0 \\ v\frac{dx_{2ss}}{d\zeta} &= \alpha(1 - x_{2ss})e^{\gamma x_{1ss}/1+x_{1ss}}, \quad x_{2ss}(0) = 0 \end{aligned} \tag{5.30}$$

The optimal control of the system at steady state is to find control $u^*(\zeta)$ which causes the system to follow an admissible trajectory $x^*(\zeta)$ while minimizing performance criterion:

$$\min_u \quad J = h[x(L)] + \int_0^L g[x(\zeta)]d\zeta \tag{5.31}$$

Here, we consider a cost criterion of the following type:

$$\min_u \quad J = (1 - A)(1 - x_2(L)) + \frac{A}{K}\int_0^L x_1^2(\zeta)d\zeta \tag{5.32}$$

where A is the trade-off coefficient between terminal and integral costs, and K is a user-defined weighting factor to bring the two costs in the same order of magnitude. The terminal cost part is a measure for the process efficiency, while the integral cost part accounts for the total heat loss.

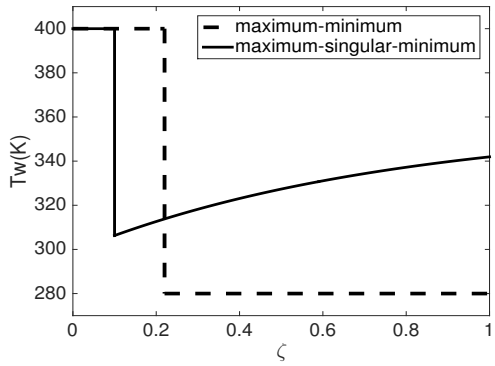

(a) Temperature in heat exchanger

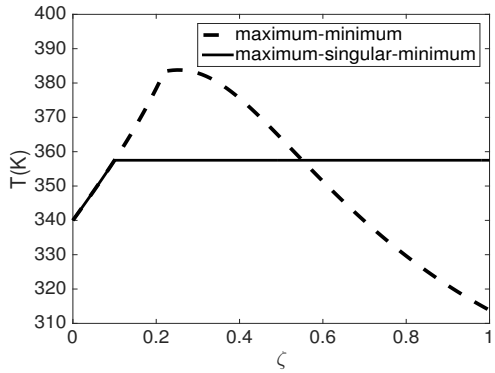

(b) Temperature in Reactor

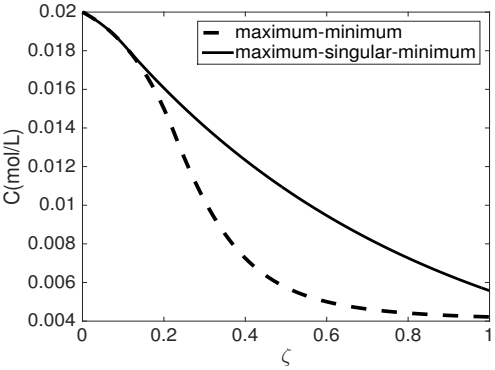

(c) Concentration in Reactor

Fig. 5.3: Optimal profiles of maximum-minimum profile (dashed line) vs. maximum-singular-minimum profile (solid line) with $A = 0.7$ and $K = 250,000$ in Eq.5.32.

According to the Minimum Principle of Pontryagin, the optimal heat exchanger profile $u^*(\zeta)$ can be maximum-minimum profile or maximum-singular-minimum profile, which is shown in Fig.5.3a. The temperature in the reactor and the reactant concentration profiles with respect to the optimal heat exchanger profiles of maximum-minimum profile as well as maximum-singular-minimum profile are illustrated in Fig.5.3b and Fig.5.3c.

This optimal steady state of interest obtained above is an unstable steady state. To make the system operate at the optimal steady state of interest, we apply single-step full state feedback control design to stabilize the system at the optimal steady state of interest. The second-order Taylor expansion of Eq.5.29 is given as follows:

$$\begin{aligned}\begin{bmatrix} \frac{\partial \tilde{x}_1}{\partial t} \\ \frac{\partial \tilde{x}_2}{\partial t} \end{bmatrix} &= -v \begin{bmatrix} \frac{\partial \tilde{x}_1}{\partial \zeta} \\ \frac{\partial \tilde{x}_2}{\partial \zeta} \end{bmatrix} + \begin{bmatrix} J_{11}(\zeta) & J_{12}(\zeta) \\ J_{21}(\zeta) & J_{22}(\zeta) \end{bmatrix} \begin{bmatrix} \tilde{x}_1 \\ \tilde{x}_2 \end{bmatrix} \\ &+ \begin{bmatrix} \frac{1}{2}H_{11}(\zeta)\tilde{x}_1^2 + H_{12}(\zeta)\tilde{x}_1\tilde{x}_2 + \frac{1}{2}H_{13}(\zeta)\tilde{x}_2^2 \\ \frac{1}{2}H_{21}(\zeta)\tilde{x}_1^2 + H_{22}(\zeta)\tilde{x}_1\tilde{x}_2 + \frac{1}{2}H_{23}(\zeta)\tilde{x}_2^2 \end{bmatrix} + \begin{bmatrix} \beta \\ 0 \end{bmatrix} \tilde{u}(t)\end{aligned} \tag{5.33}$$

where $\tilde{x} = x - x_{ss}$ and $\tilde{u} = u - u_{ss}$.

The controller synthesis goal is to apply the state feedback control law $\tilde{u} = -Kz[\tilde{x}(\zeta,t)]$ and nonlinear transformation $z[\tilde{x}(\zeta,t)] = W(\zeta)\tilde{x}(\zeta,t) + P(\zeta)\tilde{x}^2(\zeta,t)$ simultaneously, which yields the following expression:

$$\begin{aligned}\tilde{u} &= -Kz \\ &= -\begin{bmatrix} K_1 & K_2 \end{bmatrix} \begin{bmatrix} w_{11}(\zeta)\tilde{x}_1 + w_{12}(\zeta)\tilde{x}_2 + P_{11}(\zeta)\tilde{x}_1^2 + P_{12}(\zeta)\tilde{x}_1\tilde{x}_2 + P_{13}(\zeta)\tilde{x}_2^2 \\ w_{21}(\zeta)\tilde{x}_1 + w_{22}(\zeta)\tilde{x}_2 + P_{21}(\zeta)\tilde{x}_1^2 + P_{22}(\zeta)\tilde{x}_1\tilde{x}_2 + P_{23}(\zeta)\tilde{x}_2^2 \end{bmatrix}\end{aligned} \tag{5.34}$$

With control, we achieve desired closed-loop target dynamics as below:

$$\begin{bmatrix} \frac{\partial z_1}{\partial t} \\ \frac{\partial z_2}{\partial t} \end{bmatrix} = -\bar{v} \begin{bmatrix} \frac{\partial z_1}{\partial \zeta} \\ \frac{\partial z_2}{\partial \zeta} \end{bmatrix} + \begin{bmatrix} \sigma_{11}(\zeta) & \sigma_{12}(\zeta) \\ \sigma_{21}(\zeta) & \sigma_{22}(\zeta) \end{bmatrix} \begin{bmatrix} z_1 \\ z_2 \end{bmatrix} \tag{5.35}$$

where $\bar{v} = WvW^{-1}$ is identity matrix when v is identity matrix. In the simulation studies, we choose $K = [8 \;\; 4.5]$ and $\sigma = [-0.25 \;\; -0.1; 0.075 \;\; -0.45]$.

The linear control law synthesis considers only the first-order Taylor expansion of the system dynamics and is obtained by determining the numerical solution of the transformation $w(\zeta)$. In particular, with $\bar{v} = v$, the function $w(\zeta)$ is obtained by calculating the following differential equation:

$$\bar{v}\frac{dw(\zeta)}{d\zeta} = \sigma w(\zeta) - w(\zeta)J + w(\zeta)\beta K w(\zeta) \tag{5.36}$$

with initial condition $w(1)$ being design parameter. The function $w_{ij}(\zeta)$, for $i, j = 1, 2$ in Eq.5.36 is obtained by calculating the following differential equations:

$$\begin{aligned}
v\frac{dw_{11}(\zeta)}{d\zeta} &= (\sigma_{11} - J_{11})w_{11} - J_{21}w_{12} + \sigma_{12}w_{21} + \beta K_1 w_{11}^2 + \beta K_2 w_{11}w_{21} \quad (5.37)\\
v\frac{dw_{12}(\zeta)}{d\zeta} &= (\sigma_{11} - J_{22})w_{12} - J_{12}w_{11} + \sigma_{12}w_{22} + \beta K_1 w_{11}w_{12} + \beta K_2 w_{11}w_{22}\\
v\frac{dw_{21}(\zeta)}{d\zeta} &= (\sigma_{22} - J_{11})w_{21} - J_{21}w_{22} + \sigma_{21}w_{11} + \beta K_1 w_{11}w_{21} + \beta K_2 w_{21}^2\\
v\frac{dw_{22}(\zeta)}{d\zeta} &= (\sigma_{22} - J_{22})w_{22} - J_{12}w_{21} + \sigma_{21}w_{12} + \beta K_1 w_{21}w_{12} + \beta K_2 w_{21}w_{22}
\end{aligned}$$

In the simulation studies, we choose $w(1) = [0.08 \;\; 0.03; 0.005 \;\; 0.01]$, which leads to the following expression of $w(\zeta)$, see Fig.5.4. In particular, for the initial conditions given as $x_1 = x_{1ss} + 0.05e^{\zeta}$ and $x_2 = x_{2ss} - 0.1e^{\zeta}$, the linear controller is able to

stabilize the state around spatially uniform unstable steady state, see Fig.5.5.

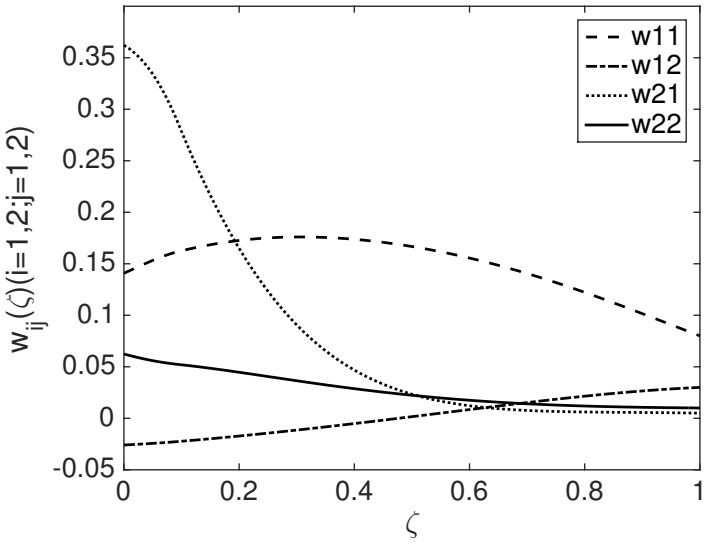

Fig. 5.4: Linear transform operator $w_{ij}(\zeta)(i,j=1,2)$ in Eq.5.36 for first-order hyperbolic PDEs described in Eq.5.29.

The quadratic control synthesis, which contains the second-order terms of the system, is obtained by determining the numerical solution of the transformation $w(\zeta)$ and $P(\zeta)$. In particular, the function $w(\zeta)$ takes the form in the Eq.5.36 and the function $P(\zeta)$ is obtained with initial condition $P(1)$. The function $P_{ij}(\zeta)$, for $i = 1,2; j = 1,2,3$ is obtained by calculating the following differential equations:

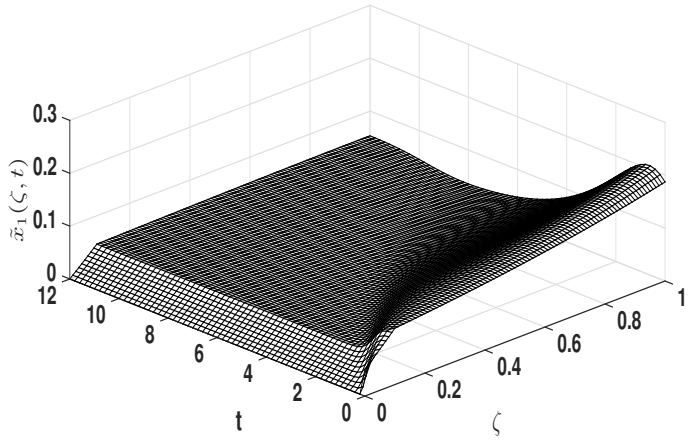

(a) Temperature $\tilde{x}_1(\zeta, t)$

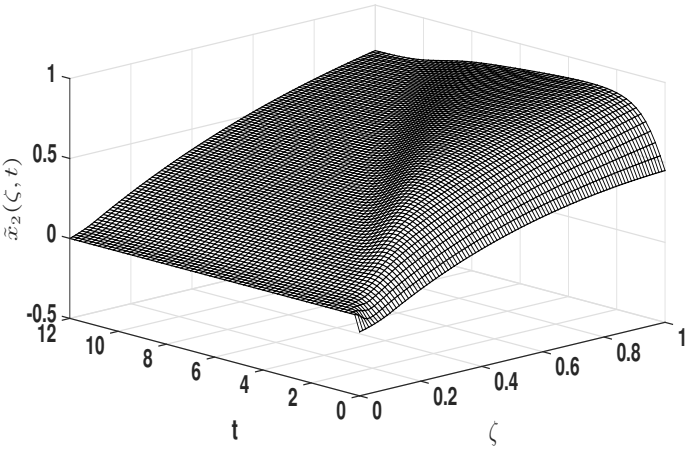

(b) Concentration $\tilde{x}_2(\zeta, t)$

Fig. 5.5: State profiles of linear single-step full state feedback control apply on first-order hyperbolic PDEs described in Eq.5.29 with transform operator $w_{ij}(\zeta)(i, j = 1, 2)$ in Eq.5.36.

$$v\frac{dP_{11}(\zeta)}{d\zeta} = \sigma_{11}P_{11} + \sigma_{12}P_{21} - (\frac{1}{2}H_{11} - \beta K_1 P_{11} - \beta K_2 P_{21})w_{11} \tag{5.38}$$
$$-2(J_{11} - \beta K_1 w_{11} - \beta K_2 w_{21})P_{11} - \frac{1}{2}H_{21}w_{12} - J_{21}P_{12}$$
$$v\frac{dP_{12}(\zeta)}{d\zeta} = \sigma_{11}P_{12} + \sigma_{12}P_{22} + \Gamma_{13}w_{21}w_{22}$$
$$-(H_{12} - \beta K_1 P_{12} - \beta K_2 P_{22})w_{11} - 2(J_{12} - \beta K_1 w_{12} - \beta K_2 w_{22})P_{11}$$
$$-(J_{11} - \beta K_1 w_{11} - \beta K_2 w_{21})P_{12} - H_{22}w_{12} - J_{22}P_{12} - 2J_{21}P_{13}$$
$$v\frac{dP_{13}(\zeta)}{d\zeta} = \sigma_{11}P_{13} + \sigma_{12}P_{23} - (\frac{1}{2}H_{13} - \beta K_1 P_{13} - \beta K_2 P_{23})w_{11}$$
$$-(J_{12} - \beta K_1 w_{12} - \beta K_2 w_{22})P_{12} - \frac{1}{2}H_{23}w_{12} - 2J_{22}P_{13}$$
$$v\frac{dP_{21}(\zeta)}{d\zeta} = \sigma_{21}P_{11} + \sigma_{22}P_{21} - (\frac{1}{2}H_{11} - \beta K_1 P_{11} - \beta K_2 P_{21})w_{21}$$
$$-2(J_{11} - \beta K_1 w_{11} - \beta K_2 w_{21})P_{21} - \frac{1}{2}H_{21}w_{22} - J_{21}P_{22}$$
$$v\frac{dP_{22}(\zeta)}{d\zeta} = \sigma_{21}P_{12} + \sigma_{22}P_{22} + \Gamma_{23}w_{21}w_{22}$$
$$-(H_{12} - \beta K_1 P_{12} - \beta K_2 P_{22})w_{21} - 2(J_{12} - \beta K_1 w_{12} - \beta K_2 w_{22})P_{21}$$
$$-(J_{11} - \beta K_1 w_{11} - \beta K_2 w_{21})P_{22} - H_{22}w_{22} - J_{22}P_{22} - 2J_{21}P_{23}$$
$$v\frac{dP_{23}(\zeta)}{d\zeta} = \sigma_{21}P_{13} + \sigma_{22}P_{23} - (\frac{1}{2}H_{13} - \beta K_1 P_{13} - \beta K_2 P_{23})w_{21}$$
$$-(J_{12} - \beta K_1 w_{12} - \beta K_2 w_{22})P_{22} - \frac{1}{2}H_{23}w_{22} - 2J_{22}P_{23}$$

In the simulation studies, we choose $P(1) = [0.01; 0.01; 0.02; 0.03; 0.01; 0.02]$, which leads to the following expression of $P(\zeta)$, see Fig.5.6. The local quadratic nature of the control law that stabilizes nonlinear plant is recognized in the case of initial conditions from which the reactor exit undergoes large excursion from the nominal operating point. For the same initial conditions in linear control simulation studies

$x_1 = x_{1ss} + 0.05e^{\zeta}$ and $x_2 = x_{2ss} - 0.1e^{\zeta}$, the quadratic controller is also able to stabilize the state around spatially uniform unstable steady state, see Fig.5.7.

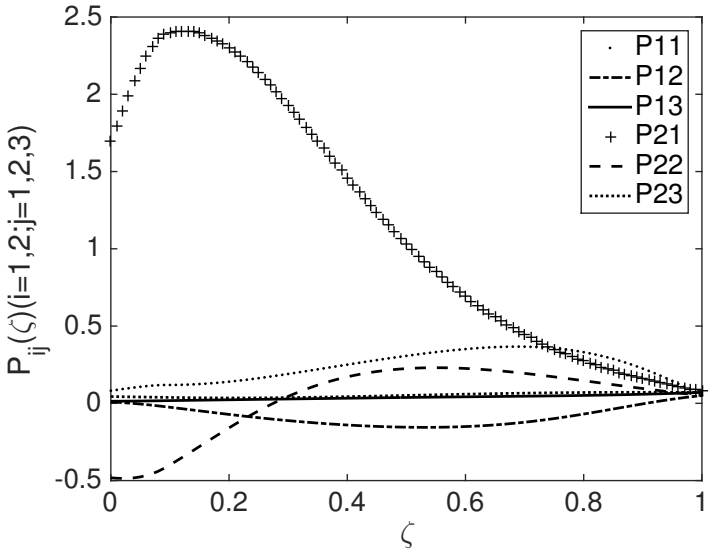

Fig. 5.6: Nonlinear transform operator $P_{ij}(\zeta)(i = 1, 2; j = 1, 2, 3)$ in Eq.5.34 for first-order hyperbolic PDEs described in Eq.5.29.

As demonstrated clearly in Fig.5.5 and Fig.5.7, the first-order hyperbolic PDEs can be stabilized around desired steady state by applying single-step controller of linear control or quadratic control. However, by comparing the norms of the state $||x(\zeta, t)||$ with the application of linear control law and quadratic control law, see Fig.5.8, it can be seen that the state norm with quadratic control is smaller than the state norm with linear control. From the simulation results, it shows that the performance of the quadratic control is better than that of the linear control. This illustrates that the single-step controller design with second-order Taylor expansion of the system's dynamics has a good control performance to stabilize the first-order nonlinear hyperbolic PDEs around desired steady state.

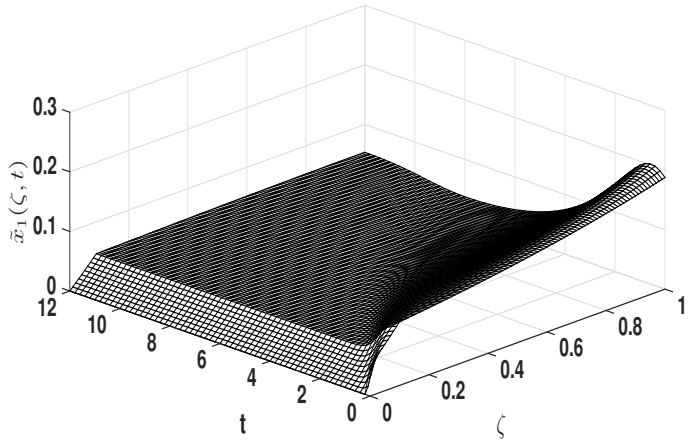

(a) Temperature $\tilde{x}_1(\zeta, t)$

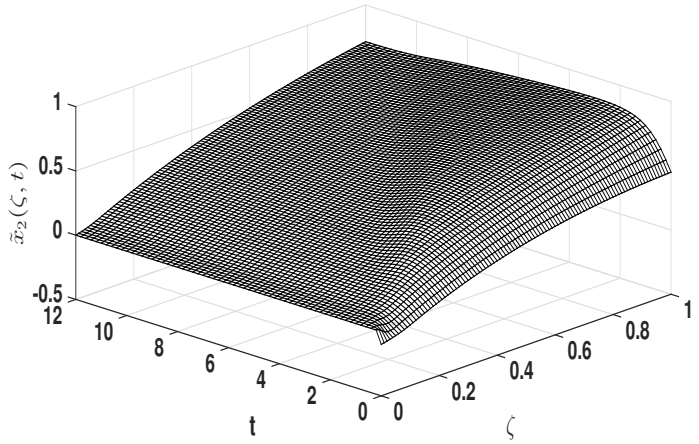

(b) Concentration $\tilde{x}_2(\zeta, t)$

Fig. 5.7: State profiles of nonlinear single-step full state feedback control apply on first-order hyperbolic PDEs described in Eq.5.29 with transform operator $P_{ij}(\zeta)(i = 1, 2; j = 1, 2, 3)$ in Eq.5.34.

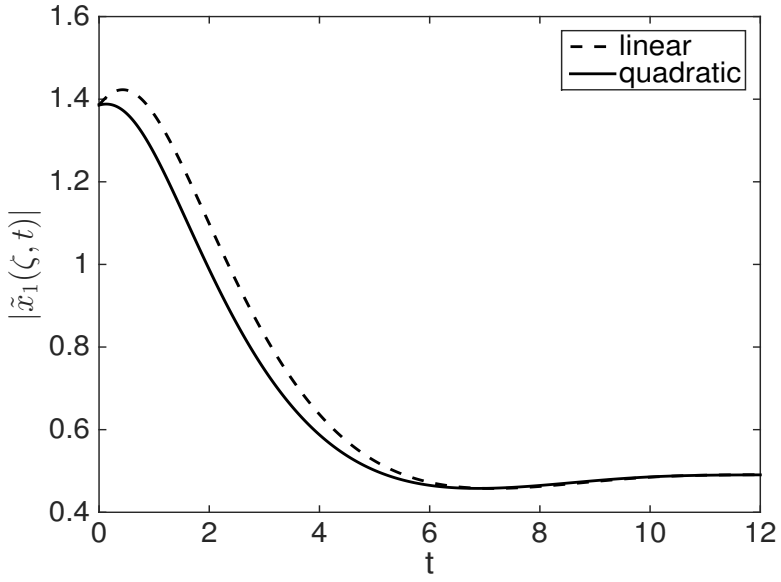

(a) Temperature norm $\tilde{x}_1(\zeta, t)$

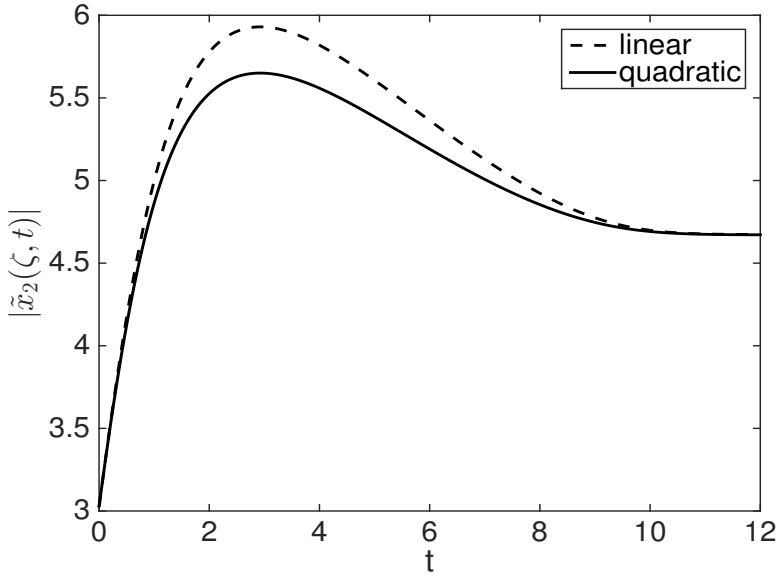

(b) Concentration norm $\tilde{x}_2(\zeta, t)$

Fig. 5.8: State norms comparison of linear (dashed line) and nonlinear (solid line) single-step full state feedback control apply on first-order hyperbolic PDEs described in Eq.5.29.

5.4.2 Second-Order Hyperbolic PDE

In this section, we consider the damped wave equation which takes the following form given as second-order hyperbolic PDE:

$$\frac{\partial^2\phi}{\partial t^2}(\zeta,t) = \nu\frac{\partial^2\phi}{\partial\zeta^2}(\zeta,t) + c\frac{\partial\phi}{\partial t}(\zeta,t) \tag{5.39}$$

with initial condition and boundary condition:

$$\begin{aligned} &\phi(\zeta,0) = \phi_0(\zeta), \quad \frac{\partial\phi}{\partial\zeta}(\zeta,0) = \phi_1(\zeta) \\ &\phi(0,t) = 0, \quad \frac{\partial\phi}{\partial\zeta}(1,t) = 0 \end{aligned} \tag{5.40}$$

where $\zeta \in [0, L]$ and $t \in [0, \infty]$.

Remark 3: The eigenvalues of the damped wave equation are $\lambda_i = \frac{c\pm\sqrt{c^2+4\nu a_i}}{2}$, where $a_i = -(\frac{2i+1}{2}\pi)^2, i = 0, 1, 2, \cdots$. According to the eigenvalues, when $c > 0$, the system is unstable; when $c < 0$, there is additional condition to determine the stability of the system, and we will not go into details here. The physical model to consider is motivated by the sucker-rod system which is described by the 1-D damped wave equation with $c < 0$ in the following form:

$$\frac{\partial^2\phi}{\partial t^2}(\zeta,t) = \nu^2\frac{\partial^2\phi}{\partial\zeta^2}(\zeta,t) + c\frac{\partial\phi}{\partial t}(\zeta,t) \tag{5.41}$$

where $\nu = \sqrt{144Eg_c/\rho}$ is the sound velocity in the rod material, ft/s; c is the damping coefficient; $\phi(\zeta,t)$ is the displacement of the rod. The application of single-step simultaneous transformation and full state feedback should ensure desired rate convergence to the steady state.

In the next controller realization, we consider an unstable damped wave equation with $\alpha = 2$ in the following form:

$$\frac{\partial^2 \phi}{\partial t^2}(\zeta, t) = \frac{\partial^2 \phi}{\partial \zeta^2}(\zeta, t) + \alpha \frac{\partial \phi}{\partial t}(\zeta, t) + \beta u(t) \tag{5.42}$$

with initial conditions and boundary conditions:

$$\begin{aligned} &\phi(\zeta, 0) = \phi_0(\zeta), \quad \frac{\partial \phi}{\partial \zeta}(\zeta, 0) = \phi_1(\zeta) \\ &\phi(0, t) = 0, \quad \frac{\partial \phi}{\partial \zeta}(1, t) = 0 \end{aligned} \tag{5.43}$$

By defining the state variables as $\frac{\partial \phi}{\partial t}(\zeta, t) = v_1(\zeta, t)$ and $\frac{\partial \phi}{\partial \zeta}(\zeta, t) = v_2(\zeta, t)$, the system reduces to the system of first-order hyperbolic PDEs:

$$\frac{\partial}{\partial t} \begin{bmatrix} v_1 \\ v_2 \end{bmatrix} = \begin{bmatrix} 0 & 1 \\ 1 & 0 \end{bmatrix} \frac{\partial}{\partial \zeta} \begin{bmatrix} v_1 \\ v_2 \end{bmatrix} + \begin{bmatrix} \alpha & 0 \\ 0 & 0 \end{bmatrix} \begin{bmatrix} v_1 \\ v_2 \end{bmatrix} + \begin{bmatrix} \beta \\ 0 \end{bmatrix} u(t) \tag{5.44}$$

Devoting $A = \begin{bmatrix} 0 & 1 \\ 1 & 0 \end{bmatrix}$, it can be shown that the matrix A can be transformed as follows:

$$A = Q \Lambda Q^{-1} \tag{5.45}$$

where $\Lambda = \begin{bmatrix} 1 & 0 \\ 0 & -1 \end{bmatrix}$, $Q = \begin{bmatrix} 1 & 1 \\ 1 & -1 \end{bmatrix}$ and $Q^{-1} = \begin{bmatrix} 0.5 & 0.5 \\ 0.5 & -0.5 \end{bmatrix}$.

Multiplying the Eq.5.44 on the left by Q^{-1}, the system transfer to a diagonal

decoupled system of first-order hyperbolic PDEs:

$$\frac{\partial}{\partial t}\begin{bmatrix} x_1 \\ x_2 \end{bmatrix} = \begin{bmatrix} 1 & 0 \\ 0 & -1 \end{bmatrix}\frac{\partial}{\partial \zeta}\begin{bmatrix} x_1 \\ x_2 \end{bmatrix} + \begin{bmatrix} 0.5\alpha & 0.5\alpha \\ 0.5\alpha & 0.5\alpha \end{bmatrix}\begin{bmatrix} x_1 \\ x_2 \end{bmatrix} + \begin{bmatrix} 0.5\beta \\ 0.5\beta \end{bmatrix} u(t) \tag{5.46}$$

where $\begin{bmatrix} x_1 & x_2 \end{bmatrix}^T = Q^{-1}\begin{bmatrix} v_1 & v_2 \end{bmatrix}^T$.

In the single-step controller design, the desired stable closed-loop target dynamics is in the following form:

$$\frac{\partial}{\partial t}\begin{bmatrix} z_1 \\ z_2 \end{bmatrix} = \begin{bmatrix} \bar{v}_{11} & \bar{v}_{12} \\ \bar{v}_{21} & \bar{v}_{22} \end{bmatrix}\frac{\partial}{\partial \zeta}\begin{bmatrix} z_1 \\ z_2 \end{bmatrix} + \begin{bmatrix} \sigma_{11} & \sigma_{12} \\ \sigma_{21} & \sigma_{22} \end{bmatrix}\begin{bmatrix} z_1 \\ z_2 \end{bmatrix} \tag{5.47}$$

The function $w(\zeta)$ of linear transformation $z[x(\zeta,t)] = w(\zeta)x(\zeta,t)$ is obtained with $\bar{v} = wvw^{-1}$ as the solution of the following differential equation:

$$w(\zeta)vw^{-1}(\zeta)\frac{dw(\zeta)}{d\zeta} = \sigma w(\zeta) - w(\zeta)J + w(\zeta)\beta K w(\zeta) \tag{5.48}$$

Let us assume the simplest set of deign parameter given as diagonal matrix $\begin{bmatrix} \sigma_{11} & 0 \\ 0 & \sigma_{22} \end{bmatrix}$ here. With linear transformation $\tilde{x} = w^{-1}z$, the desired stable closed-loop target in Eq.5.47 becomes:

$$\frac{\partial}{\partial t}\begin{bmatrix} \tilde{x}_1 \\ \tilde{x}_2 \end{bmatrix} = \begin{bmatrix} 1 & 0 \\ 0 & -1 \end{bmatrix}\frac{\partial}{\partial \zeta}\begin{bmatrix} \tilde{x}_1 \\ \tilde{x}_2 \end{bmatrix} + \begin{bmatrix} \gamma_{11}(\zeta) & \gamma_{12}(\zeta) \\ \gamma_{21}(\zeta) & \gamma_{22}(\zeta) \end{bmatrix}\begin{bmatrix} \tilde{x}_1 \\ \tilde{x}_2 \end{bmatrix} \tag{5.49}$$

where $\gamma_{11}(\zeta) = w_{22}\sigma_{11}w_{11} - w_{12}\sigma_{22}w_{21}$, $\gamma_{12}(\zeta) = w_{22}\sigma_{11}w_{12} - w_{12}\sigma_{22}w_{22}$, $\gamma_{21}(\zeta) =$

$-w_{21}\sigma_{11}w_{11} + w_{11}\sigma_{22}w_{21}$ and $\gamma_{22}(\zeta) = -w_{21}\sigma_{11}w_{12} + w_{11}\sigma_{22}w_{22}$.

Similarly, with linear transformation $\tilde{v} = Q\tilde{x}$, the above system is expressed in the following form:

$$\frac{\partial}{\partial t}\begin{bmatrix} \tilde{v}_1 \\ \tilde{v}_2 \end{bmatrix} = \begin{bmatrix} 0 & 1 \\ 1 & 0 \end{bmatrix} \frac{\partial}{\partial \zeta}\begin{bmatrix} \tilde{v}_1 \\ \tilde{v}_2 \end{bmatrix} + \begin{bmatrix} \rho_{11}(\zeta) & \rho_{12}(\zeta) \\ \rho_{21}(\zeta) & \rho_{22}(\zeta) \end{bmatrix} \begin{bmatrix} \tilde{v}_1 \\ \tilde{v}_2 \end{bmatrix} \tag{5.50}$$

where $\rho_{11}(\zeta) = 0.5(\gamma_{11} + \gamma_{21} + \gamma_{12} + \gamma_{22})$, $\rho_{12}(\zeta) = 0.5(\gamma_{11} + \gamma_{21} - \gamma_{12} - \gamma_{22})$, $\rho_{21}(\zeta) = 0.5(\gamma_{11} - \gamma_{21} + \gamma_{12} - \gamma_{22})$ and $\rho_{22}(\zeta) = 0.5(\gamma_{11} - \gamma_{21} - \gamma_{12} + \gamma_{22})$.

The corresponding second-order hyperbolic PDE of the desired stable closed-loop target in Eq.5.47 is given as below:

$$\frac{\partial^2 \tilde{\phi}}{\partial t^2}(\zeta, t) = \frac{\partial^2 \tilde{\phi}}{\partial \zeta^2}(\zeta, t) + \tilde{\alpha}\frac{\partial \tilde{\phi}}{\partial t}(\zeta, t) \tag{5.51}$$

where $\tilde{\alpha}(\zeta) = \rho_{11}(\zeta) - \frac{\rho_{12}(\zeta)\rho_{21}(\zeta)}{\rho_{22}(\zeta)}$.

In linear control synthesis for second-order hyperbolic system, the function $w_{ij}(\zeta)$, for $i, j = 1, 2$, in Eq.5.48 is obtained by calculating the following differential equations:

$$\begin{bmatrix} \bar{v}_{11} & \bar{v}_{12} \\ \bar{v}_{21} & \bar{v}_{22} \end{bmatrix} \begin{bmatrix} \frac{dw_{11}(\zeta)}{d\zeta} & \frac{dw_{12}(\zeta)}{d\zeta} \\ \frac{dw_{21}(\zeta)}{d\zeta} & \frac{dw_{22}(\zeta)}{d\zeta} \end{bmatrix} = \begin{bmatrix} \psi_{11} & \psi_{12} \\ \psi_{21} & \psi_{22} \end{bmatrix} \tag{5.52}$$

where $\bar{v}$ is in the following form:

$$\begin{aligned} \bar{v}_{11} &= \frac{w_{11}w_{22} + w_{12}w_{21}}{w_{11}w_{22} - w_{12}w_{21}} \\ \bar{v}_{12} &= \frac{-2w_{11}w_{12}}{w_{11}w_{22} - w_{12}w_{21}} \\ \bar{v}_{21} &= \frac{2w_{21}w_{22}}{w_{11}w_{22} - w_{12}w_{21}} \end{aligned} \tag{5.53}$$

$$\bar{v}_{22} = \frac{-w_{21}w_{12} - w_{11}w_{22}}{w_{11}w_{22} - w_{12}w_{21}}$$

and ψ takes the following form:

$$\begin{aligned}
&\psi_{11} = J_{11}w_{11} + J_{21}w_{12} - (\beta_1 K_1 w_{11}^2 + \beta_2 K_1 w_{11}w_{12} + \beta 1 K_2 w_{21}w_{11} \qquad (5.54)\\
&+\beta 2 K_2 w_{21}w_{12}) - (\sigma_{11}w_{11} + \sigma_{12}w_{21})\\
&\psi_{12} = J_{12}w_{11} + J_{22}w_{12} - (\beta_1 K_1 w_{12}w_{11} + \beta_2 K_1 w_{12}^2 + \beta 1 K_2 w_{22}w_{11}\\
&+\beta 2 K_2 w_{22}w_{12}) - (\sigma_{11}w_{12} + \sigma_{12}w_{22})\\
&\psi_{21} = J_{11}w_{21} + J_{21}w_{22} - (\beta_1 K_1 w_{11}w_{21} + \beta_2 K_1 w_{11}w_{22} + \beta 1 K_2 w_{21}^2\\
&+\beta 2 K_2 w_{21}w_{22}) - (\sigma_{21}w_{11} + \sigma_{22}w_{21})\\
&\psi_{22} = J_{12}w_{21} + J_{22}w_{22} - (\beta_1 K_1 w_{12}w_{21} + \beta_2 K_1 w_{12}w_{22} + \beta 1 K_2 w_{22}w_{21}\\
&+\beta 2 K_2 w_{22}^2) - (\sigma_{21}w_{12} + \sigma_{22}w_{22})
\end{aligned}$$

In linear control simulation studies, with $\beta = 1.3$, $K = [15\ 10]$, $\sigma = [-3\ \ 0; 0\ \ -3]$ and $w(1) = [0.5 \quad 0.4; 0.1 \quad 0.2]$, the numerical result of $w(\zeta)$ is shown in Fig.5.9. Fig.5.10 gives the numerical result of $\tilde{\alpha}(\zeta)$, which yields the condition $|\tilde{\alpha}(\zeta)| < |4\frac{2i+1}{2}\pi|$ for $i = 0, 1, 2, \cdots$. This condition leads to the eigenvalues $\lambda_i < 0$ $(i = 0, 1, 2, \cdots)$, which implies that the target system is a stable one, see Fig.5.10, showing that $\tilde{\alpha}(\zeta)$ is negative in $[0,\ 1]$. From the result of simulation studies, it can be seen that the single-step state feedback control shifts the eigenvalues of unstable system on the right hand side of complex plain to the left hand side, see Fig.5.11. Here, the stable eigenvalues obtained by single-step full state feedback control law in Fig.5.11 are simulated with minimum $\tilde{\alpha}(\zeta)$. The state of second-order hyperbolic PDE system is stabilized around steady state with the initial conditions given as $x_1 = x_{1ss} + e^{\zeta}cos(2\pi\zeta)$ and $x_2 = x_{2ss} + 1.2e^{\zeta}sin(2\pi\zeta)$, see Fig.5.12.

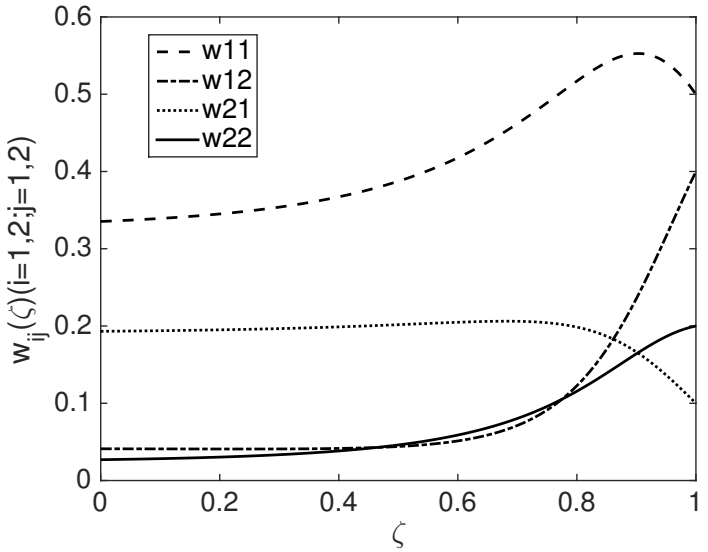

Fig. 5.9: Linear transform operator $w_{ij}(\zeta)(i, j = 1, 2)$ in Eq.5.48 for second-order hyperbolic PDE described in Eq.5.39.

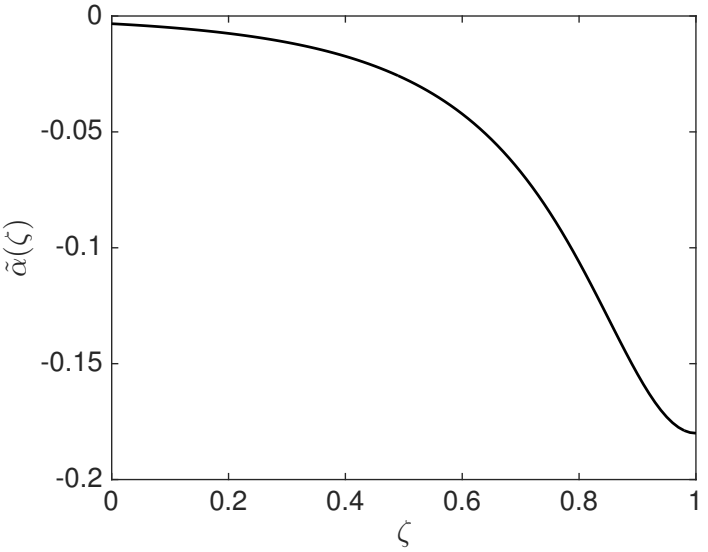

Fig. 5.10: Parameter $\tilde{\alpha}(\zeta)$ of second-order hyperbolic PDE in Eq.5.51 with the application of single-step full state feedback control.

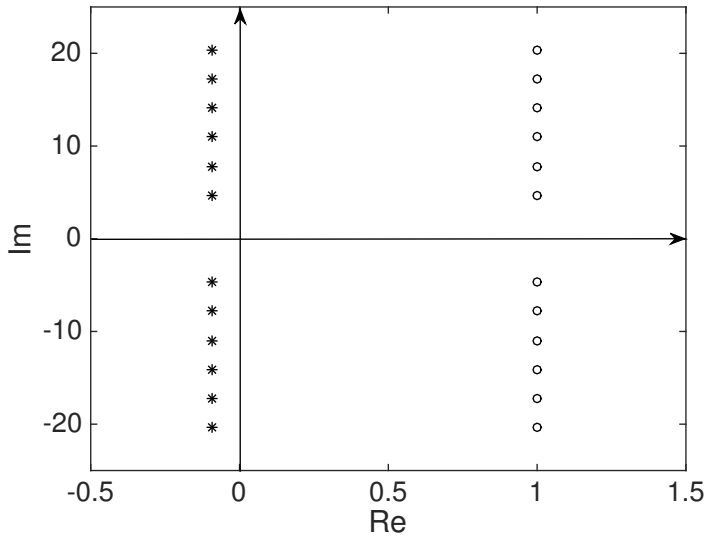

Fig. 5.11: The transformation of unstable eigenvalues on the right hand side of complex plain (o) to the left hand side ($*$) by applying single-step full state feedback control to second-order hyperbolic PDE in Eq.5.51.

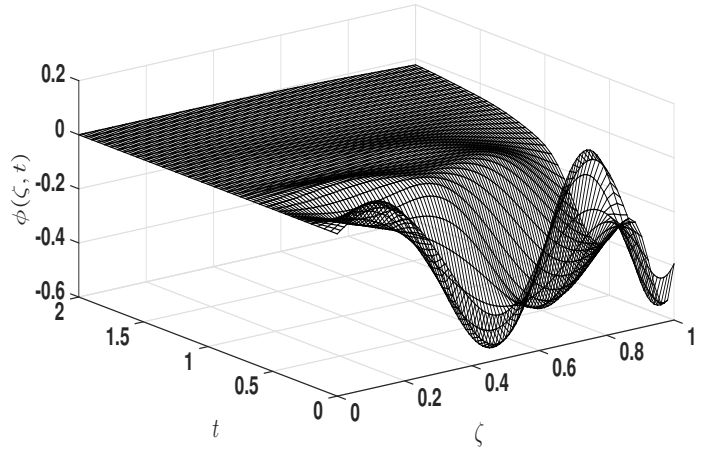

Fig. 5.12: State profiles of second-order hyperbolic PDE system described in Eq.5.39 with linear single-step full state feedback control with transform operator $w_{ij}(\zeta)(i,j=1,2)$ in Eq.5.48.

In quadratic control synthesis for second-order hyperbolic system, the function $P_{ij}(\zeta)$, for $i = 1, 2; j = 1, 2, 3$ is obtained by calculating the following differential equations:

$$\begin{bmatrix} \bar{v}_{11} & \bar{v}_{12} \\ \bar{v}_{21} & \bar{v}_{22} \end{bmatrix} \begin{bmatrix} \frac{dP_{11}(\zeta)}{d\zeta} & \frac{dP_{12}(\zeta)}{d\zeta} & \frac{dP_{13}(\zeta)}{d\zeta} \\ \frac{dP_{21}(\zeta)}{d\zeta} & \frac{dP_{22}(\zeta)}{d\zeta} & \frac{dP_{23}(\zeta)}{d\zeta} \end{bmatrix} = \begin{bmatrix} \phi_{11} & \phi_{12} & \phi_{13} \\ \phi_{21} & \phi_{22} & \phi_{23} \end{bmatrix} \tag{5.55}$$

where $\bar{v}$ takes the same form in Eq.5.53 and ϕ is in the following form:

$$\begin{aligned}
&\phi_{11} = -\sigma_{11}P_{11} - \sigma_{12}P_{21} + 2J_{11}P_{11} + 2J_{21}P_{12} + H_{11}w_{11} + H_{21}w_{12} \qquad (5.56)\\
&-2(K_1w_{11} + K_2w_{21})(\beta_1P_{11} + \beta_2P_{12}) - (\beta_1w_{11} + \beta_2w_{12})(K_1P_{11} + K_2P_{21})\\
&\phi_{12} = -\sigma_{11}P_{12} - \sigma_{12}P_{22} + J_{12}P_{11} + (J_{11} + J_{22})P_{12} + J_{21}P_{13} + H_{12}w_{11} + H_{22}w_{12}\\
&-(K_1w_{12} + K_2w_{22})(\beta_1P_{11} + \beta_2P_{12})\\
&-(K_1w_{11} + K_2w_{21})(\beta_1P_{12} + \beta_2P_{13}) - (\beta_1w_{11} + \beta_2w_{12})(K_1P_{12} + K_2P_{22})\\
&\phi_{13} = -\sigma_{11}P_{13} - \sigma_{12}P_{23} + 2J_{12}P_{12} + 2J_{22}P_{13} + H_{13}w_{11} + H_{23}w_{12}\\
&-2(K_1w_{12} + K_2w_{22})(\beta_1P_{12} + \beta_2P_{13}) - (\beta_1w_{11} + \beta_2w_{12})(K_1P_{13} + K_2P_{23})\\
&\phi_{21} = -\sigma_{21}P_{11} - \sigma_{22}P_{21} + 2J_{11}P_{21} + 2J_{21}P_{22} + H_{11}w_{21} + H_{21}w_{22}\\
&-2(K_1w_{11} + K_2w_{21})(\beta_1P_{21} + \beta_2P_{22}) - (\beta_1w_{21} + \beta_2w_{22})(K_1P_{11} + K_2P_{21})\\
&\phi_{22} = -\sigma_{21}P_{12} - \sigma_{22}P_{22} + J_{12}P_{21} + (J_{11} + J_{22})P_{22} + J_{21}P_{23} + H_{12}w_{21} + H_{22}w_{22}\\
&-(K_1w_{12} + K_2w_{22})(\beta_1P_{21} + \beta_2P_{22})\\
&-(K_1w_{11} + K_2w_{21})(\beta_1P_{22} + \beta_2P_{23}) - (\beta_1w_{21} + \beta_2w_{22})(K_1P_{12} + K_2P_{22})\\
&\phi_{23} = -\sigma_{21}P_{13} - \sigma_{22}P_{23} + 2J_{12}P_{22} + 2J_{22}P_{23} + H_{13}w_{21} + H_{23}w_{22}\\
&-2(K_1w_{12} + K_2w_{22})(\beta_1P_{22} + \beta_2P_{23}) - (\beta_1w_{21} + \beta_2w_{22})(K_1P_{13} + K_2P_{23})
\end{aligned}$$

In quadratic control law realization, function $w(\zeta)$ is given in Fig.5.9 and function $P(\zeta)$ is simulated with initial condition $P(1) = [0.00005; 0.00005; 0.00007; 0.00008; 0.00005; 0.00007]$, see Fig.5.13. The simulation result of single-step control law with nonlinear coordinate transformation is given in Fig.5.14.

Fig.5.15 illustrates that the single-step controller design with nonlinear expansion of the system has a good control performance for stabilizing the second-order hyperbolic PDE around desired steady state by comparing the state norms $||\phi(\zeta, t)||$ with the application of linear control law and quadratic control law.

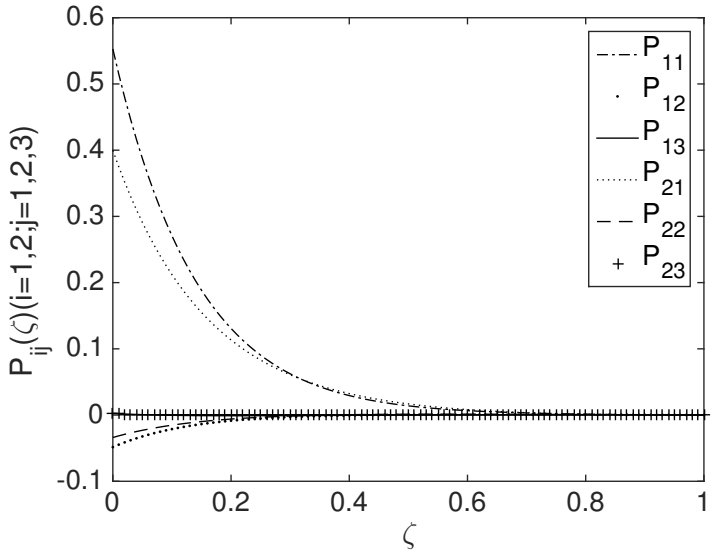

Fig. 5.13: Nonlinear transform operator $P_{ij}(\zeta)(i = 1, 2; j = 1, 2, 3)$ for second-order hyperbolic PDE described in Eq.5.39.

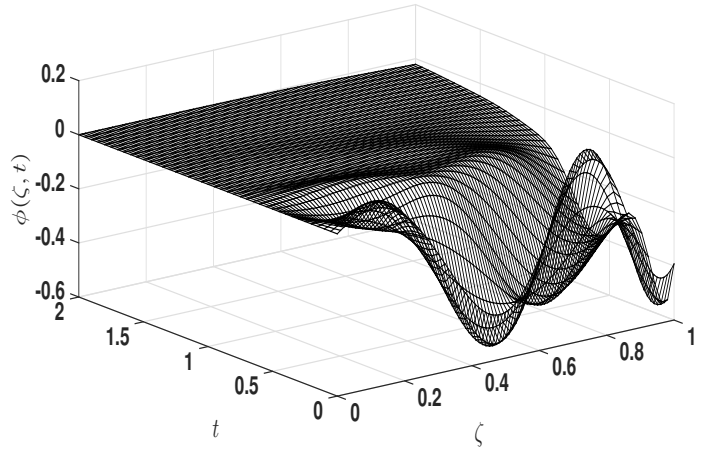

Fig. 5.14: State profiles of second-order hyperbolic PDE system described in Eq.5.39 with nonlinear single-step full state feedback control with transform operator $P_{ij}(\zeta)(i = 1, 2; j = 1, 2, 3)$.

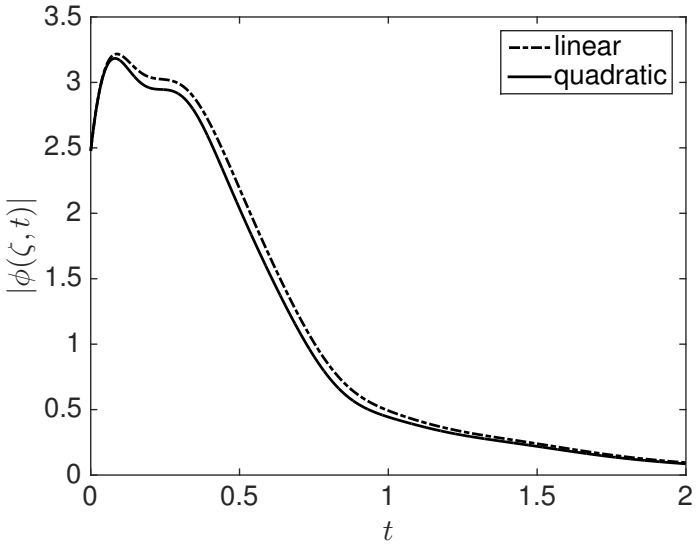

Fig. 5.15: State norms comparison of linear (dashed line) and nonlinear (solid line) single-step full state feedback control apply on second-order hyperbolic PDE described in Eq.5.39.

5.5 Conclusions

In conclusion, this chapter explores an extension of the single-step Luenberger type of feedback linearization with pole placement formulation to the class of system of nonlinear hyperbolic PDEs. In particular, single-step full state feedback controller is designed in this chapter for the nonlinear first-order hyperbolic PDEs system of the exothermic plug-flow reactor and the damped second-order hyperbolic PDE system. Simultaneous state coordinate transformation and full state feedback are realized to achieve desired pre-specified stabilization of unstable hyperbolic PDEs system. Two controller law realizations, linear and quadratic control, are developed and they can successfully stabilize the unstable nonlinear first-order hyperbolic PDEs system and unstable second-order hyperbolic PDE system. From the numerical simulation results, it can be seen that the quadratic controller has a good control performance for stabilizing various types of nonlinear or systems of hyperbolic PDEs at desired steady state.

Chapter 6

Conclusions and Future Work

6.1 Conclusions

In this thesis, model predictive control and nonlinear control are presented for distributed parameter systems. Furthermore, their performances are illustrated by hyperbolic PDE system, parabolic PDE system, coupled hyperbolic PDE and ODE system emerging from chemical transport-reaction process and solar thermal energy process.

Specifically, Chapter 2 provides foundation of systematic modelling framework for a linear DPS which uses a finite and low dimensional setting for the model predictive controller design without application of any spatial approximation or order reduction. The discrete DPS is developed by Cayley-Tustin time discretization with the application of Laplace transform applying on the continuous DPS. In this chapter, we consider the systems varying from the convection dominated plug flow reactor models described by hyperbolic PDEs to the diffusion dominated axial dispersion reactor models described by parabolic PDEs. The model predictive control algorithms

for hyperbolic PDEs and parabolic PDEs are quadratic regulator problems with the consideration of manipulated input and process state constraints.

In addition, Chapter 4 addresses the low order model predictive controller design for a coupled hyperbolic PDE and ODE system of a solar boreal thermal energy process. The model predictive control algorithm addresses a constrained optimization problem with the manipulation constraints, and accounts for possible unstable system dynamics and disturbances arising from solar and geothermal radiations. The realistic output regulation is considered by the inclusion of an observer which constructs finite and infinite dimensional states.

Along the line of controller design for DPS, Chapter 3 addresses a simple and easily realizable servo control algorithm for a coupled hyperbolic PDE and ODE system which models a complex solar thermal system with borehole seasonal storage in a real commercial community. The overall discrete system is obtained from subsystems modelling of solar power plant process, heat exchanger, borehole energy storage process, hot tank and district heating loop process. The servo controller is designed to regulate the system operating at desired thermal comfort level despite disturbances from the solar thermal plant system, the borehole geo-thermal energy storage system and/or the district heating loop system.

Finally, Chapter 5 proposes an extension of single-step formulation of full state feedback control design to the class of distributed parameter system described by nonlinear hyperbolic PDEs. The methodology lies in the fact that both feedback control and stabilization design objectives given as target stable dynamics are accomplished in one step under a simultaneous implementation of a nonlinear coordinate transformation and a nonlinear state feedback law. The mathematical formulation of the problem is realized via a system of first-order quasi-linear singular PDEs. By

using Lyapunov's auxiliary theorem for singular PDEs, the necessary and sufficient conditions for solvability are utilized. The solution to the singular PDEs is locally analytic, which enables development of a PDE series solution.

6.2 Future Work

This thesis developed model predictive control and nonlinear control for distributed parameter systems which are modelled from chemical transport-reaction process and solar thermal energy process. There remain many open questions regarding this subject and a number of them are briefly mentioned here.

In addition to chemical transport-reaction process and solar thermal energy process which are described by the classes of hyperbolic PDE system, parabolic PDE system, coupled hyperbolic PDE and ODE system, the wave equation system and beam equation system which account for a large class of distributed parameter systems can be addressed in future. Furthermore, the model predictive control can be applied to the port-Hamiltonian distributed parameter systems, such as undamped wave equation system and heat exchanger system.

Another possibility is development of advanced control algorithms such as explicit model predictive control and/or economic model predictive control for distributed parameter systems, with emphasize on the different slight variations in realization of constrained finite dimensional controllers.

Another promising area is the design of observer and/or estimation strategies such as Kalman filter and/or moving horizon estimation for linear distributed parameter systems.

Bibliography

[1] H.-X. Li and C. Qi, "Modeling of distributed parameter systems for applications—a synthesized review from time–space separation," *Journal of Process Control*, vol. 20, no. 8, pp. 891 – 901, 2010.

[2] K. R. Muske and J. B. Rawlings, "Model predictive control with linear models," *AIChE Journal*, vol. 39, no. 2, pp. 262–287, 1993.

[3] A. Alessio and A. Bemporad, "A survey on explicit model predictive control," in *Nonlinear Model Predictive Control*, pp. 345–369, Springer, 2009.

[4] E. Pahija, F. Manenti, I. M. Mujtaba, and F. Rossi, "Assessment of control techniques for the dynamic optimization of (semi-)batch reactors," *Computers & Chemical Engineering*, vol. 66, no. 0, pp. 269 – 275, 2014.

[5] W. H. Ray, *Advanced process control*. McGraw-Hill New York, 1981.

[6] W. Ray, "Some recent applications of distributed parameter systems theory—a survey," *Automatica*, vol. 14, no. 3, pp. 281 – 287, 1978.

[7] A. Armaou and P. D. Christofides, "Dynamic optimization of dissipative PDE systems using nonlinear order reduction," *Chemical Engineering Science*, vol. 57, no. 24, pp. 5083 – 5114, 2002.

[8] J. Baker and P. D. Christofides, "Finite-dimensional approximation and control of non-linear parabolic PDE systems," *International Journal of Control*, vol. 73, no. 5, pp. 439–456, 2000.

[9] M. J. Balas, "Feedback control of linear diffusion process," in *Information Linkage Between Applied Mathematics and Industry*, pp. 513 – 525, Academic Press, 1979.

[10] R. Curtain, "Finite-dimensional compensator design for parabolic distributed systems with point sensors and boundary input," *Automatic Control, IEEE Transactions on*, vol. 27, pp. 98–104, Feb 1982.

[11] M. Trainor, V. Giannakeas, C. Kiss, and L. Ricardez-Sandoval, "Optimal process and control design under uncertainty: A methodology with robust feasibility and stability analyses," *Chemical Engineering Science*, vol. 104, no. 0, pp. 1065 – 1080, 2013.

[12] S. Titouche, P. Spiteri, F. Messine, and M. Aidene, "Optimal control of a large thermic process," *Journal of Process Control*, vol. 25, no. 0, pp. 50 – 58, 2015.

[13] C. Büskens and H. Maurer, "SQP-methods for solving optimal control problems with control and state constraints: adjoint variables, sensitivity analysis and real-time control," *Journal of Computational and Applied Mathematics*, vol. 120, no. 1, pp. 85–108, 2000.

[14] S. Dubljevic, P. Mhaskar, N. H. El-Farra, and P. D. Christofides, "Predictive control of transport-reaction processes," *Computers & Chemical Engineering*, vol. 29, no. 11–12, pp. 2335 – 2345, 2005.

[15] S. Dubljevic, N. H. El-Farra, P. Mhaskar, and P. D. Christofides, "Predictive control of parabolic PDEs with state and control constraints," *International Journal of Robust and Nonlinear Control*, vol. 16, no. 16, pp. 749–772, 2006.

[16] S. Dubljevic and P. D. Christofides, "Predictive control of parabolic pdes with boundary control actuation," *Chemical Engineering Science*, vol. 61, no. 18, pp. 6239 – 6248, 2006.

[17] S. Dubljevic and P. D. Christofides, "Predictive output feedback control of parabolic partial differential equations PDEs," *Industrial & Engineering Chemistry Research*, vol. 45, no. 25, pp. 8421–8429, 2006.

[18] N. Kazantzis and C. Kravaris, "Time-discretization of nonlinear control systems via Taylor methods," *Computers & chemical engineering*, vol. 23, no. 6, pp. 763–784, 1999.

[19] V. Havu and J. Malinen, "The Cayley transform as a time discretization scheme," *Numerical Functional Analysis and Optimization*, vol. 28, no. 7-8, pp. 825–851, 2007.

[20] V. Havu and J. Malinen, "Laplace and Cayley Transforms-an approximation point of view," in *IEEE CDC.*, vol. 44, p. 5971, Citeseer, 2005.

[21] Q. Xu and S. Dubljevic, "Linear model predictive control for transport-reaction processes," *AIChE Journal*, p. 1DOI: 10.1002/aic.15592, 2016.

[22] J. Malinen, "Tustin's method for final state approximation of conservative dynamical systems," *IFAC Proceedings Volumes*, vol. 44, no. 1, pp. 4564–4569, 2011.

[23] J. Malinen, O. J. Staffans, and G. Weiss, "When is a linear system conservative?," *Quarterly of Applied Mathematics*, pp. 61–91, 2006.

[24] C. E. Garcia and M. Morari, "Internal model control. a unifying review and some new results," *Industrial & Engineering Chemistry Process Design and Development*, vol. 21, no. 2, pp. 308–323, 1982.

[25] E. Zafiriou and M. Morari, "Design of robust digital controllers and sampling-time selection for siso systems," *International Journal of Control*, vol. 44, no. 3, pp. 711–735, 1986.

[26] J. L. Lions, *Optimal control of systems governed by partial differential equations*. New York: Springer-Verlag, 1971.

[27] R. F. Curtain and K. Glover, "Robust stabilization of infinite dimensional systems by finite dimensional controllers," *Syst. & Contr. Lett.*, vol. 7, pp. 41–47, 1986.

[28] R. F. Curtain, "Finite-dimensional compensator design for parabolic distributed systems with point sensors and boundary input," *IEEE Trans. Automat. Contr.*, vol. 27, pp. 98–104, 1982.

[29] R. F. Curtain and A. J. Pritchard, *Infinite Dimensional Linear Systems Theory*. Berlin-Heidelberg: Springer-Verlag, 1978.

[30] R. F. Curtain, "On stabilizability of linear spectral systems via state boundary feedback," *SIAM J. Control and Optimization*, vol. 23, pp. 144–152, 1985.

[31] A. J. Pritchard and D. Salamon, "The linear quadratic control problem for infinite dimensional system with unbounded input and output operators," *SIAM J. Control and Optimization*, vol. 25, pp. 121–144, 1987.

[32] C. I. Byrnes, D. S. Gilliam, A. Isidori, and V. I. Shubov, "Static and dynamic controllers for boundary controlled distributed parameter systems," *Proceedings of the* 43^{rd} *IEEE Conference on Decision and Control*, pp. 3324–3325, 2004.

[33] A. Bensoussan, G. D. Prato, M. C. Delfour, and S. K. Mitter, *Representation and Control of Infinite Dimensional Systems*. New York: Birkhauser, 1993.

[34] M. Krstic and A. Smyshlyaev, *Boundary control of PDEs: A course on backstepping designs*. Philadelphia: SIAM, 2008.

[35] P. D. Christofides, *Nonlinear and Robust Control of PDE Systems: Methods and Applications to transport reaction processes*. Birkhauser, 2000.

[36] J.-M. Coron, B. d'Andrea Novel, and G. Bastin, "A strict lyapunov function for boundary control of hyperbolic systems of conservation laws," *Automatic Control, IEEE Transactions on*, vol. 52, pp. 2–11, Jan 2007.

[37] D. Ababacar, G. Bastin, and J.-M. Coron, "Lyapunov exponential stability of 1-d linear hyperbolic systems of balance laws," *Automatica*, vol. 48, no. 1, pp. 109–114, 2012.

[38] H. Zwart and R. Curtain, "An introduction to infinite-dimensional linear systems theory," *Springer-Verlag, New York*, 1995.

[39] J. Richalet, A. Rault, J. Testud, and J. Papon, "Model predictive heuristic control: Applications to industrial processes," *Automatica*, vol. 14, no. 5, pp. 413–428, 1978.

[40] J. W. Eaton and J. B. Rawlings, "Model-predictive control of chemical processes," *Chemical Engineering Science*, vol. 47, no. 4, pp. 705–720, 1992.

[41] E. S. Meadows and J. B. Rawlings, "Model predictive control," in *Nonlinear process control*, pp. 233–310, Prentice-Hall, Inc., 1997.

[42] J. B. Rawlings, "Tutorial overview of model predictive control," *IEEE Control Systems*, vol. 20, no. 3, pp. 38–52, 2000.

[43] D. Q. Mayne, J. B. Rawlings, C. V. Rao, and P. O. Scokaert, "Constrained model predictive control: Stability and optimality," *Automatica*, vol. 36, no. 6, pp. 789–814, 2000.

[44] C. Kubrusly and H. Malebranche, "Sensors and controllers location in distributed systems-a survey," *Automatica*, vol. 21, no. 2, pp. 117–128, 1985.

[45] B. Van Keulen, *H_∞-control for distributed parameter systems: A state-space approach*. Springer Science & Business Media, 2012.

[46] P. D. Christofides, *Nonlinear and robust control of PDE systems: Methods and applications to transport-reaction processes*. Springer Science & Business Media, 2012.

[47] W. Ray and J. Seinfeld, "Filtering in distributed parameter systems with moving boundaries," *Automatica*, vol. 11, no. 5, pp. 509–515, 1975.

[48] D. H. Gay and W. H. Ray, "Identification and control of distributed parameter systems by means of the singular value decomposition," *Chemical Engineering Science*, vol. 50, no. 10, pp. 1519–1539, 1995.

[49] P. Dufour and Y. Touré, "Multivariable model predictive control of a catalytic reverse flow reactor," *Computers & chemical engineering*, vol. 28, no. 11, pp. 2259–2270, 2004.

[50] J. Ng and S. Dubljevic, "Optimal control of convection–diffusion process with time-varying spatial domain: Czochralski crystal growth," *Journal of Process Control*, vol. 21, no. 10, pp. 1361–1369, 2011.

[51] J. Ng and S. Dubljevic, "Optimal boundary control of a diffusion–convection-reaction PDE model with time-dependent spatial domain: Czochralski crystal growth process," *Chemical engineering science*, vol. 67, no. 1, pp. 111–119, 2012.

[52] I. Aksikas, A. Fuxman, J. F. Forbes, and J. J. Winkin, "LQ control design of a class of hyperbolic PDE systems: Application to fixed-bed reactor," *Automatica*, vol. 45, no. 6, pp. 1542–1548, 2009.

[53] I. Aksikas, J. J. Winkin, and D. Dochain, "Optimal LQ-feedback control for a class of first-order hyperbolic distributed parameter systems," *ESAIM: Control, Optimisation and Calculus of Variations*, vol. 14, no. 4, pp. 897–908, 2008.

[54] H. Shang, J. F. Forbes, and M. Guay, "Model predictive control for quasilinear hyperbolic distributed parameter systems," *Industrial & engineering chemistry research*, vol. 43, no. 9, pp. 2140–2149, 2004.

[55] S. Dubljevic, P. Mhaskar, N. H. El-Farra, and P. D. Christofides, "Predictive control of transport-reaction processes," *Computers & chemical engineering*, vol. 29, no. 11, pp. 2335–2345, 2005.

[56] S. Dubljevic, N. H. El-Farra, P. Mhaskar, and P. D. Christofides, "Predictive control of parabolic PDEs with state and control constraints," in *American Control Conference, 2004. Proceedings of the 2004*, vol. 1, pp. 254–260, IEEE, 2004.

[57] Y. Yang and S. Dubljevic, "Boundary model predictive control of thin film thickness modelled by the kuramoto–sivashinsky equation with input and state constraints," *Journal of Process Control*, vol. 23, no. 9, pp. 1362–1379, 2013.

[58] Y. Yang and S. Dubljevic, "Linear matrix inequalities (LMIs) observer and controller design synthesis for parabolic PDE," *European Journal of Control*, vol. 20, no. 5, pp. 227–236, 2014.

[59] L. Liu, B. Huang, and S. Dubljevic, "Model predictive control of axial dispersion chemical reactor," *Journal of Process Control*, vol. 24, no. 11, pp. 1671–1690, 2014.

[60] I. Bonis, W. Xie, and C. Theodoropoulos, "A linear model predictive control algorithm for nonlinear large-scale distributed parameter systems," *AIChE Journal*, vol. 58, no. 3, pp. 801–811, 2012.

[61] Z. Emirsjlow and S. Townley, "From PDEs with boundary control to the abstract state equation with an unbounded input operator: a tutorial," *European Journal of Control*, vol. 6, no. 1, pp. 27–49, 2000.

[62] G. F. Franklin, J. D. Powell, and M. L. Workman, *Digital control of dynamic systems*, vol. 3. Addison-wesley Menlo Park, 1998.

[63] R. Curtain and K. Morris, "Transfer functions of distributed parameter systems: A tutorial," *Automatica*, vol. 45, no. 5, pp. 1101–1116, 2009.

[64] K. J. Åström and B. Wittenmark, *Computer-controlled systems: theory and design*. Courier Corporation, 2013.

[65] E. Hairer, C. Lubich, and G. Wanner, *Geometric numerical integration: structure-preserving algorithms for ordinary differential equations*, vol. 31. Springer Science & Business Media, 2006.

[66] S. L. Campbell, I. C. Ipsen, C. T. Kelley, and C. D. Meyer, "GMRES and the minimal polynomial," *BIT Numerical Mathematics*, vol. 36, no. 4, pp. 664–675, 1996.

[67] S. Campbell, I. Ipsen, C. Kelley, C. Meyer, Z. Xue, *et al.*, "Convergence estimates for solution of integral equations with GMRES," *Journal of Integral Equations and Applications*, vol. 8, no. 1, pp. 19–34, 1996.

[68] C. W. Gear, I. G. Kevrekidis, and C. Theodoropoulos, "'coarse' integration/bifurcation analysis via microscopic simulators: micro-Galerkin methods," *Computers & chemical engineering*, vol. 26, no. 7, pp. 941–963, 2002.

[69] B. Sibbitt, D. McClenahan, R. Djebbar, J. Thornton, B. Wong, J. Carriere, and J. Kokko, "The performance of a high solar fraction seasonal storage district heating system–five years of operation," *Energy Procedia*, vol. 30, pp. 856–865, 2012.

[70] T. P. McDowell and J. W. Thornton, "Simulation and model calibration of a large-scale solar seasonal storage system," in *Proceedings of 3rd National Con-*

ference of the International Buildings Performance Simulation Association-USA, Berkeley, 2008.

[71] D. McClenahan, J. Gusdorf, J. Kokko, J. Thornton, and B. Wong, "Okotoks: Seasonal storage of solar energy for space heat in a new community," in *Proceedings on*, 2006.

[72] A. Fernandez-Garcia, E. Zarza, L. Valenzuela, and M. Pérez, "Parabolic-trough solar collectors and their applications," *Renewable and Sustainable Energy Reviews*, vol. 14, no. 7, pp. 1695–1721, 2010.

[73] V. M. Zavala, J. Wang, S. Leyffer, E. M. Constantinescu, M. Anitescu, and G. Conzelmann, "Proactive energy management for next-generation building systems," in *Fourth National Conference of IBPSA-USA, New York City, New York August 11*, vol. 13, 2010.

[74] E. Camacho, F. Rubio, M. Berenguel, and L. Valenzuela, "A survey on control schemes for distributed solar collector fields. part ii: Advanced control approaches," *Solar Energy*, vol. 81, no. 10, pp. 1252–1272, 2007.

[75] Y. Zhang and V. I. Hanby, "Model-based control of renewable energy systems in buildings," *HVAC&R Research*, vol. 12, no. S1, pp. 739–760, 2006.

[76] P. M. Ferreira, S. M. Silva, and A. E. Ruano, "Energy savings in hvac systems using discrete model-based predictive control," in *Neural Networks (IJCNN), The 2012 International Joint Conference on*, pp. 1–8, IEEE, 2012.

[77] J. Gauthier and C. Xu, "H∞-control of a distributed parameter system with non-minimum phase," *International journal of control*, vol. 53, no. 1, pp. 45–79, 1991.

[78] L. Pu, D. Qi, K. Li, H. Tan, and Y. Li, "Simulation study on the thermal performance of vertical u-tube heat exchangers for ground source heat pump system," *Applied Thermal Engineering*, vol. 79, pp. 202–213, 2015.

[79] L. Dai, Y. Shang, X. Li, and S. Li, "Analysis on the transient heat transfer process inside and outside the borehole for a vertical u-tube ground heat exchanger under short-term heat storage," *Renewable Energy*, vol. 87, pp. 1121–1129, 2016.

[80] K. Astrom and B. Wittenmark, "Computer controlled systems, theory and design, 1984."

[81] B. A. Francis and W. M. Wonham, "The internal model principle of control theory," *Automatica*, vol. 12, no. 5, pp. 457–465, 1976.

[82] M. Maasoumy, A. Pinto, and A. Sangiovanni-Vincentelli, "Model-based hierarchical optimal control design for hvac systems," in *ASME 2011 Dynamic Systems and Control Conference and Bath/ASME Symposium on Fluid Power and Motion Control*, pp. 271–278, American Society of Mechanical Engineers, 2011.

[83] M. Komareji, J. Stoustrup, H. Rasmussen, N. Bidstrup, P. Svendsen, and F. Nielsen, "Optimal model-based control in hvac systems," in *American Control Conference, 2008*, pp. 1443–1448, IEEE, 2008.

[84] Q. Xu and S. Dubljevic, "Modelling and control of solar thermal system with borehole seasonal storage," *Renewable Energy*, vol. 100, no. 4, pp. 114–128, 2017.

[85] R. F. Curtain and H. Zwart, *An Introduction to Infinite-Dimensional Linear Systems Theory*. New York: Springer-Verlag, 1995.

[86] D. Salamon, *Control and observation of neutral systems*, vol. 91. Pitman Advanced Publishing Program, 1984.

[87] G. Weiss, "Transfer functions of regular linear systems. i. characterizations of regularity," *Transactions of the American Mathematical Society*, vol. 342, no. 2, pp. 827–854, 1994.

[88] V. Natarajan, D. S. Gilliam, and G. Weiss, "The state feedback regulator problem for regular linear systems," *IEEE Transactions on Automatic Control*, vol. 59, no. 10, pp. 2708–2723, 2014.

[89] X. Xu and S. Dubljevic, "Output regulation problem for a class of regular hyperbolic systems," *International Journal of Control*, vol. 89, no. 1, pp. 113–127, 2016.

[90] A. Isidori, *Nonlinear Control Systems: An Introduction*. Berlin, Germany: Springer, 1989.

[91] H. Nijmeijer and A. J. V. der Schaft, *Nonlinear Dynamic Control Systems*. New York: Springer-Verlag, 1990.

[92] T. Chen, C., *Linear System Theory and Design*. New York: Holt, Rinehart and Winston, 1984.

[93] N. Kazantzis and C. Kravaris, "Singular PDE's and the single-step formulation of feedback linearization with pole-placement," in *Proceedings of the 36th Conference on Decision & Control*, (San Diego, CA), pp. 36–41, 1997.

[94] N. Kazantzis and C. Kravaris, "Nonlinear observer design using Lyapunov's auxiliary theorem," *Syst. & Contr. Lett.*, vol. 34, pp. 241–247, 1999.

[95] I. Y. Smets, D. Dochain, and J. F. Van Impe, "Optimal temperature control of a steady-state exothermic plug-flow reactor," *AIChE Journal*, vol. 48, no. 2, pp. 279–286, 2002.

[96] F. Logist, P. Van Erdeghem, I. Smets, and J. Van Impe, "Optimal design of dispersive tubular reactors at steady-state using optimal control theory," *Journal of Process Control*, vol. 19, no. 7, pp. 1191–1198, 2009.

[97] S. Oh and R. Schmitz, "A study of the control of a tubular reactor with recycle i. theoretical results for a zero-order exothermic reaction," *Chemical Engineering Communications*, vol. 1, no. 4, pp. 199–216, 1974.

[98] R. C. McOwen, *Partial differential equations: Methods and applications*. Prentice Hall, 2003.

[99] W. Ray, *Advanced Process Control*. New York, New York: McGraw-Hill, 1981.